DEVELOPMENT OF A RESISTANCE BASED BIOSENSOR UTILIZING CONDUCTING MICROFIBERS FOR MICROBIAL PATHOGEN DETECTION

By

Shannon Katie McGraw

A DISSERTATION

Submitted to
Michigan State University
in partial fulfillment of the requirements
for the degree of

Biosystems Engineering – Doctor of Philosophy

2013

ABSTRACT

DEVELOPMENT OF A RESISTANCE BASED BIOSENSOR UTILIZING CONDUCTING MICROFIBERS FOR MICROBIAL PATHOGEN DETECTION

By

Shannon Katie McGraw

Escherichia coli O157:H7 (*E. coli* O157:H7) is one of the U.S. military's top pathogens of interest for the development of rapid diagnostic systems. The enteric pathogen can cause severe gastroenteritis and is spread through the consumption of contaminated food and water. This is of concern to the U.S. military and warfighter because an outbreak of diarrheal disease in the field has the ability to rapidly render a large number of warfighters ineffective in performing their duties. Current field "portable" detection technologies can be cumbersome and require generous quantities of chemicals to operate. In addition, the current FDA gold standard for identification of this pathogen from food matrices takes up to 3 days to generate a confirmed positive result. The objective of this dissertation research was to develop a rapid, novel electrochemical biosensor based on the use of polypropylene microfiber membranes coated with a conductive polypyrrole and antibody functionalized for the biological capture and detection of *E. coli* O157:H7. In this dissertation research, an electrotextile composed of conductive polymer coated microfibers containing functional attachment sites for biorecognition elements was developed. The electrotextiles were optically and electrically assessed based on the polymerization chemicals and reaction time to determine how these factors affected the resistance of the fibers. Based on these experiments, a mathematical model was developed, optimized, and validated.

Various methods of antibody immobilization and surface blocking on the fibers were also assessed. Using glutaraldehyde, pathogen specific antibodies were covalently attached to the conductive microfiber electrotextiles which were then blocked using a 5% bovine serum albumin solution. The functionalized membranes were exposed to *E. coli* O157:H7 cells, washed in Butterfield's phosphate buffer and added to a phosphate buffer electrolyte solution. When a voltage was applied to the system, the presence of the captured pathogen on the fiber surface resulted in an increase in resistance at the electrotextile electrode surface, indicating a positive result. It was found that the conductivity of the components of the system, other than the electrotextile fibers, was not statistically significant. Proof-of-concept experiments were conducted and it was determined that the electrotextile electrode was able to differentiate between positive and negative samples using the pathogen *E. coli* O157:H7 cells as the target over a concentration range of $10^0 – 10^9$ colony forming units per milliliter (CFU/mL). The reproducibility of the sensor results was tested and it was found that the trends in the biosensor results were reproducible. By testing the significance of the biosensor response it was determined that the biosensor can successfully function as a yes / no screening system. The results show that the biosensor has an experimental lower limit of detection of 3.23×10^0 CFU/mL for the detection of *E. coli* O157:H7 in pure culture.

ACKNOWLEDGEMENTS

I would first like to sincerely thank everyone who has contributed, assisted, and supported this research over the years. I would like to especially thank Dr. Evangelyn Alocilja for believing in me and helping make all of this possible. She has been a friend and mentor to me since my freshman year of college and has molded me into the scientist I am today. Her support has been absolutely crucial to the success of my graduate career and shaping me into a responsible scientist. I would like to thank the SMART scholarship program and in particular my SMART sponsor, Dr. Andy Senecal, who has always kept me focused on the big picture. I would also like to thank Kris Senecal and the rest of my lab mates at Natick labs for their support and assistance in helping me learn to use my research in an applied setting to help people. I would like to thank the members of my Ph.D. guidance committee: Dr. John Gerlach, Dr. Wei Liao, and Dr. Joan Rose for their support and guidance. As stressful as this experience has been at times, I know they have always been working to make me better. I would also like to take this opportunity to recognize the three people who assisted me on a day to day basis with my work: Gianna Prata, Krista Lueck, and Patrick Fewins.

I would also like to extend my sincerest gratitude to my friends and family for all their support, patience, and belief in me during my Ph.D. pursuit, in particular my mother, my father, my brother Mike, and my two closest friends through this experience, Mike Anderson and Michelle Packard. Without all of you I would have never made it this far. Everything I have accomplished has been as a result of your love and support.

Shannon McGraw

TABLE OF CONTENTS

LIST OF TABLES

LIST OF FIGURES

Chapter 1 : Introduction

Although food and waterborne pathogens do not have as significant an effect on U.S. military operations as they have in the past, enteric pathogens are the number one cause of non-combat related injuries in the field and are therefore one of the primary military medical concerns for deployed troops [1]. Gastroenteritis was the leading cause of illness among troops during Operations Desert Shield (1990 – 1991) and Desert Storm (1991) [2]. This is a significant issue for the military to address because an outbreak of diarrheal disease in the field has the ability to rapidly render a large number of warfighters ineffective in performing their duties. During Operation Restore Hope (1992 - 1993) it was shown that 16% of all hospital admissions were for diarrheal illness [3]. Of these admissions, 16% could be traced back to *Escherichia coli* (*E. coli*). Various studies on diarrheal illness in deployed troops have listed an array of enteric source pathogens with the most commonly occurring being: *Shigella*, *E. coli*, *Salmonella*, and *Campylobacter* species [1-4]. Based on this information, the pathogen of interest selected for this study is *Escherichia coli* O157:H7.

It is important to have rapid, inexpensive, highly sensitive detection technologies because of the low infectious dose, potential severity of illness, and ease of *E. coli* O157:H7 infection spreading to large populations. These technologies need to be environmentally robust and capable of detecting multiple pathogens. The standard method of detection for *E. coli* O157:H7 does not meet this standard. The U.S. Food and Drug Administration (FDA) standard screening method for *E. coli* O157:H7 requires the blending or stomaching of food samples followed by overnight enrichment before real-time polymerase chain reaction (PCR) screening can be done [5, 6]. Any

samples that are determined to be presumptive positive based on the real-time PCR screening must then be culture confirmed. Obtaining a confirmed positive sample takes a minimum of 3 days and requires an enrichment step before isolation can be performed. In addition, in order to perform a serological characterization multiple staining and agglutination tests must be performed. These methods have several drawbacks. It can be difficult to recover cells from food matrices and cells that are recovered are often not concentrated enough to provide rapid identification [5, 6]. In addition, it is difficult to discern between colonies of different strains of bacterium on culture plates. These methods are not easily implemented in the field. Even the most "portable" versions still require large instrumentation, generous quantities of chemicals, and a low risk of exposure to other contaminants [5, 6]. Because of the unreliability and long wait time for detection using current methods the development and use of a rapid, antibody-based, pathogen specific biosensor is a priority. An improved detection method would decrease the amount of time between contamination and warning, reduce the size of outbreaks, and help ensure overall public safety [7].

This dissertation describes the generation of an electrochemical based biosensor for *E. coli* O157:H7 detection using antibody-functionalized electrotextile electrodes. Chapter 2 presents a review of the literature that pertains to the technologies relevant to this project including current methods for the detection of *E. coli* O157:H7, nonwoven fiber fabrication, and the use of nonwoven fibers in electrochemical detection. Chapter 3 describes the synthesis and characterization of conductive polymer coated nonwoven fibers to create electrotextiles. Chapter 4 presents the development of an optimization model of the polymer synthesis used to develop the electrotextile fibers. Antibody immobilization and blocking of the electrotextile fibers is

presented in Chapter 5. Chapter 6 describes the use of antibody functionalized pyrrole – 3-thiopheneacetic acid (3TAA) copolymer coated nonwoven fibers as electrotextile electrodes in a working electrochemical biosensor for the detection of *E. coli* O157:H7. Chapter 7 is a discussion on the conclusions made in this dissertation and Chapter 8 presents recommendations for future research based on this project. The following sections of Chapter 1 present the research hypothesis and objectives, as well as the research significance and novelty.

1.1 Hypothesis

The research presented in this dissertation is based on the following hypothesis that electrotextile fibers can be developed from nonwoven microfibers and they can be immuno-functionalized for the rapid detection of *E. coli* O157:H7.

1.2 Research objectives

The overall objective of this dissertation research is to develop, optimize, and evaluate a rapid, portable, and novel electrochemical biosensor utilizing antibody-functionalized electrotextile electrodes for the capture and detection of *Escherichia coli* O157:H7.

The detailed objectives of this project are:

- To develop an electrotextile composed of conductive polymer coated microfibers.
- To optimize the polymerization process with the development of a mathematical model.
- To functionalize electrotextile surfaces with pathogen specific antibodies.
- To develop an electrochemical biosensor system.
- To evaluate the biosensor for the detection of the pathogen: *Escherichia coli* O157:H7.

1.3 Research significance and novelty

The novelty of the presented research in this dissertation relies on the use of polymer coated fibers as an electrode in a biosensor for the electrochemical detection of bacterial pathogen in a liquid sample. Many biosensors have been developed for the detection of *E. coli* using metallic electrodes such as gold [8], platinum [9], silver [10], or carbon [11]. By producing a conductive polymer coating on nonwoven microfibers, an electrochemical biosensor electrode can be created that is less expensive than its planar metal counterpart [12]. The overlapping fiber layers also have more available surface area than planar electrodes, resulting in more potential target attachment sites. In addition, these electrotextile electrodes can be engineered to be durable, disposable, lightweight, and require minimal attachment chemistry. These qualities make them ideal for in field use. To our knowledge, this is the first time a functionalized conductive copolymer coated nonwoven electrotextile has been used with immobilized antibodies as an electrode for the successful electrical detection of bacterial cells. A summary of the presented research is listed in Table 1-1 and a comparison with the current literature illustrates the novelty and scientific contribution [12-17].

Table 1-1. Research contribution of this dissertation project to the literature

Subject	References		
Synthesis of aqueously deposited conformal coating of polypyrrole onto electrotextile	This work, published [18]	[14]	[16]
Characterization and analysis of the effect of 3TAA inclusion in polymerization	This work	[17]	[15]
Use of electrotextile in optical detection of avidin / biotin binding	This work, published [18]	[13]	
Use of electrotextile in electrochemical detection of avidin / biotin binding	This work, published [18]	[13]	
Development and optimization of a mathematical model of electrotextile polymerization	This work		
Antibody attachment to electrotextile fibers	This work, published [19]		
Construction of electrochemical cell with electrotextile electrodes	This work, published [20]	[13]	[12]
Electrochemical detection of *E. coli* O157:H7 in pure culture using electrotextile electrodes	This work, published [20]		

Chapter 2 : Literature review

2.1 *Escherichia coli* O157 in the U.S. and military

According to the Centers for Disease Control and Prevention (CDC) “Estimates of Foodborne Illness in the United States”, published in 2011, 1 in 6 Americans (roughly 48 million people) will become sick from a foodborne illness every year [21]. Of those 128,000 will require hospitalization and 3,000 will die, with children under the age of 5 and seniors over the age of 65 being at the greatest risk to develop the severe complications that lead to hospitalizations and death. There are 31 known pathogens that are tracked by the CDC and are believed to account for 20% of all illnesses (9.4 million cases per year), but 44% of all hospitalizations and deaths (55,961 and 1,351 cases per year, respectively). The remainder of illnesses are caused by unspecified agents (microbes, chemicals, or other factors that have not yet been identified or proven to cause illness). Of these hospitalizations caused by a known pathogen, 88% can be traced to 1 of 5 pathogens. These can be seen in Table 2-1.

Table 2-1. Top 5 pathogens contributing to domestically acquired foodborne illnesses resulting in hospitalization per year, taken from the CDC 2011 Estimates: Findings.

Pathogen	Estimated Number of Hospitalizations	Percentage of All Cases (%)
Salmonella, nontyphoidal	19,336	35
Norovirus	14,663	26
Campylobacter spp.	8,463	15
Taxoplasma gondii	4,428	8
E. coli (STEC) O157	2,138	4
Subtotal		88

As can be seen in Table 2-1, *Escherichia coli* (*E. coli*) O157 is responsible for 4% of all cases or 2,138 domestically acquired foodborne illnesses that require hospitalization. *E. coli* is a gram-negative, rod shaped bacteria that is commonly found in human intestinal flora, however *E. coli* O157:H7 is a less common toxin producing strain that causes serious illness when it enters the human gastrointestinal system [22]. *E. coli* O157:H7 infection causes hemorrhagic colitis with symptoms that include severe abdominal cramping and diarrhea that while initially watery can become severely bloody and lasts an average of 8 days. Up to 15% of infections can develop into hemolytic uremic syndrome (HUS) resulting in renal failure, hemolytic anemia, and the permanent loss of kidney function. Common food sources of *E. coli* O157:H7 include ground beef, alfalfa sprouts, lettuce, unpasteurized fruit juices, and raw milk. While the infectious dose of *E. coli* O157:H7 is not known, according to the U.S. Food and Drug Administration (FDA) it may be as few as 10 cells [23]. According to the Foodborne Diseases Active Surveillance Network (FoodNet) Food Safety 2011 Report Card there has been a 25% decrease in *E. coli* O157 infections since 2008 with a rate of occurrence of 0.98 per 100,000 people [24, 25]. This number is still too high though, a goal rate of 0.6 per 100,000 people has been set for the year

2020. In addition, it is believed that for every 1 case of *E. coli* O157:H7 reported, roughly 26 cases go undiagnosed.

As frequent as foodborne illnesses are within the United States, they are of even greater concern for the U.S. military. Although combat injuries are the most significant health risk during military deployments, infectious diseases have been the largest cause of hospitalizations and lost time in every major US war for centuries [26], particularly those caused by enteric pathogens [1]. A study of aero-medical evacuations from Iraq in 2003 found that disease and non-battlefield injuries were 6 times more common than combat related injuries [27]. Improvements in sanitation and hygiene practices have improved prevention [28], however military units are still at risk due to the standard use of community kitchens, which can lead to widespread outbreaks, rapidly rendering a large number of warfighters ineffective in performing their duties. In fact, gastroenteritis was found to be the leading cause of illness among troops during Operations Desert Shield (1990 – 1991) and Desert Storm (1991) [2]. During Operation Restore Hope (1992 - 1993) it was shown that 16% of all hospital admissions were for diarrheal illness [3]. Of these admissions 16% could be traced back to *E. coli*. A study of troops stationed in Iraq in 2004 found that enterotoxigenic *E. coli* and enteroaggregative *E. coli* caused 23% and 12.5% of all diarrhea cases over one summer [29]. In Iraq and Afghanistan 77% and 54% of deployed troops were found to have experienced diarrhea at least once [30], with the rates of diarrhea correlating with local food consumption [31]. Various studies on diarrheal illness in deployed troops have listed an array of enteric source pathogens with the most commonly occurring being: *Shigella*, *E. coli*, *Salmonella*, and *Campylobacter* species [1-4].

Based on the potential to cause severe illness and the prevalence in the U.S. domestic and military populations, the pathogen of interest selected for this study was *Escherichia coli* O157:H7.

2.1.1 Traditional methods of detection

There are three traditional methods most commonly used for pathogen detection: colony counting, polymerase chain reaction (PCR), and immunological methods [32]. These methods are often used for detection because of their high sensitivity and selectivity. These methods do have drawbacks though, they are often complex and not rapid, sometimes taking up to several days to achieve a confirmed positive. The FDA has issued a Bacteriological Analytical Manual (FDA BAM) in order to standardize the methods used for the detection of multiple different foodborne pathogens in different food matrices [5, 6]. The standard method provided for the detection of *E. coli* O157:H7 from foods involves growing the sample in an enrichment broth, plating and culturing the colonies so that they can be identified phenotypically and serologically, and finally testing for Shiga toxin genes using PCR. This method has been updated in the most recent eBAM to recommend performing a quick screening using real-time PCR which can be conducted in 24 hours, however it still takes 3 days in order to get a confirmation. Detailed descriptions of these methods can be found below.

2.1.1.1 Colony counting

Colony counting involves the use of selective growth media in order to detect different bacteria species [32]. These media often contain either inhibitors or specific substrates in order to affect the growth of bacteria, either by inhibiting non-target strains or by causing particular colonies to

appear different colors in order to differentiate them [33]. Following growth of the bacteria of interest, the colonies are assessed optically and counted in order to determine the sample concentration.

Colony culturing and counting is the oldest method for the detection and enumeration of bacteria and has become the standard that every other detection method is compared against. It is generally the standard method of detection used by the FDA because of its accuracy and reproducibility [6]. Despite being the standard it has many drawbacks, first and foremost the fact that it is time consuming. It can often take multiple days to get a negative result, and more to confirm a positive one. A positive result can sometimes require additional tests and culturing to be performed, especially if it is necessary to identify the serotype of the pathogen. Colony counting also requires many different kinds of media, antibiotic supplements, and incubators, making it not viable as a field based testing system.

2.1.1.2 Immunology based methods

Immunological based methods use antibodies in order to detect pathogens. Antibodies are defined as proteins that bind to a particular target antigen [34]. For the detection of bacteria, antibodies are often generated against the bacteria surface antigens such as O (terminal sugars), K (capsule components), H (flagella), and LPS (cell surface lipopolysaccharide) antigens. Antibodies are produced by plasma cells in response to infections or immunizations. The specificity of an antibody depends on the type of antibody, the species of host used, individual differences between hosts, and the extent of purification conducted. Antibodies can be monoclonal, polyclonal, or recombinant [32]. Monoclonal antibodies are made in lag phase with

cell culture by a single clone and target the same antigen [34]. Polyclonal antibodies are typically purified from blood serum and contain a mixture of several antibodies that target multiple different portions of the same target antigen [34]. Recombinant antibodies are synthetic antibodies that are created using antibody genes either made in a laboratory or taken from human cells [35].

One of the most common immunology based tools to aid in the detection of bacteria is immunomagnetic separation (IMS), a pre-concentration step where magnetic beads that have been coated with antibodies to the pathogen of interest are inserted into the sample and then removed using a magnet [36-38]. The extracted beads pull the captured target pathogen from the sample matrix with them. IMS has been combined with nearly every type of detection method available [32]. It can be particularly useful when the sample is complex, either due to the matrix that the pathogen is in or because there are many different kinds of bacteria present.

Another standard immunologically based technique is the enzyme-linked immunosorbent assay (ELISA) [34]. ELISAs benefit from the specificity of antibodies but also the sensitivity of enzyme assays by combining the two together. In the most common version, a sandwich ELISA, an antigen specific antibody is immobilized within a well, normally the well of a 96 well plate. The sample containing the antigen is added and then removed, leaving behind any antigen that has bound to the immobilized antibodies. Then a second enzyme-labeled antibody specific to the antigen is added and removed, leaving behind only the antibodies which had bound to the bound antigen. Finally, the enzyme's substrate is added to the well and if the antigen is present a change in color in the well can be observed. The color change will only occur if the antigen is

present because the enzyme labeled antibody will only remain to react if the antigen is present in the well for it to bind to [32, 34].

The use of immunology based methods benefits from the specificity of the antibody-antigen binding. Antibodies can be expensive though and detection methods like ELISA may have to be paired with a separation step if the matrix is complex. This is especially true if the detection signal is a visual change (e.g., color), which can be obscured by a sample matrix that is opaque or brightly colored. In addition, antibodies are proteins and therefore qualities of the sample such as temperature or pH have to be monitored so as to not render the antibodies ineffective. Many antibodies available for sale have cross-reactivities, meaning that the antibody reacts and binds to an antigen that is not the antigen that was used to produce the antibody. Antibodies for *E. coli* O157:H7 have been reported to have some level of cross-reactivity with *Klebsiella*, *Enterobacter*, *Citrobacter*, and non-pathogenic *E. coli* [39].

2.1.1.3 Polymerase chain reaction

PCR is a nucleic acid amplification technique used to detect targeted bacteria based on specific short sequences of their genetic material [40]. It combines steps to perform DNA isolation, amplification, and quantification based on specific target DNA probes. In PCR many cycles are completed to exponentially amplify the sample until enough target DNA has been formed for detection. Briefly, in one cycle targeted double stranded DNA (dsDNA) is first denatured by heat then specific primers are added which recognize the corresponding DNA strands. Polymerization occurs, extending the DNA strands bound to the primers until 2 new identical dsDNA sequences are formed. These newly formed dsDNA strands are then used as the target

DNA in the next cycle. Gel electrophoresis is then used to detect the DNA. There are several different variations of PCR including: real-time PCR, multiplex PCR, and reverse transcriptase PCR. Real-time PCR is faster than regular PCR, it uses fluorescent emission with a specific dye attached to the targeted amplicon rather than gel electrophoresis for detection [41, 42]. The fluorescent intensity is then interpreted to be proportional to the amount of amplified product generated. Multiplex PCR can be used to detect several targets at the same time by using multiple different primers to amplify more than one specific gene [43, 44].

PCR can be much less time consuming than other bacterial detection techniques, however it can still take up to 24 hours and usually requires purification and enrichment steps beforehand [32]. PCR has a high level of complexity when compared to other detection techniques and is susceptible to environmental contamination, making it not viable for in field testing. PCR detection does have very high specificity of detection though, basing its detection on the DNA of the target sample. This requires the use of a primer developed to be specific to a section of the DNA sequence of the target pathogen. The primer must be known and fabricated beforehand in order to be able to perform detection though, and if the sequence is not specific enough, then detection specificity will be lost [32]. One of the biggest problems with using PCR to detect *E. coli* O157:H7 in food samples or complex matrices is that the most important virulence factors, Shiga toxin 1 (*stx1*) and Shiga toxin 2 (*stx2*), are not specific to the pathogen, they can be found in other Shiga-toxin producing *E. coli* as well [45]. This requires the use of multiplex PCR assays for the Shiga-toxin genes as well as pathogen-specific sequences in order to obtain a definitive detection. Also, components in food samples or other complex matrices (e.g., calcium,

fat, complex polysaccharides) can inhibit the PCR, requiring additional purification and sample preparation techniques be used [45].

2.1.1.4 FDA Bacteriological Analytical Manual method

In the FDA BAM method for the detection of *E. coli* O157:H7 [6] food samples are blended or stomached, followed by overnight enrichment in modified Buffered Peptone Water with pyruvate (mBPWp) [46] and Acriflavin-Cefsulodin-Vancomycin (ACV) antibiotic supplements. Using either a SmartCycler II or LightCycler ® 2.0 [47-49] platform real-time PCR is used to test the enriched samples for *stx1* and *stx2* genes as well as the +93 single nucleotide polymorphism in the *uidA* gene, which encodes for β-D-glucuronidase (GUD) enzyme [50]. If the result comes back positive, then a confirmation must be conducted using cultural isolation.

In order to perform the cultural isolation Butterfield's phosphate buffer with ACV supplements is used for overnight enrichment. The enriched sample is then serially diluted in Butterfield's phosphate buffer and spread or streak plated onto Tellurite Cefixime – Sorbitol MacConkey Agar (TC-SMAC) and a chromogenic agar such as Rainbow® Agar O157 and incubated for 18 – 24 hours. *E. coli* O157:H7 colonies will appear colorless or neutral / gray with a smoky center on TC-SMAC while non-O157 sorbitol-fermenting *E. coli* will be pink or red. On Rainbow Agar O157:H7 will appear black or blue – black. Portions of the isolated colonies that test positive for O157 antigen using a latex agglutination test are then streaked onto Trypticase Soy Agar with Yeast Extract (TSAYE) plates to check for purity. ColiComplete (CC) discs are added to the heaviest streaks on the TSAYE plates as well as a similar plate containing a positive control, MUG positive strain of *E. coli*, and incubated for 24 hours. The CC discs contain a

chromogenic assay for galactopyranosidase (X-gal) which will appear blue on and around the disc indicating coliform growth. It also contains a fluorogenic assay for glucuronidase (MUG) which will fluoresce under long wave UV (365 nm) which indicates non-O157 *E. coli*. *E. coli* O157:H7 is X-gal (+) and MUG (-). Following this test a spot indole test is conducted by taking the spot growth from the TSAYE plate and adding it to a filter wetted with Kovac's reagent, where *E. coli* O157 will appear indole (+).

Samples that are found to be X-gal (+), MUG (-), and indole (+) must have additional tests performed to confirm the positive result. The colonies from the TSAYE plate are tested using the RIM *E. coli* O157:H7 latex test using commercial antisera to confirm the presence of O157 and H7 antigens. If the latex test comes back O157 (+) and H7 (+) then the O157:H7 serotype is confirmed, however if the test comes back O157 (+) and H7 (-) then more tests must be conducted to assure that the sample is not a non-motile variant (O157:NM). Tests that are O157:H7 (+) are tested using API20E or VITEK to identify the sample as *E. coli*.
Both H7 (+) and H7 (-) samples must be retested to verify their toxigenic potential using either real-time PCR (which can also be used for initial screening) or a conventional 5P multiplex PCR. The 5P multiplex PCR looks for *stx1*, *stx2*, +93 *uidA* SNP, and the enterohemolysin (*ehxA*) genes and gamma (γ) intimin (*eae*) allele (O157:H7 virulence factors) [51].

If the food sample to be tested is complex, either due to the food matrix or the sample containing many bacterial samples, IMS beads can be used on the sample after the overnight enrichment. This will help isolate the pathogen of interest for PCR or plate counting.

2.2 Biosensors

The requirement for small, ultrasensitive, affordable, disposable sensors for medical diagnostics, environmental monitoring, and food safety has led to an increase in research in biosensor technology. The International Union of Pure and Applied Chemistry (IUPAC) has defined biosensors as "a device that uses specific biochemical reactions mediated by isolated enzymes, immunosystems, tissues, organelles or whole cells to detect chemical compounds usually by electrical, thermal, or optical signals" [52, 53], put simply, the purpose of a biosensor is to convert the occurrence of biological events into measurable responses [54]. A schematic representation of a biosensor and its components can be seen in Figure 2-1.

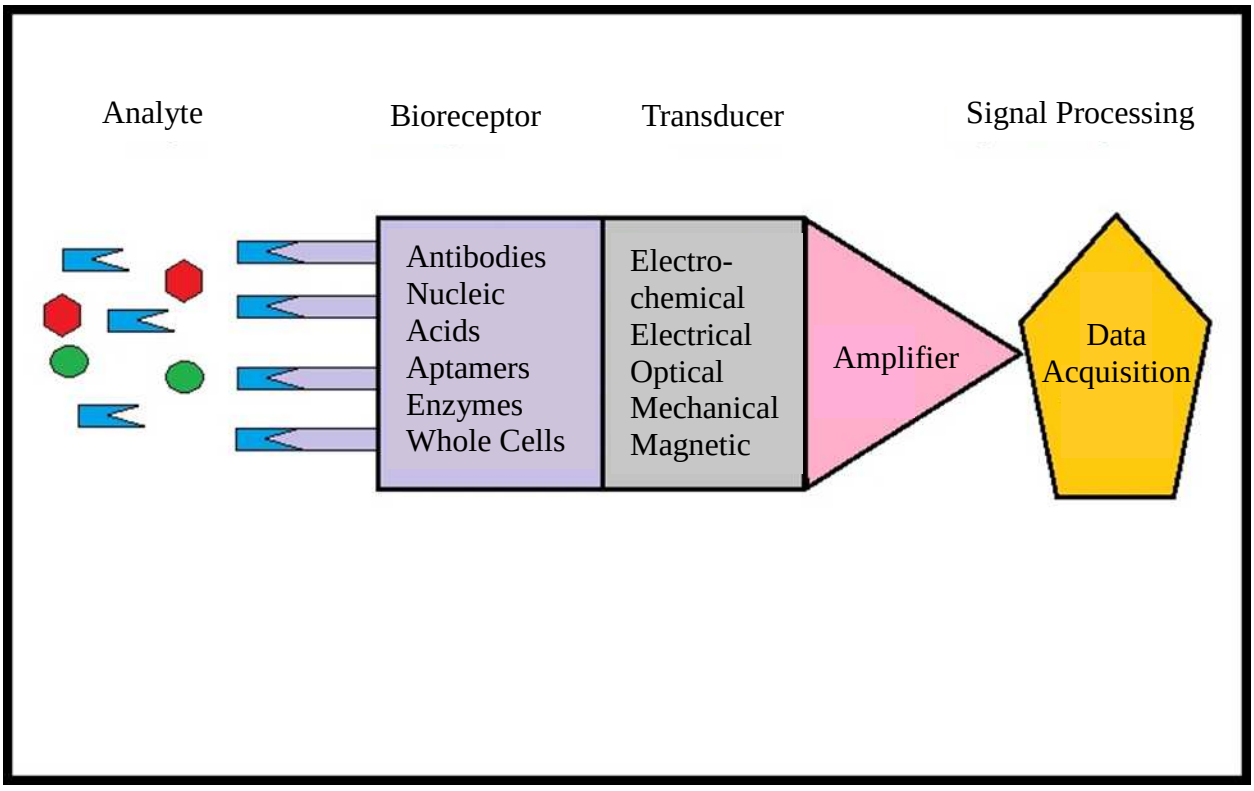

Figure 2-1. Schematic representation of a biosensor and its components. (For interpretation of the references to color in this and all other figures, the reader is referred to the electronic version of this dissertation.)

In a biosensor a bioreceptor, such as antibodies or nucleic acids, are bound or in some way closely associated with a transducer. When a biological recognition event occurs between the bioreceptor and its target analyte, the transducer converts this event into a measurable signal. Biosensors can be grouped based on several different criteria, such as their target analyte, biomolecule receptor type, or method of signal transduction. The most common method is based on signal transducer, with optical and electrochemical being the most common [52, 55-57]. Optical biosensors are often used because they have better sensitivity and selectivity than electrochemical systems, however that advantage can be greatly reduced if the sample is turbid or it is difficult to perform analyte extraction. Optical biosensing systems are also generally more expensive than electrochemical systems, making them not cost beneficial in some scenarios [58]. In order for biosensor technology to advance and surpass common pathogen detection techniques, such as PCR and culture / colony counting, the current drawbacks of biosensors must be addressed. These include high cost, low durability, a lack of environmental robustness for in field testing, detection limits that do not reach those of traditional techniques, and a necessity for extra extraction methods to be performed before use adding to the total detection time [32, 52, 59, 60].

2.2.1 Optical biosensors

Optical sensors measure changes in the optical properties of an analyte, often using fluorescence. It can also be expanded to include such techniques as surface plasmon resonance (SPR) and piezoelectric systems [32]. Optical biosensors have been developed for the detection of not just bacteria, but also toxins, drugs, and other contaminants [61-64]. Optical sensing systems are

considered to be beneficial due to their selectivity and sensitivity, these can be reduced though if the sample is complex.

2.2.1.1 Fluorescence

Fluorescence is defined as luminescence that is caused by a valence electron being excited from its ground state to an excited singlet state [65]. This excitation occurs when light of a sufficient energy is absorbed. When the electron returns to its original ground state it emits a photon of a lower energy. Fluorescence is also characterized as having little thermal loss in the system and rapid light emission after excitation. Fluorescence is the method most often used for optical biosensing [65]. It can be combined with established techniques such as ELISA or PCR or can be a detection method on its own if fluorescent markers, such as fluorescein isothiocyanate (FITC) are used [66]. Another form of fluorescent biosensing is fluorescence resonance energy transfer (FRET) where the capture of the target analyte results in a decrease in distance between donor and acceptor fluorophores associated with the bioreceptor [67]. This decrease in distance allows the acceptor fluorophore to become excited by the donor fluorophore, emitting a fluorescent signal.

2.2.1.2 Surface plasmon resonance

In SPR based sensors, structural alterations occur near a thin film metal surface resulting in changes in the measured refractive index [68]. Briefly, a glass plate that has been covered with a gold thin film is irradiated with a p-polarised light from the back using a hemispherical prism. The reflectivity is then measured as a function of the angle of incidence, θ. The resulting plot curve will contain a dip known as the SPR minimum. The properties of the gold-solution

interface will dictate the angle position of this minimum, allowing for detection. SPR has been used in the analysis of adsorption phenomena, antigen-antibody affinity binding, and bacterial detection [32, 69, 70].

2.2.1.3 Piezoelectric

Piezoelectric systems use a quartz crystal microbalance (QCM) which has observable changes in resonance frequency when there are mass changes on the sensor surface [71]. These changes are usually visualized through the use of a fluorescent label. By using immobilized antibodies on the probes a QCM has been shown to be capable of piezoelectrically detecting bacteria, such as *E. coli* K12 [72], *Listeria monocytogenes* [73], and *Salmonella* species [74].

2.2.2 Electrochemical

In an electrochemical biosensor, the biological recognition element is immobilized at an electrode which then converts the biological recognition event (e.g., antibody – antigen binding) into a measurable electrical signal. Electrochemical sensors are often subdivided based on the electrical parameter that is being observed for changes at the electrode-matrix interface as either amperometric (change in current), potentiometric (change in potential), or impedimetric (change in impedance) [32].

2.2.2.1 Amperometric detection

Amperometry uses the stepping of the potential of the working electrode from where no faradaic reaction occurs to a potential where the surface concentration of the electroactive species at the

electrode is effectively zero [75]. In this method, the current over time is monitored. Amperometry is used to measure the diffusion coefficient of electroactive species or surface area of the working electrode. It can also be used to study the mechanisms of the electrode processes. Because mass transport is diffusion based, in the conditions of amperometry the current-time curves can be used to show the change in concentration gradient in the area surrounding the surface. The gradual increase of the size of the diffusion layer paired with the depletion of the reactant results in a decreasing slope in the concentration profile over time. This can be seen in the current decay that occurs over time [75].

2.2.2.2 Potentiometric detection

Potentiometric detection monitors changes in the system potential and is the least common technique used in biosensors. This can be observed when an enzyme catalyses a reaction and consumes or generates a substance that can be detected by the ion-selective electrode. Another form of potentiometric detection are ion selective field effect transistors (ISFETs). When modified with antibodies, DNA , enzymes, or whole cells they can be used to monitor biorecognition events [76, 77]. An ISFET will create regions of excess charge in a semiconducting substrate using an electric field in order to increase or decrease conductivity. Potentiometric techniques, such as ISFET, are not often used for biosensing because they are complex and biomolecule immobilization can be difficult. In addition they can also have poor reproducibility and stability [32].

2.2.2.3 Electrochemical impedance spectroscopy

Electrochemical impedance spectroscopy (EIS) uses a small amplitude cyclic function with variable frequency applied to a transducer to calculate impedance based on the resulting current. The system impedance is determined based on the amplitude of the current and potential signals as well as the resulting phase difference that occurs between the voltage and current [78, 79]. Because EIS is very complicated to calculate, the calculations are often simplified by viewing the system as equivalent circuits consisting of capacitors and resistors. This has allowed biosensors to be developed using EIS for the detection of bacterial pathogens such as *E. coli* O157:H7 [80].

2.3 Nonwoven fibers in biosensing

One approach for addressing some of the drawbacks of current biosensor technology is through the development / use of electrotextiles. Nonwoven fabrics are one material being explored for electrotextile development due to their inherent high surface area and commercial availability [81]. The convergence of electronics, electrical engineering, and textile technologies has the potential to combine the attractive attributes of each technology into making fabric based networks for electrical systems, paving the way for the development of fully integrated high surface area smart textiles with transistors, integrated circuits, sensors and other electronic devices built into the textile structures [82].

Nonwoven fabrics are broadly defined as sheet or web structures bonded together by entangling fibers or filaments, forming flat, porous sheets made either directly from separate fibers or from molten plastic or plastic film [83]. The term nonwoven implies that the fabric was produced by a

method other than knitting, weaving, braiding, or tufting [84]. Nonwoven fibers are of particular interest because of their small diameters (in the micro or nano scale), increased surface area, and their ability to maintain membrane porosity in comparison to larger micron diameter nonwoven fibers and continuous cast films [85]. These interconnected pores can result in essentially "soldered junctions" after the annealing process is completed, resulting in higher textile durability and tensile strength. They are also inexpensive to produce and lightweight, ideal qualities for in field use [86, 87]. The chemical composition of nonwoven fibers and their coatings can also be easily changed or adjusted based on their intended use. Small changes to the processing parameters can change the fiber diameter, mesh size, porosity, texture, or weave pattern. This processing flexibility makes them a very versatile material for sensor development. They can be designed to be used with many different analytes and experimental conditions and can be designed to have high chemical stability [85].

Reviews of the literature indicate that biosensor research focusing on nonwoven fibers can be divided into the production, characteristics, and applications of nanofibers and microfibers. Nonwoven optical biosensing is a relatively new area of research and studies in this area are limited [88]. The majority of electrochemical work with nonwoven fibers has been for the development of biosensors to detect compounds, such as glucose, urea, and hydrogen peroxide [88]. Presented in the subsequent sections are descriptions of the common functional modification techniques used for the development of nonwoven based biosensors. Also presented are the current optical and electrical based systems that exist for biosensing using nonwoven fibers. The aim of the next portion of the review is to present the different biosensing applications being developed using nonwovens.

2.3.1 Fiber fabrication

Typically, commercial nonwovens are produced by dry-laid, wet-laid, spunbound, meltblown, and/or spunlaced processes [89, 90]. The production process usually consists of three primary steps: spinning the polymer, collecting continuous filaments, and bonding the fiber mat for greater strength and functionality, using either thermal, chemical and / or mechanical techniques [91]. Polymer fibers have typically been produced by solution / gel spinning, melt spinning, or electrospinning [81, 92]. There are a number of excellent review articles on electrospinning and the effects of process variables for producing polymer fibers [81, 88, 93-98]. Fiber diameters produced by these methods can range from nano to micrometer in scale, with micron diameters more reproducible. The selected method used to synthesize nonwovens will ensure specific characteristics in the material [91]. This allows for the design of nonwoven fibers with an array of characteristics, making them versatile in fabric production for commercial products.

2.3.1.1 Electrospinning

Electrospinning is a well-established process that uses electrostatic forces to produce nonwoven nanofibers [99], a schematic of which can be seen in Figure 2-2.

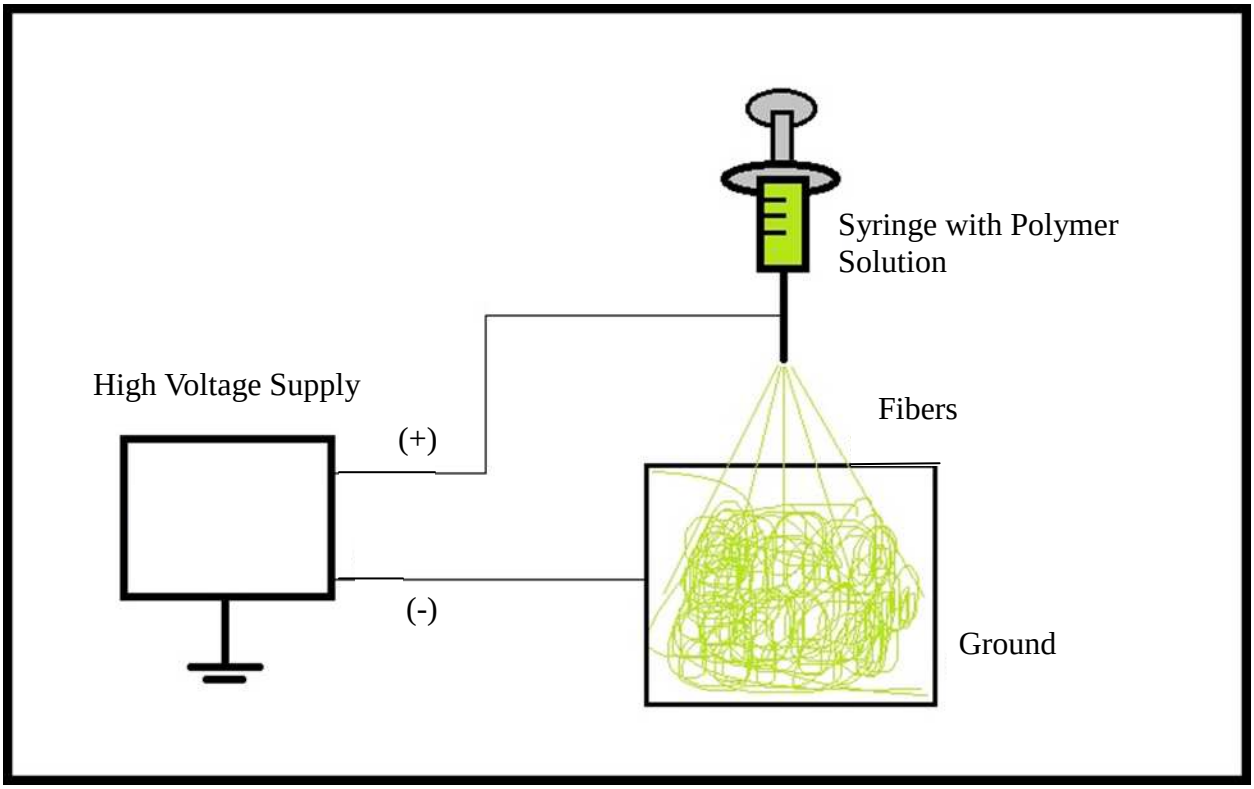

Figure 2-2. Schematic representation of electrospinning process.

Briefly, during electrospinning, the polymer is either in solution or a melt. A voltage is applied to the polymer solution / melt, producing electrically charged jets that are collected by an oppositely charged collector. As the charged jet travels to the grounded collector, the solvent / melt evaporates and cools producing nanofibers on the collector. A large number of polymers can be spun, with the only limitation being the polymer's solubility or ability to be used as a melt. Additionally, electrospinning is capable of producing fibers in the submicron range [98]. In 2009, researchers fabricated conductive nonwoven nanofibers for gas sensing applications by electrospinning solutions of zinc acetic acid with a poly 4-vinyl phenol. After the combination fibers were initially formed, zinc oxide (ZnO) nanofibers were obtained by calcinations burning off the polymer carrier [100]. Electrospinning can also be used to fabricate nanocomposite

fibers, removing the need for a separate recognition element immobilization step during fabrication. Nanocomposite fibers of urease and polyvinylpyrrolidone (PVP) were made into nonwoven mats for electrochemical sensing of urea [101]. The enzyme / polymer composite mats had increased surface area and smaller pore sizes, resulting in a larger adsorption rate and therefore decreased response time for detection. Electrospun fibers have been studied for use in several different sensor technologies such as: acoustic wave, resistive, photoelectric, optical, and amperometric [102].

2.3.1.2 Melt extrusion

Another method to create nonwovens involves a melt extrusion process. In polymer melt extrusion, the hot liquid polymer is forced through an extruding device containing either a mold or die. It is then cooled until it solidifies into the desired fiber shape [103]. At North Carolina State University, an elastomer in a coaxial configuration was used to create hollow fibers into which a specific additive, conductive eutectic gallium indium, was used to fill the fibers to form medical / diagnostic monitoring products [104]. This process can be tailored to specific applications based on the additive used.

2.3.2 Surface treatments

2.3.2.1 Drop on Demand

In many electrochemical based sensing systems the nonwoven fibers are made conductive in order to act as a substitute for a metal electrode. One method for forming conductive nonwoven fibers is drop on demand ink jet printing [105]. In drop on demand an ink composed of an

aqueous carrier, a pigment, and a polymer having either acid, base, epoxy, or hydroxyl functional moieties is applied to a textile that contains a hydroxyl, amine, amido, or carboxyl group and an organometallic or isocyanate cross-linking agent [106]. When a current is pulsed through either a heating element or piezoelectric material associated with the ink chamber it causes the ink to be propelled out of the nozzle onto the textile in a drop [107]. This method has been used for developing sensors using nonwovens of polyethylene / polypropylene and can be used to network conductive components throughout the fabric. Applications usually center on the health care field, focusing specifically on the monitoring of vital signs such as respiration and electrocardiograms [108].

2.3.2.2 Atomic layer deposition

Others in the field of conductive nonwovens have looked at utilizing processes such as atomic layer deposition (ALD), a vapor phase growth process known for its metal oxides, nitrides, and conducting thin films, where self-terminating gas-solid reactions are performed sequentially to fabricate conformal coatings as small as the nanometer range [109]. The conformal coating process for deposition of metal oxides on surfaces can be carefully controlled and tailored for thickness and content of the metal oxide layers. Plasma-enhanced ALD coating application is beneficial because it operates at low temperatures, making this method amenable to thermally sensitive materials, such as polymers [110, 111]. In the work by Jur et al [112] researchers coated various fibrous textiles with different metal oxide layers and conductivities ranging from 24 S/cm for zinc oxide (ZnO) to 1150 S/cm for tungsten oxide were observed.

2.3.2.3 Conjugated polymers

Other methods for creating conductive nonwoven fibers for use in sensors involve the use of conjugated polymers both within and coating the nonwoven fabric structure. Organic conjugated polymers in recent years have been well studied and used in such fields as energy storage, memory devices, electrocatalysts, and electrochemical devices [113]. Conductive polymer preparation can be straightforward and production of some, such as polyacetylene and polypyrrole, can be simple to form using electrochemical or chemical synthesis. In order to achieve electrical conductivity, a charge must be capable of being transferred along the conjugated chain, between chains or particles, and along grain boundaries. This is achieved when π-overlap along the polymer chain occurs, providing a half-filled band of delocalized π-electrons [114]. Their unique properties such as stability in air and compatibility with biological molecules make them ideal candidates for use in biosensing. The conductive polymer polypyrrole has been one of the most studied polymers for use in biosensing and has been found to be the most active for both deposition at neutral pH and immobilization of biomolecules [115]. A popular method for conjugating polymers with nanofibers is oxidative chemical vapor deposition (oCVD), where an electrically conductive coating can be formed directly on the fibers. This is done by simultaneously combining an oxidant and a monomer in the reaction chamber with the fiber substrates [116]. This method has shown versatility in the coating of various substrates from films to fibers. Nylon fibers were coated with the conductive co-polymers of polyethylene dioxythiophene / 3-thiopheneethanol using oCVD. These fibers have recently been studied for use in a resistance based sensor where the immobilization of biomolecules uses the built in carboxyl (–COOH) functional group of the polymer [13].

A two-step combination process has been used to develop nonwoven conductive fibers formed using polyethylene oxide (PEO) containing the oxidant ferric chloride ($FeCl_3$) [117]. The PEO fibers containing the oxidant were produced using electrospinning and in the second step the fibers were exposed to pyrrole vapor for polypyrrole (PPy) synthesis. This same method was used by Granato et al [12] to develop polypyrrole coated fibers, except the fibers were made of nylon-6 instead of PEO. In thin film devices that contain PPy, active sensing components are imbedded which can limit efficiency and sensitivity. A nanofibrous surface improves these factors because of the high surface area for the given mass / volume. In addition, the nanofiber platform can enhance the transport of ions and chemicals from the solution to the interior of the sensor component, perhaps even acting as the capture and sensing component all in one. Results showed that the composite PPy / PEO fibers were very smooth after exposure to pyrrole vapor with the average diameter of the fiber being 96 nm. The sheet conductivity of the fibers was found to be on the order of 10^{-3} S/cm [117]. The nylon-6 / PPy fibers were found to have an average diameter of 290 nm and could be used to measure an amperometric response due to increases in concentrations of a phosphate solution with a significant R^2 of 0.990 [12].

The most largely researched and easiest method for the fabrication of conductive fibers is through the use of aqueous / organic solvent deposition using chemical polymerization [118]. This can be achieved by using a bulk process where a relatively strong chemical oxidant oxidizes a monomer in solution and the resulting polymer precipitates out of the solution as a solid. For a finer, more controlled coating, the monomer or oxidant can be exposed to only the fibers, then introduced to the reacting solution resulting in the polymerization occurring directly at the

surface. Other polymer coated fibers and textiles have been generated using liquid chemical oxidation to generate PPy [119-124] and polyaniline (PANI) polymers onto fibers [125]. The resulting electrotextiles maintain the porosity and increased surface area of a fiber textile, but the polymer coating along the individual fibers are also capable of providing electrical conductivity through the membrane.

2.3.3 Covalent biosurface modification

The demands of a successful biomaterial immobilization with conductive fibers are: the biorecognition properties and / or catalytic properties of the bioreceptor remain active; the recognition elements are attached within or on the substrate to maintain activity; the chosen biorecognition elements improve selectivity of the biosensor; and the transducer is affected, whether by increasing or decreasing electron transfer, upon a binding event. In order to successfully achieve these demands, surface modification of the nanofibers is often necessary. The strategy for surface modification that is most promising is covalent attachment of biomolecules, which allows for electron interactions between the active site and the electrode [126]. Modified electrode surfaces have been examined for use in amperometric biosensors. Transfer reactions of biological molecules were observed to be normally slow at conventional metallic electrodes. Bartlett [126] sought to overcome this problem by direct coupling of the biological redox reactions to the electrodes. This involved the electrodes being modified by covalent attachment of species, by either reversible adsorption or by deposition of conducting polymers as electrode materials. Using electrodes coated with conductive poly (5-carboxyindole) they were able to use the carboxylate groups on the polymer to interact with the lysine residues on the protein surface for orientation and electron transfer upon binding events.

This study also pointed out the electrochemical constraints of electron transfer in relation to the distance to the electrode in biosensors.

A chemiresistive biosensor for the detection of the biomolecule biotin was developed using 3,4-ethylenedioxythiophene (EDOT) copolymerized with 3-thiopheneethanol (3-TE) on a nylon fiber mat [13]. The available hydroxyl (–OH) functional group found in the copolymer was covalently attached to the biomolecule avidin using p-maleimidophenylisocyanate (PMPI) molecules as a cross-linker. The naturally high affinity constant of avidin for biotin ensured the sensor would have strong selectivity and specificity. This was confirmed using laser scanning confocal microscope images of the fibers with FITC-avidin molecules before and after reacting with biotinylated red quantum dots [13].

2.3.4 Electrochemical detection using nonwoven fibers

Electrochemical based sensing does not require enzyme labels or redox mediators to facilitate detection like optical sensors do and output signals are directly related to the concentration of bound antigen to the sensor. Three of the most commonly used electrochemical detection methods in biosensing are amperometry, voltammetry, and resistivity, or looking at changes in the current, voltage, or resistance, respectively, across the system [127]. The system parameters commonly measured are: interfacial capacitance, electron transfer resistance, and medium conductivity. In developing an electrochemical based biosensor using nonwoven fibers, it is important to take into consideration such individual components as: the conductivity of the electrolyte solution, the distance between electrodes, the total electrode surface area, the electrode materials, and the temperature and pH at which the measurement is carried out [128].

Electrically based detection systems that use a polymer nanofiber-based biosensor paired with enzymes have been developed for sensing glucose [129], urea [101], and fructose [130]. Recently studies have been conducted to use nanofibers as biosensors for detecting food pathogens. Some examples of this include nitrocellulose nanofibers that have been fabricated and used as a lateral flow immunosensor for detecting *E. coli* 0157:H7 [131], *Salmonella* spp [80], *Bacillus* spp [132]. In this section, a more in depth review is made on the use of nonwoven fibrous platforms for electrochemical biosensors.

2.3.4.1 Cyclic voltammetry

Cyclic voltammetry provides information on the thermodynamics of redox processes, kinetics of heterogeneous electron-transfer reactions, coupled chemical reactions, or adsorption processes [75]. It is also used to determine the locations of redox potentials of electroactive species and evaluate media effects . In cyclic voltammetry, a linear scan of the potential of a working electrode is performed using a triangular potential waveform. A single cycle or multiple cycles can be performed. During the potential sweep the current resulting from the applied potential is measured and the current versus the potential is plotted on to a cyclic voltammogram. Forward and reverse scans will result in peaks of O to R (oxidation to reduction) and R to O, respectively. These peaks are the result of the diffusion layer formed near the electrode surface. In reversible systems the current and potential at each of the two peaks can be used for data analysis with the current being directly proportional to the concentration of the electroactive species of interest [75].

Arecchi et al. [133] used nylon nanofibrous membranes to build electrochemical biosensing devices for the detection of glucose that allowed high enzyme loading due to the high surface-to-volume ratio of nanofibers when compared to thin film technology. Glucose oxidase was attached to the nanofibers using glutaraldehyde to covalently immobilize the enzyme. The functional membrane was then securely attached to a carbon electrode, completing the electrochemical biosensor. Cyclic voltammetry was used to analyze the sensor with the nylon membranes attached. The sensor exhibited a sensitivity of 1.9 μA/mM over a response time of 20 – 30 seconds and had a limit of detection of 6×10^{-6} M.

2.3.4.2 Amperometry

Amperometry uses the stepping of the potential of the working electrode from where no faradaic reaction occurs to a potential where the surface concentration of the electroactive species at the electrode is effectively zero [75]. In this method, the current over time is monitored.

Biosensors used in glucose monitoring have been created using immobilized glucose oxidase associated with an electrospun electrode made of nanofibers consisting of polymethylmethacrylate dispersed with multiwall carbon nanotubes. Glucose was detected amperometrically in a phosphate buffer and effective electron mediation was achieved. A benefit of this nonwoven fabricated electrode is flexibility for the flow of gas and liquids through the high surface area allowing higher loading of biomolecules for improving biosensor performance. Testing looked at how stronger binding efficiency of the biomolecules / enzymes minimized leaching of the active component during the fabrication process. Results showed that

the nanofibrous nonwoven biosensor provided excellent detection levels and wide linear range response to glucose presence [134].

A tyrosinase-modified electrode was developed to be used as an electrochemical amperometric biosensor for the detection of phenolic compounds in food [135]. The enzyme had been immobilized by drop-coating onto a glassy carbon electrode that had been covered with a nanofibrous membrane made of nylon-6 that was prepared by electrospinning. A three-electrode system was used with the coated glassy carbon serving as the working electrode. At -0.2 V the amperometric response was measured, showing a decrease in current over time with the addition of standard pyrocatechol. The biosensor exhibited a response time of 16 seconds, a detection limit of 0.05 μM, and linearity up to 100 μM.

2.3.4.3 Resistivity / conductivity

In electrochemical resistance / conductance based biosensors, the biological recognition event creates either a disruption or connection for the flow of current at the working electrode and a system response is measured [136, 137]. This resistance can be correlated to different target pathogen concentrations, resulting in pathogen detection. The change of the system resistance should be proportional to the change in the amount of pathogen captured. Fabrication of a chemiresistive biosensor for detection of biomolecules was demonstrated on a high surface area, flexible electrospun nylon fibrous mat [13]. The –OH functionalized conducting copolymer of 3,4-ethylenedioxythiophene (EDOT) and 3-thiopheneethanol (3-TE) was synthesized and conformally deposited on the electro-spun mats by oxidative chemical vapor deposition (oCVD). The –OH functional groups associated with the copolymer were used for covalent

immobilization of avidin. Biotin molecules were used as the target analyte-specific molecule. The sensitivities of avidin immobilized conducting copolymer on electrospun mats were tested against micro-molar to nano-molar concentrations of biotin in aqueous solutions. Results showed the sensor response was 6 times higher than when a flat substrate was used. It also significantly lowered the response time.

E. coli O157:H7 bacteria and bovine viral diarrhea virus (BVDV) detection has been conducted using electrospun fibers of nitrocellulose [131]. Nanofibers were functionalized to contain antibodies by glutaraldehyde crosslinking chemistry. Silver electrodes were then fabricated on the nanofibers. To complete the circuit for detection, those same antibodies were attached to conductive (polyaniline) magnetic nanoparticles which attached when exposed to target pathogens in solution. This complex then attached to the modified surface of the membrane completing the charge transfer between the electrodes. Detection of the targets for the fabricated device was found to be linear in response to the amounts of analyte in solution. In an 8 minute detection process sensitivity of the biosensor was 61 colony forming units per milliliter (CFU/ml) for *E. coli* and 103 cell culture infectious dose per milliliter (CCID/ml) for BVDV [131].

2.4 Conclusions / outlook

Although a lot of research activity has gone into the development of biosensors, there is still a disconnect in getting this technology transitioned to real world with commercially available systems. The biggest cause for this is the common drawbacks that still exist in current biosensors such as high cost, low durability, a lack of environmental robustness for in field

testing, detection limits that do not reach those of traditional techniques, and a necessity for extra extraction methods to be performed before use adding to the total detection time. Optical biosensors have better sensitivity and selectivity than electrochemical systems; however they are very sensitive to the characteristics of the sample matrix. Electrochemical systems are subject to high levels of system noise, which can reduce the sensitivity of the sensor. Other drawbacks of current biosensor technology include the need for chemical labels or reporters, a lack of multiplexing capabilities, short shelf lives, complex production methods, and a lack of reproducibility of materials and results [32, 52]. The use of durable nonwoven fibers is one new field that can be explored to help address some of these issues. Their low cost, material durability, ease of production, and material stability make them particularly promising for sensing applications.

There are many different approaches available for the formation and use of nonwoven fibers for biosensing. Nonwoven fibers can be utilized as optical or electrical based sensors with appropriate design considerations such as choice of polymer, fiber packing density, biomolecule attachment chemistries, signal attenuation, dopants, and detector / reader design. Care must be taken to choose materials that will be able to maintain their optical or conductive properties in the presence of biological systems. The requirement for small, ultrasensitive, affordable, disposable sensors for medical diagnostics, environmental monitoring, and food safety has led to an increase in this research.

Chapter 3 : Synthesis and characterization of electrotextile fibers

This chapter is adapted from our recently published work in the journal, Biosensors: McGraw, Shannon K.; Alocilja, Evangelyn; Senecal, Andre; Senecal, Kris. Synthesis of a Functionalized Polypyrrole Coated Electrotextile for Use in Biosensors. Biosensors. 2012; 2(4):465-478. DOI: 10.3390/bios2040465.

3.1 Introduction

Electrochemical biosensors combine a biological recognition element with an electrical readout. There is a large array of biorecognition elements to choose from including: DNA / RNA aptamers, proteins, antibodies, enzymes, and DNA probes. These biorecognition elements can be used directly in their natural form or can be biochemically altered [138-141]. Biological recognition is accomplished when the element is immobilized at an electrode transducer which converts the biological recognition event (i.e., antibody - antigen binding) into a measurable electrical signal [54, 75, 142, 143]. Biosensor transducers can be electrochemical, optical, thermal, mass related, or based on electrical impedance. Impedance based sensing is advantageous because it does not require enzyme labels or reduction/oxidation mediators to facilitate detection as optical based sensing does [127]. In electrochemical impedance based systems a measurable system response is created when the biological recognition event disrupts the flow of the current at the working electrode while the reference electrode maintains a constant potential [75].

High-surface area nonwoven fibers are versatile and can be developed into electrotextile smart membranes designed for use with all forms of sensor signal transduction. However, research into the integration of electrotextile, biological, and electrical technologies to create novel biosensor systems for food protection is limited. Previously published studies have been conducted on the development of electrically active non-metallic textile coatings made of doped polypyrrole (PPy) polymers [13, 14, 19, 121, 122, 144]. By producing a conductive polymer coating on non-woven microfibers, an electrochemical biosensor electrode can be created that is less expensive than its planar metal counterpart, with more available surface area [12].

In addition, these electrotextile electrodes can be engineered to be durable, disposable, and require minimal attachment chemistries. The ability to use antibody functionalized fibers for capture and concentration was previously demonstrated with electrospun nanofibers and a carboxyl functional group [19, 145]. With the attachment of biological recognition elements to the electrotextile surface, these electrodes have the capacity to act as the transducer in a biosensor while also performing pathogen capture, concentration, and detection [13]. This combination would simplify a food pathogen detection biosensor, resulting in a significantly smaller and lighter detection system.

The inclusion of a carboxyl group in the polymerization of such an electrotextile based sensor would provide the needed functional group sites for the attachment of biorecognition elements necessary to a biosensor design (i.e., antibodies, avidin). Various types of molecules have previously been included during the polymerization of pyrrole in order to create biosensors with built in biological receptor sites, such as biotin [146], benzophenone [147], pyrrole-3-carboxylic

acid [148] and 3-thiopheneacetic acid (3TAA) [17]. Rapid, highly specific sensing of target analytes can be achieved due to the use of these elements at a relatively low cost. The faster speed and lower cost of biosensors versus standard detection methods have made them especially marketable to the food industry [149-151].

The objective of this study was to develop and produce an electrotextile with a biosensing focus composed of conductive polymer coated microfibers that contain functional attachment sites for biorecognition elements. Experiments were conducted to select a functional group, fiber platform, and polymerization solvent. The effects of dopant inclusion and post-polymerization wash steps were also analyzed. Investigations were conducted to determine if the inclusion of 3TAA in the polymerization process would have an effect on the availability of binding sites for biorecognition elements in the high-surface area electrotextile and how the increase in the concentration of 3TAA would affect several properties of the coating such as the physical characteristics, resistivity of the sample, and the availability of binding sites. Finally, the successful attachment of avidin to the electrotextile was examined as well as the avidin's ability to capture biotin (a common biorecognition model). This was evaluated optically and electrochemically.

3.2 Materials and methods

3.2.1 Materials

Nylon 6 (NY6) and polypropylene (PP) nonwoven microfibers were obtained from North Carolina State Nonwovens Cooperative Research Institute. The fibers were cut into circular discs with a diameter of 1.2 cm. The monomer solution contained 98% pyrrole and either 3TAA or

pyrrole-3-carboxylic acid (3-COOH), all obtained from Sigma-Aldrich (St. Louis, MO, USA). Iron (III) chloride ($FeCl_3$), acetonitrile, methanol, and 5-sulfosalicylic acid (5SSA) were also obtained from Sigma-Aldrich. Covalent attachment of the biorecognition elements was performed using N-(3-dimethylaminopropyl)-N'-ethylcarbodiimide hydrochloride (EDC) (Sigma-Aldrich) and N-hydroxysulfosuccinimide (sulfo-NHS) (Invitrogen, Carlsbad, CA, USA) with 50 mM 2-(N-morpholino)ethanesulfonic acid (MES) buffer, pH 6.0, (Thermo Fisher Scientific, Waltham, MA, USA), fluorescein isothiocyanate (FITC) labeled avidin (Thermo Fisher Scientific, Waltham, MA), avidin (Thermo Fisher Scientific), biotin (Thermo Fisher Scientific), and biotinylated quantum dots (Qdot 655 biotin conjugate kit, Invitrogen).

3.2.2 Synthesis

3.2.2.1 Functional group selection

A circular NY6 membrane sample was dipped into a solution of 1 mg/mL 3TAA in pyrrole, removed, and placed into a reaction vessel where 10 mL of 0.1 M $FeCl_3$ in acetonitrile was added and allowed to react for 18 hours at room temperature, during which oxidative polymerization of the pyrrole based monomer occurred [121, 152-156]. The second sample was dipped into a solution of 0.5 mg/mL 3-COOH in pyrrole, removed, and placed into a container where 10 mL of 0.1 M $FeCl_3$ in acetonitrile was added and allowed to react for 18 hours at room temperature. Both samples were removed from their respective solutions and left to dry for 4 hours at room temperature.

3.2.2.2 Dopant inclusion and solvent selection

Six polymer samples were generated and evaluated using NY6 as the fiber platform. The fibers were dipped into a solution of 1 mg / mL 3TAA in pyrrole, removed, and placed into separate reaction vessels. Two samples each were oxidized with 10 mL of 0.1 M $FeCl_3$ suspended in acetonitrile, methanol, or deionized (DI) water. A volume of 1 mL of 0.1 M 5SSA was added immediately after the addition of the $FeCl_3$ to act as a dopant. All samples were allowed to react for 30 minutes at room temperature. After polymerization, the samples were removed and dried for 4 hours at room temperature.

3.2.2.3 Post-polymerization treatment

NY6 membrane samples were dipped into a solution of pyrrole containing 1 mg/mL 3TAA, removed, and placed into an empty container. $FeCl_3$ (10 mL, 0.1 M) was added to each followed immediately by 5SSA (1 mL, 0.1 M). Samples were allowed to react for 30 minutes. Samples were subject to 3 conditions: no post-polymerization treatment, a DI water wash, or a DI water wash and sonication for 5 minutes. Following treatment the samples were dried for 4 hours at room temperature.

3.2.2.4 Fiber platform selection

A spot melted PP disc was coated with the PPy conductive polymer. The fiber disc was dipped into a solution of 1 mg / mL 3TAA in pyrrole, removed, and placed into a separate reaction vessel where polymerization occurred. A volume of 10 mL of 0.1 M $FeCl_3$ in DI water was used

as the oxidant and 1 mL of 0.1 M 5SSA was used as the dopant. The sample reacted for 30 minutes at room temperature and was then removed, washed with DI water, and dried for 4 hours at room temperature. A sample using NY6 as the fiber platform was also prepared with an identical coating method.

3.2.2.5 3TAA analysis

PP microfiber discs were briefly submerged in a 10% pyrrole and 3TAA (concentrations of 0, 0.1, 1, 10, 20, 50, or 100 mg / mL) solution. The functionalized monomer was absorbed onto the fiber mat. The wet fiber sample was then removed from the solution and placed in a glass container for polymerization. $FeCl_3$ (0.1M, 10 mL) was added to the sample to initiate the chemical reaction while a dopant, 5SSA (0.1M, 1 mL), was simultaneously added. The fibers in solution were incubated at room temperature for 30 minutes with constant agitation, thereby ensuring that polymerization occurred on both sides of the mat. The nonwoven fiber sample was removed from the solution, gently rinsed on both sides with distilled (DI) water, and dried at room temperature overnight.

3.2.3 Physicochemical characterization

A visual assessment of each sample was conducted using scanning electron microscopy (SEM). The samples were gold sputter coated (~15 nm thickness) and imaged with a Zeiss EVO 60 scanning electron microscope fitted with an energy dispersive spectroscopy (EDS) attachment (Carl Zeiss Microscopy, LLC, Thornwood, NY, USA). The images were taken at a setting of 1,024 × 768 pixels with 4× line integration (noise reduction technique). Slow scan speed 8 was

used with a spot size of 370 for a measurement beam current of 70 picoamps. The EHT voltage was 30.0 kV and the working distance was 6 mm, except where noted otherwise. EDS measurements were performed with 102.4µS amp time for 500 counts at magnifications of 100x. Electrical resistance measurements of the polymer were taken across the fiber membranes using a four point probe (Pro-4, Signatone, Gilroy, CA) and a Keithley 2400 Sourcemeter (Keithley Instruments, Cleveland, OH, USA) after an interval of 10 seconds.

3.2.4 Biological experiments

3.2.4.1 Optical analysis

PPy / 3TAA coated PP membrane discs were prepared according to the method listed in Section 3.2.2.4 and washed with DI water. FITC labeled avidin (FITC-avidin) was attached to the functionalized membranes through EDC / sulfo-NHS crosslinking. The discs were washed with distilled water and dried for 10 minutes. A volume of 200 µL of EDC and sulfo-NHS in MES buffer was added and reacted with gentle agitation for 15 minutes. The discs were washed twice in MES buffer and 250 µL of FITC-avidin was added to each disc. The discs were reacted with gentle agitation for 4 hours and were washed with MES buffer. Finally, the discs were washed three times with phosphate buffered saline (PBS). For 3TAA analysis the samples were read using a Fluoroskan Ascent microplate fluorometer (Thermo Scientific) and measured for fluorescence at an excitation wavelength of 490 nm. Emission was measured at 535 nm. Triplicate readings were taken for each sample and then averaged to obtain an average fluorescent output value. Imaging was performed using a Zeiss LSM710 confocal microscope (Carl Zeiss Microscopy, LLC, Thornwood, NY, USA).

To visually assess the avidin functionalized fibers' ability to capture a target molecule a total volume of 500 µL of biotinylated Qdots was added to the fibers at a 1:400 dilution. The samples were incubated with agitation for 1 hour at room temperature and were stored at 4 °C overnight. The samples were washed three times with PBS and then imaged using a Zeiss LSM710 confocal microscope (Carl Zeiss Microscopy, LLC, Thornwood, NY, USA).

3.2.4.2 Electrochemical analysis

PPy / 3TAA coated PP membrane discs were prepared according to the method listed in Section 3.2.2.4, cut into 2 cm × 2 cm squares, and washed with DI water. Avidin was attached to the functionalized membranes through EDC / sulfo-NHS crosslinking as described in Section 3.2.4.1. Resistance measurements were obtained by connecting the avidin attached membrane discs to a PalmSens using two alligator clips on opposing sides of the membrane. The membrane was submerged in 10 mL of 0.1 M phosphate buffer (PB) and then a 10 mL sample of biotin solution at varying concentrations was added. The resistance values were recorded every 30 seconds for 15 minutes. The system response (Rp) was calculated using Equation 3-1 [13].

$$Rp(\%)=((R_1-R_0)/R_0)\times 100 \qquad (3\text{-}1)$$

Where R_1 is the resistance of the avidin attached sensor after the biotin sample has been added.

R_0 is the resistance of the avidin attached sensor that has not been exposed to biotin.

3.3 Results and discussion

Table 3-1 summarizes the different treatments, platforms, and reaction times that were examined in this manuscript as well as their impact on material resistance and coating morphology.

Analysis of the results from each tested combination is explained in the subsequent sections. Supplementary data, calculations, and images can be found in Appendix B.1.

Table 3-1. Summary of treatments and effects. All reaction times are 30 minutes except for the samples from Figure 3-1 and Figure 3-2 which had reaction times of 18 hours.

Materials and Methods Tested					Results		
Platform	**Monomer**	**Dopant**	**Solvent**	**Wash Treatment**	**Resistance**	**Figure #**	**Notes**
NY6	3-COOH/ Pyrrole	none	acetonitrile	none	397 kΩ	3-1	Coating even, black, and conformal on fibers. Heavy buildup of polymer clusters along fibers.
NY6	3TAA/ Pyrrole	none	acetonitrile	none	23.71 kΩ	3-2	Coating even, black, and conformal on fibers. Clusters of polymers buds scattered along fibers.
NY6	3TAA/ Pyrrole	none	acetonitrile	none	189.98 kΩ	none	Coating uneven, gray, and brittle.
NY6	3TAA/ Pyrrole	5SSA	acetonitrile	none	291 kΩ	none	Coating uneven, gray, with dark black spots, brittle.
NY6	3TAA/ Pyrrole	none	methanol	none	35.31 MΩ	none	Coating uneven, gray, slight brittleness.

Table 3-1 (cont'd).

NY6	3TAA/ Pyrrole	5SSA	methanol	none	710 Ω	3-4	Coating uneven and gray with black spots. Polymer forms a solid sheet across fibers.
NY6	3TAA/ Pyrrole	none	water	none	557 Ω	none	Coating smooth and even, black, slightly brittle
NY6	3TAA/ Pyrrole	5SSA	water	none	91.5 Ω, 51.2 Ω	3-5 3-6	Coating smooth, even, and black. Polymer clusters are small and build along fiber surfaces
NY6	3TAA/ Pyrrole	5SSA	water	DI water wash and sonication	60.5 Ω	3-8	Coating smooth, even, and black. Coating is slightly lighter than other samples with better porosity

Table 3-1 (cont'd).

NY6	3TAA/ Pyrrole	5SSA	water	DI water wash	42.6 Ω	3-7 3-9	Coating smooth, even, black, and slightly brittle. Coating is slightly lighter than unwashed sample
PP	3TAA/ Pyrrole	5SSA	water	DI water wash	55.1 Ω	3-10	Coating smooth, even, and black. Not brittle. Coating is conformal along fibers.

3.3.1 Functional group selection

The inclusion of a pendant carboxyl functional group associated with the conductive polymer coating provides attachment sites for the covalent binding of antibodies to the fibers, giving a biosensor its ability to detect pathogens and specificity of capture [157]. The groups 3TAA and 3-COOH were evaluated as potential functional group additions in the electrotextile polymer. The SEM images of the samples can be seen in Figures 3-1 and 3-2 and the results can be seen in Table 3-1.

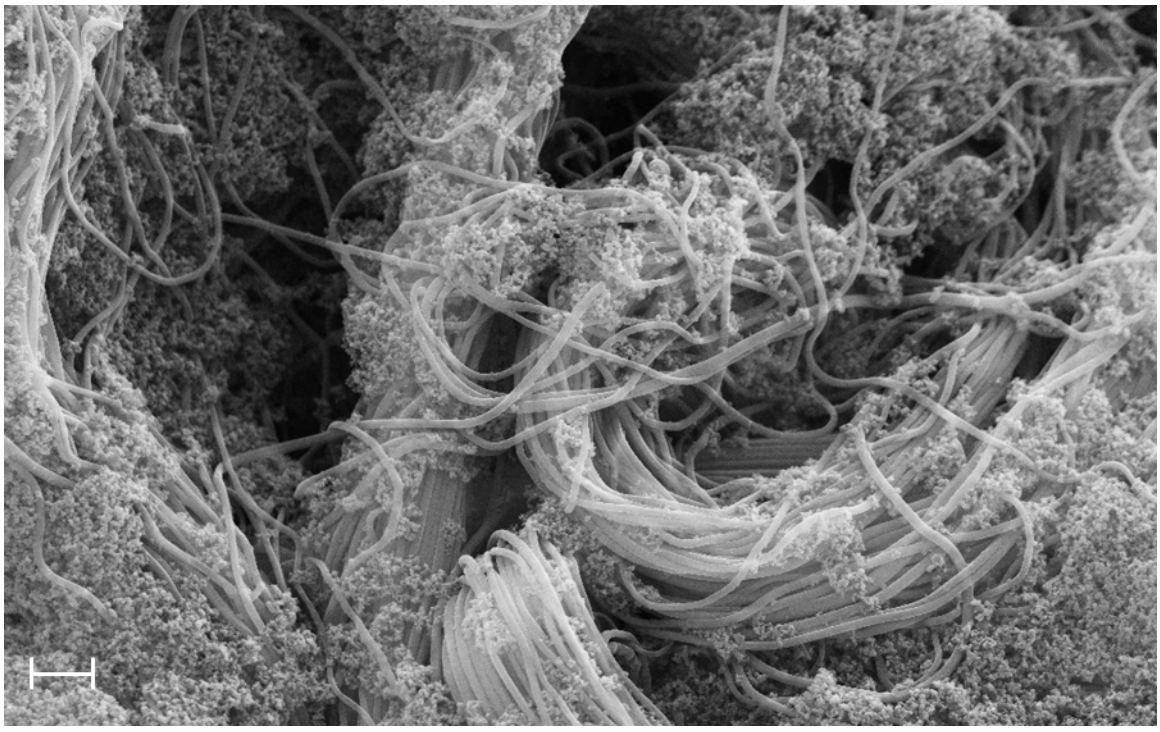

Figure 3-1. SEM image of nylon 6 fibers coated in polypyrrole with 3-COOH. Scale bar equal to 10 µm, magnification of 2,000x, EHT of 30 kV and working distance of 6.0 mm.

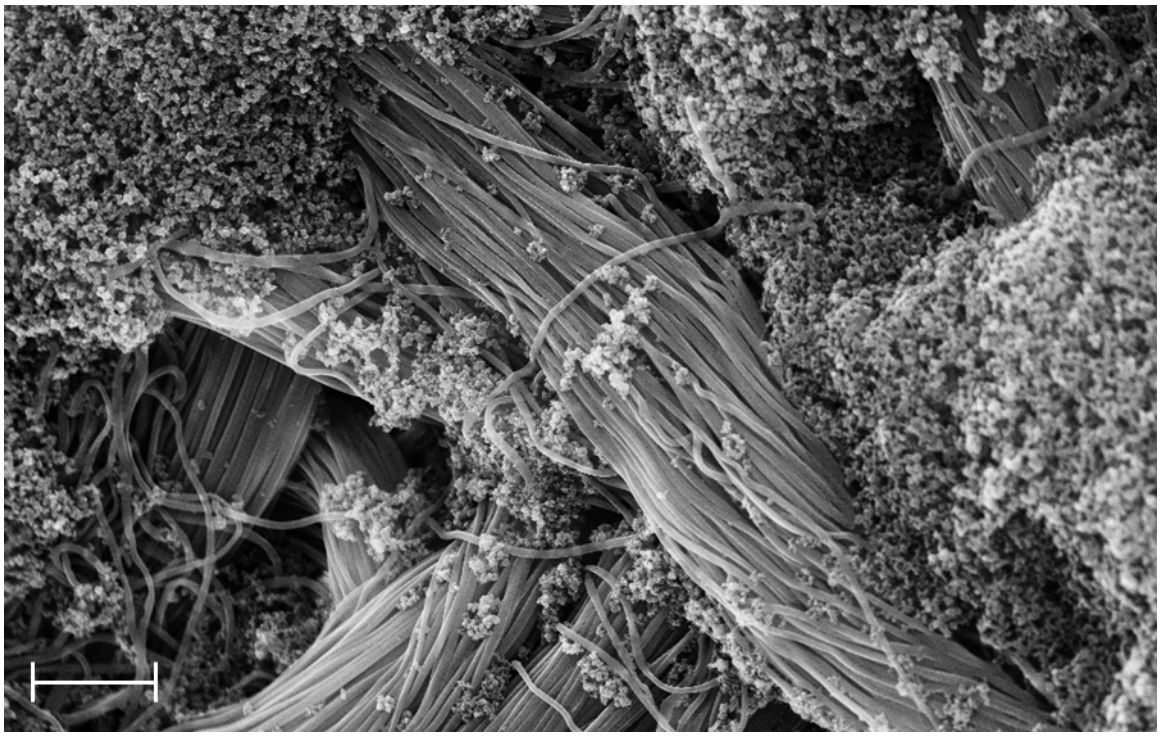

Figure 3-2. SEM image of nylon 6 fibers coated in polypyrrole with 3TAA. Scale bar equal to 20 µm, magnification of 2,000x, EHT 30 kV, and working distance of 6.0 mm.

The sample using 3TAA formed an even black coating across the fiber surface. SEM analysis showed that the coating was conformal on the individual fibers on the membrane with clusters of polymer buds scattered along the fibers. The measured resistance for the sample was 23.71 kΩ. The sample with 3-COOH additive had an evenly dispersed black coating across the surface as well. SEM analysis showed that the fibers were conformally coated, however the buildup of polymer clusters on the fibers was much heavier than in the sample where 3TAA was used as the additive. This buildup of polymer on the sample using 3-COOH pyrrole caused an increased resistance of 397 kΩ for the sample. In the development of an electrotextile electrode, it is important to minimize material resistance and for the conductive polymer coating to be continuous throughout the fibrous platform. This ensures consistency across the electrode surface for recognition element attachment and that any change in electrical signal is due to target

binding to the recognition site instead of variations between fabricated electrodes. Based on this information, 3TAA was selected as the functional group additive to be used in the polymerization for the remaining experiments.

The chemical structure of the poly(pyrrole-3TAA) copolymer can be seen in Figure 3-2.

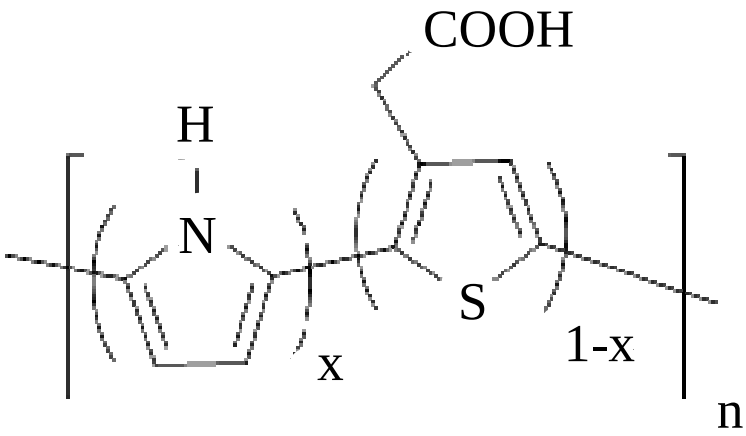

Figure 3-3. Schematic representation of the chemical structure of poly(pyrrole-3TAA).

Previous work has been done exploring the polymerization of pyrrole with additional molecules added to create a co-monomer in order to build biological receptor sites into the polymer. These include biotin [146], benzophenone [147], 3-COOH [148] and 3TAA [17]. The structure is the same as that published in Vaddiraju et al. [17], however because the deposition method is aqueous instead of oCVD there are differences in the coating thicknesses, morphologies, and conductivities. The addition of an organic acid dopant will also affect these parameters.

3.3.2 Dopant inclusion and solvent selection

The inclusion of the dopant 5SSA was evaluated as a result of previous research indicating that the use of planar dopant ions increases conductivity in PPy coatings [14, 122, 158]. The effect of the polymerization solvent was evaluated as well. These results can be seen in Table 3-1.

The samples with acetonitrile as a solvent were both unevenly coated, with the sample containing dopant having dark black spots across the surface. The coating was very brittle. As shown in Table 3-1, the measured resistance for the sample oxidized in acetonitrile with 5SSA was 291 kΩ. The resistance of the sample without the inclusion of the dopant was 189 kΩ. The samples where methanol was used as the solvent had uneven black coatings. The sample that did not have 5SSA added had a measured resistance of 35 MΩ, however the sample where 5SSA was added had a measured resistance of 710 Ω.

The samples that were oxidized using $FeCl_3$ in water had smooth and even black coatings. The sample without 5SSA had a slightly heavier surface coating and appeared more brittle. The sample without 5SSA had a measured resistance of 557 Ω. The sample with 5SSA had a resistance of 91.5 Ω.

The samples containing 5SSA that were oxidized in methanol and in water were selected for further evaluation using SEM. These images can be seen in Figures 3-4 and 3-5.

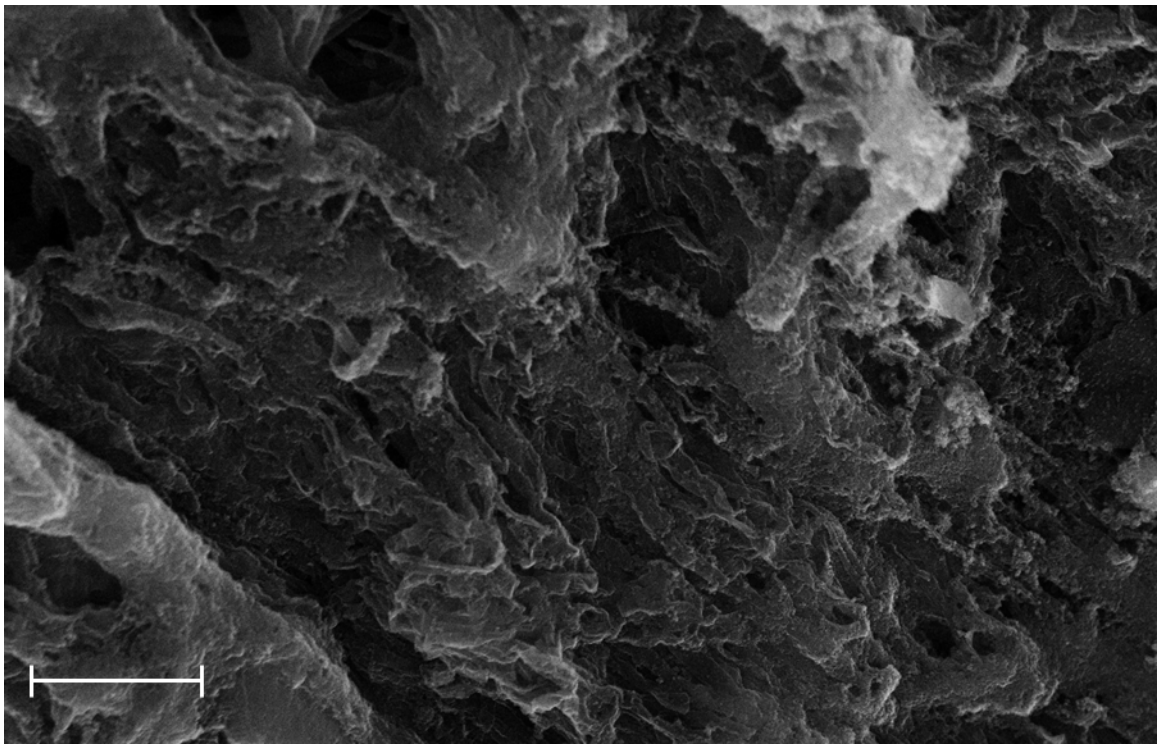

Figure 3-4. SEM image of nylon 6 fibers coating in doped polypyrrole with methanol as solvent. Scale bar equal to 20 µm, magnification of 2,000x, EHT of 30 kV and working distance of 6.0 mm.

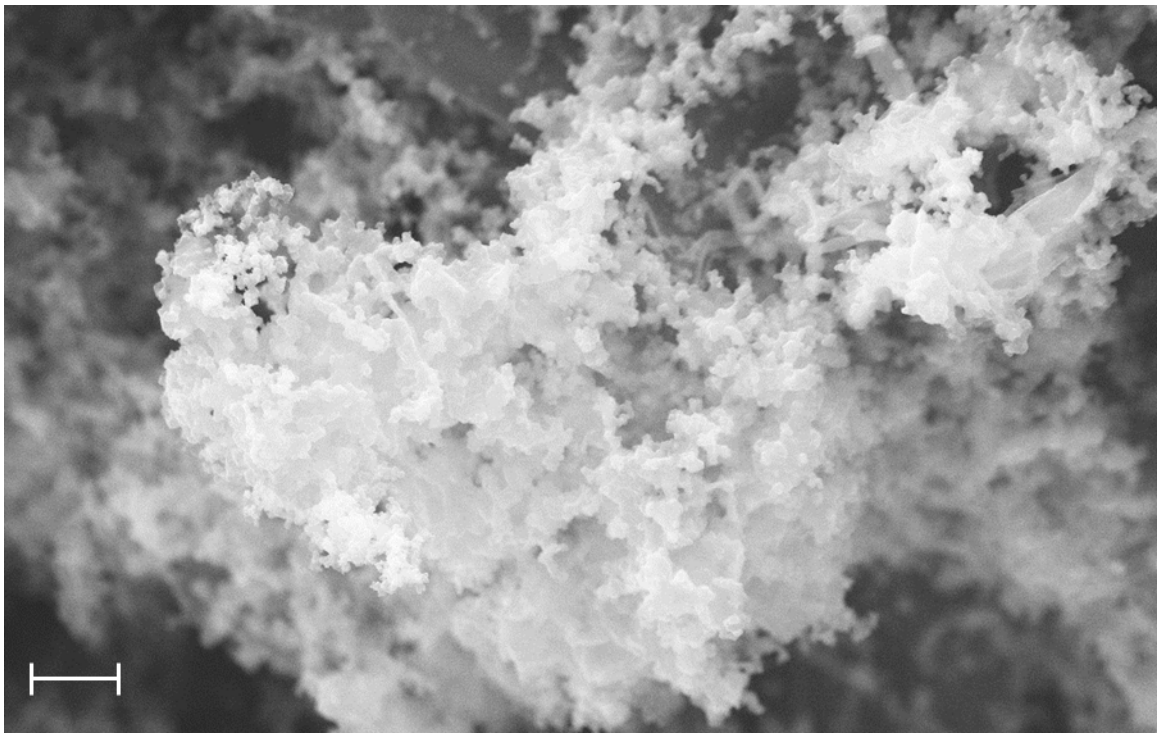

Figure 3-5. SEM image of nylon 6 fibers coated in doped polypyrrole with water as solvent. Scale bar equal to 10 µm, magnification of 2,000x, EHT of 30 kV, and working distance of 8.0 mm.

The sample oxidized using methanol had a less globular appearance than previously seen in the acetonitrile samples without the dopant, however it appeared more like a solid sheet of coating across the fibers. In comparison, the samples that were oxidized in water were very globular, the polymer clusters seen previously were present, but much smaller and building along each individual fiber.

When comparing the samples shown in Figures 3-4 and 3-5 with the samples from Figures 3-1 and 3-2, it can be seen that the choice of solvent for the reaction was shown to affect polymer formation on the fiber surface, directly relating to overall polymer conductivity. The inclusion of a dopant resulted in increased conductivity across the fiber membranes in less reaction time. The inclusion of the dopant had the greatest impact on conductivity when the conductive polymer

was chemically oxidized in water resulting in the lowest sample resistance among the tested combinations.

3.3.3 Post-polymerization treatment

In order to evaluate the strength of the attachment of the coating to the fiber surface, a wash step and sonication were introduced post-polymerization to remove excess, unattached polymer. Each cleaning step was tested for effect on resistance. Untreated, washed, and sonicated samples were measured using a four point probe to determine the resistance. These results can be seen in Table 3-1. Their resistances were 51.2 Ω, 42.6 Ω, and 60.5 Ω, respectively. With a range of 17.9 Ω, the difference observed between the resistance measurements of the three samples was minimal and did not appear significant.

SEM analysis, shown in Figures 3-6, 3-7, and 3-8, shows heavy, clustered polymer coatings along the fibers from each sample, with the sample that was not washed appearing to have a slightly heavier surface coating.

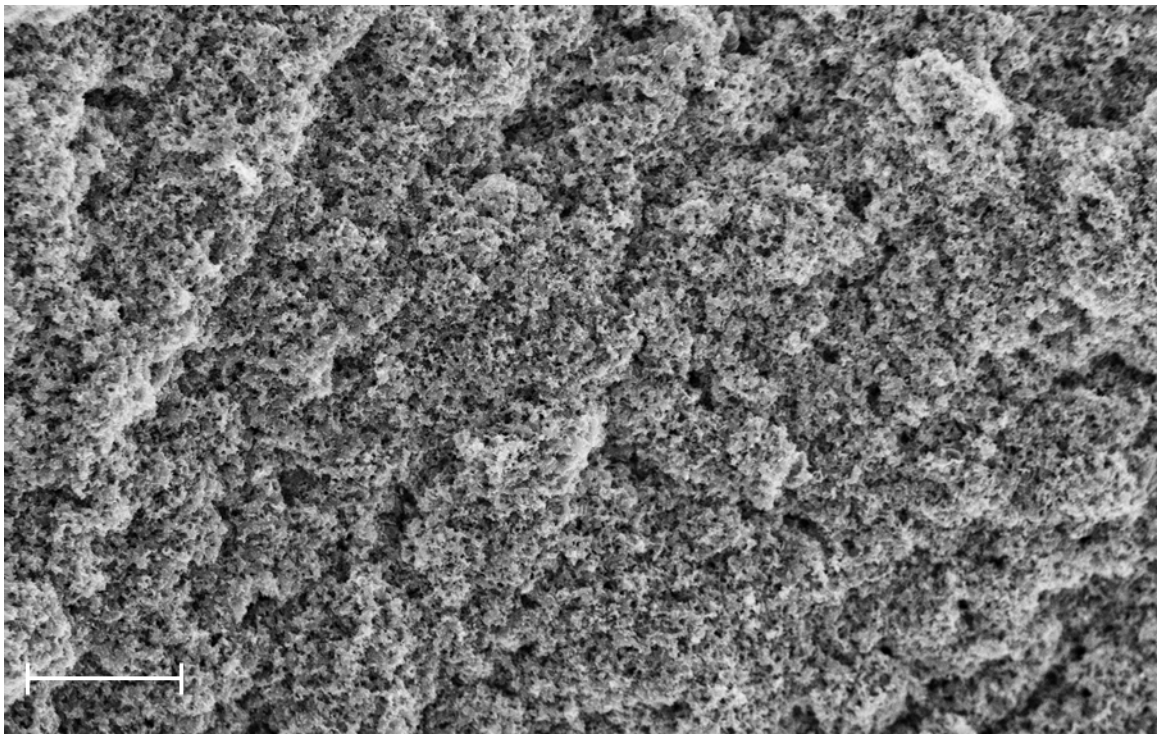

Figure 3-6. SEM image of nylon 6 fibers coated in doped polypyrrole with no rinse post-polymerization. Scale bar equal to 100 µm, magnification of 500x, EHT of 30 kV and working distance of 6.0 mm.

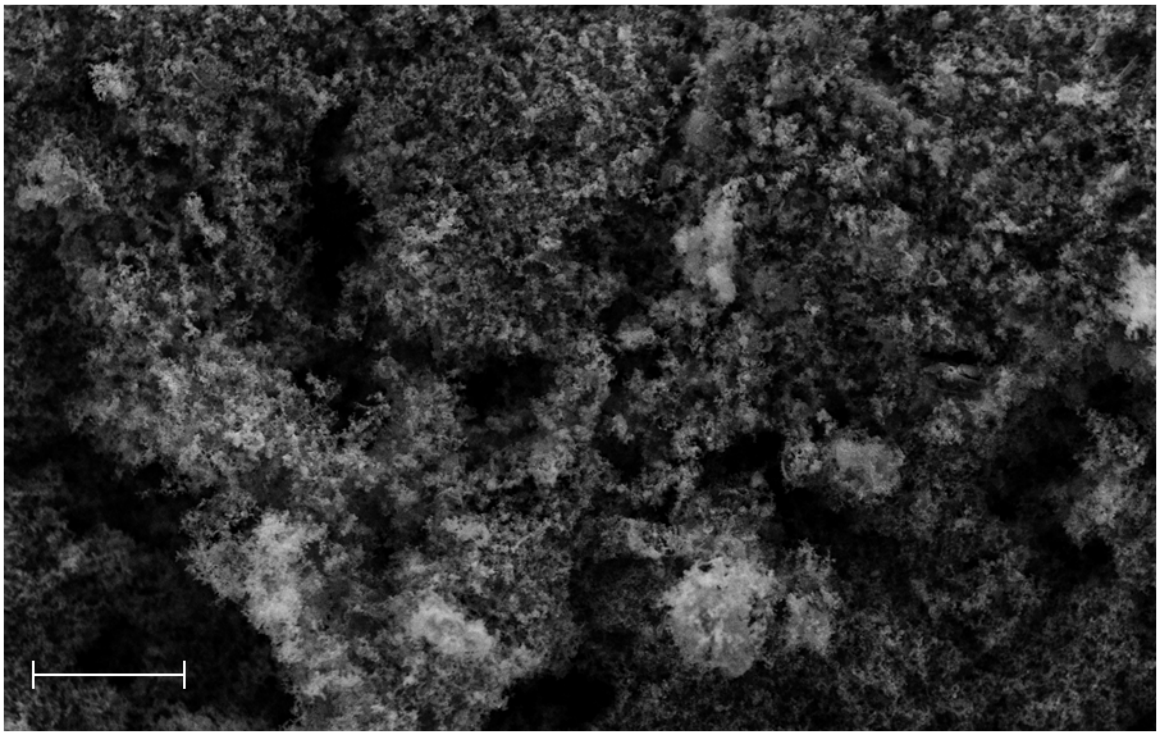

Figure 3-7. SEM image of nylon 6 fibers coated in doped polypyrrole with a DI water wash post-polymerization. Scale bar equal to 100 µm, magnification of 500x, EHT of 30 kV and working distance of 6.0 mm.

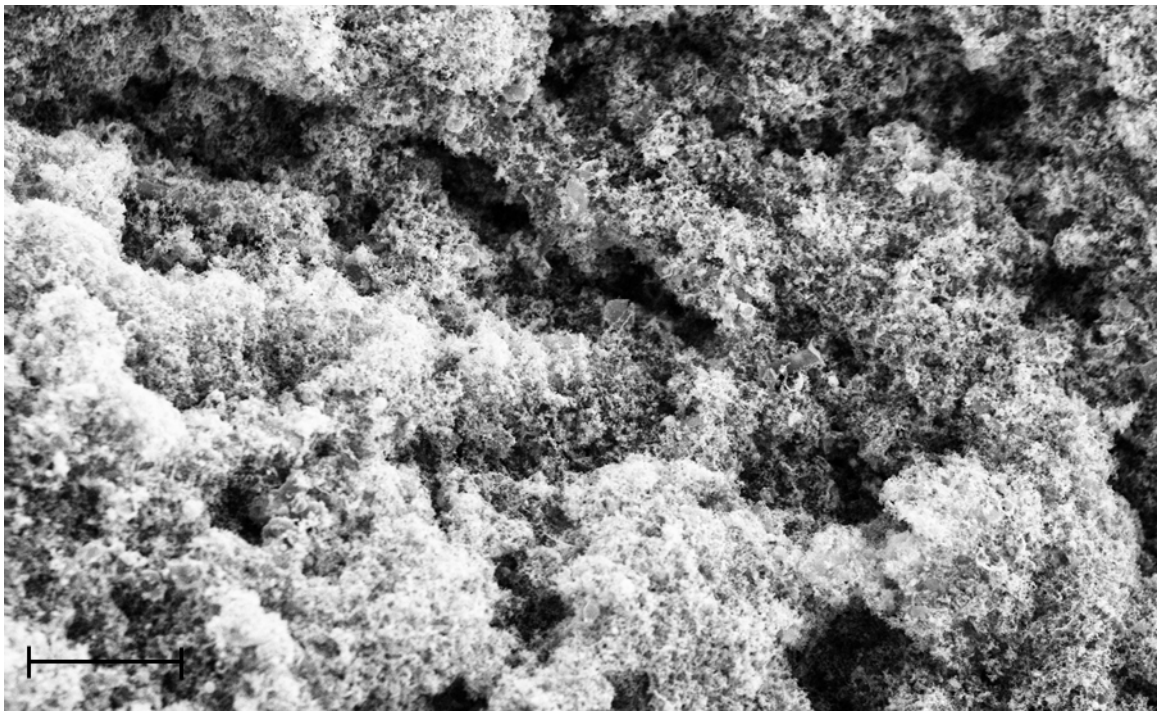

Figure 3-8. SEM image of nylon 6 fibers coated in doped polypyrrole with DI water wash and sonication post-polymerization. Scale bar equal to 100 µm, magnification of 500x, EHT of 30 kV and working distance of 6.0 mm.

The addition of a rinse step and sonication did not result in a significant loss of polymer coating from the fiber discs, however those samples did show better porosity between the individual fibers in the SEM images. The lack of a change in resistance and SEM images indicated that the polymer had bound to the nylon microfiber lattice. The larger clusters of polymer, where the polymer was attached to itself as opposed to the fiber surface, had weaker bonds, was removable and did not significantly change the resistance. Washing of the fibers post-polymerization was added to the protocol to allow for the removal of weakly bound excess, resulting in better fiber porosity and ensuring that the biorecognition elements would have access to the lower layers of the fiber mat.

3.3.4 Fiber platform selection

During drying the coated NY6 fibers contracted, resulting in the discs becoming slightly smaller in diameter than before polymerization occurred. The coated fibers also became more brittle, occasionally fracturing when bent or twisted. To address this effect, a spot melted PP disc, a more robust material, was coated with the PPy conductive polymer using the procedure described in Section 3.2.2.4 in a 30 min reaction and compared to an identically coated NY6 membrane. After being washed with DI water SEM images of the samples were taken. These results can be seen in Table 3-1 and Figures 3-9 and 3-10.

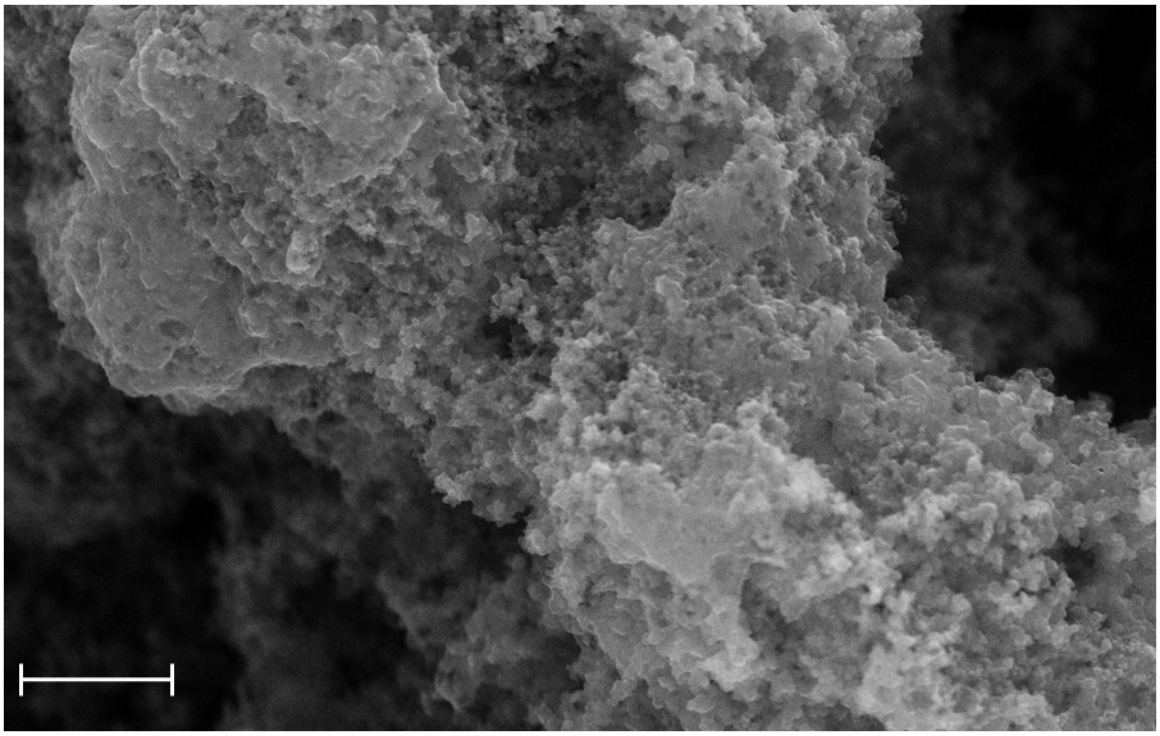

Figure 3-9. SEM image of nylon 6 fibers coated in doped polypyrrole. Scale bar at 10 µm, magnification of 5,000x, EHT of 30 kV and working distance of 6.0 mm.

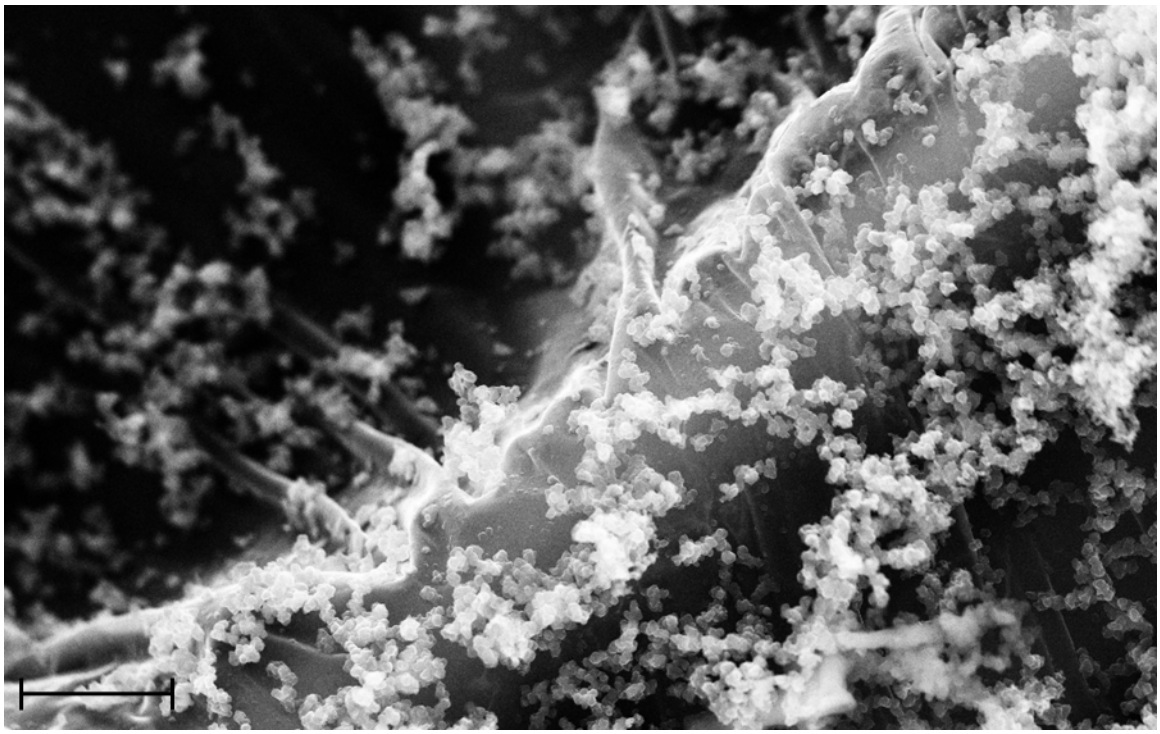

Figure 3-10. SEM image of polypropylene fibers coated in doped polypyrrole. Scale bar at 10 µm, magnification of 5,000x, EHT of 30 kV and working distance of 6.0 mm.

The PP disc in Figure 3-10 has an even black coating and a measured resistance of 55.1 Ω. The PP microfibers were conformally coated with the PPy polymer. The surface coating on the PP fibers appears smoother than the coating on the NY6 fibers. Nanoscale buds of polymer were seen scattered across the polymer surface ranging in size from 0.5 to 1 µm. At the areas where the nonwoven fibers were melted together, buds of polymer coating are seen in the range of 200 to 400 nm in diameter. It was observed that the coated PP discs also have better durability than its NY6 counterpart. The PP discs were able to be folded, rolled, and handled with less fracturing and loss of coating.

3.3.5 Effects of 3TAA concentration

Increases in resistivity, sulfur weight percent, and fluorescent output were all observed as the concentration of 3TAA increased in the samples. This increase became pronounced at a concentration of 10 mg/mL of 3TAA in the monomer solution. A summary of results can be found in Table 3-2.

Table 3-2. Characterization of polypyrrole copolymer with increasing concentrations of 3TAA.

Concentration of 3TAA (mg / mL)	Average Resistivity (Ω·cm)	Sulfur Weight (%)	Fluorescent Output Average (RFU)
0	4.55	0.93	1.0287
0.1	4.58	0.78	1.0950
1	3.43	0.55	1.3870
10	6.29	1.30	1.4770
20	8.14	1.54	1.2677
50	9.44	2.24	1.6453
100	1587.45	3.83	3.9623

3.3.5.1 SEM analysis

The increase in concentration of 3TAA in the polymerization process resulted in an increase in the buildup of the coating on the PP fibers. Little visible difference was observed between the samples ranging in concentration from 0 – 10 mg / mL. The four samples tested within this range showed a conformal polymer coating around the individual PP fibers. A comparison of two fiber samples with different concentrations of 3TAA can be seen in Figures 3-11 and 3-12.

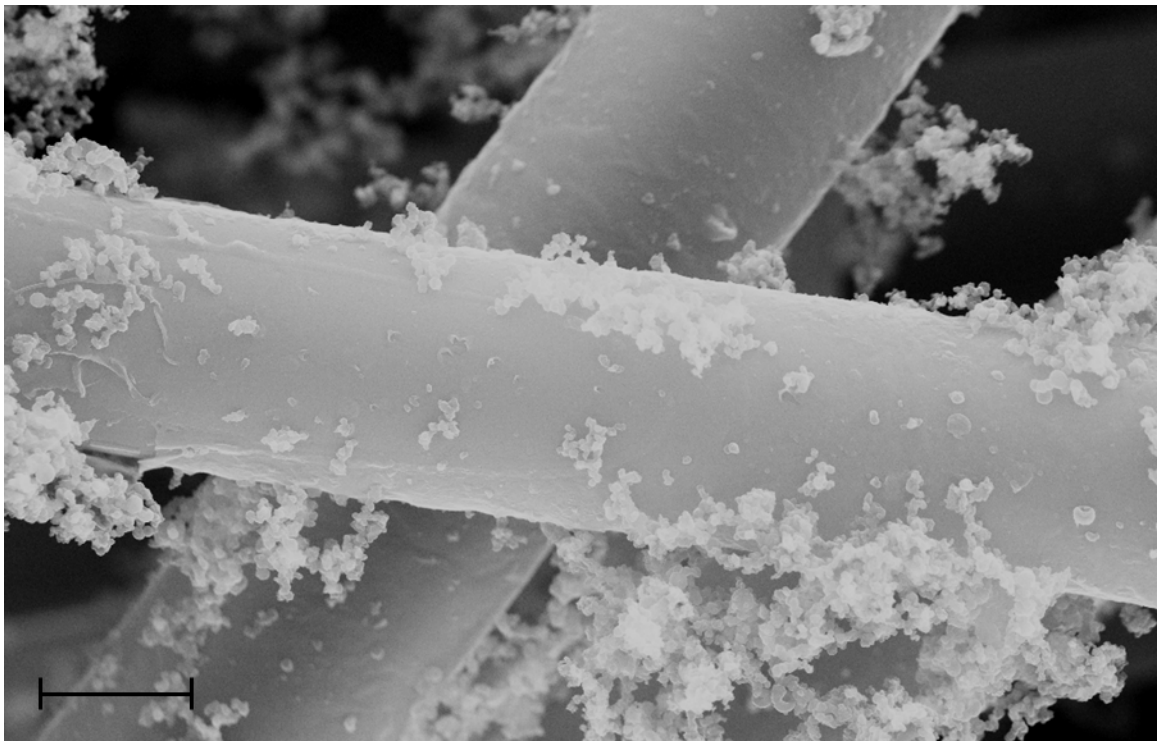

Figure 3-11. SEM image of fibers with polymer coating with a 3TAA concentration of 10 mg/mL. A smooth conformal polymer coating was observed along the individual fibers with minimal polymer clusters. Scale bar equal to 10 µm, magnification of 5,000x, EHT of 30 kV and working distance of 6.0 mm.

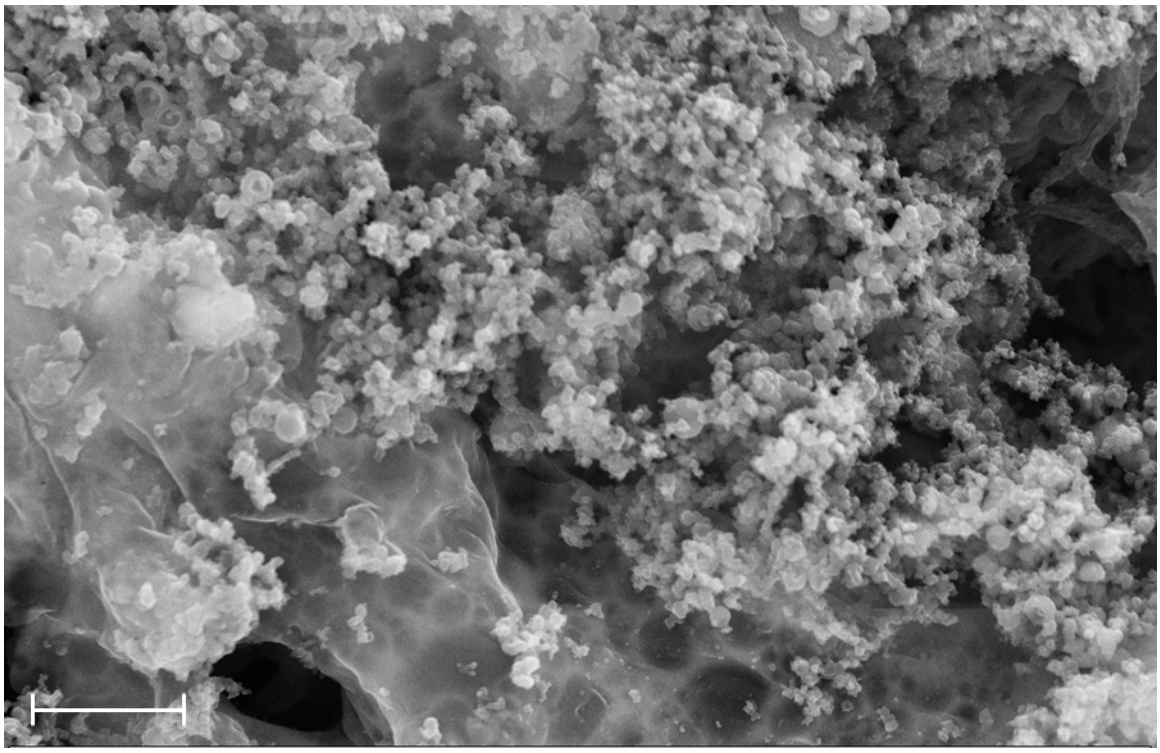

Figure 3-12. SEM image of fibers with polymer coating with a 3TAA concentration of 100 mg/mL. The coating was rough with a large amount of polymer built up along the surface, engulfing several fibers and reducing the porosity of the membrane. Scale bar equal to 10 µm, magnification of 5,000x, EHT of 30 kV and working distance of 6.0 mm.

Along the fibers small buildup of polymer could be observed. An example of this can be seen in Figure 3-11, where fibers were coated with a concentration of 10 mg/mL. Samples with higher 3TAA concentration displayed large buildups of polymer that had collected together to form aggregates measuring roughly 400 – 500 µm in diameter on the fiber surface. As seen in Figure 3-12, fibers coated at a concentration of 100 mg/mL show polymer build up along the surface, engulfing several fibers and reducing the porosity of the membrane instead of forming a smooth conformal polymer coating along the individual fibers. It was also observed that as the concentration of 3TAA was increased, the polymer coating became more brittle. Flakes of polymer fell off of the samples containing 50 and 100 mg/mL when handled.

3.3.5.2 Electrical resistivity

As can be seen in Table 3-2, the measured resistivities of the samples ranged from 3.43 to 1587.5 Ω•cm. The relationship between the concentration of 3TAA in each sample and the resistivity of the sample can be seen in Figures 3-13 and 3-14.

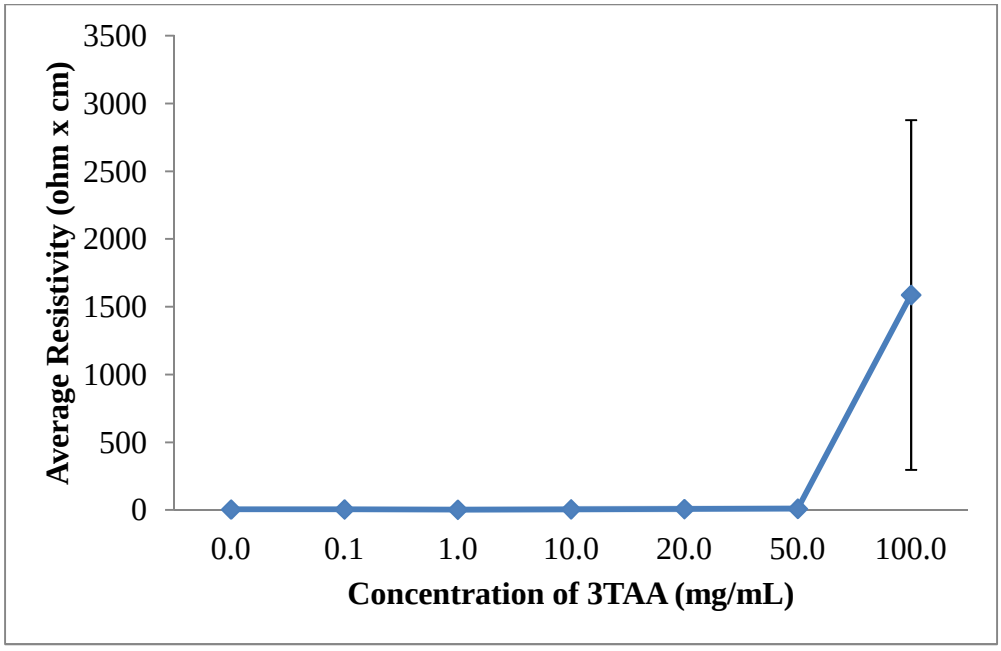

Figure 3-13. Change in sample resistivity based on increasing 3TAA concentrations, with error bars representing the standard deviation of each sample. The overall trend showed resistivity increasing as concentration of 3TAA increases, starting at 1 mg/mL.

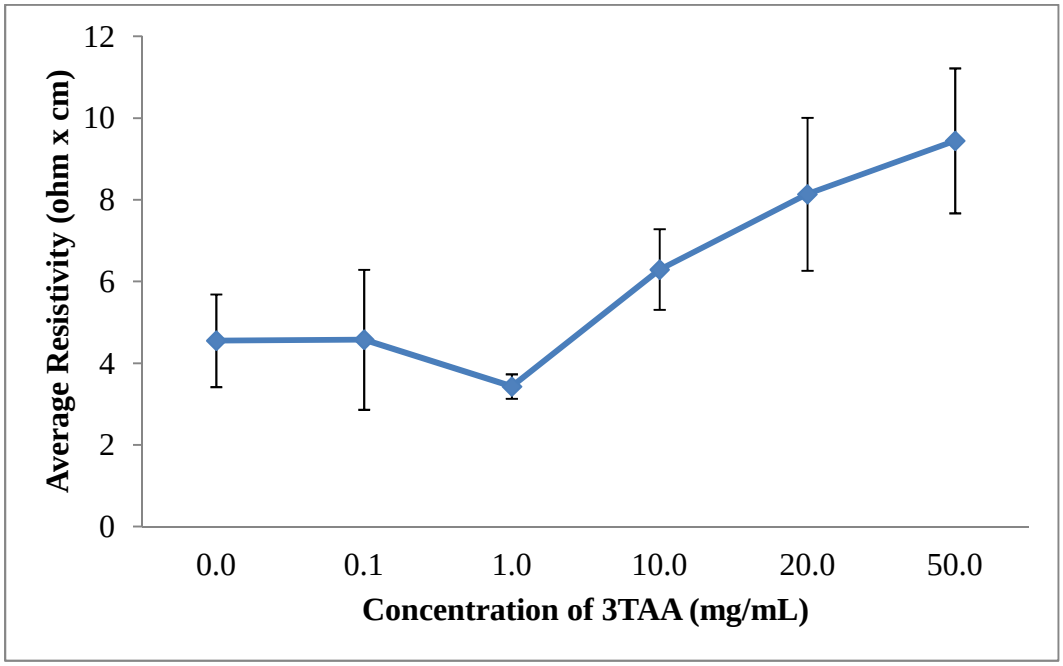

Figure 3-14. Change in sample resistivity based on increasing 3TAA concentrations excluding 100 mg/mL 3TAA, with error bars representing the standard deviation of each sample.

The samples containing 0, 0.1, 1, 10, 20, and 50 mg/mL of 3TAA all have resistivities under 10 Ω•cm, with the samples ranging from 0 to 1 mg/mL under 5 Ω•cm. A sharp increase was observed in the resistivities of the samples containing 100 mg/mL of 3-TAA, with the resistivity being over 150 x larger than the sample containing 50 mg/mL. A steady increase in resistivity was observed as the concentration increased starting at 1 mg/mL.

3.3.5.3 Elemental weight percent

Because the chemical structure of 3TAA contains a free carboxyl attached to a sulfur ring, the presence of sulfur was used as an indicator of carboxyl groups present in the coating surface for covalent binding, this relationship can be seen in Figure 3-3. Energy dispersive spectroscopy

was used to determine the elemental weight percentages for each sample. The sulfur weight percent measured in each sample can be seen in Table 3-2 ranging from 0.55% to 3.83%. The relationship between the weight percent of sulfur and the concentration of 3TAA in each sample can be seen in Figure 3-15.

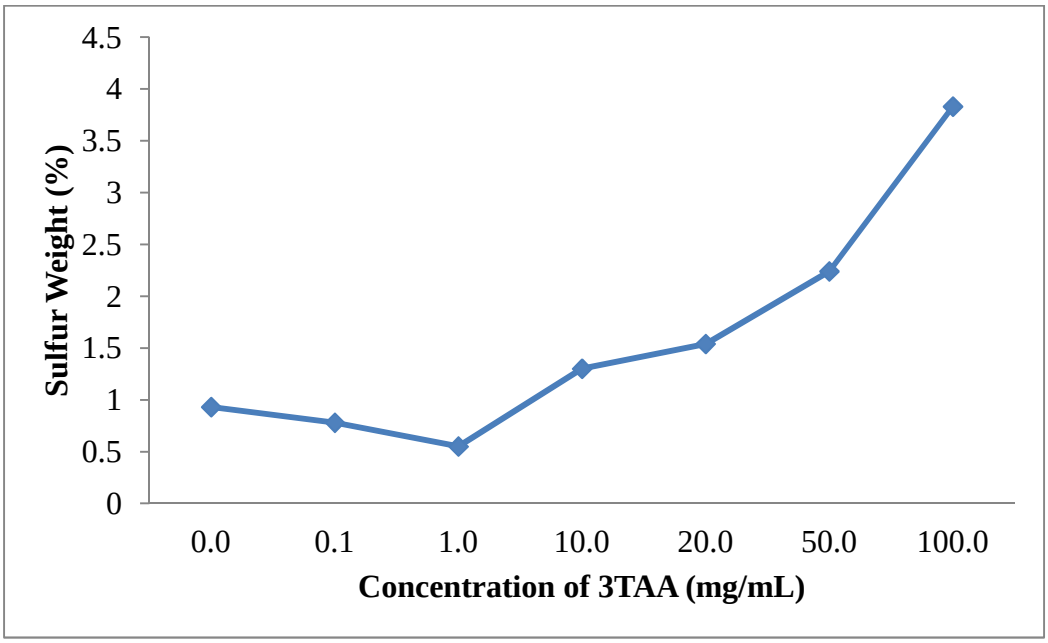

Figure 3-15. Change in sulfur weight percent at 100x magnification using EDS based on increasing 3TAA concentrations. The overall trends shows the sulfur weight percentage increasing as the concentration of 3TAA increases in the sample, starting at 1 mg/mL.

All of the samples with 3TAA concentrations of 10 mg/mL or higher had a sulfur weight percent of greater than 1%. The range between the measurements of the samples containing 10 and 20 mg/mL of 3TAA is 0.24%. A sharp increase in the weight percent of sulfur was observed between the samples containing 50 and 100 mg/mL of 3TAA with a range of 1.59%.

3.3.5.4 Fluorescence

The intensity of the FITC signal measured following the crosslinking reaction was used as an indicator of the relative amount of avidin that was successfully attached to the available binding

sites provided by the presence of carboxyl groups in the polymer coating. The average fluorescence output for each sample can be seen in Table 3-2. The relationship between the average fluorescent readout value and concentration of 3TAA in each sample can be seen in Figure 3-16.

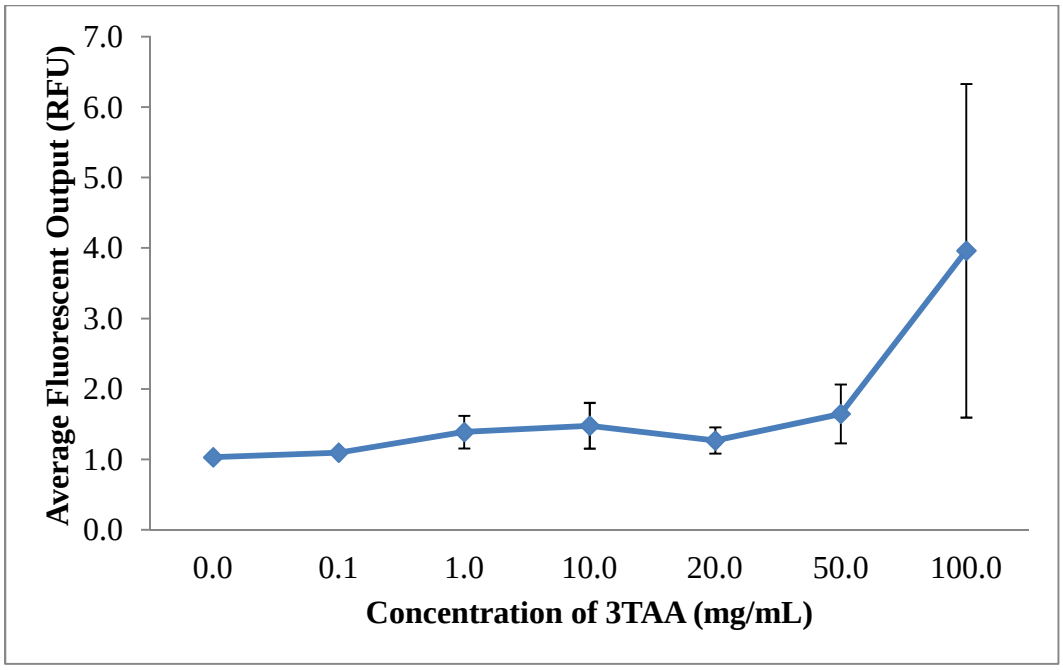

Figure 3-16. Change in average fluorescent output after FITC-avidin binding based on increasing 3TAA concentrations with error bars showing the standard deviation for each sample. The overall trend shows the average fluorescence output increasing as the concentration of 3TAA increases in the sample, starting at 0.1 mg/mL.

The average fluorescence signal measured range from 1.0287 to 3.9623 relative fluorescence units (RFUs). Only the samples containing 0 and 0.1 mg of 3TAA measure below the value of 1.1 RFUs. The samples containing 50 and 100 mg/mL both exceed 1.5 RLUs. The sharpest increase in signal comes between the samples containing 50 and 100 mg/mL with the difference being 2.317 RFUs. The increase in concentration of 3TAA in each sample coincide with an increase in fluorescent signal for every sample except between 10 and 20 mg/mL.

3.3.5.5 Selecting 3TAA concentration

In all 4 characterization methods used, a difference was observed between samples that did and did not include 3TAA. The trend was observed for each characterization that after an initial threshold was met, the measured difference increased as the concentration of 3TAA increased. The addition of 3TAA resulted in an increase in the size and buildup of the polymer coating along the individual polypropylene fibers, with the largest accumulation of polymer observed with the addition of 100 mg/mL of 3TAA. The addition of 3TAA also resulted in a higher resistivity being measured for the sample, a higher elemental weight percent of sulfur in the sample, and a higher fluorescent reading after the samples were put through the EDC / sulfo-NHS / FITC-avidin binding reaction. The additional carboxyl groups from the 3TAA reacted with the EDC / sulfo-NHS cross-linking to result in this increase in the attachment of the FITC labeled avidin. However, the increase in available functional groups for additional antibody attachment came at a cost to the material's resistivity. Increasing 3TAA changed the polymer morphology ultimately resulting in a larger, more globular, and less conductive coating.

When developing an electrochemical biosensor, it is important that a balance be found between increasing the available binding sites for reactions to take place and decreasing the membrane sample resistivity to achieve maximum sensitivity. It is also important that the membrane maintain its porosity and therefore increased surface area as well as be environmentally robust. In our research no observable difference could be found between a sample containing 0.1 mg of 3TAA and one that did not have 3TAA added. A Student's t-test (2 tail, $\alpha = 0.05$) showed no significant difference between the resistivities of the samples containing 0 and 0.1 mg/mL of 3TAA. In all samples tested, the concentration vs. signal outputs showed an observable

difference between a sample with a 3TAA concentration at 10 mg/mL and a sample without 3TAA. At a concentration of 10 mg/mL, the membrane sample had a resistivity 38.3% higher than the sample containing no 3TAA, a sulfur weight percentage 39.8% higher, and an increase in fluorescence output of 43.6%. Increases in sulfur weight percents and fluorescence outputs were also observed at concentrations of 20, 50, and 100 mg/mL, however all three showed an increase in polymer buildup on the fibers which resulted in a lower polymer durability and higher sample resistivity. For these reasons, 10 mg/mL of 3TAA was selected as the optimum tested concentration for use in our electrotextile biosensor assembly.

3.3.6 Biorecognition element attachment

3.3.6.1 Optical analysis

Generating a conductive polymer coating onto the fiber membranes has two purposes. The first is to make the fibers capable of conducting an electrical signal through the fibrous platform and the second is to provide attachment sites for biorecognition elements on these fibrous surfaces. Confocal microscopy was used to determine if FITC labeled avidin was covalently bound to the polymer coating. Qdot labeled biotin was then used to indicate if the surface bound avidin had maintained its capture ability. Figures 3-17 and 3-18 confirm the presence of functional groups for bio-recognition attachment in the polymer. Figure 3-17 shows a coated fiber that has FITC-labeled avidin attached to it.

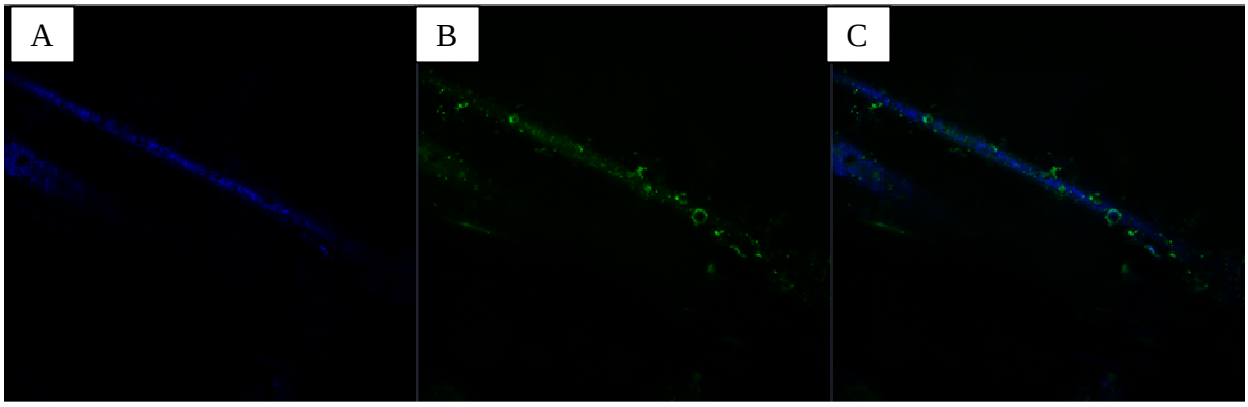

Figure 3-17. False colored confocal images of single fibers with FITC-avidin attachment. A: Fiber reflectance. B: Bound FITC-avidin. C: Composite image. All at 4,000× with lasers at 405 and 488 nm.

The fiber can be seen reflecting the blue wavelength, while the FITC-avidin fluoresces green. The composite image, Figure 3-17(C), shows the attachment of the avidin on the fiber surface, with a buildup of avidin found on the polymer buds that run along the fiber. This indicates that a biorecognition element, avidin, can be successfully bound to the polymer coating using covalent attachment chemistry, however it does not prove that the avidin is still available to react with a sample and perform capture.

Figure 3-18 shows the same fiber sample, after the addition of Qdot labeled biotin.

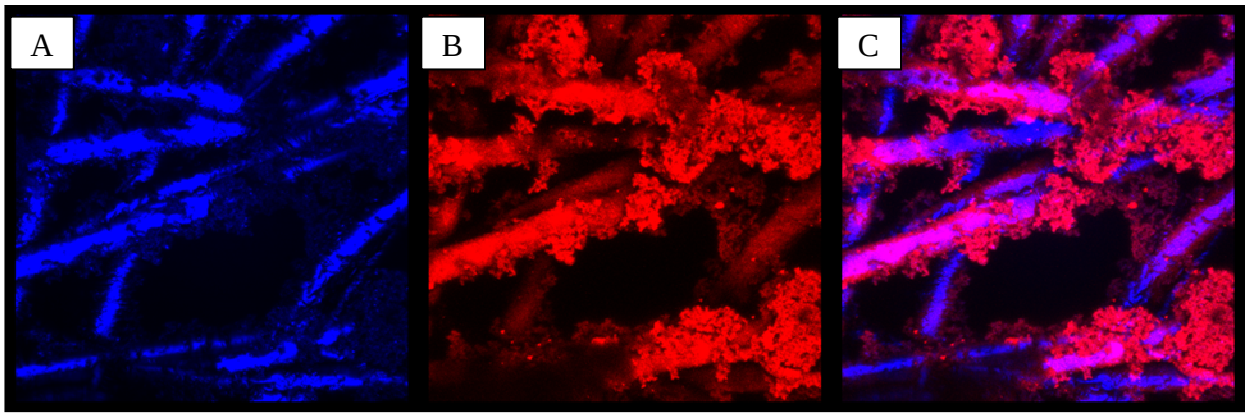

Figure 3-18. False colored confocal images of fibers with biotinylated quantum dot attachment. A: Fiber reflectance. B: Bound biotinylated quantum dots. C: Composite image. All at 4,000× with lasers at 405 nm.

The fibers can be seen reflecting the blue wavelength, while the biotinylated Qdots emit red. The composite image, Figure 3-18(C), shows the attachment of the Qdots on the fiber surface, with heavier concentrations of Qdots found where there are heavier concentrations of polymer. Based on the information gained from Figure 3-17, it can be assumed that the avidin has bound to the polymer coating and then conjugated with the biotin. This indicates that a biorecognition element, avidin, can be successfully bound to the polymer coating using covalent attachment chemistry and can be used to perform capture.

3.3.6.2 Electrochemical analysis

Preliminary experiments were conducted taking multiple measurements using the fiber membranes as electrodes to determine if a biological recognition signal can be observed. Triplicate measurements were taken using the conductive fiber membrane electrodes to establish the resistance values for a control sample (0.1 M PB) and biotin solutions at concentrations of 0.5, 5, 50, and 500 µM. A time of 3 minutes was determined to be necessary to reach system

equilibrium. The responses for each concentration at each time point were averaged and the value after the initial 3 minute equilibrium time can be seen in Figure 3-19.

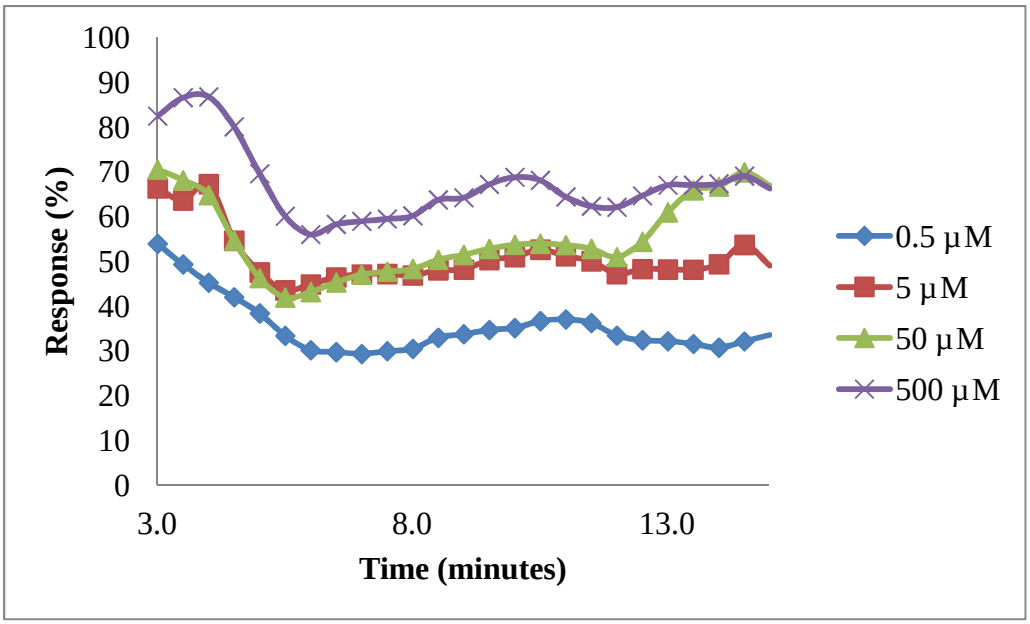

Figure 3-19. Average response over a period of 12 minutes (after a 3 minute equilibrium time) for the electrochemical detection with varying biotin solution concentrations.

The response of the system at each sample concentration was plotted over the 12 minute period following a 3 minute equilibrium time, showing that the system response increases as the concentration of biotin increase. There was a slight drop in signal between 3 and 5 minutes for each sample indicating that the electrode was still reaching equilibrium up to roughly the 5 minute point. The average percent response at a concentration of 0.5 µM was 35.4%. For the biotin concentrations of 5, 50, and 500 µM the average responses were 55.3%, 50.8%, and 67.2%, respectively. Figure 3-19 shows that the average responses at concentrations of 5 µM, 50 µM, and 500 µM were all significantly larger than the average response at 0.5 µM. Also, the average responses at these three concentrations are very close, with the average response at 5 and 50 µM crossing multiple time points. This is most likely due to the fibers reaching a threshold

for attachment on the surface, so that the increase of biotin in the sample is no longer generating a proportional increase on the system resistance. The surface attachment capabilities could be improved by increasing the size and therefore surface area of the fiber mats, attaching a higher concentration of avidin to the fibers, and increasing the amount of carboxyl group attachment sites on the fibers.

The resistance of the sensor at each biotin solution concentration was tested against the values of the control using a Student's t-test (2 tails, $\alpha = 0.05$) to determine significance. The resistance at each concentration of biotin tested was determined to be significantly different from the blank control. This shows that the electrotextile electrode is capable of detecting changes in conductivity due to the addition of biotin to the system. It also has the potential to eventually be used as a simple sample capture and read system for pathogen detection.

3.4 Conclusions

The initial results from this study show a nonwoven fiber matrix can be successfully coated in a conductive, functionalized polymer while still maintaining surface area and fiber durability. A polypropylene fiber platform with a conductive polypyrrole coating using $FeCl_3$ as an oxidant, water as a solvent, and 5SSA as a dopant exhibited the best coating consistency, material durability, and lowest resistance. The addition of 3TAA to the polymerization process resulted in a change of coating morphology, resistivity, elemental sulfur presence, and available binding sites for biorecognition elements. The polymer coated membrane sample containing 10 mg/mL of 3TAA was selected as the best for future biosensor development. Furthermore, biological attachment using avidin-biotin can be achieved on the fibers through the inclusion of a carboxyl

functional group via 3TAA in the monomer. When put into a simple electrochemical system, the membranes could be used to successfully detect biotin in solution at concentrations of 0.5, 5, 50, and 500 µM. This technology will be extremely useful in the formation of electrotextiles for use in biosensor systems.

A mathematical model of this polymerization process was developed and optimized in Chapter 4. This technology was further used for antibody attachment and *E. coli* O157:H7 detection as part of an electrochemical biosensor in Chapters 5 and 6, respectively.

Chapter 4 : An optimization model for the development of a conductive polymer coated nonwoven electrotextile for use in biosensors

4.1 Introduction

A biosensor is an analytical device used to convert the occurrence of biological recognition events into measurable electrical responses [54]. It consists of a biological sensing element that has been integrated with electronic transducers [142, 159]. Biosensor transducers can be electrochemical, optical, thermal, or mass related. Electrochemical biosensors are designed to combine the analytical power of electrochemical techniques with the specificity and binding efficiency of biological recognition processes [75]. In an electrochemical biosensor the biological recognition element is immobilized at an electrode which then converts the biological recognition event (e.g. antibody – antigen binding) into a measurable electrical signal. This output signal will be directly related to the concentration of bound antigen to the sensor.

One new field of research in the development of electrochemical biosensors is the creation of electrotextiles to be used as electrode transducers. "Electrotextiles refer to fabrics that can electrically function as electronics and physically behave as textiles" [160]. High-surface area electrospun membranes are versatile and can be developed into electrotextile "smart membranes" designed for use with all forms of sensor signal transduction, however very little research has been done into the integration of electrotextile, biological, and electrical technology to create novel biosensor systems for food defense. Previous work has been done to develop electrically active non-metallic textile coatings that are conductive using doped polypyrrole (PPy) polymer [14, 121, 122, 144]. By producing a conformal conductive polymer coating on non-woven

microfibers an electrochemical biosensor electrode can be created that is less expensive and has more surface area for attachment than its planar metal counterparts [12]. In addition these electrotextile electrodes are durable, disposable, and have the potential for minimal required attachment chemistry. With the attachment of biological recognition elements to the electrotextile electrode surface the electrodes would have the capacity to perform pathogen capture, concentration, and detection. This would simplify a food pathogen detection biosensor, allowing the overall system to be produced significantly smaller and lighter than many current systems.

Previous work has been conducted and published on the creation of an electrotextile made by performing aqueous deposition of a conductive PPy and 3-thiopheneacetic acid (3TAA) copolymer onto nonwoven polypropylene (PP) microfibers [18-20]. This combination of co-polymer provides sites where bio-recognition elements (antibodies) can covalently attach to the fiber based platform. These functionalized conductive membranes serve as the sites of pathogen collection and detection within the system. Captured pathogens impede the flow of electrons across the electrode resulting in an increased resistance in the circuit. The measured resistance across the electrotextile electrode increases as the concentration of target pathogen within the sample increases [20].

There are many factors that influence the formation of this electrotextile. Several of these factors have been previously identified and analyzed [18]. Of these, five have been identified as particularly significant to the formation and resistance of the polymer coating: the concentration of each co-monomer, the concentration of the oxidant, the concentration of the dopant, and

polymerization time. It is important in the development of an electrotextile electrode for biosensing that the electrotextile have the lowest resistance possible in order to not mask small observable changes that may be obscured with system noise. By decreasing the resistance and variability of the electrotextile, the sensitivity of the biosensor will increase.

Despite the fact that previous work has identified the importance of five factors in the formation of conductive textiles [14, 18, 121, 122], a comprehensive study is needed to investigate the effects of these factors and their interactions in polymer formation. Multiple regression analysis, a tool often used for estimating probabilities and relationships between variables in fields as diverse as economics to microbiology to psychology [161-164], can be used to generate a mathematical model of the electrotextile resistance dependent on the factors of monomer, oxidant, and dopant concentrations as well as polymerization time.

The objectives of this study included: first, investigating the effects of each monomer concentration, oxidant concentration, dopant concentration, and reaction time on the synthesized electrotextile's resistance; second, developing a multiple regression model based on these effects; third, determining the optimal conditions of these factors in order to generate the lowest experimentally possible electrotextile resistance; and finally, experimentally validating the optimized model conditions.

4.2 Materials and methods

4.2.1 Materials

Nonwoven polypropylene microfibers were obtained from North Carolina State Nonwovens Cooperative Research Institute. For polymer synthesis, the monomer used was a pyrrole solution that was copolymerized with carboxylic acid functional 3TAA. The oxidant was iron (III) chloride ($FeCl_3$). The polymer was doped using 5-sulfosalicylic acid (5SSA). All of the polymerization chemicals were obtained from Sigma-Aldrich (St. Louis, MO).

4.2.2 Experimental design

4.2.2.1 Electrotextile synthesis

Electrotextile synthesis was conducted according to previously published techniques [18-20]. Briefly, an aqueous deposition process was used to create a conductive and functional polymer coating upon a PP fiber matrix, as described below. A 6 cm x 8 cm polypropylene microfiber mat was submerged in a pyrrole and 3TAA solution (pyrrole and 3TAA concentrations were varied based on different experiments mentioned in the ensuing sections), creating a functionalized monomer that was absorbed onto the fiber mat. The wet fiber sample was then removed from the solution and laid flat in a glass reaction vessel for polymerization. A volume of 30 mL of $FeCl_3$ was added to the sample to initiate the chemical reaction while a dopant, 3 mL of 5SSA, was simultaneously added (the concentrations of $FeCl_3$ and 5SSA were varied based on experiments described in ensuing sections). The fibers in solution were incubated at room temperature (the reaction times were varied based on experiments mentioned in ensuing

sections) with constant agitation, thereby ensuring that polymerization occurred on both sides of the mat. The nonwoven fiber sample was removed from the solution, gently washed on both sides with deionized (DI) water, and dried at room temperature overnight.

4.2.2.2 Optimization of electrotextile

Optimization experiments were fulfilled by a response surface method, where the response surface plot is a 3D representation of the relationship between the factors and the response. The optimum response will fall somewhere in the experimental region along the generated curved surface at a maxima or minima [165]. In order to generate this curve based on the effects of the concentrations of pyrrole, 3TAA, $FeCl_3$, and 5SSA as well as reaction time on the final resistance of the electrotextile, a central composite design with five coded levels was used. This was used to develop a mathematical model which was able to predict the electrotextile resistance as a function of component concentrations and time. The design matrix with both codes and real values of factors is presented in Table 4-1 [165].

Table 4-1. Central composite design, from Haaland. Code values are in the parentheses, actual values are outside of the parentheses.

Run	Factors				
	Pyrrole Concentration (% volume)	3TAA Concentration (g/mL)	$FeCl_3$ Concentration (M)	5SSA Concentration (M)	Reaction Time (min)
1	32.5 (-1)	0.0125 (-1)	0.075 (-1)	0.15 (-1)	97.5 (+1)
2	32.5 (-1)	0.0125 (-1)	0.075 (-1)	0.35 (+1)	52.5 (-1)
3	32.5 (-1)	0.0125 (-1)	0.125 (+1)	0.15 (-1)	52.5 (-1)
4	32.5 (-1)	0.0125 (-1)	0.125 (+1)	0.35 (+1)	97.5 (+1)
5	32.5 (-1)	0.0375 (+1)	0.075 (-1)	0.15 (-1)	52.5 (-1)
6	32.5 (-1)	0.0375 (+1)	0.075 (-1)	0.35 (+1)	97.5 (+1)
7	32.5 (-1)	0.0375 (+1)	0.125 (+1)	0.15 (-1)	97.5 (+1)
8	32.5 (-1)	0.0375 (+1)	0.125 (+1)	0.35 (+1)	52.5 (-1)
9	77.5 (+1)	0.0125 (-1)	0.075 (-1)	0.15 (-1)	52.5 (-1)
10	77.5 (+1)	0.0125 (-1)	0.075 (-1)	0.35 (+1)	97.5 (+1)
11	77.5 (+1)	0.0125 (-1)	0.125 (+1)	0.15 (-1)	97.5 (+1)
12	77.5 (+1)	0.0125 (-1)	0.125 (+1)	0.35 (+1)	52.5 (-1)
13	77.5 (+1)	0.0375 (+1)	0.075 (-1)	0.15 (-1)	97.5 (+1)
14	77.5 (+1)	0.0375 (+1)	0.075 (-1)	0.35 (+1)	52.5 (-1)
15	77.5 (+1)	0.0375 (+1)	0.125 (+1)	0.15 (-1)	52.5 (-1)
16	77.5 (+1)	0.0375 (+1)	0.125 (+1)	0.35 (+1)	97.5 (+1)
17	10 (-2)	0.025 (0)	0.1 (0)	0.25 (0)	75 (0)
18	100 (+2)	0.025 (0)	0.1 (0)	0.25 (0)	75 (0)
19	55 (0)	0 (-2)	0.1 (0)	0.25 (0)	75 (0)
20	55 (0)	0.05 (+2)	0.1 (0)	0.25 (0)	75 (0)
21	55 (0)	0.025 (0)	0.05 (-2)	0.25 (0)	75 (0)
22	55 (0)	0.025 (0)	0.15 (+2)	0.25 (0)	75 (0)
23	55 (0)	0.025 (0)	0.1 (0)	0.05 (-2)	75 (0)
24	55 (0)	0.025 (0)	0.1 (0)	0.45 (+2)	75 (0)
25	55 (0)	0.025 (0)	0.1 (0)	0.25 (0)	30 (-2)
26	55 (0)	0.025 (0)	0.1 (0)	0.25 (0)	120 (+2)
27	55 (0)	0.025 (0)	0.1 (0)	0.25 (0)	75 (0)
28	55 (0)	0.025 (0)	0.1 (0)	0.25 (0)	75 (0)
29	55 (0)	0.025 (0)	0.1 (0)	0.25 (0)	75 (0)
30	55 (0)	0.025 (0)	0.1 (0)	0.25 (0)	75 (0)

The experiments were run based on the conditions described in the design matrix. The response was the resistance of a 1.2 cm diameter sample of the electrotextile. Each run was conducted in

triplicate with 3 sample measurements taken per experiment, resulting in 9 response values per run. These values were averaged together to provide each run response and 270 data points for regression analysis. Optimal conditions for the creation of an electrotextile with the lowest resistance were obtained from the model. A verification run was then conducted using the optimal conditions to assess the level of accuracy of the predicted result.

4.2.3 Statistical analysis

The conductivity of the electrotextile from the central composite design was analyzed by multiple regression analysis using Minitab 15 (Minitab, Inc., State College, PA). A second-order polynomial equation was applied to correlate the factors, Equation 4-1.

$$Y = a_0 + a_1X_1 + a_2X_2 + a_3X_3 + a_4X_4 + a_5X_5 + a_{11}X_1^2 + a_{22}X_2^2 + a_{33}X_3^2 + a_{44}X_4^2 + a_{55}X_5^2 + a_{12}X_1X_2 + a_{13}X_1X_3 + a_{14}X_1X_4 + a_{15}X_1X_5 + a_{23}X_2X_3 + a_{24}X_2X_4 + a_{25}X_2X_5 + a_{34}X_3X_4 + a_{35}X_3X_5 + a_{45}X_4X_5 \quad (4\text{-}1)$$

Where Y represents the electrotextile resistance in ohms and a_0 is the intercept coefficient. The values a_1, a_2, a_3, a_4, and a_5 represent the coefficients of the linear terms. The values a_{11}, a_{22}, a_{33}, a_{44}, a_{55}, a_{12}, a_{13}, a_{14}, a_{15}, a_{23}, a_{24}, a_{25}, a_{34}, a_{35}, and a_{45} represent the coefficients of the quadratic terms. The values X_1, X_2, X_3, X_4, and X_5 represent the variables of pyrrole concentration, 3TAA concentration, $FeCl_3$ concentration, 5SSA concentration, and reaction time.

Variables that were found to be highly correlated with other X variables were removed from the equation. An ANOVA table and R-square of the model were obtained from analyses, which were used to evaluate the model. Finally, the optimal conditions for synthesizing a low resistance electrotextile were concluded from the model equation using MATLAB 7.12 (Mathworks, Inc., Natick, MA).

4.2.4 Analytical methods

Resistance measurements were taken across the fiber membranes using a four point probe and Keithley 2400 Sourcemeter (Keithley Instruments, Cleveland, OH). A visual assessment was conducted using scanning electron microscopy. The samples were gold sputter coated and imaged with a Zeiss EVO 60 scanning electron microscope. (Carl Zeiss Microscopy, LLC, Thornwood, NY).

4.3 Results and discussion

4.3.1. Mathematical model

Experimental data of electrotextile resistance is presented in Table 4-2. Supplementary data and calculations can be found in Appendix B.2.

Table 4-2. Experimental results from central composite design.

Run	Average Resistance (Ω)	Run	Average Resistance (Ω)
1	73.80	16	33.88
2	72.03	17	76.63
3	45.51	18	51.78
4	38.89	19	55.24
5	102.17	20	68.92
6	110.51	21	95.31
7	71.49	22	40.24
8	66.88	23	75.34
9	226.93	24	56.09
10	77.00	25	62.38
11	55.20	26	46.84
12	44.17	27	51.54
13	45.38	28	45.61
14	52.61	29	41.89
15	42.27	30	44.01

Runs were conducted in triplicate testing with 3 samples measured per testing, resulting in 9 measurements per run. These 9 measured resistance values were averaged together to obtain the average resistance. Multiple regression analysis was performed to fit the response function with the data. The resulting coefficients, standard errors, T-values, and P-values can be seen in Table 4-3.

Table 4-3. Results of regression analysis.

Predictor	Coefficient	Standard Error	T-value	P-value
Constant	549.27	65.14	8.43	<0.001
X_1	-0.251	1.225	-0.21	0.838
X_2	-4162	1114	-3.73	<0.001
X_3	-3090.4	467	-6.62	<0.001
X_4	-749.7	135.4	-5.54	<0.001
X_5	-3.0857	0.5619	-5.49	<0.001
X_1^2	0.052653	0.009688	5.43	<0.001
X_1X_2	-77.773	7.799	-9.97	<0.001
X_1X_3	-10.074	3.899	-2.58	0.011
X_1X_4	-4.3741	0.9748	-4.49	<0.001
X_1X_5	-0.020077	0.004333	-4.63	<0.001
X_2X_3	33969	7019	4.84	<0.001
X_2X_4	8597	1755	4.90	<0.001
X_2X_5	31.353	7.799	4.02	<0.001
X_3X_4	2636.7	877.4	3.01	0.003
X_3X_5	16.41	3.899	4.21	<0.001
X_4X_5	5.4333	0.9748	5.57	<0.001

The predictor values correspond to the variables in Equation 4-1. A P-value of 0.05 or less was considered to be significant. X_1 was kept in the equation despite having a P-value larger than 0.05 because of the significance of X_1^2. The variables of X_2^2, X_3^2, X_4^2, and X_5^2 were found to be highly correlated with other X variables and were removed from the equation. The resulting

equation, Equation 4-2, represents the electrotextile's resistance as a function of pyrrole concentration, 3TAA concentration, $FeCl_3$ concentration, 5SSA concentration, and time.

$$Y_{resistance} = 549.27 - 0.251X_1 - 4162X_2 - 3090.4X_3 - 749.7X_4 - 3.0857X_5 + 0.052653X_1^2 - 77.773X_1X_2 - 10.074X_1X_3 - 4.3741X_1X_4 - 0.020077X_1X_5 + 33969X_2X_3 + 8597X_2X_4 + 31.353X_2X_5 + 2636.7X_3X_4 + 16.41X_3X_5 + 5.4333X_4X_5 \quad (4\text{-}2)$$

Where Y represents the resistance of the electrotextile, X_1 is the concentration of pyrrole, X_2 is the concentration of 3TAA, X_3 is the concentration of $FeCl_3$, X_4 is the concentration of 5SSA, and X_5 is the reaction time.

An ANOVA table was used to evaluate the statistical significance of the model (Table 4-4).

Table 4-4. Analysis of variance (ANOVA) for the regression model from 5-factor central composite design.

	Sum of squares	Degree of freedom	Mean square	F-value	P-value
Regression	315000	16	19688	28.42	<0.001
Residual Error	112922	163	693		
Total	427922	179			
R-square	0.736				

The R-square of the model was 73.6%, which indicated that the observations fell reasonably well on the fitted regression surface.

The response surfaces are shown in Figures 4-1 – 4-10 to demonstrate the effects of the factors on the electrotextile resistance during synthesis.

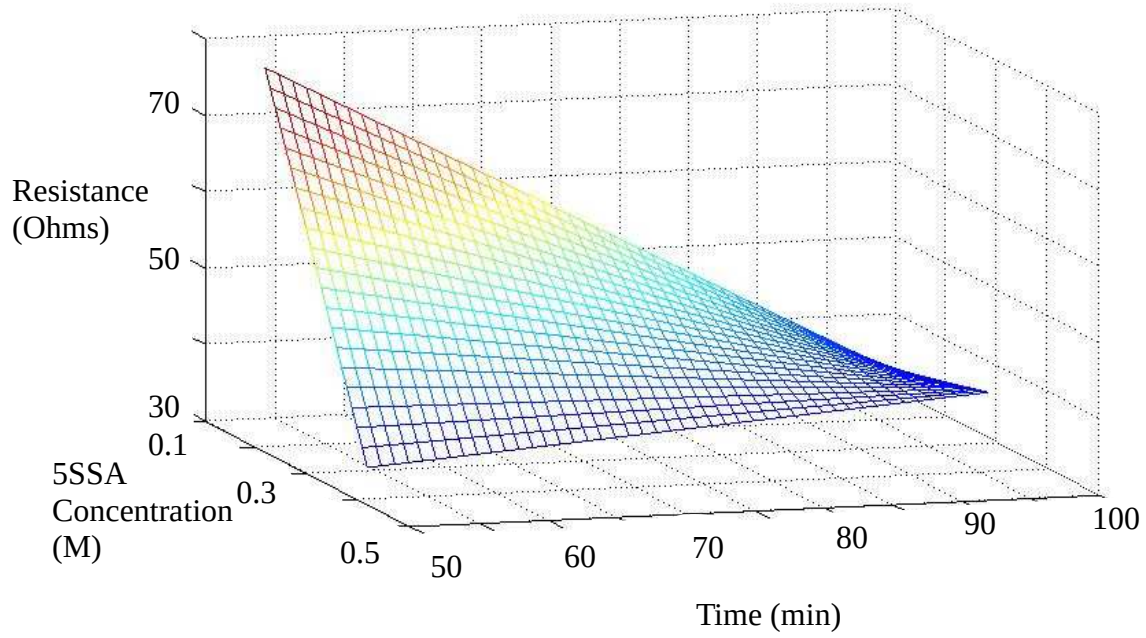

Figure 4-1. The effects of reaction conditions on electrotextile resistance at 55% pyrrole, 0.025 g/mL 3TAA, and 0.1 M $FeCl_3$.

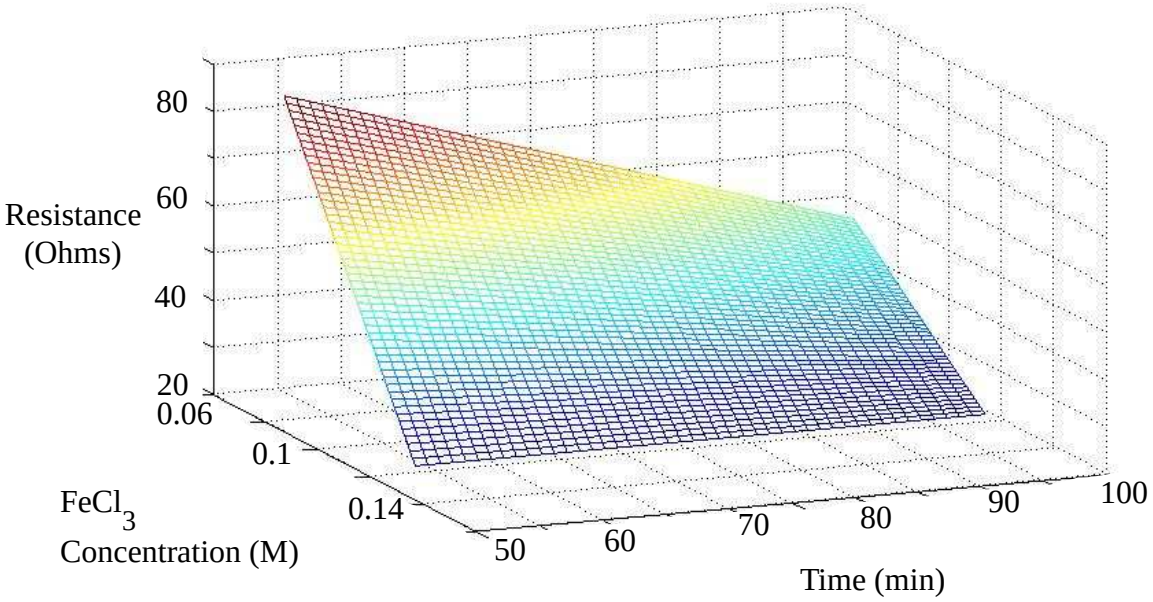

Figure 4-2. The effect of reaction conditions on electrotextile resistance at 55 % pyrrole, 0.025 g/mL 3TAA, and 0.25 M 5SSA.

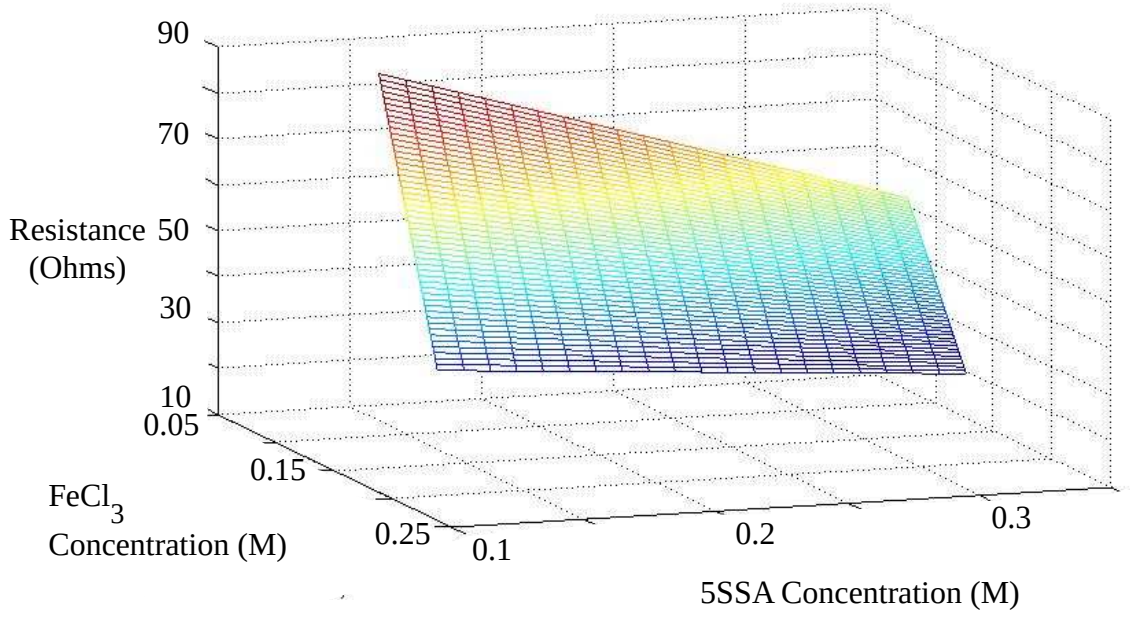

Figure 4-3. The effect of reaction conditions on electrotextile resistance at 55 % pyrrole, 0.025 g/mL 3TAA, and 75 minutes.

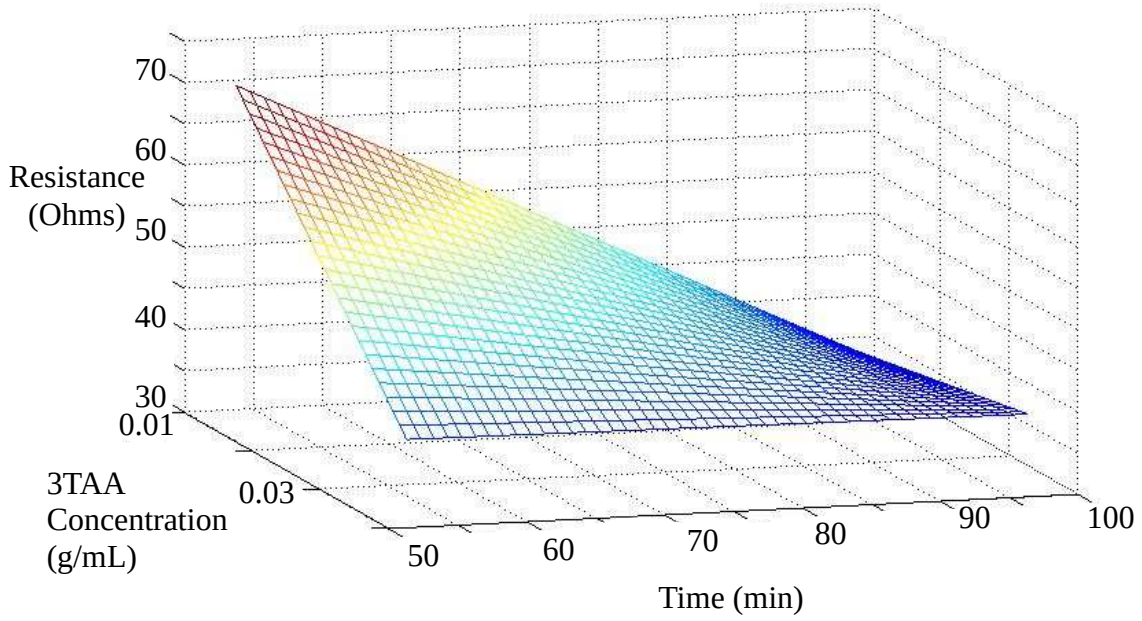

Figure 4-4. The effect of reaction conditions on electrotextile resistance at 55 % pyrrole, 0.1 M $FeCl_3$, and 0.25 M 5SSA.

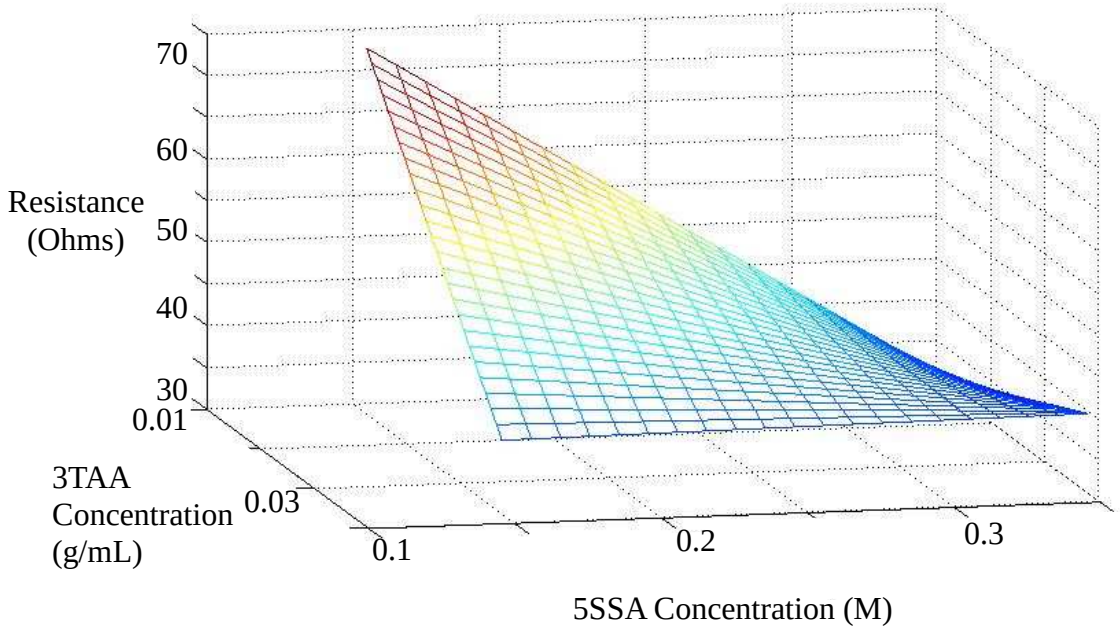

Figure 4-5. The effect of reaction conditions on electrotextile resistance at 55 % pyrrole, 0.1 M $FeCl_3$, and 75 minutes.

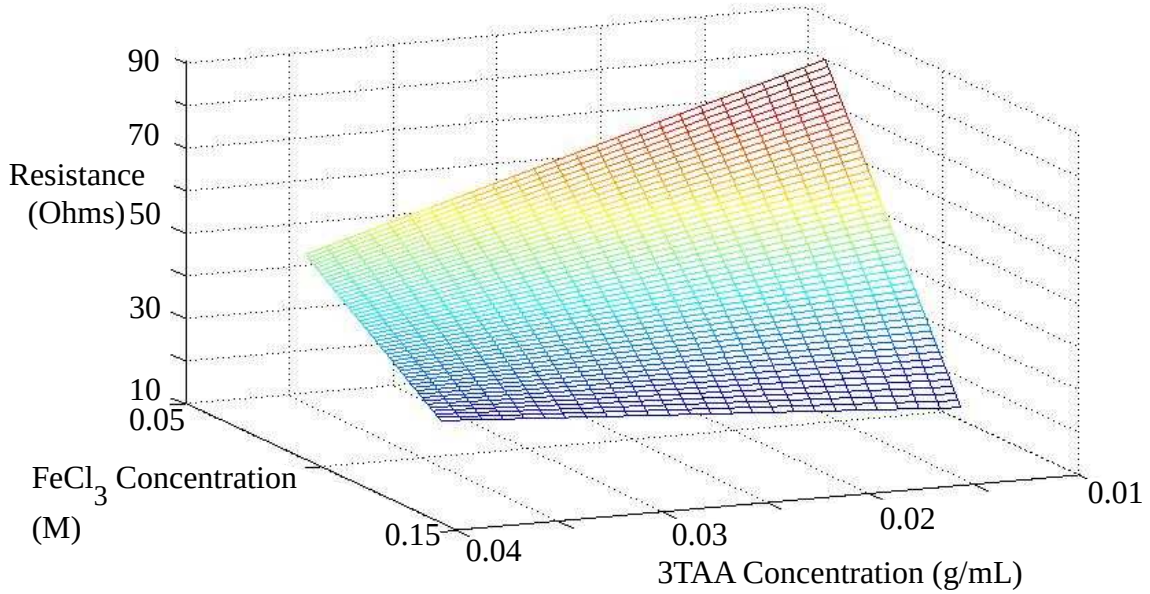

Figure 4-6. The effect of reaction conditions on electrotextile resistance at 55 % pyrrole, 0.25 M 5SSA, and 75 minutes.

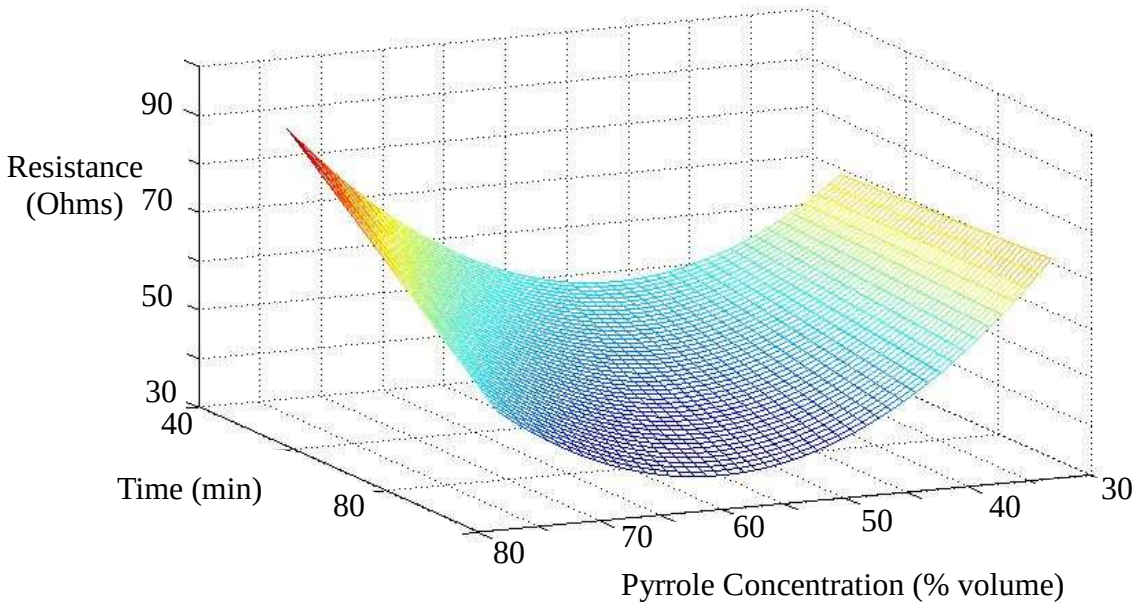

Figure 4-7. The effect of reaction conditions on electrotextile resistance at 0.025 g/mL 3TAA, 0.1 M $FeCl_3$, and 0.25 M 5SSA.

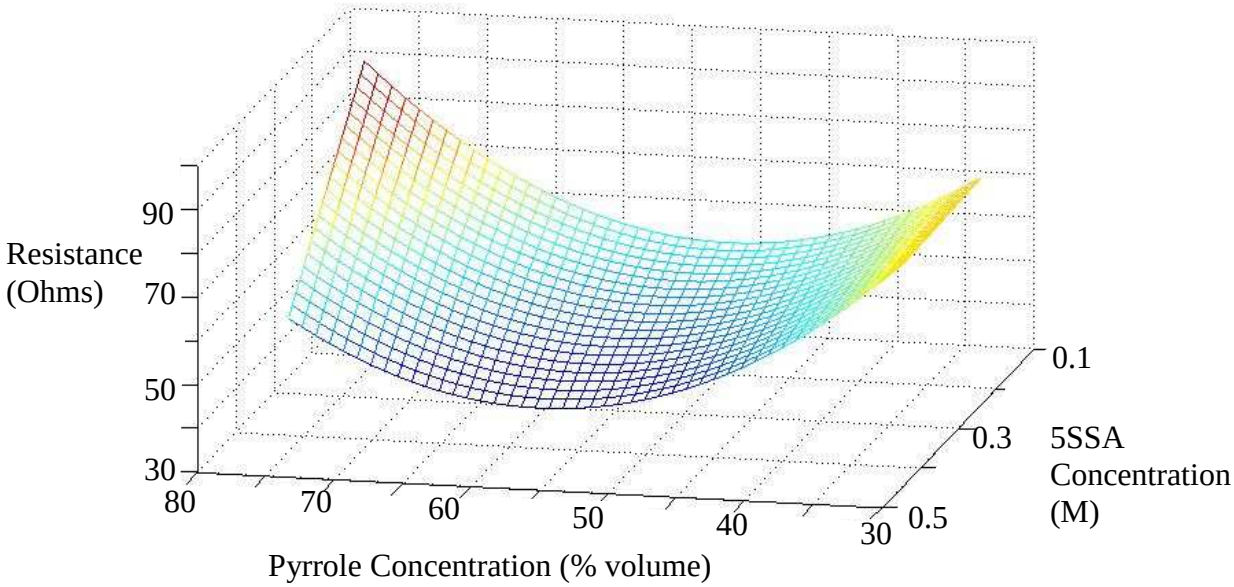

Figure 4-8. The effect of reaction conditions on electrotextile resistance at 0.025 g/mL 3TAA, 0.1 M $FeCl_3$, and 75 minutes.

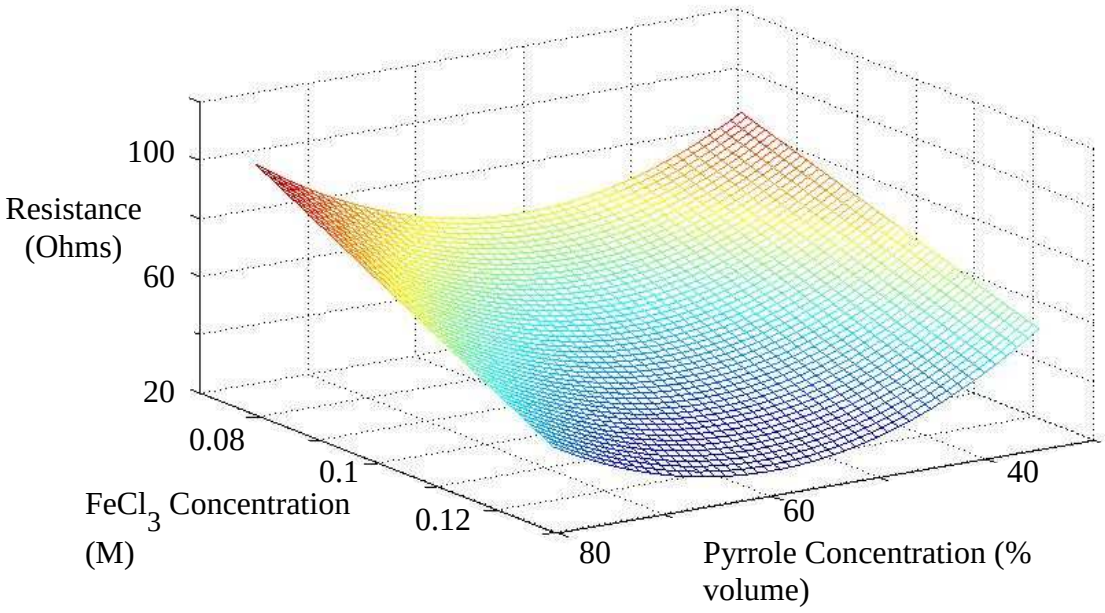

Figure 4-9. The effect of reaction conditions on electrotextile resistance at 0.025 g/mL 3TAA, 0.25 M 5SSA, and 75 minutes.

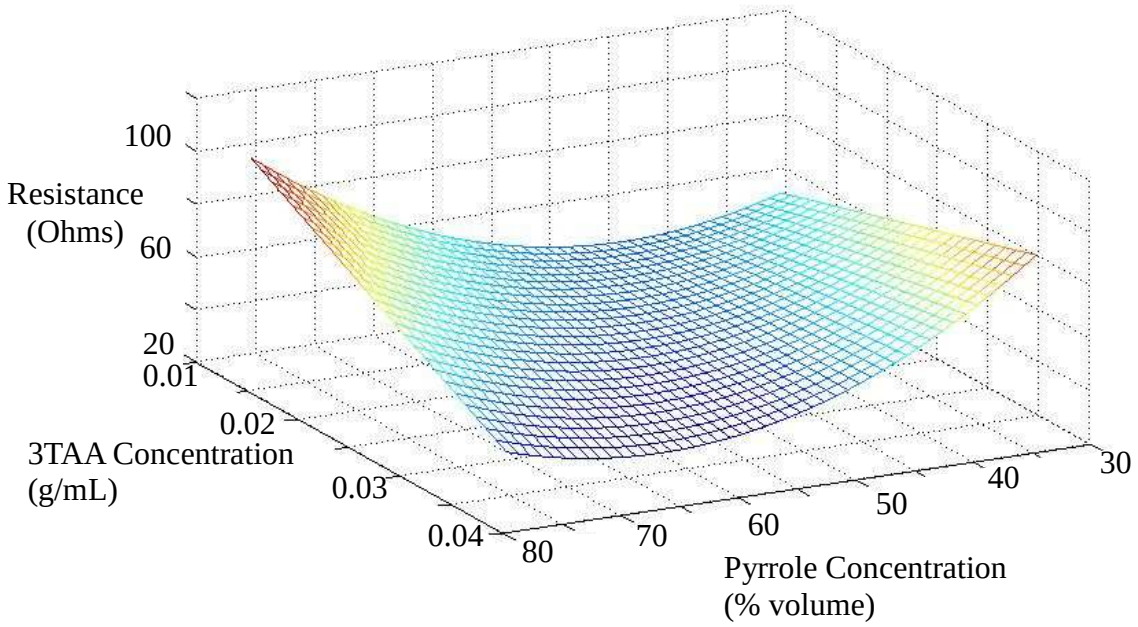

Figure 4-10. The effect of reaction conditions on electrotextile resistance at 0.1 M $FeCl_3$, 0.25 M 5SSA, and 75 minutes.

Resistance was graphed against two of the modeled factors, while the other 3 factors were held constant at the central composite center point. Electrotextile resistance decreased as the reaction time and dopant concentration increased (Figure 4-1). Increasing the reaction time and the oxidant concentration also reduced the electrotextile resistance (Figure 4-2). The combination of increased oxidant and dopant concentrations decreased the electrotextile resistance (Figure 4-3). Figure 4-4 shows that increasing the reaction time resulted in decreased resistance, regardless of 3TAA concentration, however at short reaction times the increase in 3TAA provided a slight decrease in resistance. Likewise, increased dopant concentration also resulted in decreased electrotextile resistance, regardless of 3TAA concentration (Figure 4-5). Figure 4-6 shows that increases in oxidant concentration have a less significant effect on resistance when the 3TAA

concentration is higher and that a very low resistance can be achieved with a lower oxidant concentration if the 3TAA concentration is high. In Figure 4-7 it can be seen that increasing reaction time will decrease resistance, but that the lowest resistances can be found with a mid-range pyrrole concentration. Approaching either the high or low extremes of the pyrrole concentration will result in resistance increases. The trend of a mid-range pyrrole concentration resulting in the optimum (lowest) possible electrotextile resistance can also be seen in Figures 4-8, 4-9, and 4-10. In Figure 4-8 changes in dopant concentration have nearly no effect at pyrrole concentrations less than 45%. The highest resistances can be seen with high concentrations of pyrrole and low concentrations of dopant. Increases in oxidant concentration can be seen to reduce resistance, regardless of pyrrole concentration (Figure 4-9). Figure 4-10 shows that increases in 3TAA concentration reduce electrotextile resistance at high pyrrole concentrations, but will increase electrotextile resistances at low pyrrole concentrations.

4.3.2 Optimization

One of the most important tasks of the model was to find the optimal conditions in order to produce the electrotextile with the lowest resistance for use in an electrochemical biosensor. The optimization was conducted using the optimization toolbox in Matlab 7.12 based on the model from Equation 4-2. The optimal values of each factor are listed in Table 4-5.

Table 4-5. Optimal conditions for minimum electrotextile resistance.

Factors	Optimal Conditions
Pyrrole Concentration (% volume)	58.79
3TAA Concentration (g/mL)	0.03
$FeCl_3$ Concentration (M)	0.11
5SSA Concentration (M)	0.25
Reaction Time (min)	70
Predicted Optimal Resistance (Ω)	35.41

Under the optimal conditions, the model predicted an electrotextile resistance of 35.41 Ω.

4.3.3 Model Verification

Verification experiments were carried out to confirm the optimal conditions. Ten runs were conducted under the optimal conditions, with each run's generated sample measured in triplicate. The results of the verification experiment can be seen in Table 4-6.

Table 4-6. Experimental results of optimal conditions.

Sample	Resistance (Ω)
1	30.30
2	39.63
3	31.40
4	50.60
5	42.80
6	35.13
7	33.00
8	39.10
9	38.20
10	39.87
Average	38.00
Standard Deviation	6.01

The experimental data showed an average electrotextile resistance of 38.0 Ω. The results were analyzed using a Student's t-test (1 tail, $\alpha = 0.025$) and showed that the calculated t value of 1.36 was less than the tabulated t value of 2.26, therefore there was no significant difference and demonstrated that the model fit the experimental data favorably. Thus, the optimal conditions obtained from the central composite experimental design were valid. An SEM image of the optimized electrotextile fibers can be seen in Figure 4-11.

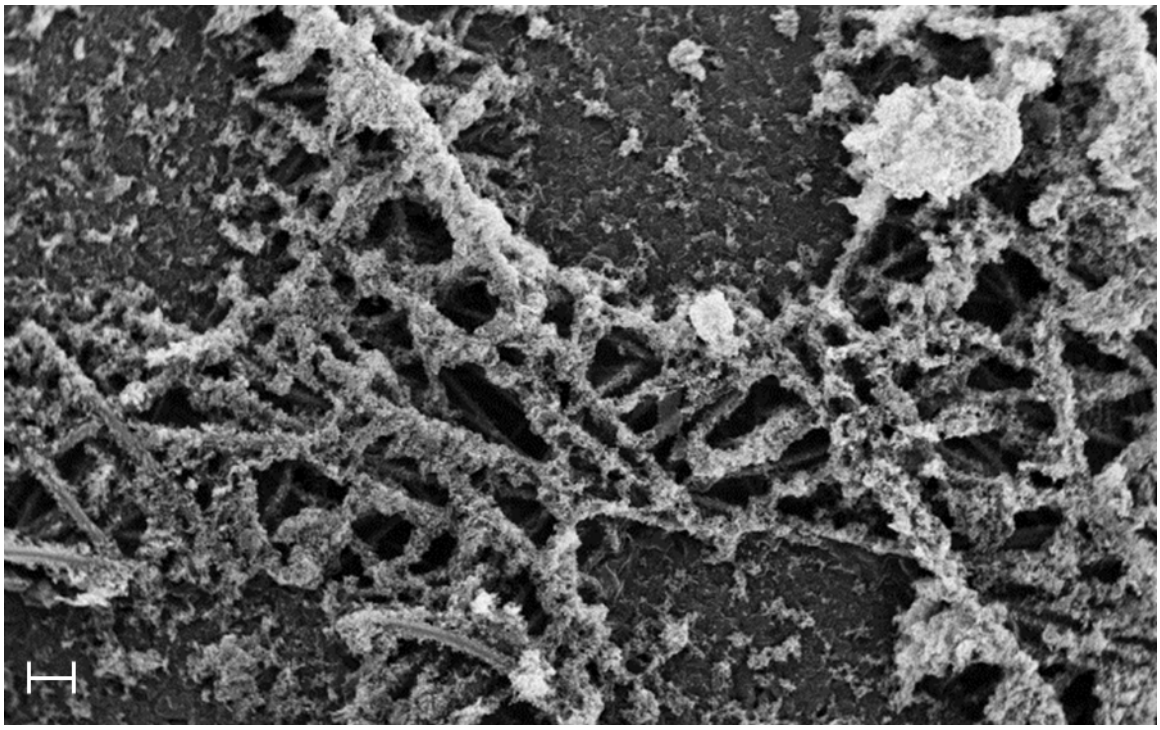

Figure 4-11. SEM image of fibers made using optimal conditions for polymer coating synthesis. Scale bar equal to 100 µm, magnification of 100x, EHT of 30 kV and working distance of 6.0 mm.

4.4 Conclusions

There are many factors that contribute to the formation and resistance of conductive polymer coatings. Five factors were identified in the synthesis of a conductive PPy – 3TAA co-polymer used to create an electrotextile for the development of an electrochemical biosensor. They were: concentration of pyrrole (monomer), concentration of 3TAA (monomer), concentration of $FeCl_3$ (oxidant), concentration of 5SSA (dopant), and polymerization time. These factors were varied in a central composite experimental design in order to develop a multiple regression model of the polymerization reaction. This model was then used to find the optimal conditions for each factor in order to generate the lowest experimentally possible electrotextile resistance. The optimal conditions were: 58.79% volume of pyrrole, 0.03 g/mL of 3TAA, 0.11 M $FeCl_3$, 0.25M 5SSA,

and 70 minutes of reaction time to generate an electrotextile resistance of 35.41 Ω. These conditions were experimentally verified and the mathematical model was statistically validated. The optimization results can be used to aid in the production of a conductive electrotextile electrode for electrochemical biosensors.

Chapter 5 : Antibody immobilization on conductive polymer coated nonwoven fibers for biosensors

This chapter is adapted from our recently published work in Sensors and Transducers Journal: McGraw, Shannon K.; Anderson, Michael J.; Alocilja, Evangelyn C.; Mareck, Patrick J.; Senecal, Kris J.; and Senecal, Andre G. Antibody Immobilization on Conductive Polymer Coated Nonwoven Fibers for Biosensors. Sensors and Transducers Journal. 2011. 13(12):142-149. http://www.sensorsportal.com/HTML/DIGEST/P_SI_176.htm

5.1 Introduction

High-surface area nonwoven membranes are versatile and can be applied to biosensor development [145]. One way to achieve this high surface area material is through the creation of electrotextiles. Electrotextiles are fabrics that can function as conductive "wires" and physically behave as textiles [160]. Electrotextile "smart membranes" can be designed for use with many types of sensor signal transduction, however limited research has been conducted with the integration of electrotextile, biological, and electrical technologies to create novel biosensor systems for food safety [13]. Previous work has been done to develop electrically active non-metallic textile coatings that are conductive using doped polypyrrole (PPy) polymer [14, 121, 122, 144, 166]. By producing a conformal conductive polymer coating on non-woven microfibers, an electrochemical biosensor electrode can be created that is less expensive and has more surface area for attachment than its planar metal counterparts [12]. In addition, these electrotextile electrodes are durable, disposable, and have the potential for minimal required attachment chemistry. With the attachment of biological recognition elements to the

electrotextile electrode surface, the electrodes would have the combined ability to perform pathogen capture and detection [167, 168]. The creation of this type of electrode would simplify a food pathogen detection biosensor, allowing the device to be smaller and lighter than current systems. Small foot print biosensors with multiplexing capabilities, environmental robustness and high sensitivity are needed for rapid presumptive testing. With membranes being designed for the capture, the sample readers can be simplified and significantly reduced in size.

The objectives of this part of the study were: to determine the best immobilization method for the attachment of antibodies to the electrotextile fibers, to determine the necessary concentration of antibody to be used, and to determine what (if any) blocking agent should be used on the antibody immobilized electrotextile fibers. In order to achieve these objectives, fluorescence based measurements were taken using anti-*Escherichia coli* (*E. coli*) O157:H7 antibody labeled with fluorescein isothiocyanate (FITC) and PicoGreen ® stained *E. coli* O157:H7 cells as optical reporters. Three different immobilization methods were analyzed: passive adsorption, glutaraldehyde attachment, and N-(3-dimethylaminopropyl)-N'-ethylcarbodiimide hydrochloride (EDC) / N-hydroxysulfosuccinimide (sulfo-NHS) cross-linking. These attachment methods were each analyzed using 3 different antibody concentrations: 1, 10, and 100 µg / mL, as well as with a negative control where no antibody was present. Finally, the use of either BSA or goat serum as a blocking agent was compared. We have shown that antibodies can be successfully attached to the electrotextile surface and still maintain the capability to capture their target pathogen, making them viable for use in a biosensor system.

5.2 Materials and methods

5.2.1 Materials

Nonwoven polypropylene (PP) microfibers were obtained from North Carolina State Nonwovens Cooperative Research Institute. For polymer synthesis, the monomer used was a pyrrole solution that was copolymerized with carboxylic acid functional 3-thiopheneacetic acid (3TAA). This co-polymer provides sites for covalent attachment of the bio-recognition (active) component of the biosensor to the fiber based platform. The oxidant was iron (III) chloride ($FeCl_3$). The polymer was doped using 5-sulfosalicylic acid (5SSA). All polymerization chemicals were obtained from Sigma-Aldrich (St. Louis, MO). The fiber characterization was conducted in Chapter 3 [18]. Covalent attachment was performed using glutaraldehyde (Sigma-Aldrich) or EDC (Sigma-Aldrich) and sulfo-NHS (Invitrogen, Carlsbad, CA, USA) with 50 mM 2-(N-morpholino)ethanesulfonic acid (MES) buffer, pH 6.0, (Thermo Fisher Scientific, Waltham, MA, USA). Blocking was conducted using 5% (w/v) bovine serum albumin (BSA) (Sigma-Aldrich) or 5% normal goat serum (KPL, Gaithersburg, MD, USA). PicoGreen ® (Invitrogen) was used for staining bacterial cells.

Two different antibodies against *E. coli* O157:H7 were used in this study, both polyclonal whole IgG: (1) BacTrace antibody goat anti-*E. coli* O157:H7 (KPL) and (2) BacTrace antibody goat anti-*E. coli* O157:H7 labeled with FITC (KPL). The antibodies were diluted in phosphate buffered saline (1x PBS) to a concentration of either 1, 10, or 100 µg / mL immediately before use.

5.2.2 Electrotextile synthesis

Electrotextile synthesis was conducted according to previously published techniques [18-20]. Briefly, an aqueous deposition process of conductive and functional polymer coatings upon a PP fiber matrix was used, as described below. A 6 cm x 8 cm polypropylene microfiber mat was submerged in a 10% pyrrole and 3TAA (10 mg/mL) solution, creating a functionalized monomer that was absorbed onto the fiber mat. The wet fiber sample was then removed from the solution and laid flat in a glass reaction vessel for polymerization. $FeCl_3$ (0.1 M, 30 mL) was added to the sample to initiate the chemical reaction while a dopant, 5SSA (0.1 M, 3 mL), was simultaneously added. The fibers in solution were incubated at room temperature for 30 minutes with constant agitation, thereby ensuring that polymerization occurred on both sides of the mat. The nonwoven fiber sample was removed from the solution, gently washed on both sides with deionized (DI) water, and dried at room temperature overnight. The fibers were then cut into 6.35 mm diameter circular discs.

5.2.3 Cell culture preparation

Cultures of *E. coli* O157:H7 Sakai strain (the strain isolated from the Sakai outbreak, 1996 in Sakai City, Osaka, Japan [169]) and *Salmonella enterica enterica*, serovar Enteritidis (*S.* Enteritidis) were obtained from the Michigan State University Food Safety and Toxicology Center. *E. coli* O157:H7 cell cultures were grown for 4 hours in tryptic soy broth (TSB) at 37°C. The growth time was selected based on a strain specific growth curve to give a concentration in excess of 10^8 colony forming units (CFU)/mL [170]. *S.* Enteritidis cultures were grown overnight in lactose broth at 37˚ C. A volume of 1 mL of cell culture was removed and pelleted

for 3 minutes at 5,000 x g. The pelleted cells were resuspended with 5 µL of PicoGreen and 500 µL of water. The cells were vortexed and stained for 5 minutes at room temperature while rotating in order for the dye to cross-link with the DNA of the cells. The cells were then washed, pelleted, and resuspended to a volume of 10 mL. PicoGreen is a fluorescent nucleic acid stain used for quantitating double-stranded DNA (dsDNA). Any excess PicoGreen stain that was not removed should have no effect due to the fact that it is non-fluorescent when unbound [171].

5.2.4 Antibody immobilization

Each immobilization and reporter combination was performed in triplicate, with the negative control receiving no immobilization or staining chemistry. Each immobilization method was performed with a series of 0 µg / mL, 1 µg / mL, 10 µg / mL, and 100 µg / ml of antibody. Each series was done twice: with FITC-labeled antibodies immobilized on them and blocked with a 5% BSA solution and with PicoGreen stained *E. coli* O157:H7 cells with a 5% BSA block. Each of the stains was also applied to samples without any antibodies immobilized to determine the background noise from the stains and non-specific binding.

5.2.4.1 Passive adsorption

The conductive nonwoven fiber discs were washed with sterile distilled water and dried for 10 minutes. After drying, a volume of 250 µL of the desired antibody concentration was applied to each disc and allowed to incubate for 1 hour with gentle agitation. After incubation, the discs were washed twice with PBS [157].

5.2.4.2 Glutaraldehyde attachment

The conductive nonwoven fiber discs were washed with distilled water and dried for 10 minutes. After drying, a volume of 25 µL of 2.5 mM glutaraldehyde was applied to each disc and incubated for 1 hour at 4°C. After incubation, the discs were washed with distilled water and dried for 10 minutes. A volume of 250 µL of antibody was then applied to each disc and incubated for 15 minutes at 37°C. The discs were washed with distilled water, dried for 10 minutes, and then 50 µL of deactivating buffer (0.2 M Tris, 10 mM sodium cyanoborohydride) [157] was applied and allowed to react at 37°C for 15 minutes. The discs were washed twice with PBS [172].

5.2.4.3 EDC / sulfo-NHS cross-linking

The conductive nonwoven fiber discs were washed with distilled water, dried for 10 minutes, and treated with 200 µL of EDC and sulfo-NHS in MES buffer with gentle agitation for 15 minutes. The discs were then washed twice with MES buffer and a volume of 250 µL of antibody was added and reacted with gentle agitation for 4 hours at room temperature. After incubation, the discs were washed with MES buffer and then twice in PBS [157].

5.2.5 Blocking of the fibers

A volume of 50 µL of the blocking agent was added to the electrotextile fibers and allowed to react for 1 hour. The samples were then washed twice with PBS and once with PBS containing 0.1 % Tween-20 (PBS-T).

5.2.6 Antibody immobilization analysis

The electrotextile fibers were separated into groups based on antibody attachment method: passive adsorption, glutaraldehyde, or EDC / sulfo-NHS. Each group was split in half, with FITC labeled antibodies being immobilized on half and non-FITC labeled antibodies being immobilized on the other half. The antibody concentration was varied with concentrations of 0, 1, 10, and 100 µg/mL used. The fibers were then blocked with 5% BSA using the method described in Section 5.2.5. The fibers that had non-FITC labeled antibody immobilized to the surface received a volume of 200 µL of an approximate cell count of 1×10^7 CFU/mL of *E. coli* O157:H7 cells stained with PicoGreen applied to them. The discs were incubated with the cells at 37°C for 15 minutes and then washed three times with PBS. All experiments were performed in triplicate.

5.2.7 Blocking agent analysis

BacTrace goat-anti *E. coli* O157:H7 antibodies were immobilized onto the electrotextile surface at a concentration of 10 µg/mL using the glutaraldehyde attachment method described in section 5.2.4.2. Samples were prepared using no blocking agent (PBS as a negative control), 5% (w/v) BSA, or 5% goat serum. Each sample was tested in triplicate. Bacterial cells of *E. coli* O157:H7 and *S.* Enteritidis were grown and prepared as described in section 5.2.3. Each blocking agent was tested using 1 of 3 target samples: *E. coli* O157:H7 (positive control), *S.* Enteritidis (negative control), or PBS containing no cells (system background noise) in order to determine the effect of the blocking agents on non-specific binding onto the fibers. The target samples were added in a volume of 200 µL to the discs at an assumed concentration of 1×10^7 CFU/mL.

The fibers were incubated with the target samples at 37˚C for 15 minutes and then washed with PBS. The number of washes were varied, with either 0, 1, or 3 washes performed in order to see if there was a change in non-specific attachment as more washes were performed.

5.2.8 Analytical methods

Fluorescence of the samples was measured using the Victor3 multilabel counter (PerkinElmer) using a 490 +10 nm excitation bandpass filter and a 535 +25 nm emission bandpass filter. The samples were analyzed and photographed using a fluorescent microscope (Olympus BX41 with Q Color 3 camera and a QBC ParaLens Advance kit with blue excitation). All fluorescent samples were excited at a wavelength of 490 nm and emission was measured at a wavelength of 535 nm.

5.3 Results and discussion

For this study, antibody-antigen binding assays were performed to determine the capture capability of the antibody-functionalized conductive membranes. Attachment and capture efficiency were determined through the use of fluorescent labels that were measured using a fluorometer and visualized with confocal microscopy. Two different fluorescent indicators were evaluated: FITC labeled to the antibody and PicoGreen stained *E. coli* O157:H7 Sakai cells. *E. coli* O157:H7 Sakai was selected for use as the positive control based on its positive result when tested against the KPL antibody using a Western blot. Three different antibody immobilization techniques were evaluated: passive adsorption, covalent binding using glutaraldehyde, and EDC / sulfo-NHS cross-linking. For these experiments, three different antibody concentrations (1, 10, and 100 µg / mL) were evaluated against a control with no antibody exposure. The effect of the

inclusion of 5% (w / v) bovine serum albumin (BSA) or 5% goat serum as blocking agents was also evaluated. Supplementary data, calculations, and images can be found in Appendix B.3.

5.3.1 Selecting a fluorescent indicator

At an emission of 535 nm, the average fluorescence of the non-treated fibers was 35.3 relative fluorescence units (RFU). The fluorescence intensity for each attachment method at antibody concentrations of 0, 1, 10, and 100 µg / mL using FITC and PicoGreen stained *E. coli* O157:H7 cells as indicators is shown in Figure 5-1.

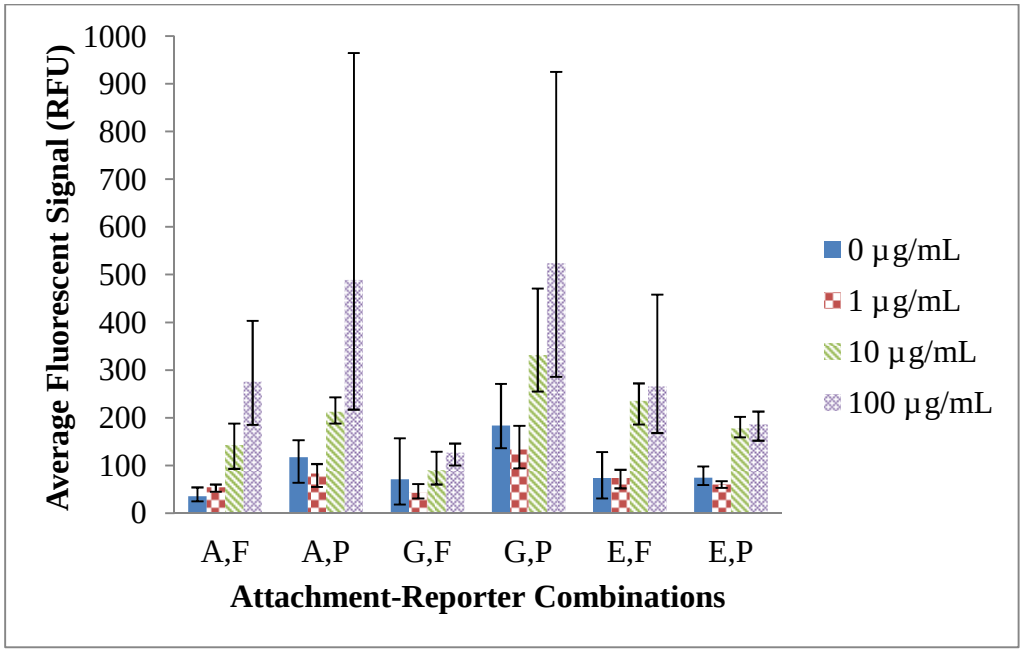

Figure 5-1. Average fluorescence due to attachment-reporter combinations when blocked at varying antibody concentrations. Where 'A' stands for passive adsorption, 'G' for glutaraldehyde attachment, 'E' for EDC attachment, 'F' for FITC labeling, and 'P' for PicoGreen stain. Error bars show the range of the signal for each data set.

The lowest average fluorescence across all four concentrations was seen with glutaraldehyde bound antibodies labeled with FITC. The highest average fluorescent signal was seen with glutaraldehyde bound antibodies exposed to PicoGreen stained cells. In both passive adsorption and glutaraldehyde binding, the PicoGreen stained cells outperformed their FITC labeled counterparts at every concentration. At an antibody concentration of 100 µg/mL, the passively adsorbed antibodies bound to PicoGreen stained cells emitted an intensity 188% higher than the passively adsorbed antibodies labeled with FITC. The glutaraldehyde immobilized antibody with the PicoGreen stained cells had an average RFU signal 535% higher than those with FITC at 100 µg/mL. The higher fluorescent output of the PicoGreen stained cells can be due to the fact that the PicoGreen stain causes the entire cell to fluoresce thus providing more signal than the FITC labeled antibody which is significantly smaller in area. PicoGreen stained *E. coli* O157:H7 cells were selected as the best fluorescent indicator of binding when compared to the FITC labeling because of a higher RFU signal and its ability to indicate if bound antibodies were present and had retained their capture ability.

5.3.2 Selecting an attachment method and antibody concentration

A comparison between the three different immobilization methods at three different antibody concentrations with blocking using 5% BSA can be seen in Figure 5-2.

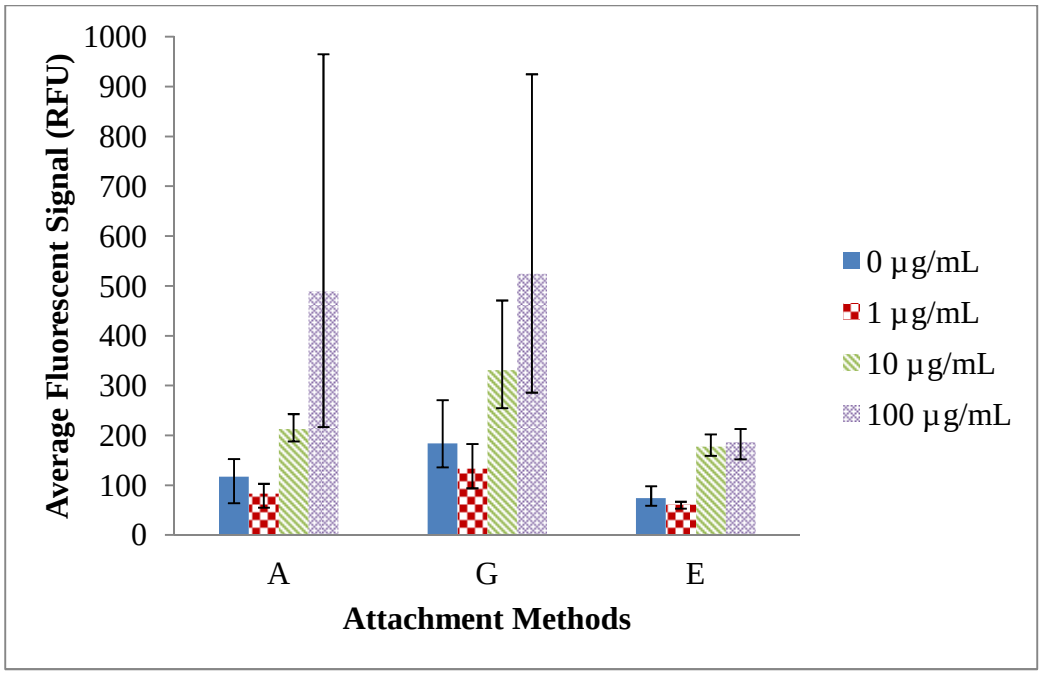

Figure 5-2. Average fluorescence for attachment methods at varying antibody concentrations with blocking and PicoGreen reporter. Where 'A' stands for passive adsorption, 'G' for glutaraldehyde attachment, and 'E' for EDC attachment. Error bars show the range of signal for each data set.

PicoGreen stained *E. coli* O157:H7 cells were used as the fluorescent indicator. The highest overall output was seen when using glutaraldehyde for covalent attachment, the lowest when using EDC and sulfo-NHS. This trend was also previously seen in Figure 5-1. The relatively small difference of 9.3 RFUs between the output values for the EDC immobilization at concentrations of 10 and 100 µg/mL appears to indicate that all available binding sites for EDC attachment are occupied with an antibody concentration of 10 µg/ml. The excess antibody available at 100 µg/mL was unable to bind and washed off during rinsing. The results show that all three methods tested were effective for pathogen capture to the fiber surfaces at antibody concentrations of 10 or 100 µg/mL. At 1 µg/mL of antibody, there is no significant difference from where no antibody is present. The differences in binding and fluorescent intensity is also seen in Figure 5-3.

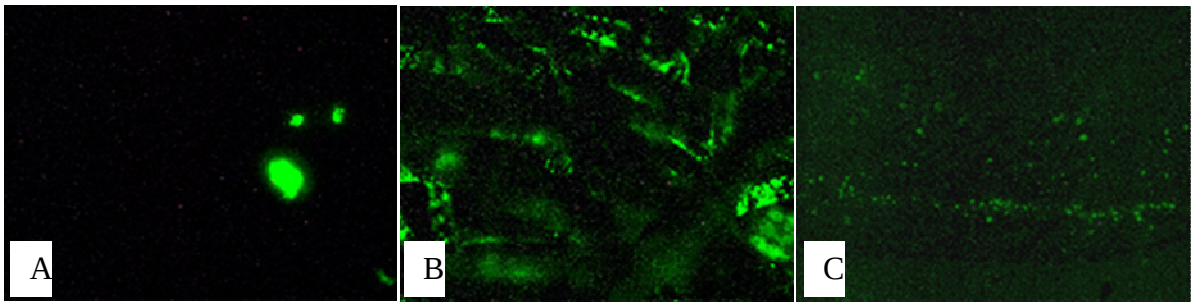

Figure 5-3. Fluorescent images of fibers at 200x with each attachment method, blocked, at an antibody concentration of 100 µg/mL, with PicoGreen reporter. A: passive adsorption. B: glutaraldehyde attachment. C: EDC / sulfo-NHS attachment.

The results in Figures 5-1 and 5-2 show that EDC and sulfo-NHS cross-linking have a lower fluorescence than passive adsorption or glutaraldehyde. While some variability is expected due to non-specific binding, it is probable that while the EDC and sulfo-NHS is binding the antibodies to the surface, the EDC may not be accessible to bind the antibody due to steric hindrance of the antibody and the surface. EDC is a zero length cross-linker while glutaraldehyde has a six carbon spacer arm that allows better accessibility on a solid surface. Also, since the antibodies are covalently attached directly to the carboxyl groups on the membrane by the EDC and sulfo-NHS method there may be less antibody immobilized on the membrane compared to the other methods due to a lack of potential binding sites. There is also the potential for the orientation of the immobilized antibodies on the membrane surface to not be optimal for analyte capture. Taking this into consideration, the method for antibody immobilization on the conductive polymer coated nonwoven fibers that shows the most promise is covalent binding using glutaraldehyde. When the need to produce the most cost effective sensor is considered, it is determined that an antibody concentration of 10 µg/ml is required to see a fluorescent change from samples with no antibody present.

5.3.3 Blocking agent selection

In order to determine the effects of the use of a blocking agent, such as BSA or goat serum, samples treated with each of the two blocking agents were compared to one another as well as to samples that had no blocking agent treatment. Figure 5-4 shows the average RFU output for samples with either no blocking agent added, a BSA block added, or a goat serum block added. These blocks were tested against target samples that contained either no cells, *E. coli* O157:H7, or *S.* Enteritidis.

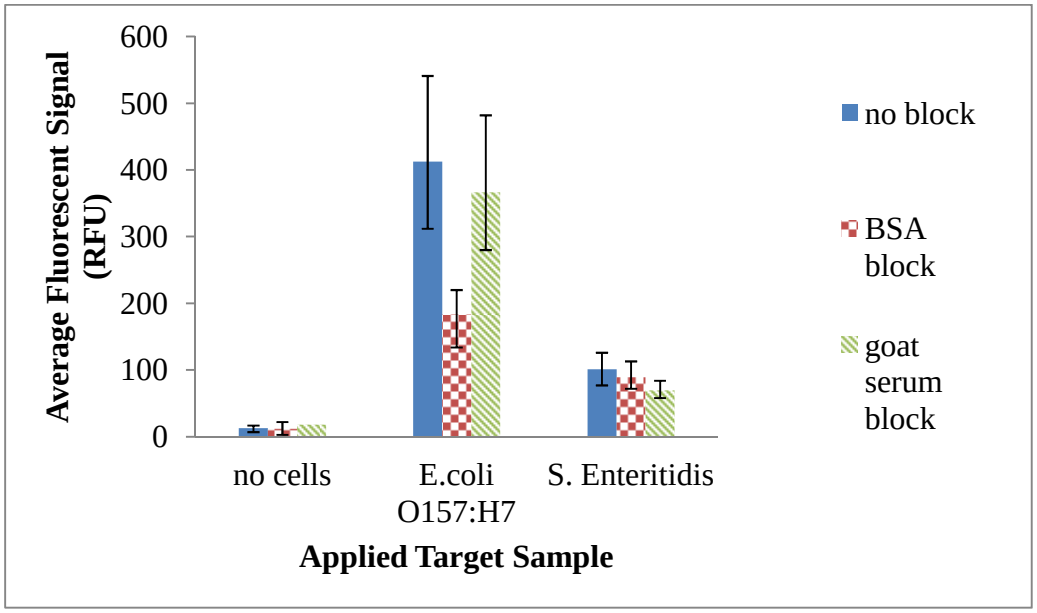

Figure 5-4. Average fluorescence for electrotextile fibers with 10 µg/mL of antibody attached using glutaraldehyde and varying blocking methods with either no cells added, PicoGreen stained *E. coli* O157:H7 added, or PicoGreen stained *S.* Enteritidis cells added and 1 wash performed. Error bars show the range of signal of each data set.

As can be seen in Figure 5-4, there is very minimal background noise (signal generated when no cells are added) for all of the blocking methods, with all three reporting an average output of less than 20 RFUs. All of the samples that had *E. coli* O157:H7 applied generated larger signals than the other samples, this was expected since the antibody target for the fibers was *E. coli* O157:H7.

The average signal when *E.* coli O157:H7 cells are applied ranges from 183.33 RFUs (BSA block) to 412.67 RFUs (no block). The largest signal was expected to be found at the *E.* coli sample with no blocking because *E. coli* O157:H7 is the target pathogen and should bind to the antibodies, with no blocking being performed it is expected that non-specific binding to the fibers is also occurring, adding to the signal. Of the samples that were exposed to *S.* Enteritidis, the non-specific pathogen, the highest RFU output was from the unblocked sample with an average value of 101 RFUs. The RFU signal from the non-specific binding of the *S.* Enteritidis is much smaller than any of the signals resulting from the binding of the target *E. coli* indicating that blocking reduces non-specific binding on the fibers.

Figures 5-5 and 5-6 show how the fluorescent output of the *E. coli* O157:H7 and *S.* Enteritidis exposed samples changed for each blocking method as more washes were applied, respectively.

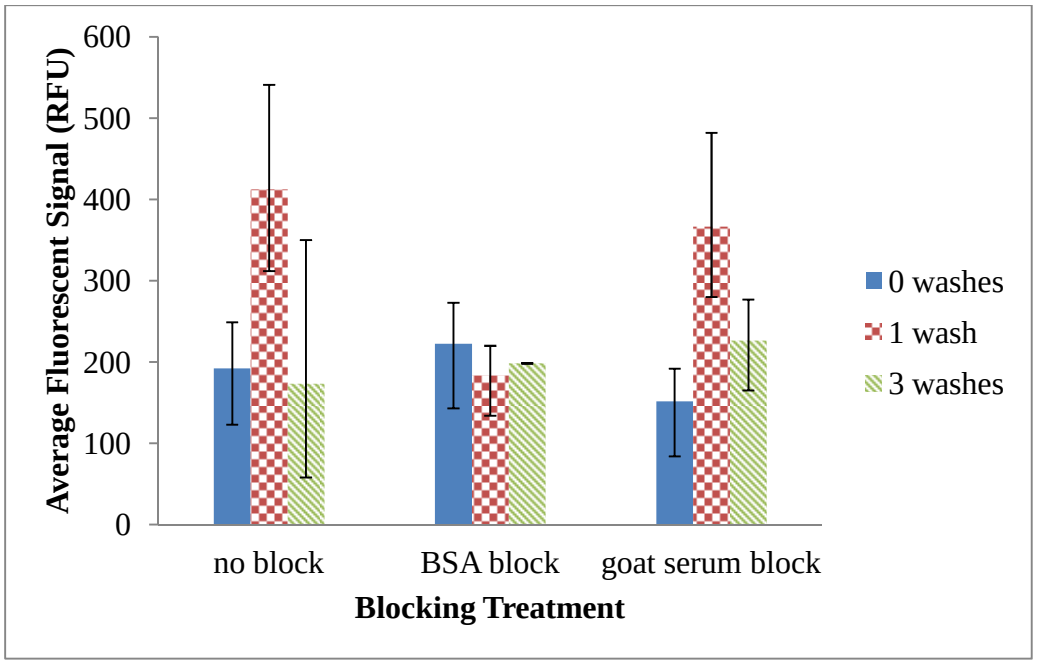

Figure 5-5. Average fluorescence for electrotextile fibers functionalized with anti-*E. coli* O157:H7 antibodies with different blocking treatments over multiple washes with PicoGreen stained *E. coli* O157:H7 cells as the fluorescent reporter. Error bars shows the range of signal of each data set.

The highest signal is seen from the sample with no blocking, but after 1 wash the signal, increased. An increase in signal after 1 wash can also be seen in the sample blocked with goat serum. The lowest signal comes from the sample blocked using goat serum, but with 0 washes. At 0 washes all of the outputs signals are within 71 RFUs of each other. After 3 washes both of the blocked samples have higher values than the sample that was not blocked. This shows that the addition of a blocking agent to the fibers does not hinder the binding between the target and antibodies. The variability between replicates of each data set was analyzed. The average variability between points when no blocking was used was found to be 215.67 RFUs. The average variability between data sets when the fibers were blocked with BSA or goat serum were found to be 72.33 RFUs and 140.67 RFUs, respectively. The addition of the blocking agent reduces the variance within samples. A possible explanation for the variability in each treatment set as washes are added is that the antibody and target bacteria are not strongly bound. The additional wash steps are then not just removing non-specifically bound cells, but also cells that were captured to the target antibody.

Figure 5-6, the fluorescent output of the *S.* Enteritidis exposed samples for each blocking method as more washes were applied, provides a better understanding of the effect of each blocking method on non-specific binding.

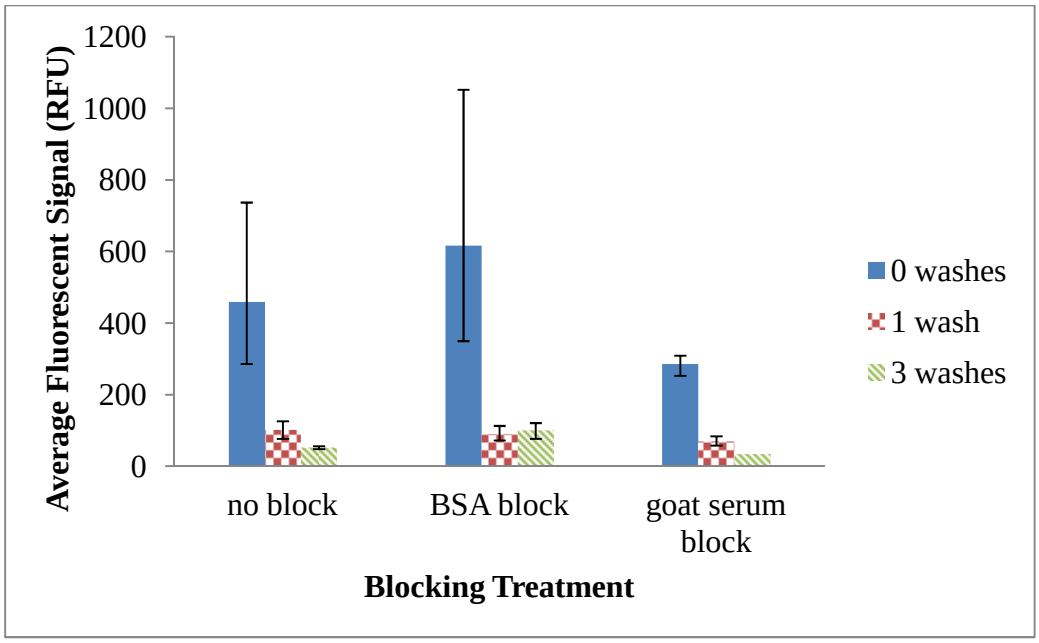

Figure 5-6. Average fluorescence for electrotextile fibers functionalized with anti-*E. coli* O157:H7 antibodies with different blocking treatments over multiple washes with PicoGreen stained *S.* Enteritidis cells as the fluorescent reporter. Error bars show the range of signal of each data set.

Figure 5-6 shows that all three blocking treatments reduced significantly after one wash, implying that there was not a high amount of non-specific binding occurring on the fibers regardless of blocking method if at least 1 wash step was used. The average RFU output of the samples blocked using goat serum with 0 washes had a value of 286 RFUs. A value 173.33 RFUs less than the samples that had no blocking treatment and 330 RFUs less than the samples blocked with BSA. After each wash step the samples blocked with goat serum had the lowest average RFU output of all of the blocking treatments, ending with an output of only 34 RFUs after 3 washes as compared to 52 RFUs for the samples with no blocking treatment and 100.67 RFUs for the samples blocked using BSA. By looking at the range of the data points within each sample set it can also be seen that the addition of wash steps reduced variability. The addition of a single wash step reduced the range in data points for samples with no blocking from 451 RFUs

to 49 RFUs. With BSA as the blocking agent the range went from 702 RFUs to 41 RFUs and with goat serum blocking 56 RFUs to 26 RFUs.

Based on these results it was found that it is necessary to block and wash the electrotextile fibers in order to prevent or remove non-specific binding. BSA and goat serum were both shown to block non-specific binding on the fibers while not inhibiting target binding, however the goat serum performs better because it results in lower initial non-specific binding as well as lower variability in samples. The use of 1 wash step instead of 3 was also found to be beneficial. The use of 1 wash reduced the non-specific binding on the fibers significantly and also did not appear to reduce signal when the target pathogen was applied to the fibers. Additional wash steps may remove captured target bacteria that are weakly bound to the immobilized antibodies.

5.4 Conclusions

The initial results from this study show that antibodies can be attached to conductive polymer coated non-woven fibers. Passive adsorption, covalent binding using glutaraldehyde, or EDC and sulfo-NHS are all effective immobilization methods, with glutaraldehyde demonstrating the best antibody attachment. These results indicate that the best nonwoven sensor construction will utilize glutaraldehyde attachment of 10 µg/mL of antibody with BSA blocking. This is confirmed by challenging the sensor with PicoGreen stained cells and fluorescent detection. Non-specific binding does occur on the fiber surfaces, however the addition of a blocking agent, such as goat serum, and a wash step can reduce the effects of non-specific binding, aiding in the specificity of the sensor. This technology was used in the capture and detection of live *E. coli* O157:H7 cells in Chapter 6.

Chapter 6 : A resistance based biosensor that utilizes conductive microfibers for microbial pathogen detection

This chapter is adapted from our recently published work in Open Journal of Applied Biosensor: McGraw, Shannon K.; Alocilja, Evangelyn; Senecal, Kris and Senecal, Andre. A Resistance Based Biosensor That Utilizes Conductive Microfibers for Microbial Pathogen Detection. Open Journal of Applied Biosensor. 2012. 1(3):36-43. DOI: 10.4236/ojab.2012.13005.

6.1 Introduction

Although food and waterborne pathogens do not have as significant an effect on U.S. military operations as they have in the past, enteric pathogens are still one of the top causes of non-combat related injuries in the field and are therefore one of the primary military medical concerns for deployed troops [1]. Gastroenteritis was the leading cause of illness among troops during Operations Desert Shield (1990 – 1991) and Desert Storm (1991) [2]. This is a significant issue for the military to address because an outbreak of diarrheal disease in the field has the ability to rapidly affect a large number of warfighters. During Operation Restore Hope (1992 - 1993), it was shown that 16 % of all hospital admissions were for diarrheal illness [3]. Of these admissions, 16 % could be traced back to *Escherichia coli* (*E. coli*). Various studies on diarrheal illness in deployed troops have listed an array of enteric pathogens as the source with the most commonly occurring ones being: *Shigella*, *E. coli*, *Salmonella*, and *Campylobacter* species [2-4, 173]. The ability to rapidly and accurately detect enteric pathogens with low infective doses, such as *E. coli* O157:H7, in the field has significant importance.

Biosensors are one technology being developed in order to improve pathogen detection and reduce response times. Immunobiosensors utilize pathogen specific antibodies coupled to a transducer as the biological recognition element for detection [75]. The use of antibodies in the design of a biosensor is beneficial because, as the field of clinical immunoassays has shown, the benefits of the antibody-antigen reaction include high binding efficiency and specificity for detection. In addition, antibodies can be generated against nearly any bacterial pathogen. The faster speed and lower cost of immunobiosensors versus standard detection methods and biosensors using other biorecognition techniques, such as DNA, have made them especially marketable for use in food matrices [149-151]. In an electrochemical biosensor, the biological recognition element is immobilized on an electrode, which then converts the biological recognition event (i.e. antibody – antigen binding) into a measurable electrical signal [75]. Electrochemical biosensors are generally less expensive than optical detection methods and are easier to use with turbid samples. Electrochemical impedance / resistance based sensing also does not require enzyme labels or redox mediators to facilitate detection the way optical based sensing does [127]. Instead, a measurable system response is created when the biological recognition event disrupts the flow of either the current or the potential at the working electrode while the reference electrode maintains a constant potential [75]. In order for biosensor technology to advance and surpass common pathogen detection techniques, such as polymerase chain reaction (PCR) and culture / colony counting, the current drawbacks of biosensors must be addressed. These include high cost, low durability, a lack of environmental robustness for in field testing, detection limits that do not reach those of traditional techniques, and a necessity for extra extraction methods to be performed before use which adds to the total detection time.

One approach for addressing some of the drawbacks of current biosensor technology is through the development / use of nonwoven fibers to create “electrotextiles”. High-surface area nonwoven electrotextile membranes are versatile materials that can be developed into “smart membranes” designed for use with all forms of sensor signal transduction. Research is scarce, however, regarding the integration of electrotextile, biological, and electrical technology to create novel biosensor systems for applications such as food protection and environmental sampling. Previous work has been done to develop electrically active non-metallic textile coatings made of doped polypyrrole (PPy) polymer [14, 121, 122, 144]. By producing a conductive polymer coating on nonwoven microfibers, an electrochemical biosensor electrode can be created that is less expensive than its planar metal counterpart [12]. The overlapping fiber layers also have more available surface area than planar electrodes, resulting in more potential target attachment sites. In addition, these electrotextile electrodes can be engineered to be durable, disposable, lightweight, and require minimal attachment chemistry. These qualities make them ideal for in field use. The chemical composition of nonwoven fibers and their coatings can also be easily changed or adjusted based on their intended use. Small changes to the processing parameters can change the fiber diameter, mesh size, porosity, texture, or weave pattern. This processing flexibility makes them a very versatile material for sensor development. They can be designed to be used with many different analytes and experimental conditions and can be designed to have high chemical stability [85]. The ability to use antibody functionalized fibers for the capture and concentration of target analytes has been previously demonstrated with electrospun nanofibers and a carboxyl functional group (-COOH) [19, 145]. With the attachment of biological recognition elements to the electrotextile surface, these electrodes have the capacity

to perform pathogen capture, concentration, and detection. This would simplify a food pathogen biosensor, resulting in a significantly smaller and lighter detection system.

A nonwoven polypropylene (PP) electrotextile coated with a pyrrole and 3-thiopheneacetic acid (3TAA) conductive copolymer has been developed (Chapter 3) [18]. Studies were conducted to look at the effects of the inclusion of different monomers, reaction solvents, and a dopant. Analysis was also done to determine the best concentration of oxidant and functionalizing monomer to use. The successful attachment of antibodies to the coated fibers for the capture of bacterial cells using this electrotextile has been previously reported [19]. Bhattacharyya et al. have shown that a nylon electrotextile coated with a 3,4-ethylenedioxythiophene (EDOT) and 3-thiopheneethanol (3-TE) copolymer functionalized with avidin can be used to detect biotin in solution [13]. They observed that the textile resistance increased as the concentration of biotin protein in the solution increased and that the resistance of each sample also increased over time. These increases in resistance were theorized to be the result of the surface bound avidin on the electrotextile reacting with the biotin in solution and that the attachment of the biotin to the surface altered the electrical environment close to the electrode layer. This same theory can be applied to our sensor, the average resistance for each bacterial sample increases as the bacterial cells impede the flow of electricity through the electrode. This response becomes larger and more significant as the concentration of cells in solution increases.

There were three objectives to this study in order to establish a proof of concept for our sensor: first, to determine the resistance of the electrotextile membrane in the electrochemical cell; second, to determine what effect the rest of the system has on the total resistance and if that

effect is significant; and third, to determine if the electrotextile electrode can differentiate between small changes in the conductivity of a solution due to the addition of target bacterial pathogens. In order to achieve these objectives, experiments were conducted using serial dilutions of *E. coli* O157:H7. First, resistances were measured in the system with and without the conductive electrotextile in order to determine the baseline resistances for the system components and how much they contribute to the total measured sensor resistance. Next, multiple measurements were conducted over a large range of bacterial concentrations and evaluated to determine if the detected change at each concentration was significantly different from the blank (no bacteria) values. We have shown that a rapid, novel electrochemical biosensor based on the use of polypropylene microfiber membranes coated with a conductive polypyrrole and antibody functionalized can be used for the detection of *E. coli* O157:H7. To our knowledge, this is the first time a functionalized conductive copolymer coated nonwoven electrotextile has been used with immobilized antibodies as an electrode for the successful electrical detection of bacterial cells.

6.2 Materials and methods

6.2.1 Materials

Nonwoven PP microfibers were obtained from North Carolina State Nonwovens Cooperative Research Institute. For the polymer synthesis, the monomer used was a 10% pyrrole solution that was copolymerized with carboxylic acid functional 3TAA. The oxidant was iron (III) chloride ($FeCl_3$). The polymer was doped using 5-sulfosalicylic acid (5SSA). All of the polymerization chemicals were obtained from Sigma-Aldrich (St. Louis, MO). Covalent

attachment of KPL (Gaithersburg, MD) BacTrace antibody goat anti-*E. coli* O157 was performed using glutaraldehyde (Sigma-Aldrich) and a deactivating buffer (0.2 M Tris, 10 mM sodium cyanoborohydride (Sigma-Aldrich)) and blocked with 5% (w/v) bovine serum albumin (BSA) (Sigma-Aldrich).

6.2.2 Electrotextile synthesis

Electrotextile synthesis was conducted according to previously published techniques [19]. Briefly, an aqueous deposition process of conductive and functional polymer coatings upon a PP fiber matrix was used, as described below. A 6 cm x 8 cm PP microfiber mat was submerged in a 10% pyrrole and 3TAA (10 mg/mL) solution, creating a functionalized monomer that was absorbed onto the fiber mat. The wet fiber sample was then removed from the solution and laid flat in a glass reaction vessel for polymerization. $FeCl_3$ (0.1 M, 30 mL) was added to the sample to initiate the chemical reaction while a dopant, 5SSA (0.1 M, 3 mL), was simultaneously added. The fibers in solution were incubated at room temperature for 30 minutes with constant agitation, thereby ensuring that polymerization occurred on both sides of the mat. The nonwoven fiber sample was removed from the solution, gently washed on both sides with deionized (DI) water, and dried at room temperature overnight.

6.2.3 Antibody Immobilization

Covalent attachment of the anti-*E. coli* O157 antibodies onto the electrotextile fiber surface was conducted following a previously published technique [19]. Briefly, the conductive nonwoven fiber mats were cut into 2 cm x 2 cm squares. The fiber squares were washed with 0.01 M

phosphate-buffered saline (PBS), pH 7.4, and dried for 10 minutes. After drying, a volume of 3 mL of 2.5 mM glutaraldehyde was applied to each disc and incubated for 1 hour at 4°C. After incubation, the discs were washed with 0.01 M PBS and dried for 10 minutes. A volume of 4 mL of antibody (10 µg/mL in PBS) was then applied to each disc and incubated for 15 minutes at 37°C. The discs were washed with 0.01 M PBS, dried for 10 minutes, and then 3 mL of deactivating buffer was applied and allowed to react at 37°C for 15 minutes. A 5% BSA block was added and reacted at room temperature for 1 hour. The discs were washed twice with PBS, and then once with PBS containing 0.1 % Tween-20 (PBST).

6.2.4 Cell culture preparation and enumeration

E. coli O157:H7 Sakai strain was obtained from the Michigan State University Food Safety and Toxicology Center. It was selected as the target pathogen after testing positive against the KPL antibody using a Western blot. Cell cultures were grown to a concentration of roughly 10^8 colony forming units (CFU)/mL based on a strain specific growth curve [170] in tryptic soy broth (TSB) at 37°C. A 10 mL volume of cell culture was removed and centrifuged for 5 minutes at 5,000 rpm. The pelleted cells were washed with Butterfield's phosphate buffer (BPB), pH 7.2. This wash procedure was performed in triplicate. The cells were resuspended (10 mL) and then serially diluted using BPB. A volume of 100 µL of the 5th, 6th, 7th, and 8th dilutions as well as the blank control sample, sterile BPB, was plated in triplicate onto MacConkey-sorbitol (SMAC) agar and incubated overnight at 37˚C. Sample concentration estimates were calculated using standard estimation methods based on the average plate counts [174, 175].

6.2.5 Resistance measurements and electrical theory

Resistance values were obtained by connecting the electrotextile electrodes to a potentiostat with two stainless steel alligator clip. The experimental setup can be seen in Figures 6-1and 6-2.

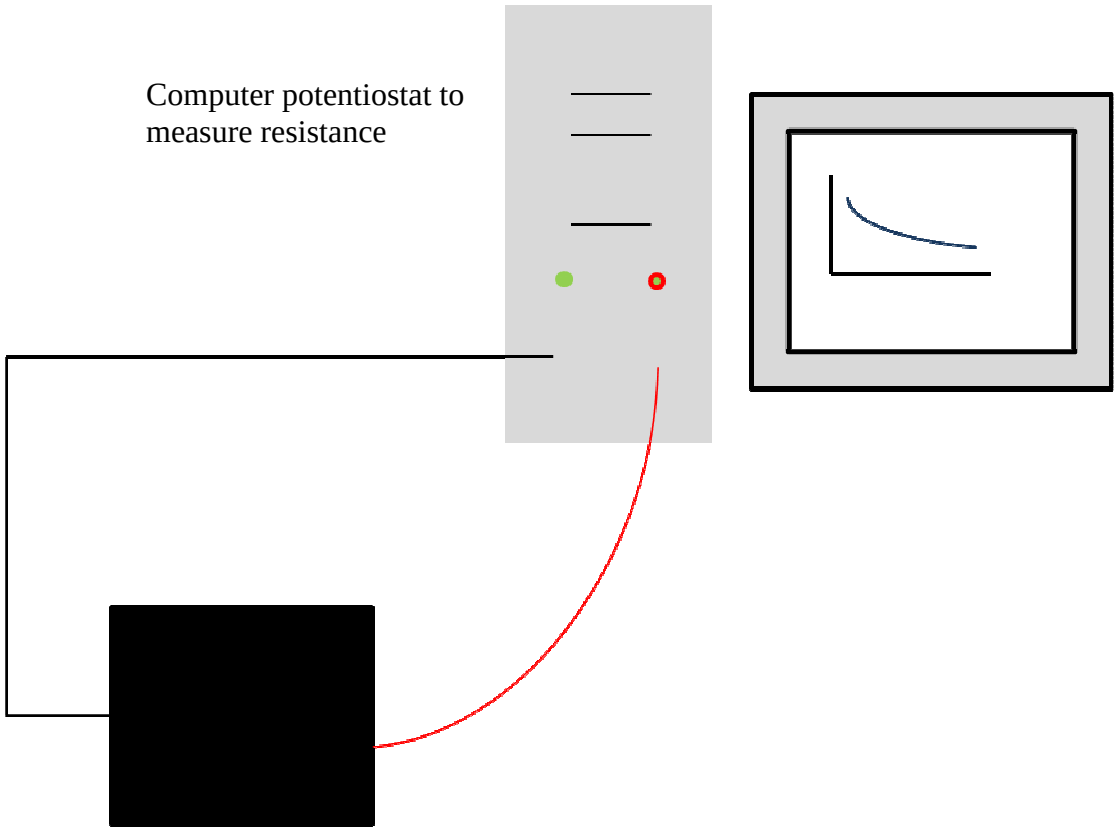

Figure 6-1. Schematic of the system design. The electrotextile fibers are connected to the computer / potentiostat for resistance measurements.

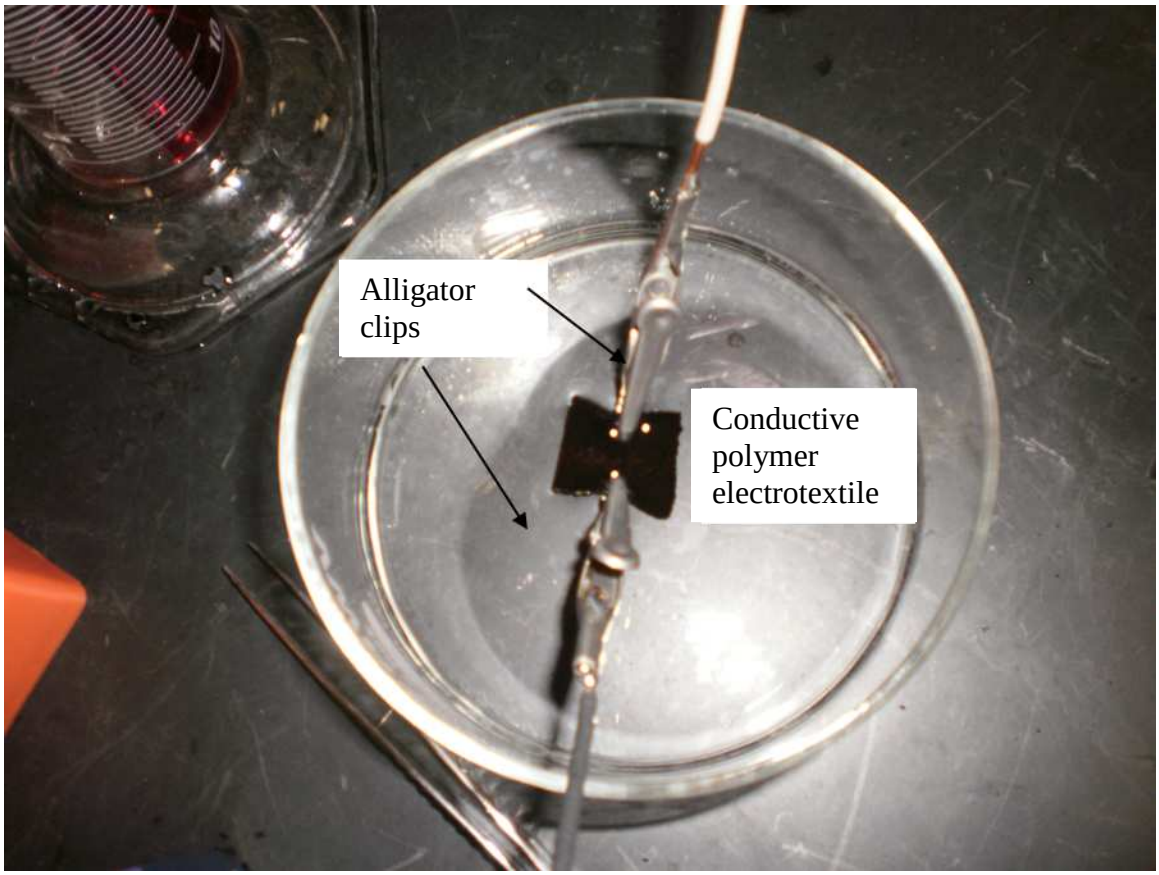

Figure 6-2. Experimental set-up that measures the change in resistance of the antibody bound electrotextile electrode when bacteria are added to the buffer solution. Alligator clips connect the conductive polymer electrotextile to the computer / potentiostat where the measured current of the system is recorded.

Briefly, the antibody bound 2 cm x 2 cm electrotextile squares were completely submerged in a beaker containing 0.1 M phosphate buffer (18 mL, pH 7.4) while attached to the potentiostat in order to establish a baseline resistance for the fibers. After 30 minutes, a 2 mL sample from the *E. coli* O157:H7 serial dilutions was added, bringing the total solution volume to 20 mL. Constant potential amperometry (0.5 V), where a constant potential is applied and the current is measured, was used and the current values were recorded at fixed time intervals over 15 minutes. Previous studies have demonstrated that a potential of 0.2 V to 0.8 V is a preferable input signal

when dealing with whole cells or other biological elements [176-179]. Based on this information, the potential of 0.5 V was arbitrarily selected.

6.2.5.1 Screening for ohmic behavior

Because a direct current (DC) power source was used with a constant potential, the measured currents at each time point could be used to calculate the total resistance of the system based on Ohm's law, Equation 6-1. Ohm's law states that the current flowing through a conductor, at a constant temperature, is directly proportional to the potential difference across the points of applied voltage.

$$V=IR \tag{6-1}$$

Where V is the potential across, I is the current through, and R is the resistance of the system. The ratio of V / I indicates the resistance value at that point in time. To validate the use of this equation, a linear sweep was performed on the electrotextile. A linear sweep is a voltammetric method where the applied potential to the electrode is linearly varied in time. A material that produces a linear response to a linear sweep is described as an ohmic material, a material that exhibits ohmic behavior

6.2.5.2 Circuit with two resistors in parallel

The complete system setup can be viewed as a simple circuit with two resistors in parallel, as can be seen in Figure 6-3.

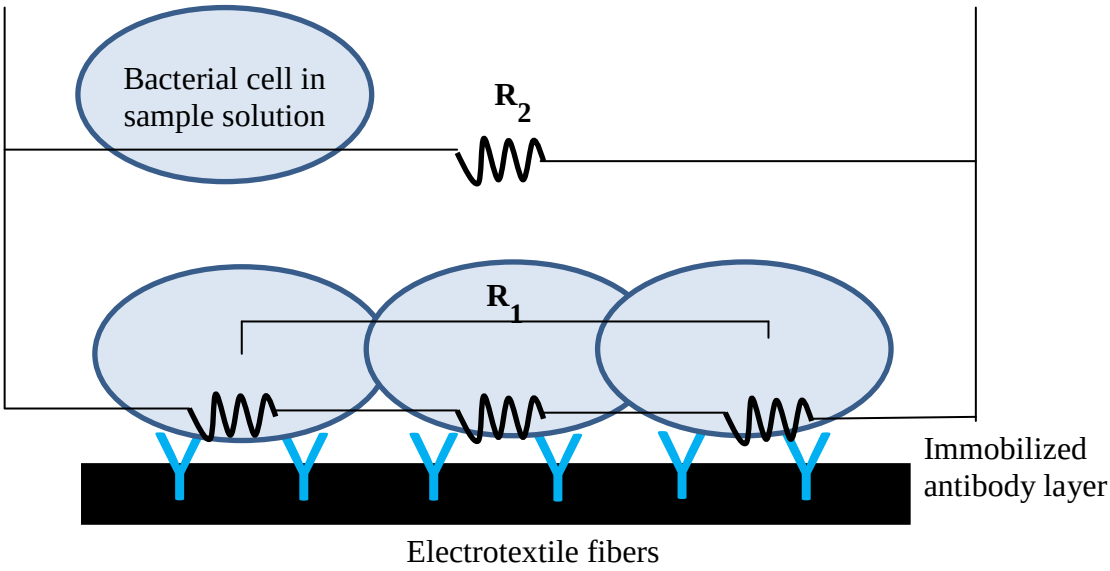

Figure 6-3. Circuit model of the antibody immobilized fibers with bacteria present. The system acts as a circuit with two resistors in parallel. R_1 is the resistance at the electrotextile surface. R_2 is the resistance in the buffer solution.

The resistance caused by interactions at the conductive fiber electrode surface would be considered resistor 1 (R_1) and any resistance occurring due to interactions between the buffer solution and the rest of the system components would be considered resistor 2 (R_2). Based on the theory of parallel resistors, these two resistances combine to form the total resistance of the system (R_T) as seen in Equation 6-2.

$$1/R_T = 1/R_1 + 1/R_2 \qquad (6\text{-}2)$$

R_2 can be determined by measuring the resistance of the system when the conductive fiber electrode is not present. Once measured values for R_T and R_2 have been obtained, R_1 can be calculated. In order to determine if the effect of R_2 is significant in the system, it is important to

look at how much it contributes to R_T. Equation 6-3 was used to determine what percentage of the total system resistance, R_T, was due to R_2.

$$R_2 \text{ \% contribution to } R_T = \Delta R / R_T \times 100 \quad (6\text{-}3)$$

Equation 6-3 calculates the contribution to R_T from R_2 as a percentage, where ΔR is equal to the difference between R_T and R_1, or the difference in the total system resistance due to R_2.

6.2.6 Determining system resistances

In order to address objective 1, squares (2 cm x 2 cm) of the electrotextile fabric were attached to the potentiostat in phosphate buffer (PB) and their amperometric response to the addition of *E. coli* O157:H7 samples at calculated concentrations of 10^0, 10^3, 10^5, and 10^8 (log 0, 3, 5, and 8, respectively) CFU/mL as well as a control (BPB, 0 CFU / mL) at fixed time points over 15 minutes was recorded. Using Equation 6-1, R_T was calculated.

6.2.7 Determining the system's component contributions

In order to address objective 2, the procedure described in Section 6.2.6 was performed using 2 cm x 2 cm squares of non-coated, non-functionalized PP fibers. Using Equation 6-1, these values were designated as R_2. Using Equation 6-2, the value of R_1 at each time point was calculated. Once the values of R_1, R_2 and R_T were established, Equation 6-3 was used to

determine the percent contribution to R_T that was due to the resistance from R_2. Significance was tested by using a Student's t-test (2 tail, $\alpha = 0.05$).

6.2.8 Using the electrotextile as a resistance based sensor

To address objective 3, squares (2 cm x 2 cm) of the electrotextile fabric were attached to the potentiostat in PB and multiple measurements were first taken using the electrotextile electrodes and constant potential amperometry with a pure BPB solution over several days to establish the range of the initial baseline values for the system. Triplicate measurements were taken using the electrotextile electrode and constant potential amperometry to establish the resistance values for a control sample (BPB, 0 CFU/mL) and *E. coli* O157:H7 at concentrations of 10^1, 10^4, 10^6, and 10^9 CFU/mL. The resistances for each concentration at each time point were averaged to determine an average resistance value for each concentration. The resistance of the sensor at each bacterial concentration was tested against the values of the control using a Student's t-test (2 tail, $\alpha = 0.05$) to determine significance. The measured biosensor resistances were normalized using Equation 3-1 to determine the system response (Rp) [13].

$$Rp(\%)=((R_1-R_0)/R_0)\times 100 \qquad (3\text{-}1)$$

Where R_1 is the resistance of the biosensor after the positive bacteria sample has been added. R_0 is the resistance of the biosensor that has not been exposed to bacteria (blank). This was done in order to pool and analyze multiple experiments with one another to determine if the biosensor results were reproducible.

6.3 Results and discussion

The purpose of this study was to determine: the resistance of the membrane in the electrochemical cell; what effect the buffer solution has on the total resistance of the system and if that effect is significant; and if the electrotextile electrode can differentiate between small changes in the conductivity of a solution due to the addition of target bacterial pathogens. As a result of this study a functionalized conductive copolymer coated nonwoven electrotextile was successfully used as an electrode with immobilized antibodies on the surface for the successful electrical detection of bacterial cells for the first time. This technology has the potential to be used in the development of light-weight, flexible, inexpensive, and disposable field based systems for the rapid detection of various target pathogens. Supplemental data and calculations can be found in Appendix B.4.

6.3.1 Screening for ohmic behavior

Data showing ohmic behavior of the electrotextile is shown in Figure 6-4.

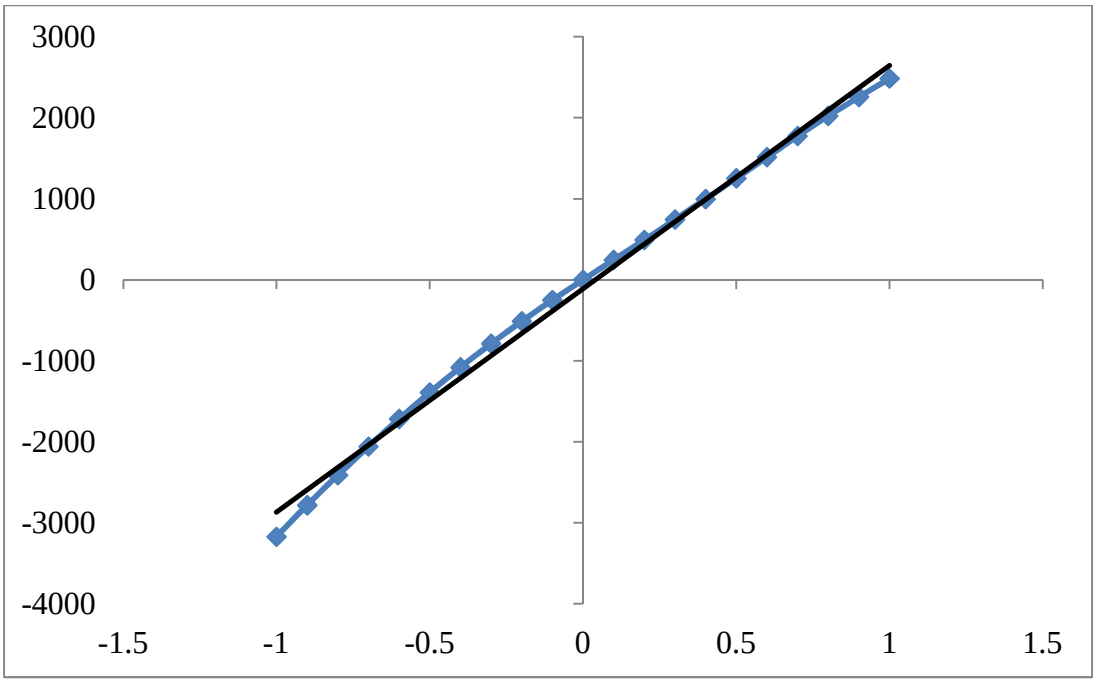

Figure 6-4. The average linear sweep of the electrotextile fibers over the potential range of interest, -1.0 to 1.0 V. The vertical axis is measured current output in micro amps. The solid line shows the linear best fit of the data points with an equation of y=2756.4x-112.49 and has an R_2 value of 0.9949.

The electrotextile exhibits ohmic behavior across the potential range of interest, meaning that it obeys Ohm's law, as the potential increases, the measured current increases proportionally. The electrotextile can therefore be used as an electrode for this study.

6.3.2 Determining system resistances

Using the method described in Section 6.2.6, amperometric responses to the addition of *E. coli* O157:H7 samples at calculated concentrations of 8.37 x 10^0, 10^3, 10^5, and 10^8 CFU/mL as well as a control (BPB, 0 CFU/mL) at fixed time points over 15 minutes were recorded. Using Equation 6-1, R_T was calculated, achieving objective 1. These results can be seen in Figure 6-5.

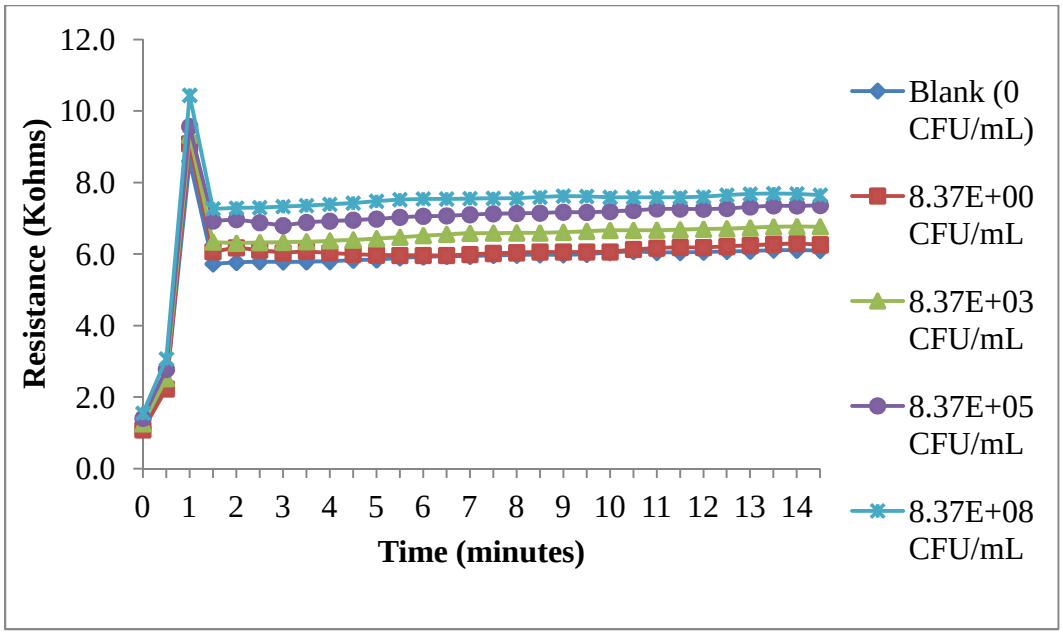

Figure 6-5. Total system resistance (R_T) over 15 minutes at varied bacterial cell concentrations. As the concentration of bacterial cells increases, so does the measured system resistances.

The average total system resistance (R_T) ranged from 5.8 to 7.3 kΩ, with the resistance increasing as the concentration of bacterial cells in solution increased. The cytoplasm of live bacterial cells has been previously reported to have a resistivity of 10^6 Ω / cm^2, which explains this phenomenon [180, 181]. The measurements appeared to settle at a near constant resistance after roughly 2-3 minutes had passed and the system had reached equilibrium.

6.3.2 Determining the system's component contributions

In order to complete objective 2 the method described in Section 6.2.7 was performed. The difference between the methods described in Sections 6.2.6 and 6.2.7 is that in Section 6.2.7 2 cm x 2 cm squares of non-coated, non-functionalized PP fibers were used. Using Equation 6-1,

these values were designated as R_2. Using Equation 6-2, the value of R_1 at each time point was calculated. The results of this experiment can be seen in Figure 6-6.

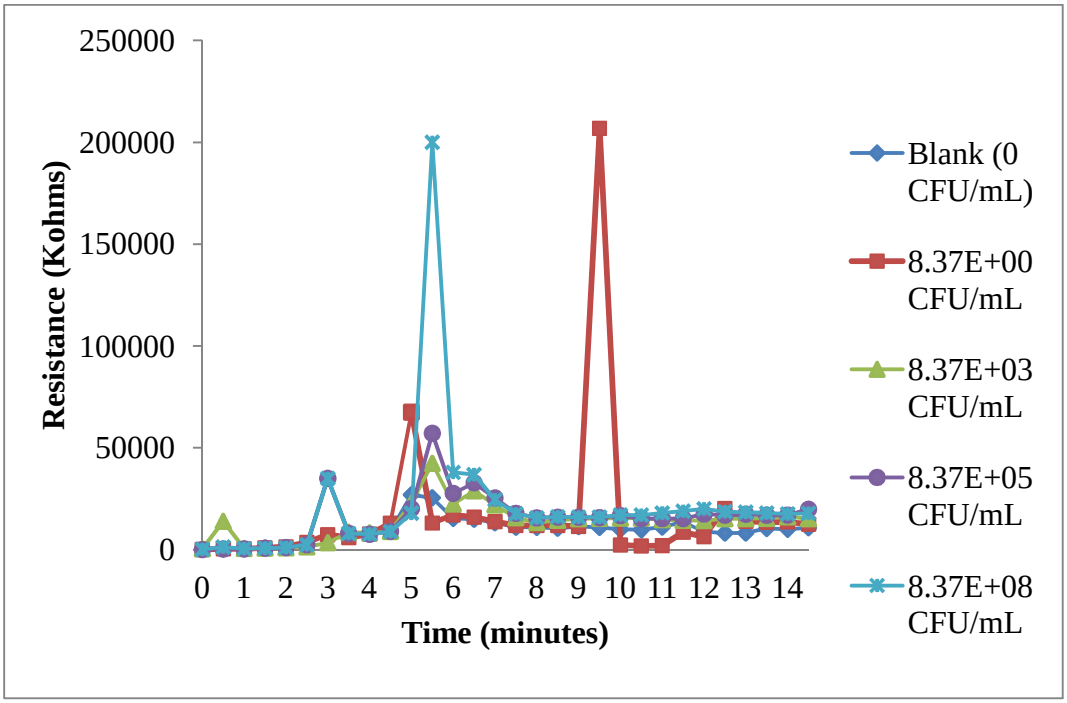

Figure 6-6. Resistance of the buffer solution (R_2) without the electrotextile present over 15 minutes at varied bacterial cell concentrations.

The average resistance of the system without the coated fibers (R_2) ranged from 10.5 MΩ to 21.5 MΩ, a 10^3 magnitude difference from the values of R_1. The values of R_2 for each cell concentration exhibited the same general trend as seen with the values of R_T, but were more variable with random fluctuations occurring as late as 10 minutes into the measurement. As can be seen in Figure 6-6, at 2 different points during the experiment the measured resistance peaked to a value of roughly 200,000 kΩ. This is most likely due to the fact that at such high resistance, and therefore low current levels, the measured values were near the limit of sensitivity for the potentiostat and difficult to separate from the regular system noise. The values of R_2 also had

larger standard deviations, ranging from 7.8 to 37.8 MΩ, as compared to 1.2 to 1.5 kΩ for the values of R_T.

With the values of R_1, R_2 and R_T established, Equation 6-3 was used to determine that at its maximum point, the contributed resistance from R_2 was calculated to be 2.8% of the total system resistance. After 2 minutes, R_2 contributed at maximum only 0.73% to the total system resistance, with the average percentage of R_T due to R_2 being 0.09%. A Student's t-test (2 tail, $\alpha = 0.05$) was performed and found no significant difference between R_T and R_1 at any of the tested concentrations. With R_1 contributing over 97% of the value of R_T, R_T and R_1 were determined to be essentially equivalent. All future reported resistances and analysis for the sensor are based on the value of R_T.

6.3.3 Using the electrotextile as a resistance based sensor

Multiple measurements were taken using the electrotextile electrodes and constant potential amperometry with a pure BPB solution to establish a baseline range for the system. Within the experimental lot the sensor was found to have an initial resistance range of 5.8 kΩ to 13.0 kΩ with an average value of 9.6 kΩ (standard deviation = 3.1 kΩ). This range can be attributed to variability in the polymer synthesis and deposition process as well as the potential for inconsistencies of the amount and orientations of the bound antibodies and blocking proteins between the fiber membranes.

Triplicate measurements were taken using the electrotextile electrode and constant potential amperometry to establish the resistance values for a control sample (BPB, 0 CFU/mL) and *E. coli* O157:H7 at concentrations of 10^1, 10^4, 10^6, and 10^9 (log 1, 4, 6, and 9, respectively) CFU/mL. A time of 3 minutes was determined to be necessary to reach system equilibrium. The resistances for each concentration at each time point were averaged and the value after the initial 3 minute equilibrium time can be seen in Figure 6-7.

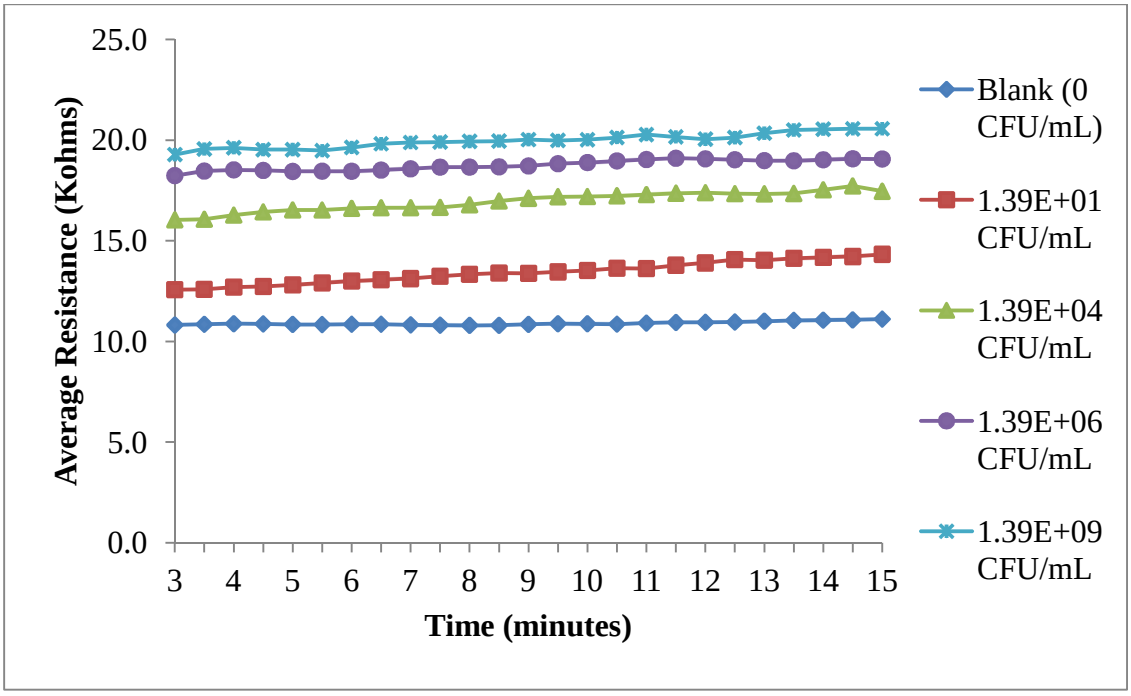

Figure 6-7. Average resistances over a period of 12 minutes (after a 3 minute equilibrium time) for the triplicate runs of the electrotextile biosensor with varying bacterial cell concentrations, fibers from experiment A. The resistances increase as the concentration of cells increases. A visible difference in response can be observed between all of the samples and the control.

At each concentration, the change in the resistance values between 3 and 15 minutes was less than 2kΩ, the resulting relatively smooth stacked lines for each of the samples indicate that the resistance of the sensor at each concentration is not significantly changing over the 12 minute period. The resistance for each sample increases as the concentration of cells increases. This

trend can also be seen in Figure 6-8, where the individual resistance values at each time point after 3 minutes for each sample concentration were averaged together to determine an average resistance for each sample.

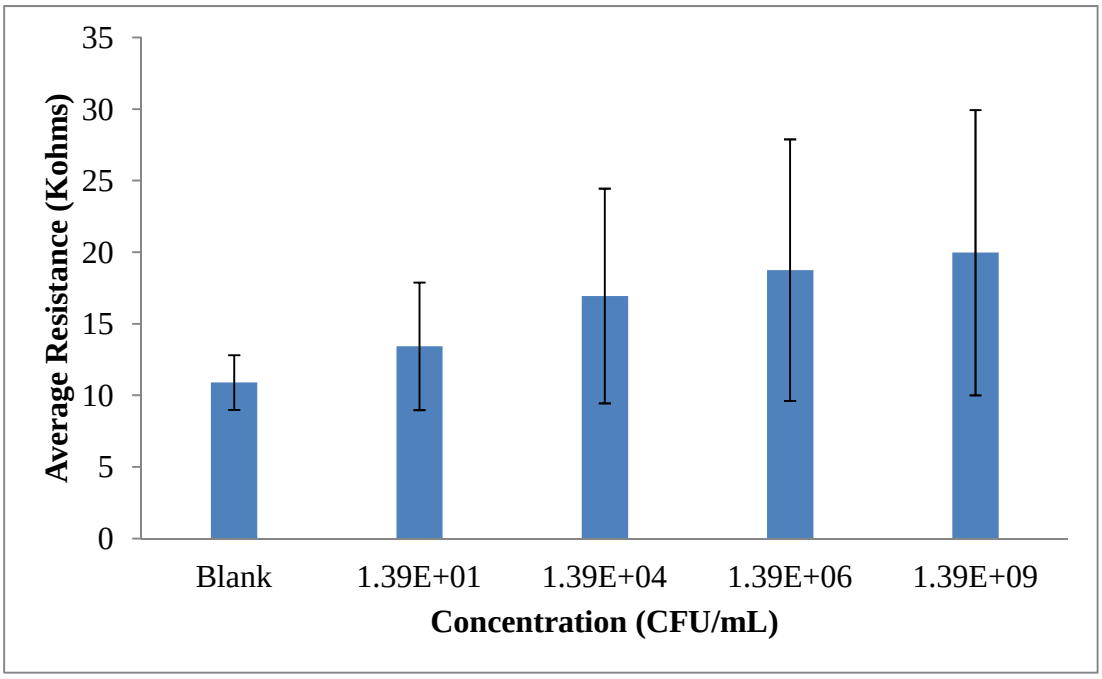

Figure 6-8. Average resistances for varying bacterial cell concentrations, fibers from experiment A. Resistances taken after 3 minutes equilibrium time for each cell concentration were averaged to provide a single resistance value. Error bars show the standard deviations of the experimental data.

In Figure 6-8, it can be seen that the change in average resistance values is smaller between the high concentrations than the changes observed between the lower half of the concentrations. This is most likely due to the fibers reaching a threshold for attachment on the surface, so that the increase of cells in the sample is no longer generating a proportional increase on the system resistance. The surface attachment capabilities could be improved by decreasing the size of the fibers, allowing more fibers per square centimeter and therefore increasing the surface area of the fiber mats. It can also be improved by attaching more antibodies to the fibers and decreasing the amount of blocking agent being used.

The resistance of the sensor at each bacterial concentration was tested against the values of the control using a Student's t-test (2 tail, $\alpha = 0.05$) to determine significance. The resistance at each concentration of *E. coli* O157:H7 tested was determined to be significantly different from the blank. The Student's t-test was also used to determine that, after 3 minutes, the resistances measured at each concentration were significantly different than at every other tested concentration with two exceptions: between 1.39×10^4 CFU/mL and 1.39×10^6 CFU/mL and between 1.39×10^6 CFU/mL and 1.39×10^9 CFU/mL. Within each individual run of the triplicate, the electrotextile electrode was capable of differentiating between each of the samples, with resistance at each concentration found to be significantly different than the resistance at every other tested concentration. This shows that the electrotextile electrode is capable of differentiating between a positive and negative sample, but cannot be used for quantitative analysis. Due to manufacturing variations resulting in different initial resistances for the sensor when no bacteria are present, it is important for each experiment to have a blank control run with fibers from the same lot and for the data to be normalized in order to accurately determine positive / negative results.

6.3.4 Sensor reproducibility

The experiment conducted in Section 6.3.3 was repeated 3 more times in order to test for reproducibility of the results. Each individual run was tested in triplicate. In order to compensate for the variability in the initial resistance values between sensors, the data was normalized into a percent response using Equation 3-1. The responses for each dilution at each time point across the triplicates were averaged together to provide an average performance of the

sensor for each experiment set. The results of these additional experiments can be seen in Figures 6-9, 6-10, and 6-11.

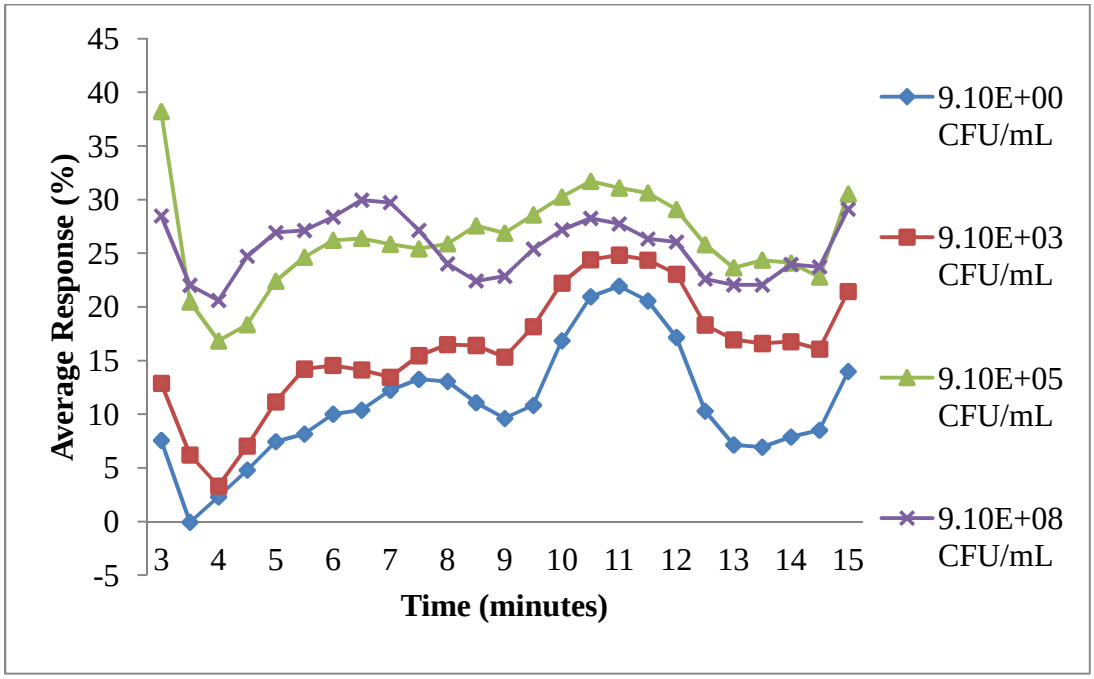

Figure 6-9. Average response over a period of 12 minutes (after a 3 minute equilibrium time) for the electrotextile biosensor with varying bacterial cell concentrations, fibers from experiment B.

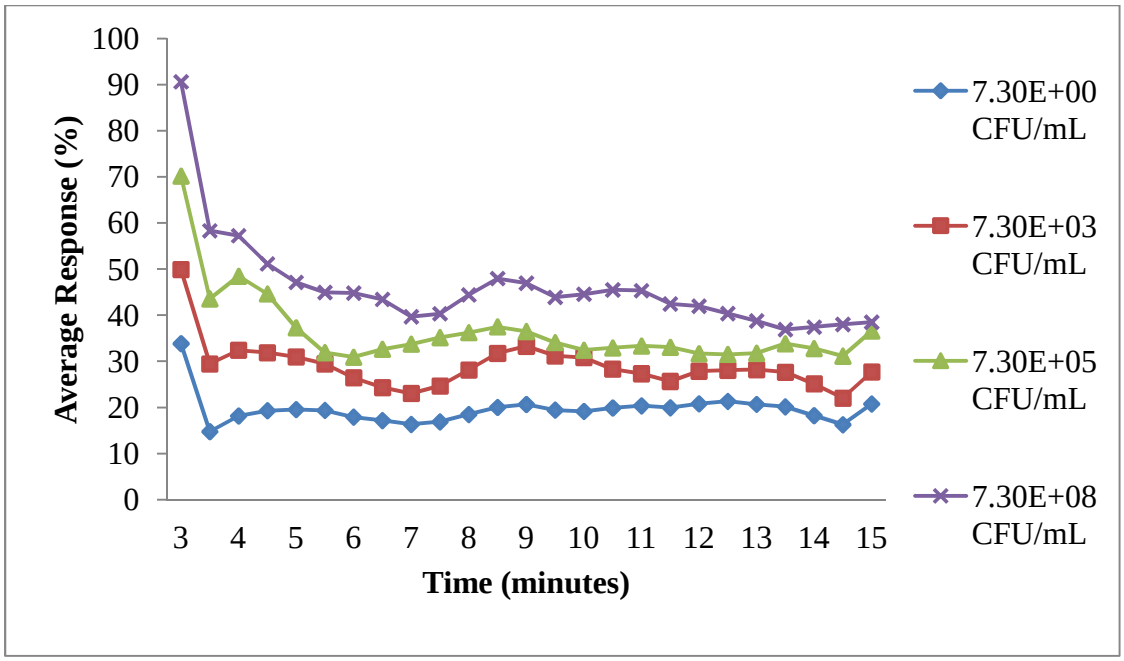

Figure 6-10. Average response over a period of 12 minutes (after a 3 minute equilibrium time) for the electrotextile biosensor with varying bacterial cell concentrations, fibers from experiment C.

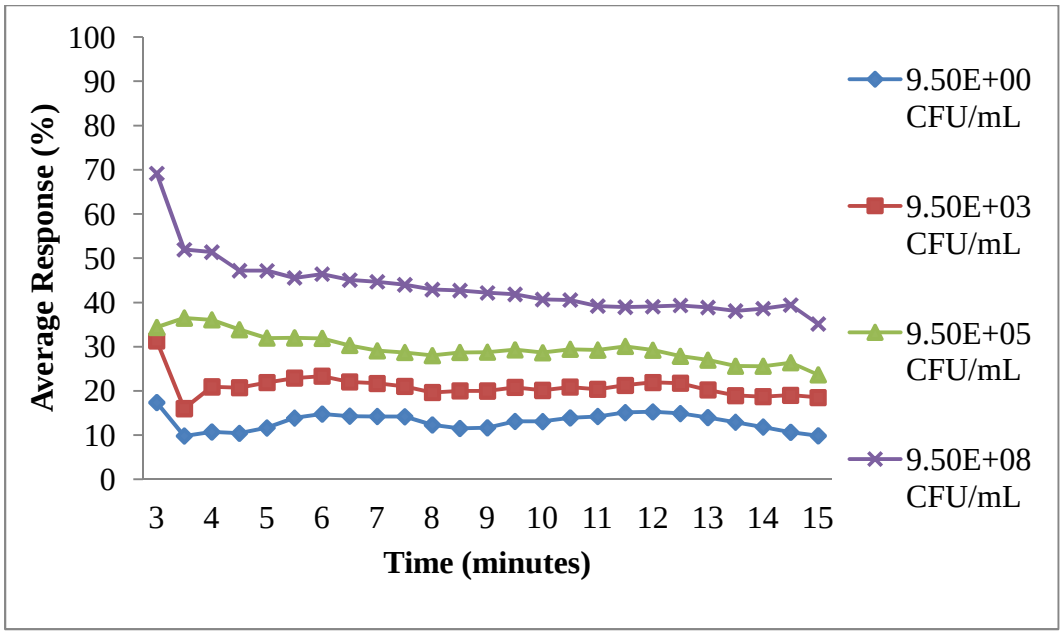

Figure 6-11. Average response over a period of 12 minutes (after a 3 minute equilibrium time) for the electrotextile biosensor with varying bacterial cell concentrations, fibers from experiment D.

When all 4 experimental sets conducted in triplicate were pooled together, the average resistance of the blank study (no bacteria) had a wide variation of 10.9 kΩ to 225.2 kΩ with an average value of 119.5 kΩ (standard deviation = 88.9 kΩ). This range can be attributed to variability in the manufacturing processes (polymer synthesis and deposition), the potential for inconsistencies of the amount and orientations of the bound antibodies and blocking proteins between the fiber membranes, and variability in the biosensor connections between runs. Because the range in the initial baseline for the system between lots is large, it is necessary to evaluate the system based on the response of the sensor and the average observed trends across multiple sensors. Normalizing the data using the signal to noise ratio to look at the sensor response can help minimize the effect caused by that variability.

All of the experiments were shown to follow the same trend, horizontal lines vertically stacked for each of the samples, with the samples with concentrations in the 10^0 CFU/mL range having the lowest response and the samples with concentrations in the 10^8 CFU/mL range having the highest response. The sensor response increases as the concentration of bacterial cells in the samples increases. Using a Student's t-test (2-tails, $\alpha = 0.05$) showed the in each experiment the sensor response for each positive concentration was significantly different than the blank sample. Lots A, B, and C could not significantly differentiate between the samples with concentrations in the range of 10^5 CFU/mL and 10^8 CFU/mL. Lot B could also not significantly differentiate between the samples with concentrations of 9.10×10^0 CFU/mL and 9.10×10^3 CFU/mL.

A total of 18 runs over 8 experiments conducted over multiple days were pooled together. The cumulative average response can be seen in Figure 6-12.

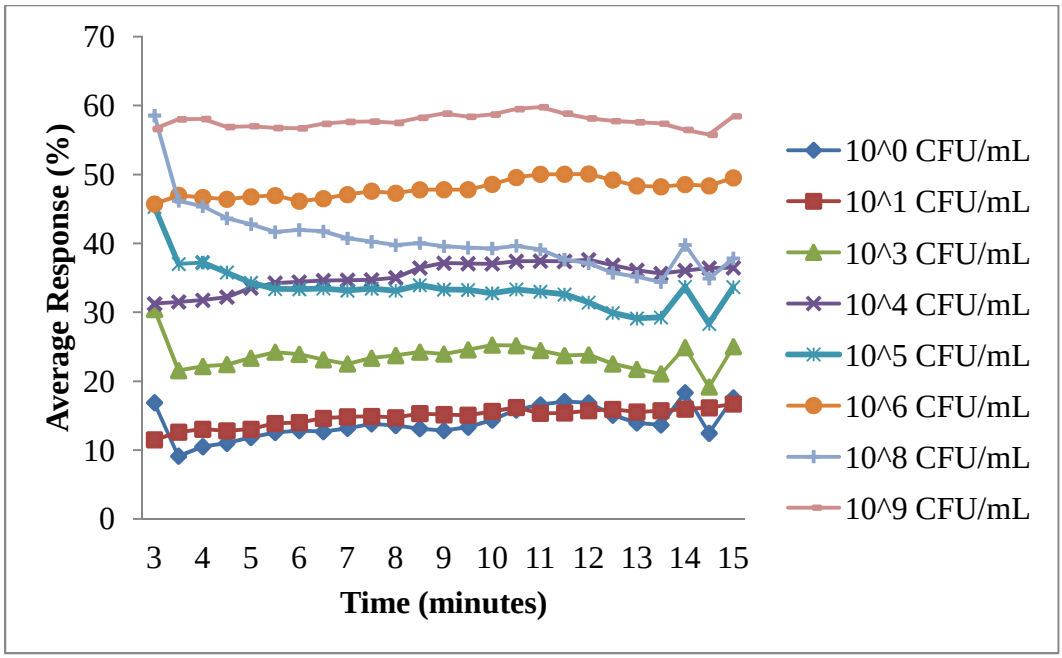

Figure 6-12. Cumulative average response at each time point of pooled multiple day data over a period of 12 minutes (after a 3 minute equilibrium time) for the electrotextile biosensor with varying bacterial cell concentrations.

In Figure 6-12, it can be seen that the original general trend of vertically stacked horizontal lines, with the response increasing as the concentration increases is still observed. There is overlap, however, between samples with close concentrations. Using a Student's t-test (2 tails, $\alpha = 0.05$) each sample was found to be significantly different from the blank. The t-test also showed that the sensor cannot significantly differentiate between positive samples, especially samples that are close in concentration (e.g. 10^0 and 10^1 CFU/mL, 10^8 and 10^9 CFU/mL). Within each of the experiments, a Student's t-test showed that the response of the sensor at each of the tested positive concentrations was significantly different than the blank. The lowest tested concentration was 3.23×10^0 CFU/mL. The highest tested concentration was 1.39×10^9 CFU/mL.

Based on the data, the trends in the biosensor results were found to be reproducible, however due to the variations between lots and the difficulty in differentiating between concentrations, the biosensor is not yet capable of being used as a quantitative detection system. The biosensor does work as a yes / no screening system. The results show that the biosensor has an experimental lower limit of detection of 3.23×10^0 CFU/mL for the detection of *E. coli* O157:H7 in pure culture.

6.4 Conclusions

A high surface area electrotextile based biosensor has been developed by the aqueous deposition of a functionalized conductive copolymer onto a nonwoven polypropylene microfiber mat. Pathogen specific antibodies were covalently attached to the fibers using glutaraldehyde. The proof of concept for the system was established by measuring the resistance response of the fibers when they were exposed to a target pathogen in solution over 15 minutes. By evaluating the system as a circuit with two resistors in parallel, it was found that the resistance of the system not associated with the electrotextile fibers contributed to only 2.8% of the total system resistance, and was determined not to be a significant contribution. The biosensor was shown to be able to differentiate between changes in conductivity due to the presence of a target pathogen in a solution over a sensitivity range of $10^0 - 10^9$ CFU/mL. By normalizing the resistance data using the signal to noise ratio to calculate the biosensor response, the reproducibility of the biosensor results was analyzed. It was found that the trends in the biosensor results were reproducible, however due to the variations between lots and the difficulty in differentiating between samples of different concentrations, the biosensor is not yet capable of being used as a

quantitative detection system. The ability of the biosensor to detect significant differences between samples that do and do not contain bacteria, as shown using a Student's t-test, indicates that the biosensor can work as a yes / no screening system. The initial results show that the biosensor has an experimental lower limit of detection of 3.23×10^{0} CFU/mL for the detection of *E. coli* O157:H7 in pure culture. This technology has the potential for application in the development of a light-weight, flexible, inexpensive, and disposable field based system for the rapid detection of various target pathogens.

Chapter 7 : Discussion and conclusions

The combined research presented in Chapters 3-6 describe the development of an electrochemical biosensor based on the use of nonwoven microfiber membranes coated with a conductive polymer and functionalized with antibodies for the biological capture and detection of *Escherichia coli* O157:H7, one of the U.S. military's top pathogens of interest for the development of rapid diagnostic systems. *E. coli* O157:H7 can cause severe gastroenteritis and is often spread through the consumption of contaminated food and water, which would rapidly render a large number of warfighters ineffective in performing their duties. Current standard detection technologies can be cumbersome and require generous quantities of chemicals and time to operate. The current FDA gold standard for identification of this pathogen from food matrices takes up to 3 days to generate a confirmed result. The research in this dissertation presents a rapid, novel, and inexpensive approach to the detection of *E. coli* O157:H7. The developed biosensor uses pathogen specific antibodies attached to conductive polymer coated nonwoven fibers for identification in 15 minutes.

The fabrication of electrically conductive fabrics is not a new concept. Previously, this type of material has been created by blending or mixing a conductive powder such as carbon black or silver particles with a polymer melt that is then extruded to form fibers [182]. The disadvantage of this method is that in order to achieve conductivity, the concentration of conductive powder must be high enough that the particles touch each other in order to conduct electricity [121]. This can result in changes to the fibers' physical properties that are unintended and undesired. To address this Gregory, Kimbrell, and Kuhn have published on the creation of conductive

fabrics by polymerizing pyrrole onto the surface to textile fibers (e.g. cotton, quartz, polyethylene terephthalate) [14, 16, 122, 166]. The most commonly used fiber material in these works is nylon. Gregory, Kimbrell, and Kuhn all reported performing a slow (2 – 6 hours), low concentration chemical oxidation onto the surface of nylon fabrics by combining the monomer (pyrrole) and oxidant ($FeCl_3$) and allowing them to react and form a pre-polymer species. This pre-polymer was then epitaxially deposited onto the surface of the fibers where polymerization was completed. The method detailed in this work for the fabrication of a conductive polymer coated fabric differs from these works in three significant ways. First, although the previous works cited did not report any material deformation or loss of strength when using nylon as the fiber platform, this was observed during the work detailed in Chapter 3. In this work, a nonwoven polypropylene fiber platform was coated in a conductive polypyrrole polymer coating using $FeCl_3$ as an oxidant, water as a solvent, and 5SSA as a dopant. The polypropylene fibers were found to better maintain their original material strength and durability post-polymerization. The previously published methods may not have suffered from this post-polymerization deformation because the solutions used were at relatively dilute concentrations and the order of addition to the fibers differed from this work. While the previously cited works formed a pre-polymer from the monomer and oxidant that was then applied to the fibers and allowed to react over several hours, in this work a two stage process was used where the monomer was adsorbed into the fibers and then reacted with the oxidant. The change in addition order, higher concentrations, and additional doping using 5SSA resulted of the fabrication of a black polypyrrole coating (more heavily oxidized) on the fiber surfaces in far less time (30 minutes). This change in the addition order of the reactants to the fibers helped improve the conformal nature of the coating at the higher concentrations used. Additionally, a carboxyl functional

group was added to the polymer via the addition of 3TAA as a co-monomer with the pyrrole in order to provide potential binding sites for biorecognition elements. The coated fibers were found to be conductive while still maintaining surface area and fiber durability.

In order for the conductive fibers to be used in a resistance based biosensor, there must also be a method available to bind biological molecules to the surface. One way of achieving this binding is by building a functional group into the fiber. In Chapter 3, a carboxyl functional group was added to the polymer by adding 3TAA as a co-monomer with the pyrrole. The binding of biological molecules such as antibodies to surfaces functionalized with carboxyls is a well-established process [157]. The use of 3TAA as an individual monomer or as a co-monomer with pyrrole to create conductive polymer thin films has been previously published [15, 183-185], however the combination of 3TAA and pyrrole for the synthesis of a functionalized conducting polymer thin film to be used for biological attachment has only been published once using vapor deposition [17]. Our approach however is liquid adsorption onto the fibers. In Chapter 3, the addition of a carboxyl functional group via 3TAA as a co-monomer with the pyrrole was analyzed using three-dimensional polypropylene fibers as the platform surface for the aqueous polymerization reaction. It was found to result in changes to the coating morphology, resistivity, elemental sulfur presence, and available binding sites for biorecognition elements, with each increasing as the concentration of 3TAA increased. This result was consistent with previously published work that found that increasing the ratio of pyrrole to 3TAA resulted in higher polymer conductivities [15, 17] but less binding potential for biological attachment [17]. Because increasing the concentration of 3TAA in the monomer solution resulted in increased

binding sites for biorecognition elements but also decreased the conductivity of the fibers, a concentration of 10 mg/mL was initially selected for use in developing the biosensor.

Biological attachment using avidin-biotin was achieved on the fibers and assessed optically and electrochemically. The use of a functionalized electrotextile for the detection of the avidin-biotin binding reaction was previously done by Bhattacharyya et al. [13] where an electrospun nylon fiber mat was coated with the conducting copolymer 3,4-ethylenedioxythiophene (EDOT) and 3-thiopheneethanol (3-TE) using oxidative chemical vapor deposition in order to make the coating conformal. This combination of reagents built a hydroxyl group into the polymer coating that was then used for avidin attachment. The avidin bound fibers were then assessed both optically and electrochemically for the attachment of biotin. Using the same methodologies as Bhattacharyya et al. for optical and electrochemical detection (confocal microscopy of FITC-avidin and biotinylated quantum dots and a simple electrochemical cell setup) the fiber membranes developed in Chapter 3 were found to be able to successfully detect biotin in solutions of 0.5, 5, 50, and 500 µM when a carboxyl functional group was present in a polypyrrole based electrotextile as a result of the 3TAA inclusion in the polymer.

Five factors were identified as significant in the synthesis of the conductive polypyrrole – 3TAA co-polymer. They were: concentration of pyrrole (monomer), concentration of 3TAA (monomer), concentration of $FeCl_3$ (oxidant), concentration of 5SSA (dopant), and polymerization time. These process conditions must be carefully controlled in order to generate a reproducible and effective polymer [121]. A central composite experimental design varying these factors was conducted in order to develop a multiple regression model of the

polymerization reaction. The use of a central composite design is a well-established method for performing regression / optimization analyses in many fields [165]. This includes the fields of biosensor development and polymer synthesis. Multiple regression modeling has been used to optimize biosensor performance based on influencing factors, such as signal output, structural parameters, electrical parameters and bacterial concentrations [186-188]. The use of multiple regression modeling is particularly useful for predicting and optimizing polymer properties which are often complex and non-linear and therefore not easy to accurately predict [189]. The effects of modifications to the polymerization process are difficult to predict because of the possibility of a large number of interactions between reagents resulting in multiple changes to the polymer. The use of multiple regression modeling and optimization has not been previously used with electrotextile fibers for biosensor development. This model was used to find the optimal conditions for each factor in order to generate the lowest experimentally possible electrotextile resistance. The optimal conditions were: 58.79% volume of pyrrole, 0.03 g/mL of 3TAA, 0.11 M $FeCl_3$, 0.25M 5SSA, and 70 minutes of reaction time to generate an electrotextile with a predicted resistance of 35.41 Ω. These conditions were experimentally verified and the mathematical model was statistically validated. The use of a multiple regression model provided a comprehensive means for not only optimizing but also characterizing the polymerization reaction.

In order for the fibers to be used as a biosensor, the target pathogen must be captured / attached to the fibers. *E. coli* O157:H7 specific antibodies were selected as the biorecognition element, but the necessary concentration and the method of attachment still needed to be determined. Antibody-antigen binding assays were then performed using standard attachment chemistry

techniques to determine the capture capability of the antibody-functionalized conductive membranes [157]. Attachment and capture efficiency were determined through the use of fluorescent labels and assessed using a fluorometer and confocal microscopy. The effect of blocking the fibers was also assessed. Passive adsorption, covalent binding using glutaraldehyde, and cross-linking using EDC and sulfo-NHS were all found to be effective immobilization methods, however glutaraldehyde demonstrated the best antibody attachment. While each of the tested methodologies is well established, analysis had not previously been done on comparing their effectiveness for attachment to electrotextile surfaces. With their three-dimensional, fibrous, porous structure, electrotextiles are a more complex attachment surface than planar metal electrodes, metallic or plastic beads, or polystyrene plates. One of the biggest issues that had to be assessed when performing attachment and capture on electrotextile surfaces was non-specific binding which is a common issue with membranes and textiles [190, 191]. Blocking of the fibers using BSA or goat serum combined with a wash step was found to reduce non-specific binding on the fibers. The tested scenario found to perform the best was using glutaraldehyde to attach the antibodies at a concentration of 10 µg/mL with goat serum used to block against nonspecific binding.

Granato et al. have previously shown that electrodes could be made from disposable electrospun fibers that were coated with a conductive polypyrrole polymer [12]. It was demonstrated that these electrodes could function as part of an electrochemical cell as a simple sensor system for the detection of phosphate and carbonate organic anions. Bhattacharrya et al. has also demonstrated that polymer coated fibers can function as an electrode in a simple electrochemical cell to perform sensing (avidin-biotin reaction) [13]. Neither Granato or Bhattacharrya,

however, have adapted their sensors to evaluate their performance as functioning biosensors for the detection of pathogens. In Chapter 6, the developed antibody-functionalized conductively coated nonwoven fibers were used as the electrode transducer in the design of an electrochemical biosensor for the detection of *E. coli* O157:H7. The proof of concept for the system was established by measuring the resistance response of the fibers when they were exposed to a target pathogen in solution over 15 minutes. By evaluating the system as a circuit with two resistors in parallel, it was found that the resistance of the system not associated with the electrotextile fibers was calculated to contribute only 2.8% of the total system resistance and was determined not to be a significant contribution. The biosensor was shown to be able to differentiate between small changes in conductivity due to the presence of the target pathogen in a solution over a concentration range of $10^0 – 10^9$ CFU/ mL. The sensor results were normalized for comparison between experiments. The trends in the biosensor results were reproducible, however due to the variations between lots and the difficulty in differentiating between positive samples, the biosensor is not yet capable of being used as a quantitative detection system. The ability of the biosensor to detect significant differences between samples that do and do not contain bacteria indicates that the biosensor can work as a yes / no screening system. The results show that the biosensor has an experimental lower limit of detection of 3.23×10^0 CFU/mL for the detection of *E. coli* O157:H7 in pure culture.

In summary, this research demonstrates the successful integration of conductive polymer synthesis, mathematical modeling and optimization of the polymerization process, biorecognition element immobilization, and electrochemistry for the development of an electrotextile based biosensor. The successful use of an electrotextile in the fabrication of an

electrochemical biosensor for the detection of a bacterial pathogen has the potential to result in the creation of a light-weight, flexible, inexpensive, and disposable method for the detection of various target pathogens. In Chapter 8 I will briefly discuss the necessary steps to advance this work for field readiness.

Chapter 8 : Future work

Future work is required to fully optimize the biosensor detection system for real world use. In order to improve the sensor for field readiness the variability of the sensor must be reduced through the use of coating optimization, further analysis of antibody immobilization and blocking techniques, and the development of an extraction method. After modifications to the sensor and experimental procedures have been made, the sensor system will still need to be tested to establish its functioning parameters such as limits of detection and specificities as well as validated before any sort of field testing can be introduced.

The optimization of the polymerization process on the nonwoven fibers, described in Chapter 4, and the blocking of the fibers using goat serum, described in Chapter 5, were the last experiments to be completed and therefore the optimized fibers with goat serum block have not been assessed in the biosensor yet. Optimizing the polymerization parameters in Chapter 4 appeared to reduce the variability in the initial electrotextile conductivity as well as lowering the overall electrotextile resistance when compared to the original established coating from Chapter 3. Comparison experiments will need to be conducted to determine if this is true and determine if there are any other coating parameters in the synthesis procedure that need to be optimized in order to improve the base material. Because the initial uncoated fibers are variable in thickness and direction, it is essential to try to reduce the variability between the coated fibers at every other component and fabrication step in order to have a functional sensing material. Because the fiber coating is heavier, has a different chemical makeup, and is more conductive than the coating that was used for establishing the antibody attachment protocol (Chapter 5) and for

establishing the initial biosensor sensitivity (Chapter 6), these tests will need to be repeated with the optimized fibers to establish if they need to be altered for the new fibers. The increase in concentration of 3TAA in the optimized fibers may improve the capture efficiency when using EDC / sulfo-NHS binding, resulting in the establishment of a new antibody attachment method for the sensor. Because the coating is heavier on the fibers, it may be necessary to add more wash steps in order to remove any excess unbound coating or nonspecifically attached pathogens. In addition, the fibers will need to be tested with several different potential electrolyte solutions in order to find one that allows the system to be conductive, but not reactive with the coating. Finally, the effect of goat serum as a blocking agent on the fiber conductivity will also need to be analyzed. While it was shown in Chapter 5 that a blocking agent is necessary, the concentration could potentially be reduced if it is found to have a significant effect on the electrotextile conductivity.

Although the current system has a low limit of detection, successfully detecting *E. coli* O157:H7 at levels as low as 10^0 CFU/ mL, this has only been done using pure culture that is added directly to the system. An extraction protocol must be developed for the biosensor in order for it to be useful in real world situations. One possibility is for the antibody-functionalized electrotextile membrane to be placed into diluted samples and allowed to react for 5 minutes. The bacteria within the sample will be captured by the antibodies attached to the surface and concentrated on the membrane forming a bacterial layer. When the electrotextile membrane is removed from the sample it will be rinsed in order to remove any non-specifically bound bacteria and inserted into the electrochemical cell as the working electrode, where the change in conductivity will indicate the presence or absence of the pathogen of interest. Another option would be to use

immunomagnetic separation to extract the target pathogen from the sample and then apply the extract directly to the electrotextile in the biosensor.

The use of an antibody coated bead for performing a separation step before the sample is added to the biosensor could also help with improving the biosensor specificity. Because only one type of antibody is being used for detection the biosensor is subject to the specificity of that antibody and has the potential for cross-reactivity with other non-target pathogens. Using a secondary antibody on non-conductive nanoparticle beads that differed from the antibody used on the fibers would help reduce the potential for false positives due to cross-reactivity. The non-conductive nanoparticles would only be attached to the pathogen that bound to both the primary and secondary antibodies and would create a second impedance layer. This second impedance layer could also be used to improve biosensor sensitivity by amplifying the measured resistance when the target pathogen is bound to the electrotextile surface.

The sensitivity of the biosensor could also be improved through the incorporation of an incubation step. At low bacterial concentrations, the change in the resistance of the circuit may be too low to differentiate from system noise. In order to increase system sensitivity at low concentrations, a short (<6 hours) incubation period could be built into the system protocol. An incubation of less than 6 hours allows for testing to still be conducted and a result generated within 1 work day shift. The use of an incubation period is already used in the gold standard methods of real-time PCR or plate counting recommended by the FDA [6].

Following the validation of the biosensor for detection with pure samples, a sensitivity study will need to be conducted for detection of *E. coli* O157:H7 in inoculated food samples, such as vegetables and fruits. The food samples may be inoculated with cell concentrations of $10^0 – 10^6$ CFU/mL. Testing will then be conducted with an identical procedure to the one used to determine the sensitivity of the biosensor with pure culture samples, as presented in Chapter 6. To determine the specificity of the biosensor, pure culture samples of *E. coli* O157:H7 may be tested and compared to the results of samples containing other common food and waterborne pathogens such as enterotoxigenic *Escherichia coli* (ETEC) strains, *Salmonella typhimurium*, *Shigella sonnei*, and *Campylobacter jejuni*. Samples would be prepared, diluted, plated and tested in an identical method to the one used to determine pure culture sensitivity.

In order to establish the robustness of the studies that determined the sensitivities, specificities, and limits of detection established for the sensor using varying food samples it will be necessary to validate the sensor data by completing blind studies as well as across lab testing. This will remove any potential experimenter's bias from the results. In addition, the sensor will need to be tested against other established comparative methods such as ELISA or PCR in order to determine if the sensor will actually be beneficial for real world use.

The goal of this work is to eventually develop a handheld reader for the electrotextile electrodes so that the biosensor can be used as a snap and read system where the electrotextile is exposed to the sample, removed, and inserted into the reader to be read with minimal handling and steps in-between. Once the sensor has been validated for food samples in the laboratory setting, the handheld reader will have to be developed and the system will have to be revalidated with the

new reader under actual in field conditions. In order to complete a comprehensive validation, the entire system will need to again be tested for sensitivity and specificity limits by using blind studies, across lab testing, and comparative studies against established detection methodologies under in field conditions. This will establish the feasibility and parameters for the successful use of the biosensor for detection of *E. coli* O157:H7 in foods for military use.

In summary, this research demonstrates the successful integration of conductive polymer synthesis, mathematical modeling and optimization of the polymerization process, biorecognition element immobilization, and electrochemistry for the development of an electrotextile based biosensor. More work is needed in order to create a biosensor that is viable for being used in the field. This work includes reduction in material variability via optimization and improvement of the electrotextile synthesis procedures, development of an extraction protocol for measuring samples, establishing sensitivity and specificity limits for the sensor with pure culture and food samples both in the lab and eventually in the field, and validating those procedures and limits by using blind studies and multi-lab testing to prevent experimenter's bias in the results.

APPENDICES

APPENDIX A: STANDARD OPERATING PROCEDURES

A.1 FIBER SYNTHESIS PROTOCOL

Project: Conductive Polymer Coated Non-Woven Fiber Based Biosensor

Protocol: Polymerization of Doped Polypyrrole on Fibers

PPE: BSL-1; standard lab coat and latex or nitrile gloves, long pants, close-toed shoes, protective eye wear

Materials:

I. Chemicals

a. Ferric Chloride ($FeCl_3$)

b. Pyrrole (C_4H_5N)

c. 3-Thiopheneacetic Acid, 3TAA ($C_6H_6O_2S$)

d. 5-Sulfosalicylic Acid Hydrate, 5SSA ($HO_3SC_6H_3$-2-$(OH)CO_2H$•xH_2O)

e. Reagent Grade Water

II. Equipment

a. Glass staining box

b. Scissors

c. Pipettors

d. 10mL and 1mL Pipette Tips

e. Forceps

f. Oscillator or Rocker

g. Punch and hammer

Procedure:

1. Measure and cut fiber sheet to dimensions of 6 cm x 8 cm so it can lay flat in reaction container.
2. Soak fiber sample in pyrrole-3TAA solution (10% volume pyrrole to water with 10 mg/mL 3TAA) for 1 minute.
3. Lay wet sheet flat on bottom of glass staining box.
4. Add 30mL of 0.1 M $FeCl_3$ in water solution to box.
5. Add 3mL of 0.1M 5SSA in water solution to box.
6. Secure lid and place on oscillator or rocker on low setting so liquid is moving over and under fiber sample, but not washing it against the side of the box. Let to react for 30 min.
7. Remove sample and rinse both sides with water. Lay flat to dry.
8. If in chemical hood, flip after 15 min.
9. If on benchtop, flip after 1 hr.
10. Cut sample using punch and mallet for resistance measuring and testing.

A.2 OPTIMIZED FIBER SYNTHESIS PROTOCOL

Project: Conductive Polymer Coated Non-Woven Fiber Based Biosensor

Protocol: Optimized Polymerization of Doped Polypyrrole on Fibers

PPE: BSL-1; standard lab coat and latex or nitrile gloves, long pants, close-toed shoes, protective eye wear

Materials:

I. Chemicals

a. Ferric Chloride ($FeCl_3$)

b. Pyrrole (C_4H_5N)

c. 3-Thiopheneacetic Acid, 3TAA ($C_6H_6O_2S$)

d. 5-Sulfosalicylic Acid Hydrate, 5SSA ($HO_3SC_6H_3$-2-$(OH)CO_2H$•xH_2O)

e. Reagent Grade Water

II. Equipment

a. Glass staining box

b. Scissors

c. 10mL and 1mL Pipette Tips

d. Pipettors

e. Forceps

f. Oscillator or Rocker

g. Punch and hammer

Procedure:

1. Measure and cut fiber sheet to dimensions of 6 cm x 8 cm so it can lay flat in reaction container.
2. Soak fiber sample in pyrrole-3TAA solution (58.79% volume pyrrole to water with 0.03 g/mL 3TAA) for 1 minute.
3. Lay wet sheet flat on bottom of glass staining box.
4. Add 30mL of 0.11 M $FeCl_3$ in water solution to box.
5. Add 3mL of 0.25 M 5SSA in water solution to box.
6. Secure lid and place on oscillator or rocker on low setting so liquid is moving over and under fiber sample, but not washing it against the side of the box. Let to react for 70 min.
7. Remove sample and rinse both sides with water. Lay flat to dry.
8. If in chemical hood, flip after 15 min.
9. If on benchtop, flip after 1 hr.
10. Cut sample using punch and mallet for resistance measuring and testing.

A.3 ANTIBODY PASSIVE ADSORPTION PROTOCOL

Project: Conductive Polymer Coated Non-Woven Fiber Based Biosensor

Protocol: Antibody Immobilization, Passive Adsorption (96 well size)

PPE: BSL-1; standard lab coat and latex or nitrile gloves, long pants, close-toed shoes, protective eye wear

Materials:

I. Chemicals

a. Sterile Distilled Water

b. KPL Bactrace ® Goat Anti-*E.coli* O157:H7 diluted to desired concentration in 1x PBS

c. Blocking Agent (5% w/v Bovine Serum Albumin or 5% KPL Normal Goat Serum)

d. Phosphate Buffered Saline (1x PBS)

e. Phosphate Buffered Saline with 0.1% Tween-20 (PBST)

II. Equipment

a. Conductive Fiber Electrotextile

b. Scissors

c. Punch and Hammer

d. 96 well plate

e. Pipette Tips, 1mL and 100 µL

f. Pipettors

g. Forceps

h. Oscillator or Rocker

i. Refrigerator

Procedure:

1. Cut nonwoven fibers into 96 well size discs using punch and hammer.
2. Put 1 disc into each well of a 96 well plate.
3. Wash nonwoven fiber discs with sterile water and dry for 10 minutes.
4. Add 250 µL of antibody at desired concentration to each disc.
5. Incubate fiber discs with antibody for 1 hr at room temperature with gentle agitation.
6. Remove antibody solution and apply 50 µL of blocking agent solution.
7. Allow fibers and blocking agent to react at room temperature with gentle agitation for 1 hour.
8. Wash fibers twice with PBS.
9. Wash fibers once with PBST and refrigerate until use.

A.4 ANTIBODY GLUTARALDEHYDE PROTOCOL (96 WELL PLATE)

Project: Conductive Polymer Coated Non-Woven Fiber Based Biosensor

Protocol: Antibody Immobilization, Glutaraldehyde (96 well size)

PPE: BSL-1; standard lab coat and latex or nitrile gloves, long pants, close-toed shoes, protective eye wear

Materials:

I. Chemicals

a. Sterile Distilled Water

b. Glutaraldehyde

c. KPL Bactrace ® Goat Anti-*E.coli* O157:H7 diluted to desired concentration in 1x PBS

d. Deactivating Buffer (0.2 M Tris, 10 mM Sodium Cynaoborohydride)

e. Blocking Agent (5% w/v Bovine Serum Albumin or 5% KPL Normal Goat Serum)

f. Phosphate Buffered Saline (1x PBS)

g. Phosphate Buffered Saline with 0.1% Tween-20 (PBST)

II. Equipment

a. Conductive Fiber Electrotextile

b. Scissors

c. Punch and Hammer

d. 96 well plate

e. Pipette Tips, 1mL and 100 µL

f. Pipettors

g. Forceps

h. Oscillator or Rocker

i. Incubator

j. Refrigerator

Procedure:

1. Cut nonwoven fibers into 96 well size discs using punch and hammer.
2. Put 1 disc into each well of a 96 well plate.
3. Wash nonwoven fiber discs with sterile water and dry for 10 min.
4. Add 25 µL of 2.5 mM glutaraldehyde to each disc and incubate for 1 hr at 4˚C.
5. Wash fibers with distilled water and dry for 10 min.
6. Add 250 µL of antibody at desired concentration to each disc.
7. Incubate fiber discs with antibody for 15 min at 37˚C.
8. Wash fibers with distilled water and dry for 10 min.
9. Add 50 µL of deactivating buffer and incubate for 15 min at 37˚C.
10. Wash fibers with distilled fibers and dry for 10 min.
11. Apply 50 µL of blocking agent solution.
12. Allow fibers and blocking agent to react at room temperature with gentle agitation for 1 hr.
13. Wash fibers twice with PBS.
14. Wash fibers once with PBST and refrigerate until use.

A.5 ANTIBODY GLUTARALDEHYDE PROTOCOL (2 CM X 2 CM SQUARE)

Project: Conductive Polymer Coated Non-Woven Fiber Based Biosensor

Protocol: Antibody Immobilization, Glutaraldehyde (2 cm x 2 cm squares)

PPE: BSL-1; standard lab coat and latex or nitrile gloves, long pants, close-toed shoes, protective eye wear

Materials:

I. Chemicals

a. Glutaraldehyde

b. KPL Bactrace ® Goat Anti-*E.coli* O157:H7 (10 µg/mL in 1x PBS)

c. Deactivating Buffer (0.2 M Tris, 10 mM Sodium Cynaoborohydride)

d. Blocking Agent (5% w/v Bovine Serum Albumin or 5% KPL Normal Goat Serum)

e. Phosphate Buffered Saline (1x PBS)

f. Phosphate Buffered Saline with 0.1% Tween-20 (PBST)

II. Equipment

a. Conductive Fiber Electrotextile

b. Scissors

c. 6 well plate

d. Pipette Tips, 1mL and 100 µL

e. Pipettors

f. Forceps

g. Oscillator or Rocker

h. Incubator

i. Refrigerator

Procedure:

1. Cut nonwoven fibers into 2 cm x 2cm squares.
2. Put 1 square into each well of a 6 well plate.
3. Wash nonwoven fiber squares with 0.01 M PBS and dry for 10 min.
4. Add 3 mL of 2.5 mM glutaraldehyde to each well and incubate for 1 hr at 4˚C.
5. Wash fibers with 0.01 M PBS and dry for 10 min.
6. Add 4 mL of antibody to each square.
7. Incubate fiber squares with antibody for 15 min at 37˚C.
8. Wash fibers with 0.01 M PBS and dry for 10 min.
9. Add 3 mL of deactivating buffer and incubate for 15 min at 37˚C.
10. Wash fibers with 0.01 M PBS and dry for 10 min.
11. Apply 3 mL of blocking agent solution.
12. Allow fibers and blocking agent to react at room temperature with gentle agitation for 1 hr.
13. Wash fibers twice with PBS.
14. Wash fibers once with PBST and refrigerate until use.

A.6 ANTIBODY EDC / SULFO-NHS PROTOCOL (96 WELL PLATE)

Project: Conductive Polymer Coated Non-Woven Fiber Based Biosensor

Protocol: Antibody Immobilization, EDC / Sulfo-NHS (96 well size)

PPE: BSL-1; standard lab coat and latex or nitrile gloves, long pants, close-toed shoes, protective eye wear

Materials:

I. Chemicals

a. Sterile Distilled Water

b. N-(3-dimethylaminopropyl)-N'-ethylcarbodiimide Hydrochloride (EDC)

c. N-hydroxysulfosuccinimide (Sulfo-NHS)

d. 2-(N-morpholino)ethanesulfonic Acid Buffer (MES), 50 mM

e. KPL Bactrace ® Goat Anti-*E.coli* O157:H7 diluted to desired concentration in 1x PBS

f. Blocking Agent (5% w/v Bovine Serum Albumin or 5% KPL Normal Goat Serum)

g. Phosphate Buffered Saline (1x PBS)

h. Phosphate Buffered Saline with 0.1% Tween-20 (PBST)

II. Equipment

a. Conductive Fiber Electrotextile

b. Scissors

c. Punch and Hammer

d. 96 well plate

e. Pipette Tips, 1mL and 100 µL

f. Pipettors

g. Forceps

h. Oscillator or Rocker

i. Refrigerator

Procedure:

1. Cut nonwoven fibers into 96 well size discs using punch and hammer.
2. Put 1 disc into each well of a 96 well plate.
3. Wash nonwoven fiber discs with sterile water and dry for 10 min.
4. Add 200 µL of EDC and Sulfo-NHS in MES buffer at manufacturer's recommended concentrations to fibers and react with gentle agitation at room temperature for 15 minutes.
5. Wash fibers twice with MES buffer.
6. Add 250 µL of antibody at desired concentration to each disc.
7. Incubate fiber discs with antibody with gentle agitation for 4 hrs at room temperature.
8. Wash fibers with MES buffer.
9. Apply 50 µL of blocking agent solution.
10. Allow fibers and blocking agent to react at room temperature with gentle agitation for 1 hr.
11. Wash fibers twice with PBS.
12. Wash fibers once with PBST and refrigerate until use.

A.7 PICOGREEN STAINING OF CELLS

Project: Conductive Polymer Coated Non-Woven Fiber Based Biosensor

Protocol: PicoGreen Staining of Bacterial Cells

PPE: BSL-1; standard lab coat and latex or nitrile gloves, long pants, close-toed shoes, protective eye wear

Materials:

I. Reagents
   a. Full Grown Bacterial Culture in Growth Medium Broth
   b. PicoGreen dsDNA stain
   c. Sterile Distilled Water

II. Equipment
   a. 2 mL Centrifuge Tubes
   b. Pipette Tips, 10 mL, 1 mL and 10 µL
   c. Pipettors
   d. Centrifuge
   e. Vortex
   f. Oscillator

Procedure:

1. Remove 1 mL of cell culture and pellet in centrifuge for 3 min at 5,000 x g.
2. Remove supernatant and resuspend pellet in 5 µL PicoGreen and 500 µL water, vortex.
3. Place sample in rotating oscillator and rotate for 5 min at room temperature with no light while stain cross-links with cells.

4. Pellet stained cells in centrifuge for 3 min at 5,000 x g.
5. Remove supernatant and resuspend pellet with 1 mL of water, vortex.
6. Dilute stained cells to necessary volume / concentration with water.

A.8 FLUORESCENT MEASUREMENT OF CAPTURED STAINED CELLS

Project: Conductive Polymer Coated Non-Woven Fiber Based Biosensor

Protocol: Measuring Fluorescence of Captured Cells (96 well plate)

PPE: BSL-1; standard lab coat and latex or nitrile gloves, long pants, close-toed shoes, protective eye wear

Materials:

I. Reagents

a. PicoGreen Stained Bacteria Cells (approximate concentration of 10^7 CFU/mL)

b. Phosphate Buffered Saline (1x PBS)

II. Equipment

a. Conductive electrotextile fibers (96 well plate size) with immobilized antibodies

b. 96 well plate (black)

c. Pipette Tips, 1 mL

d. Pipettors

e. Victor3 MuliLabel Counter

Procedure:

1. Place antibody functionalized fibers into wells of 96 well plate.
2. Add 200 µL of PicoGreen stained cells to each well.
3. Incubate fibers with cells for 15 min at 37˚C.
4. Wash fibers 3 times with PBS.
5. Pipette all excess liquid off of each fiber, make sure fibers are lying flat in the bottom of each well.

6. Place plate with fibers into Victor.
7. Read fluorescence output of plate using FITC program, excitation of 490 nm and emission of 535 nm.

A.9 ELECTROCHEMICAL MEASUREMENT USING BIOSENSOR

Project: Conductive Polymer Coated Non-Woven Fiber Based Biosensor

Protocol: Measuring Resistance Across Fibers in Biosensor

PPE: BSL-1; standard lab coat and latex or nitrile gloves, long pants, close-toed shoes, protective eye wear

Materials:

I. Reagents

a. Sterile Distilled Water

b. Bacterial Serial Dilutions (Cells Washed Using Centrifuge and Resuspended in Butterfield's Phosphate Buffer)

c. Butterfield's Phosphate Buffer (Blank)

d. Phosphate Buffer (0.1 M PB)

e. Bleach

f. Ethanol

II. Equipment

a. Conductive electrotextile fibers (2 cm x 2 cm) with immobilized antibodies

b. Glass beaker

c. Pipettors

d. Pipette Tips, 10 mL and 1 mL

e. Alligator Clip Leads

f. Potentiostat

Procedure:

1. Turn on potentiostat and attach alligator clip leads.
2. Place leads into beaker with 20 mL of distilled water and secure leads to opposing sides of beaker.
3. Run potentiostat for constant potential amperometry with a constant voltage of 0.5 V for 30 min – 2 hr to warm up system, taking a measurement every minute.
4. If result at end of warm up is a horizontal line, system is ready for use.
5. Empty beaker.
6. Attach electrotextile fibers to alligator clip leads, with each lead attached at opposing sides, facing each other, going into the fibers to the depth of the 3rd tooth.
7. Insert fibers with alligator clip leads into glass beaker.
8. Attach alligator clip leads to the potentiostat.
9. Secure wires to opposing sides of beaker so fibers are lying flat on bottom of the beaker and pulled taut, but not being strained.
10. Submerge fibers in 18 mL of PB.
11. Add 2 mL of sample and stir gently with pipette tip to mix sample with solution.
12. Run potentiostat using constant potential amperometry at a constant voltage of 0.5 V for 15 min taking a measurement every 30 s.
13. Record measured current over time.
14. Clean glassware, alligator clip leads, and forceps between different bacterial concentration samples.
15. Repeat for each sample.

A.10 BACTERIAL CULTURE TRANSFER AND GROWTH

Project: Conductive Polymer Coated Non-Woven Fiber Based Biosensor

Protocol: Transfer of *E. coli* O157:H7 Sakai Strain Cultures and Growth

PPE: BSL-1; standard lab coat and latex or nitrile gloves, long pants, close-toed shoes, protective eye wear

Materials:

I. Reagents

   a. Trypticase Soy Broth (TSB)

   b. CHROMagar O157 plate with *E. coli* O157:H7 Sakai Strain Culture

II. Equipment

   a. Biosafety cabinet

   b. Vortex

   c. 15 ml Sterile Tubes

   d. Inoculating Loop

   e. 1000 µl pipette

   f. 1000 µl pipette tips with filter (sterile)

Procedure (all in biosafety cabinet):

1. Remove CHROMAGAR O157 plate with bacterial culture from refrigerator and remove one colony from plate using inoculating loop.
2. Transfer colony to 9 mL of sterile TSB.
3. Incubate at 37˚C for 48 hrs to bring culture to maximum concentration.
4. Vortex 48 hr microbial culture.

5. Transfer 1 mL of the culture into 9 mL of sterile TSB.
6. Vortex
7. Incubate the new culture tube for 4 hrs at 37°C.

APPENDIX B: DATA

B.1 CHAPTER 3 DATA

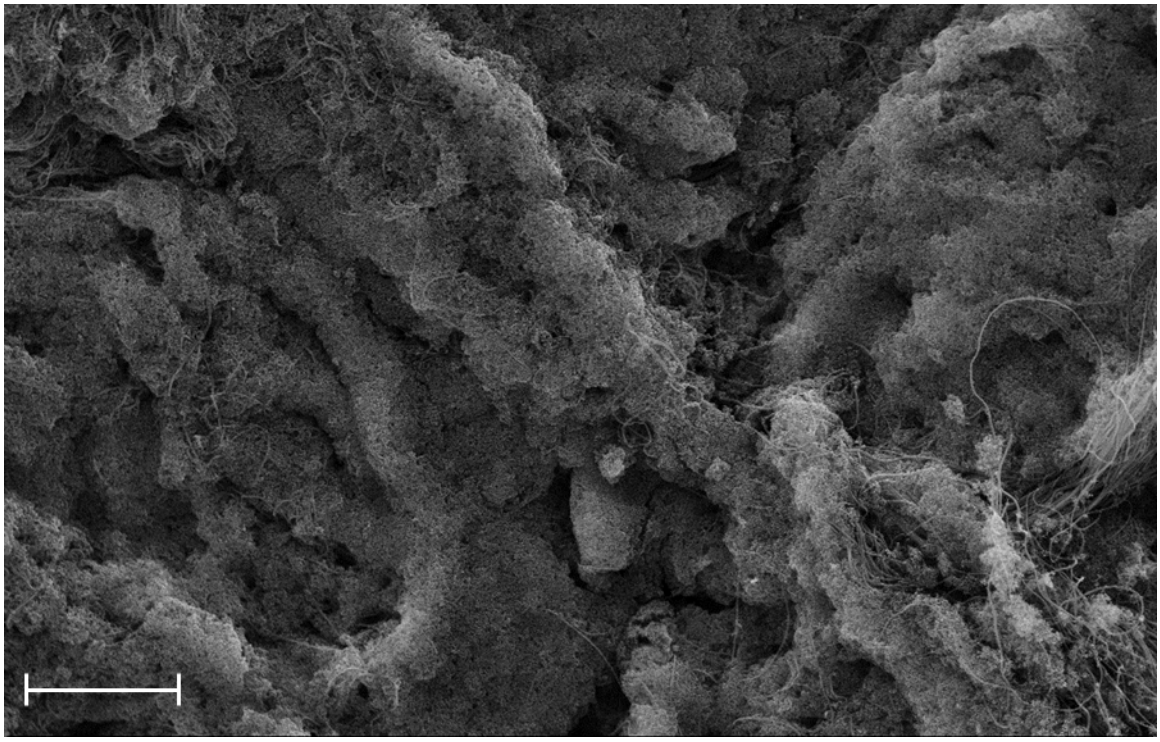

Figure B- 1. SEM image of Nylon 6fibers with 3-COOH and pyrrole polymer coating, acetonitrile solvent, 18 hour reaction time. Scale bar equal to 100 µm, magnification at 500x, EHT of 30 kV and working distance of 6.0 mm.

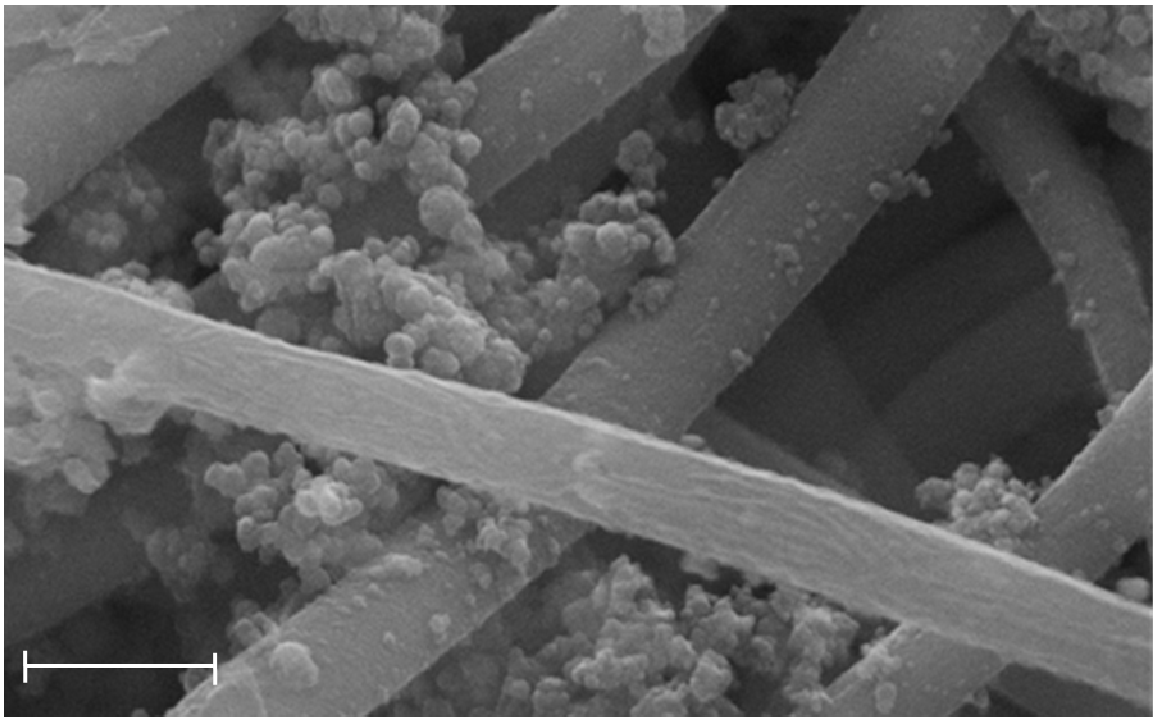

Figure B- 2. SEM image of Nylon -6 fibers with 3-COOH and pyrrole polymer coating, acetonitrile solvent, 18 hour reaction time. Scale bar equal to 2 µm, magnification of 30,000x, EHT of 30 kV and working distance of 6.0 mm.

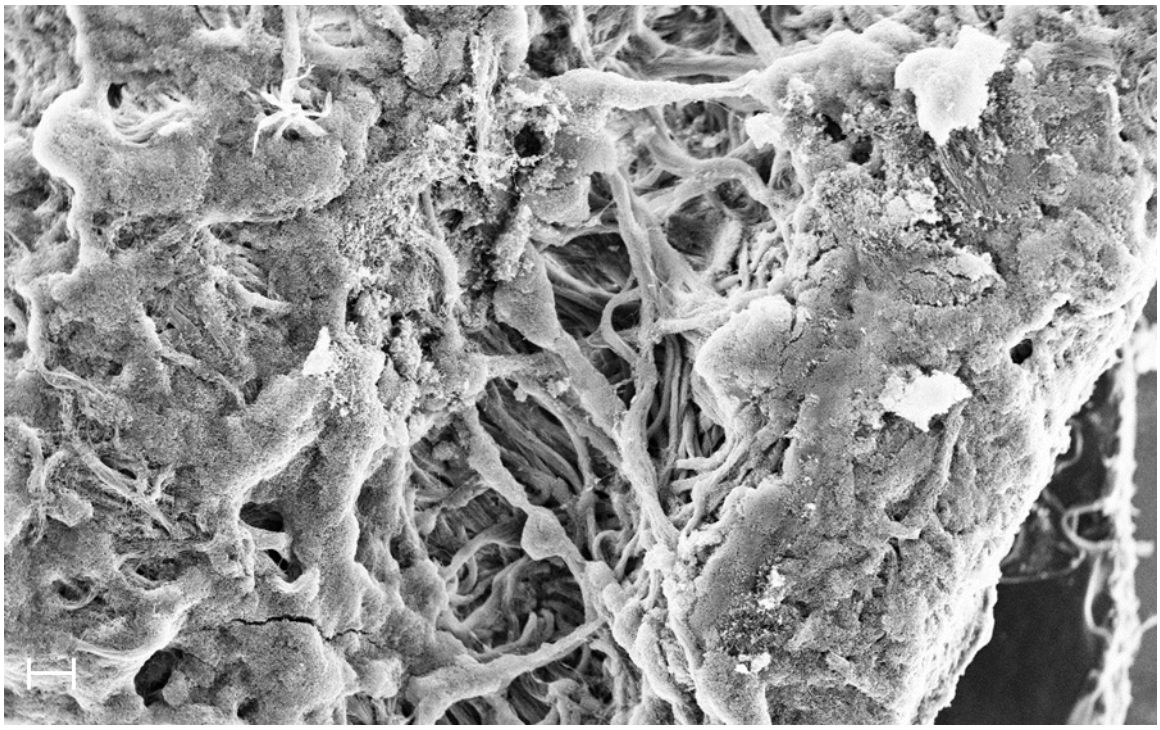

Figure B- 3. SEM image of Nylon-6 fibers with 3TAA and pyrrole polymer coating, acetonitrile solvent, 18 hour reaction time. Scale bar equal to 100 µm, magnification of 150x, EHT of 30 kV and working distance of 6.0 mm.

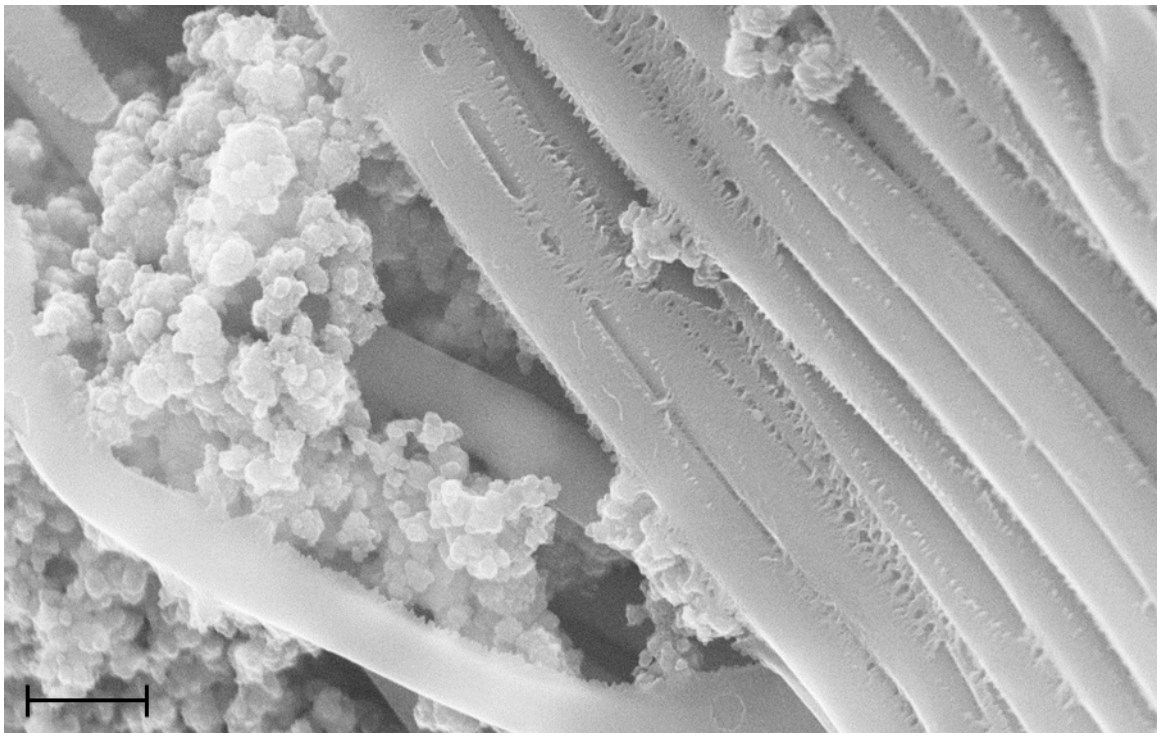

Figure B- 4. SEM image of Nylon-6 fibers with 3TAA and pyrrole polymer coating, acetonitrile solvent, 18 hour reaction time. Scale bar equal to 2 µm, magnification of 20,000x, EHT of 30 kV and working distance of 6.0 mm.

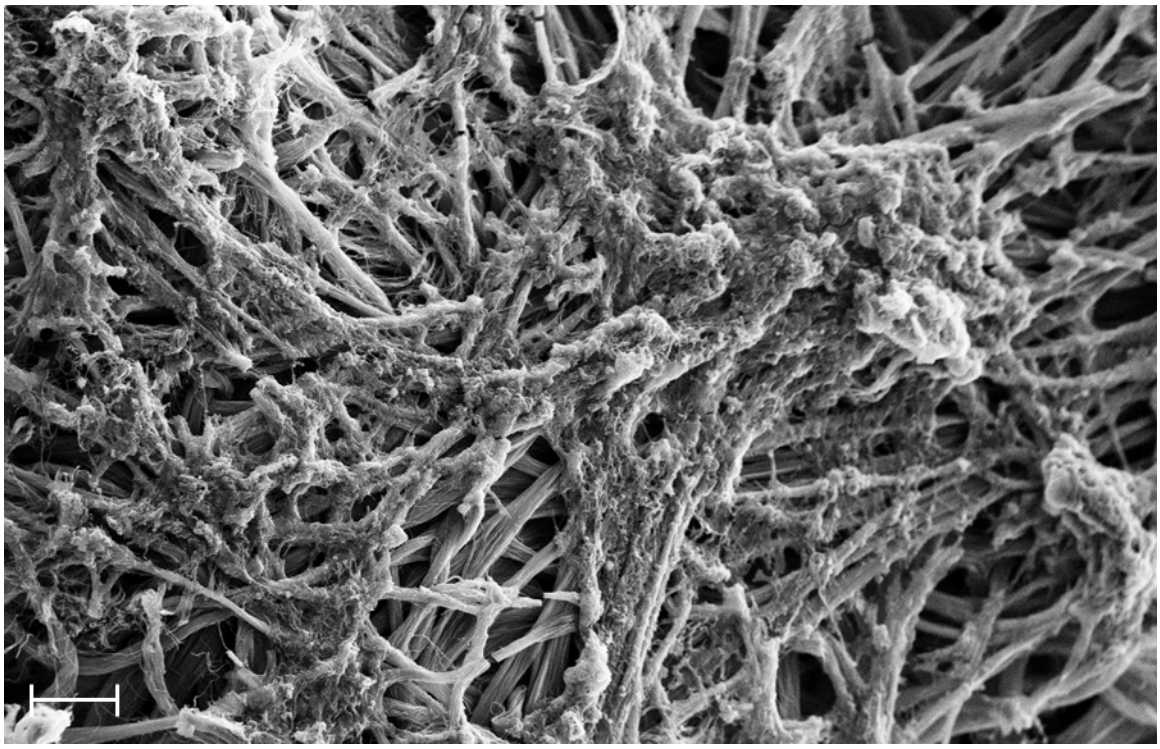

Figure B- 5. SEM image of Nylon-6 fibers with 3TAA and pyrrole polymer coating, methanol solvent, 5SSA dopant, 30 minute reaction time. Scale bar equal to 100 µm, magnification of 200x, EHT of 30 kV and working distance of 6.0 mm.

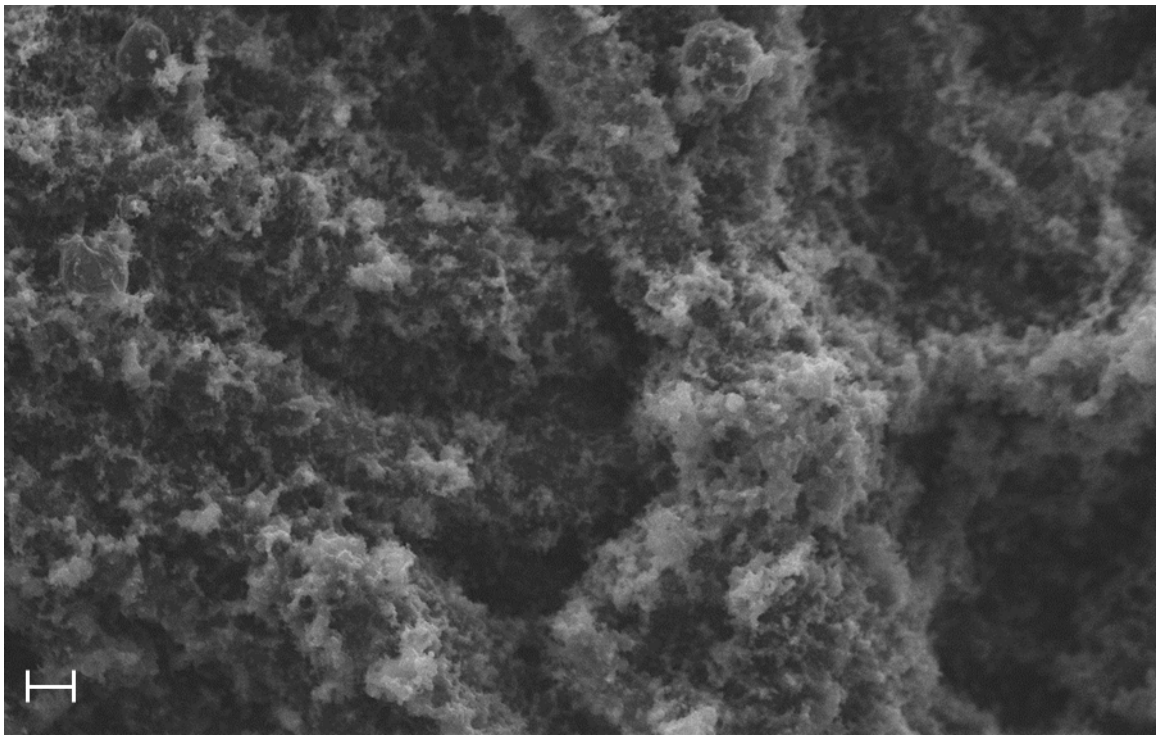

Figure B- 6. SEM image of Nylon-6 fibers with 3TAA and pyrrole polymer coating, water solvent, 5SSA dopant, 30 minute reaction time. Scale bar equal to 20 µm, magnification of 500x, EHT of 30 kV and working distance of 8.0 mm.

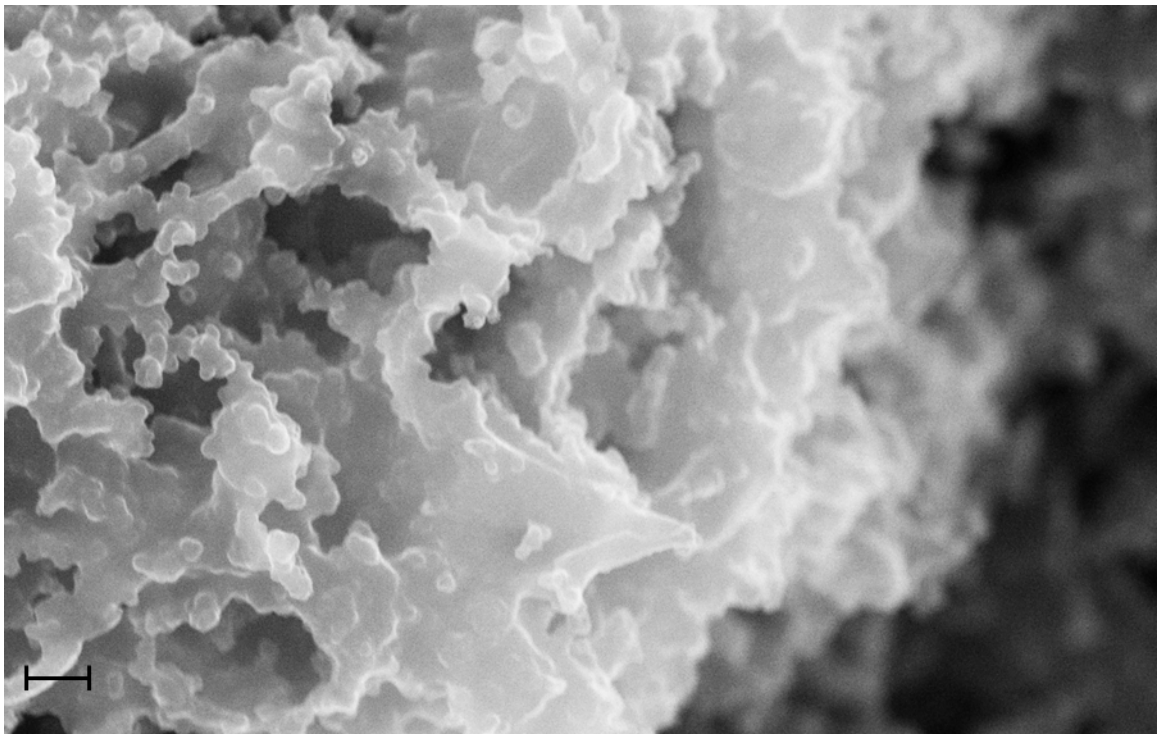

Figure B- 7. SEM image of Nylon-6 fibers with 3TAA and pyrrole polymer coating, water solvent, 5SSA dopant, 30 minute reaction time. No rinse. Scale bar equal to 2 µm, magnification of 10,000x, EHT of 30 kV and working distance of 6.0 mm.

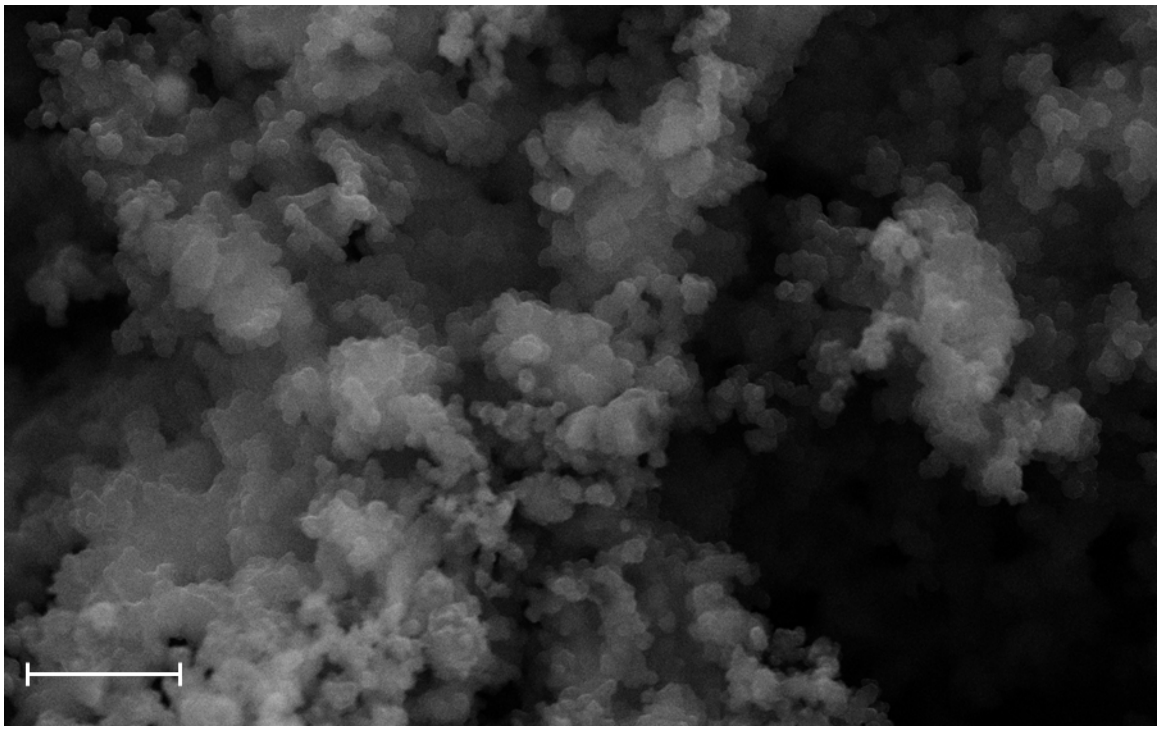

Figure B- 8. SEM image of Nylon-6 fibers with 3TAA and pyrrole polymer coating, water solvent, 5SSA dopant, 30 minute reaction time. DI water rinse. Scale bar equal to 10 µm, magnification of 5,000x, EHT of 30 kV and working distance of 6.0 mm.

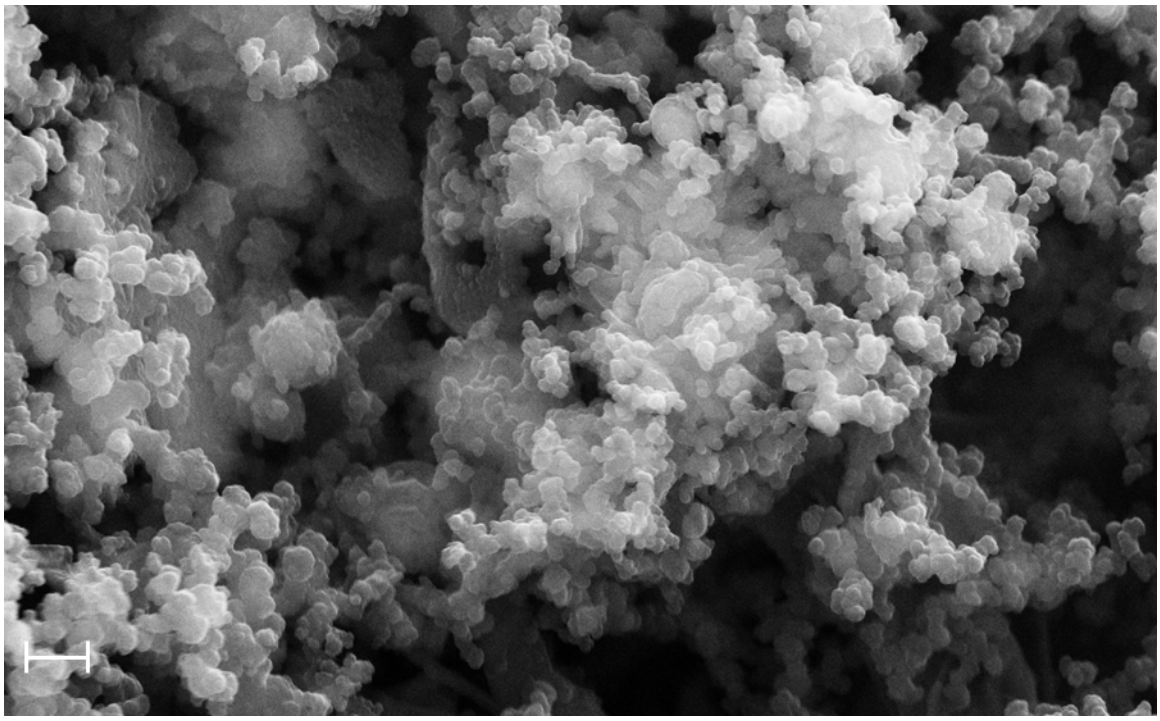

Figure B- 9. SEM image of Nylon-6 fibers with 3TAA and pyrrole polymer coating, water solvent, 5SSA dopant, 30 minute reaction time. DI water rinse and sonication. Scale bar equal to 2 µm, magnification of 10,000x, EHT of 30 kV and working distance of 6.0mm.

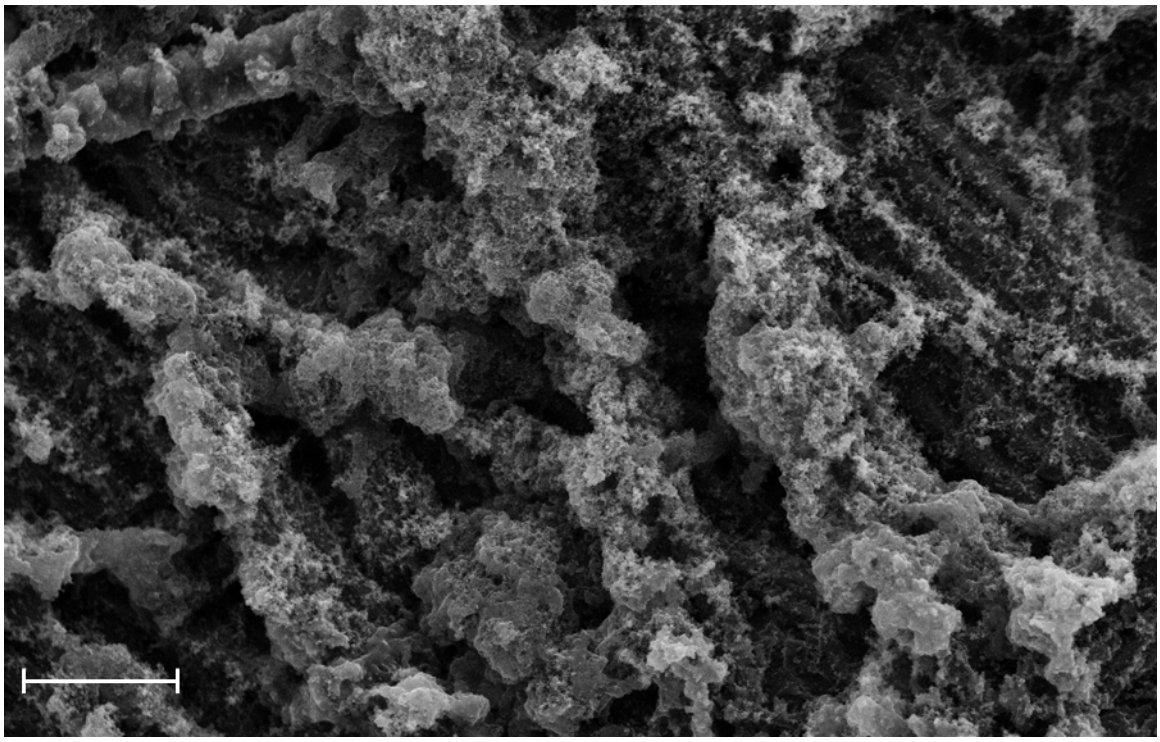

Figure B- 10. SEM image of Nylon-6 fibers with 3TAA and pyrrole polymer coating, water solvent, 5SSA dopant, 30 minute reaction time. DI water rinse. Scale bar equal to 100 µm, magnification of 500x, EHT of 30 kV and working distance of 6.0 mm.

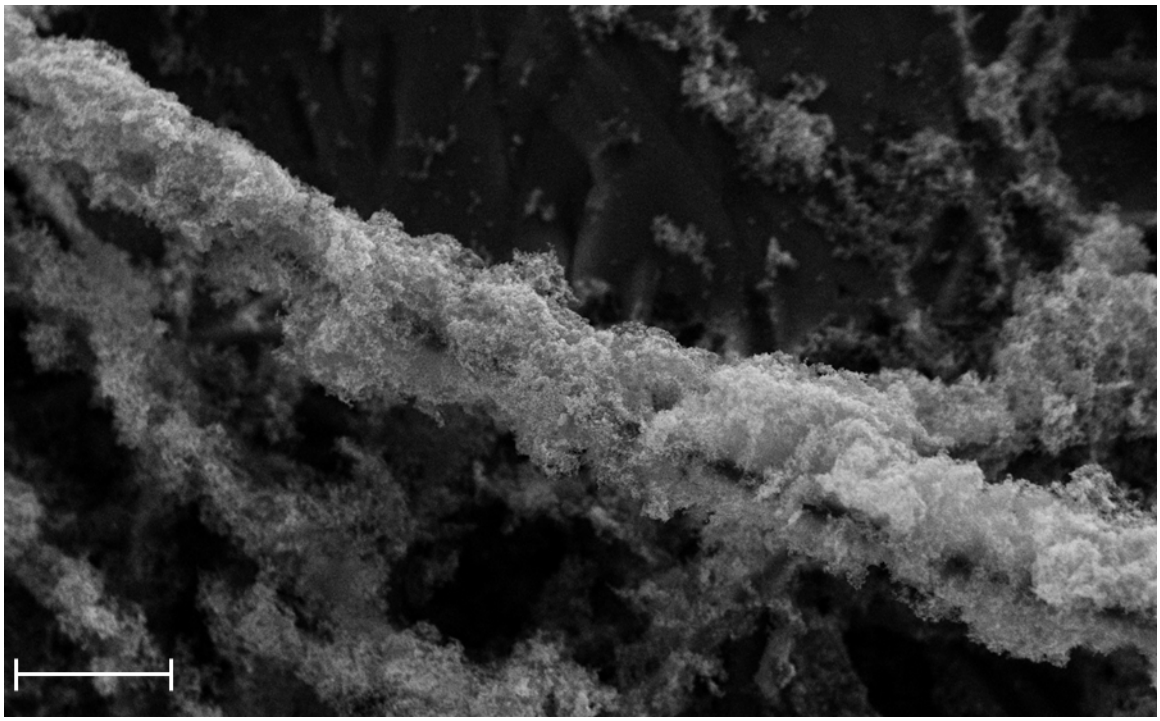

Figure B- 11. SEM image of polypropylene fibers with 3TAA and pyrrole polymer coating, water solvent, 5SSA dopant, 30 minute reaction time. DI water rinse. Scale bar equal to 100 µm, magnification of 500x, EHT of 30 kV and working distance of 6.0 mm.

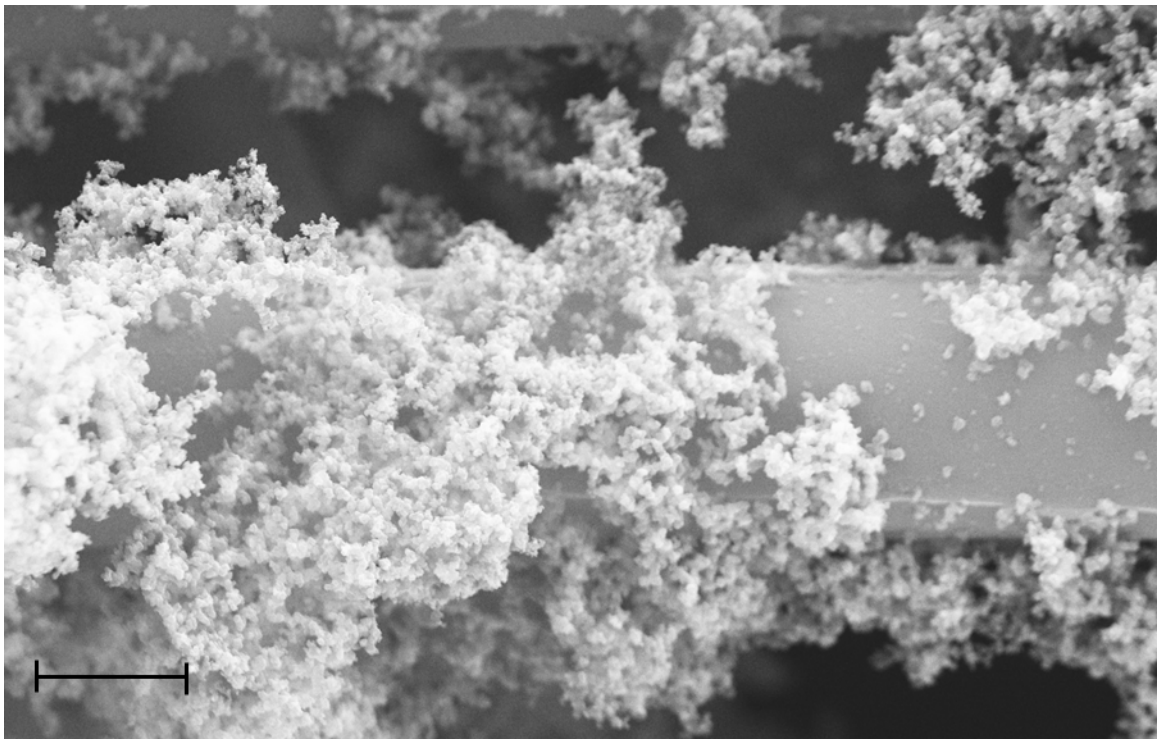

Figure B- 12. SEM image of fibers with polymer coating containing 0 mg/mL 3TAA. Scale bar equal to 10 µm, magnification of 5,000x, EHT of 30 kV and working distance of 6.0 mm.

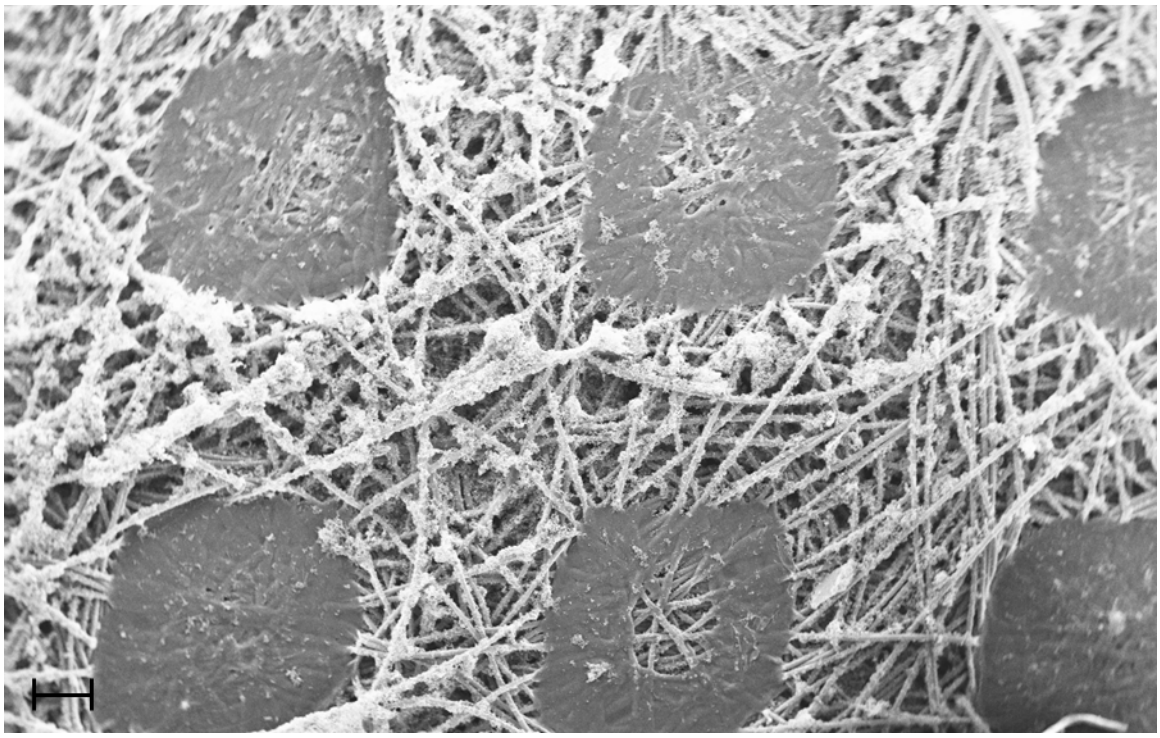

Figure B- 13. SEM image of fibers with polymer coating containing 0 mg/mL 3TAA. Scale bar equal to 200 µm, magnification of 100x, EHT of 30 kV and working distance of 6.0 mm.

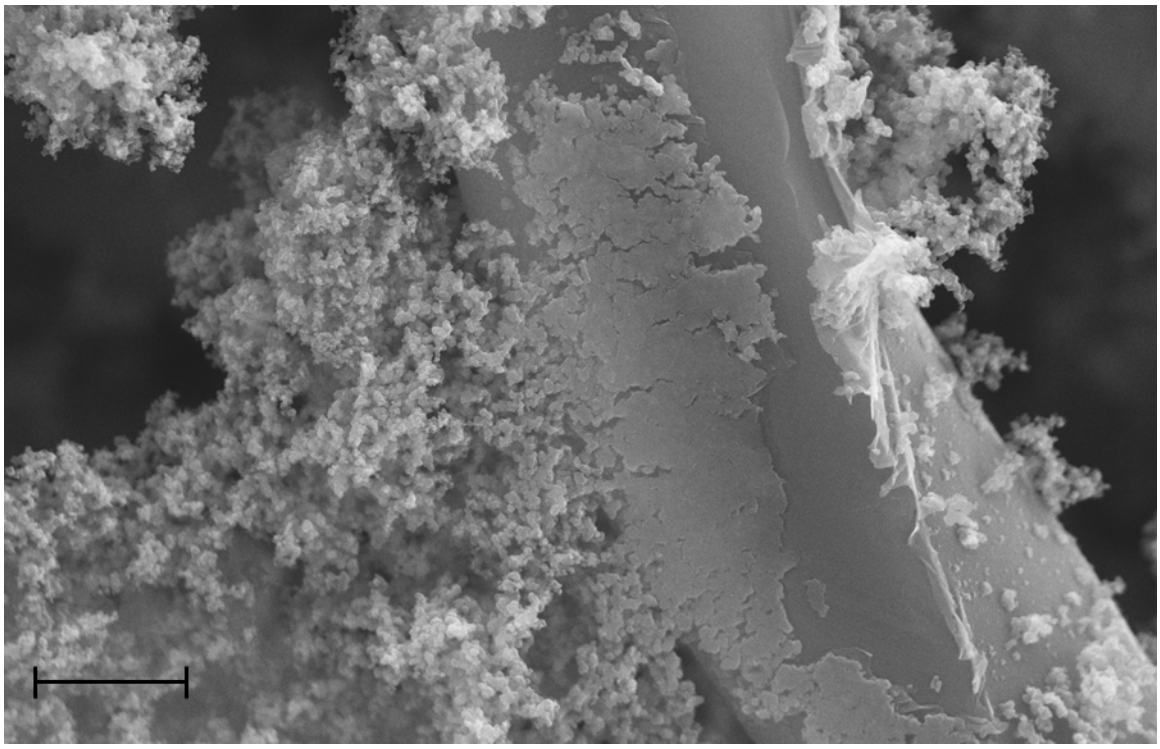

Figure B- 14. SEM image of fibers with polymer coating containing 0.1 mg/mL 3TAA. Scale bar equal to 10 µm, magnification of 5,000x, EHT of 30 kV and working distance of 6.0 mm.

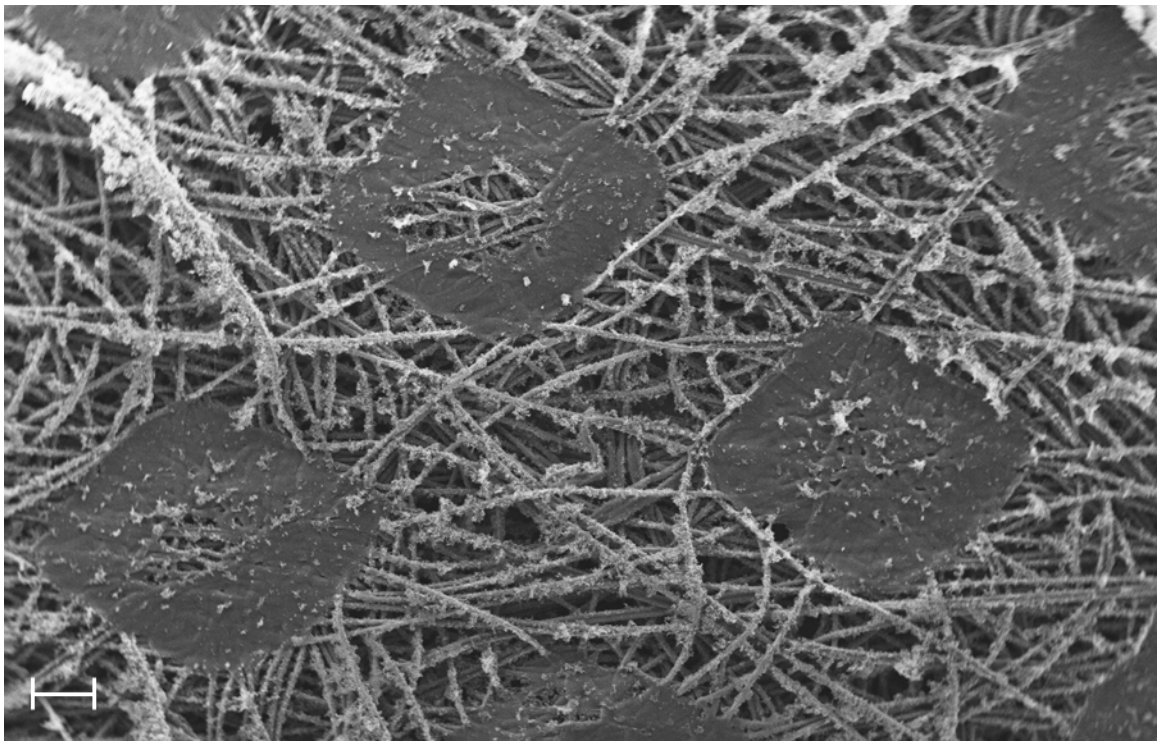

Figure B- 15. SEM image of fibers with polymer coating containing 0.1 mg/mL 3TAA. Scale bar equal to 200 µm, magnification of 100x, EHT of 30 kV and working distance of 6.0 mm.

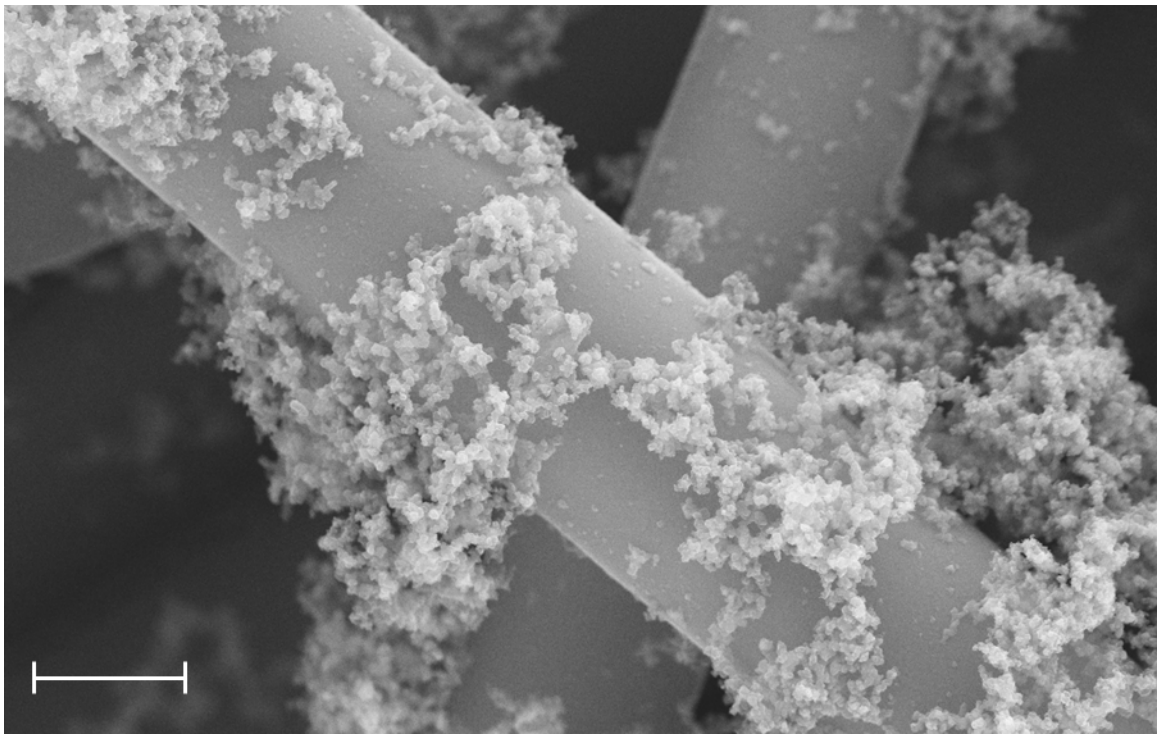

Figure B- 16. SEM image of fibers with polymer coating containing 1 mg/mL 3TAA. Scale bar equal to 10 µm, magnification of 5,000x, EHT of 30 kV and working distance of 6.0 mm.

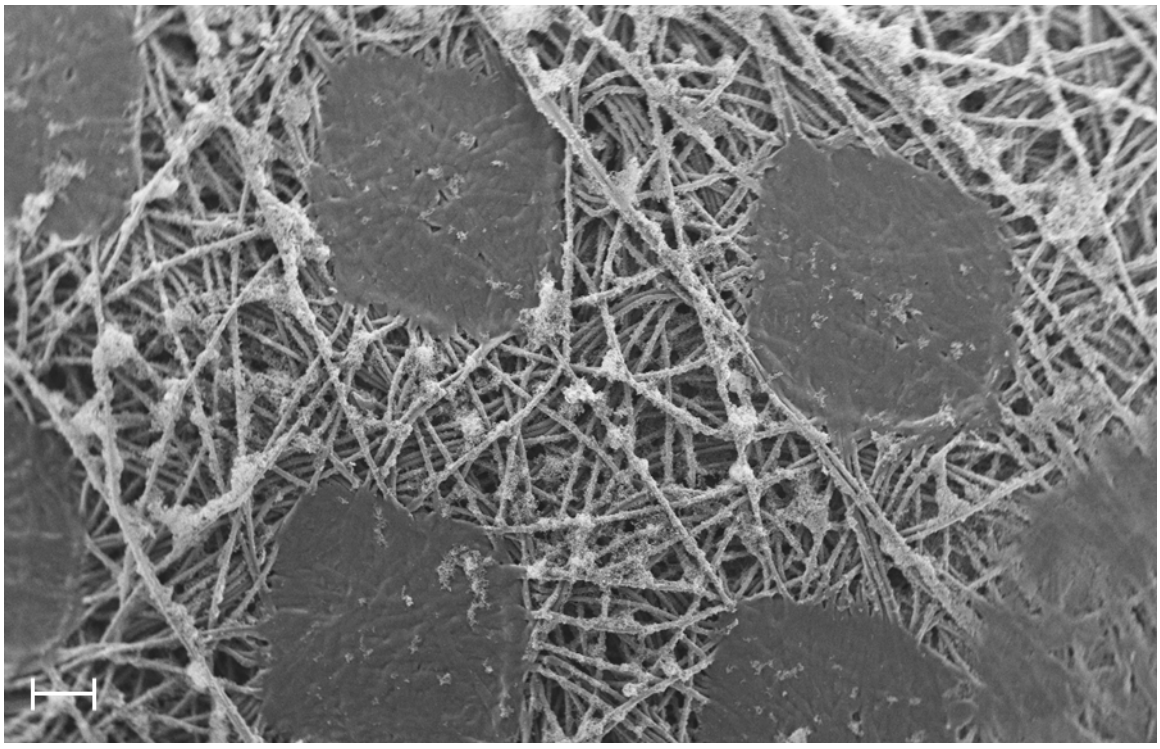

Figure B- 17. SEM image of fibers with polymer coating containing 1 mg/mL 3TAA. Scale bar equal to 200 µm, magnification of 100x, EHT of 30 kV and working distance of 6.0 mm.

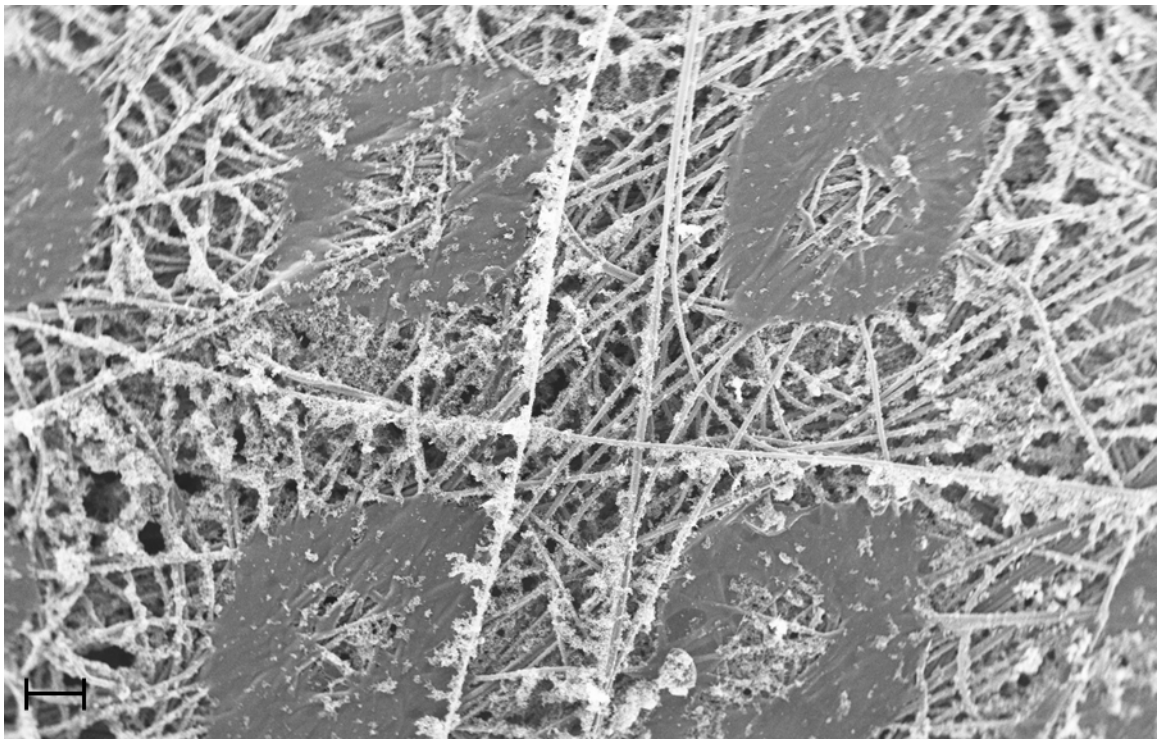

Figure B- 18. SEM image of fibers with polymer coating containing 10 mg/mL 3TAA. Scale bar equal to 200 µm, magnification of 100x, EHT of 30 kV and working distance of 6.0 mm.

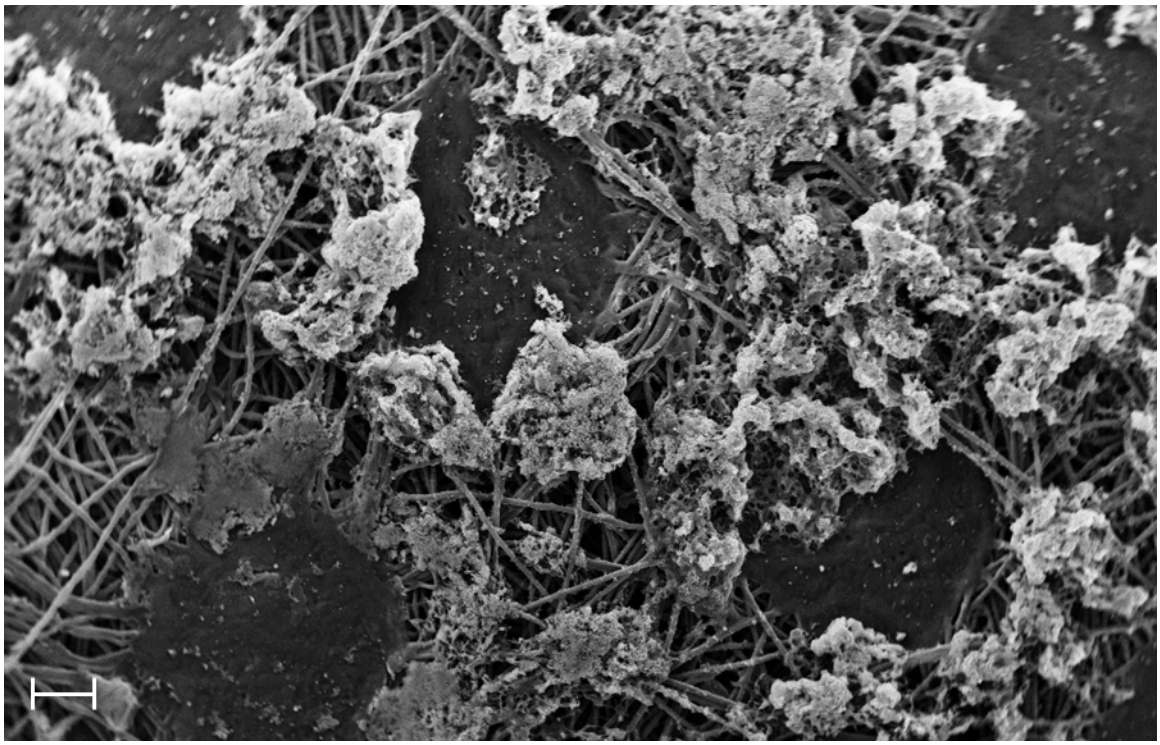

Figure B- 19. SEM image of fibers with polymer coating containing 100 mg/mL 3TAA. Scale bar equal to 200 µm, magnification of 100x, EHT of 30 kV and working distance of 6.0 mm.

Table B- 1. Data for Figure 3-7.

3TAA Concentration (mg/mL)	Resistivity				
	Run 1	Run 2	Run 3	Run 4	Run 5
0.0	5.19	5.95	5.44	3.8	3.58
0.1	3.13	3.65	4.32	4.46	8.67
1.0	3.6	3.45	3.7	3.01	3.32
10.0	6.51	6.55	6.6	4.77	5.31
20.0	8.22	7.73	7.17	7.69	6.23
50.0	10.38	10.67	12.44	8.56	11.09
100.0	2519.13	76.9	769.32	1530.53	610.98

3TAA Concentration (mg/mL)	Resistivity			
	Run 6	Run 7	Run 8	Run 9
0.0	6.19	3.37	4.04	3.41
0.1	5.79	3.84	3.71	3.61
1.0	3.01	3.78	3.25	3.75
10.0	5.11	7.04	7.37	7.38
20.0	7.04	8.5	7.86	12.79
50.0	8.14	7.21	8.88	7.62
100.0	1229.93	693.67	2784.62	4071.96

3TAA Concentration (mg/mL)	Average Resistivity	Standard Deviation
0.0	4.552222	1.135053
0.1	4.575556	1.713433
1.0	3.43	0.300915
10.0	6.293333	0.986927
20.0	8.136667	1.871042
50.0	9.443333	1.774197
100.0	1587.449	1289.793

Table B- 2. Data for Figure 3-8.

3TAA Concentration (mg/mL)	Sulfur Weight Percent at 100 x magnification (%)
0.0	0.93
0.1	0.78
1.0	0.55
10.0	1.3
20.0	1.54
50.0	2.24
100.0	3.83

Table B- 3. Data for Figure 3-9.

3TAA Concentration (mg/mL)	Fluorescent Output (RFU)			Average Fluorescent Output	Standard Deviation
	Run 1	Run 2	Run 3		
0.0	1.015	1.002	1.069	1.0287	0.035529
0.1	1.092	1.09	1.103	1.0950	0.007
1.0	1.432	1.135	1.594	1.3870	0.232785
10.0	1.102	1.66	1.669	1.4770	0.324791
20.0	1.102	1.233	1.468	1.2677	0.185446
50.0	1.235	1.632	2.069	1.6453	0.41716
100.0	6.683	2.845	2.359	3.9623	2.368664

Table B- 4. Student's T-Test of Resistivities (2 tails, $\alpha = 0.05$)

Sample 1	Sample 2	P value	Significant Difference
0.0 mg/mL	0.1 mg/mL	0.973	No

Table B- 5. Data for Figure 3-12, resistances.

Time (min)	Resistance (Ω)				
		Biotin Concentration			
	Blank	0.5 µM	5 µM	50 µM	500 µM
180.3	71355.76	62752.13	118946.49	86580.07	111731.84
210.3	73035.53	62625.81	113119.89	88133.45	122860.90
240.3	73915.68	62596.41	120872.01	85937.01	125910.62
270.4	73895.19	62708.56	114552.23	85005.61	124036.48
300.4	73597.06	64128.99	112130.07	86433.08	124593.95
330.4	73556.45	65166.29	112848.63	87412.59	121601.66
360.4	73356.03	66550.99	115193.39	87672.60	119535.49
390.5	73202.61	66907.21	116932.37	89694.71	119750.76
420.5	74298.15	68382.75	117037.28	93057.26	124257.22
450.5	76065.25	68302.68	116354.86	95037.67	126885.13
480.6	77368.64	68936.65	115400.63	96068.07	129810.52
510.6	77747.06	69473.73	115001.72	97137.89	131352.09
540.6	77461.47	70873.51	115031.78	99065.95	129413.32
570.6	76126.06	70871.72	116047.86	100250.63	128504.38
600.7	75211.70	71190.66	116260.22	101567.04	128820.63
630.7	75331.14	71776.46	116255.55	101298.79	127323.72
660.7	75986.29	73261.98	115356.41	102448.14	124668.16
690.8	76878.72	74064.76	114550.00	102808.88	125975.81
720.8	78480.28	74300.11	113534.98	102189.41	131283.59
750.8	79675.60	73929.83	113353.44	109339.11	136365.86
780.8	80121.32	73675.00	112855.89	124431.16	137767.99
810.9	81496.03	73371.89	111544.90	137392.27	137297.31
840.9	82290.01	72000.25	112182.63	136066.97	138735.78
870.9	81383.52	70546.73	116026.11	134273.25	140795.49
901.0	84210.53	72727.27	118500.96	136565.38	139664.80
180.3	58079.23	55522.51	54448.49	56145.98	52434.46
210.3	57767.69	55801.90	54836.38	56044.83	53359.00
240.3	58403.91	55744.69	54412.52	56186.26	53784.09
270.4	59585.88	55991.04	54054.05	56457.30	53685.93
300.4	58460.00	56198.94	53724.49	57007.61	53750.79
330.4	57427.65	56063.91	53745.90	57450.03	53850.36
360.4	58061.17	55913.89	53621.36	57582.07	53899.79
390.5	58295.69	56150.48	53535.75	57464.18	53985.59
420.5	58369.81	56207.97	53445.31	57601.31	54105.69
450.5	57937.42	55932.88	54260.94	57627.69	54188.00
480.6	58162.48	55734.43	54502.27	57625.09	54244.64

Table B-5 (cont'd).

510.6	57770.07	55902.38	54417.80	57564.60	54298.01
540.6	58062.37	56186.10	54120.85	57549.02	54323.84
570.6	58259.29	56236.19	54355.21	57772.38	54648.06
600.7	58141.95	56182.53	54363.33	58150.56	54727.05
630.7	57019.51	56321.76	54388.73	58675.52	55007.66
660.7	55799.12	56603.96	54519.19	58763.67	55279.43
690.8	55105.90	56959.64	54777.10	59064.25	55599.68
720.8	55022.46	57154.99	55021.17	59790.73	55386.38
750.8	55112.68	57187.20	55243.99	60959.68	55271.25
780.8	54830.39	57081.69	55641.11	60659.88	55308.98
810.9	54690.70	57014.86	55953.00	59886.64	55306.18
840.9	55189.47	56953.98	56090.30	60216.35	55536.61
870.9	56022.41	56777.85	55983.20	61871.62	55904.96
901.0	56219.26	56377.72	55401.66	61208.87	55594.16
180.3	181971.77	506329.11	434108.42	534351.14	546875.01
210.3	160256.41	425693.50	386206.85	459581.63	479452.12
240.3	170161.04	435036.06	416976.97	479780.61	506924.95
270.4	172498.73	426374.14	376141.78	438527.63	486956.39
300.4	173826.64	403095.13	344742.71	389158.97	430272.60
330.4	174939.56	374231.61	321137.80	361944.04	387061.01
360.4	176436.24	359008.93	326682.94	372093.02	374456.66
390.5	174883.02	352430.61	328304.15	375798.57	382336.07
420.5	173334.02	346080.40	333086.85	376582.02	376000.35
450.5	170306.98	346500.35	332044.78	372464.17	371402.04
480.6	167230.51	345331.29	330594.25	370870.63	367097.49
510.6	163293.89	347442.03	329933.91	369895.81	372761.84
540.6	162691.36	346394.72	329830.10	370059.52	377506.07
570.6	160963.00	345110.58	330359.66	366242.95	384673.38
600.7	161019.50	344717.51	329696.78	364112.23	388069.50
630.7	160987.30	347542.01	335106.04	361521.14	384546.76
660.7	163394.85	348518.03	333244.02	360769.62	376015.62
690.8	165539.67	345995.86	333835.64	360176.05	367894.58
720.8	168561.98	340045.14	331914.73	360885.76	368139.99
750.8	168714.58	338453.92	341359.37	363418.05	375441.90
780.8	168672.63	338173.73	341018.29	365924.52	384911.47
810.9	167475.12	335607.86	343769.25	367776.32	387813.05
840.9	164890.14	332258.59	346470.33	372179.44	383877.16
870.9	160998.19	335429.77	351957.77	377180.58	377358.49
901.0	161812.30	346320.35	336275.75	371574.55	378787.88

Table B- 6. Data for Figure 3-12, responses.

Time (min)	Response (%) Biotin Concentration 0.5 µM	5 µM	50 µM	500 µM
180.3	-12.06	66.70	21.34	56.58
210.3	-14.25	54.88	20.67	68.22
240.3	-15.31	63.53	16.26	70.34
270.4	-15.14	55.02	15.04	67.85
300.4	-12.86	52.36	17.44	69.29
330.4	-11.41	53.42	18.84	65.32
360.4	-9.28	57.03	19.52	62.95
390.5	-8.60	59.74	22.53	63.59
420.5	-7.96	57.52	25.25	67.24
450.5	-10.21	52.97	24.94	66.81
480.6	-10.90	49.16	24.17	67.78
510.6	-10.64	47.92	24.94	68.95
540.6	-8.50	48.50	27.89	67.07
570.6	-6.90	52.44	31.69	68.80
600.7	-5.35	54.58	35.04	71.28
630.7	-4.72	54.33	34.47	69.02
660.7	-3.59	51.81	34.82	64.07
690.8	-3.66	49.00	33.73	63.86
720.8	-5.33	44.67	30.21	67.28
750.8	-7.21	42.27	37.23	71.15
780.8	-8.05	40.86	55.30	71.95
810.9	-9.97	36.87	68.59	68.47
840.9	-12.50	36.33	65.35	68.59
870.9	-13.32	42.57	64.99	73.00
901.0	-13.64	40.72	62.17	65.85
180.3	-4.40	-6.25	-3.33	-9.72
210.3	-3.40	-5.07	-2.98	-7.63
240.3	-4.55	-6.83	-3.80	-7.91
270.4	-6.03	-9.28	-5.25	-9.90
300.4	-3.87	-8.10	-2.48	-8.06
330.4	-2.37	-6.41	0.04	-6.23
360.4	-3.70	-7.65	-0.83	-7.17
390.5	-3.68	-8.17	-1.43	-7.39
420.5	-3.70	-8.44	-1.32	-7.31
450.5	-3.46	-6.35	-0.53	-6.47
480.6	-4.17	-6.29	-0.92	-6.74

Table B-6 (cont'd).

510.6	-3.23	-5.80	-0.36	-6.01
540.6	-3.23	-6.79	-0.88	-6.44
570.6	-3.47	-6.70	-0.84	-6.20
600.7	-3.37	-6.50	0.01	-5.87
630.7	-1.22	-4.61	2.90	-3.53
660.7	1.44	-2.29	5.31	-0.93
690.8	3.36	-0.60	7.18	0.90
720.8	3.88	0.00	8.67	0.66
750.8	3.76	0.24	10.61	0.29
780.8	4.11	1.48	10.63	0.87
810.9	4.25	2.31	9.50	1.13
840.9	3.20	1.63	9.11	0.63
870.9	1.35	-0.07	10.44	-0.21
901.0	0.28	-1.45	8.88	-1.11
180.3	178.25	138.56	193.65	200.53
210.3	165.63	140.99	186.78	199.18
240.3	155.66	145.05	181.96	197.91
270.4	147.18	118.05	154.22	182.30
300.4	131.89	98.33	123.88	147.53
330.4	113.92	83.57	106.90	121.25
360.4	103.48	85.16	110.89	112.23
390.5	101.52	87.73	114.89	118.62
420.5	99.66	92.16	117.26	116.92
450.5	103.46	94.97	118.70	118.08
480.6	106.50	97.69	121.77	119.52
510.6	112.77	102.05	126.52	128.28
540.6	112.92	102.73	127.46	132.04
570.6	114.40	105.24	127.53	138.98
600.7	114.08	104.76	126.13	141.01
630.7	115.88	108.16	124.56	138.87
660.7	113.30	103.95	120.80	130.13
690.8	109.01	101.67	117.58	122.24
720.8	101.73	96.91	114.10	118.40
750.8	100.61	102.33	115.40	122.53
780.8	100.49	102.18	116.94	128.20
810.9	100.39	105.27	119.60	131.56
840.9	101.50	110.12	125.71	132.81
870.9	108.34	118.61	134.28	134.39
901.0	114.03	107.82	129.63	134.09

Table B- 7. Data for Figure 3-12, average response.

Time (min)	Average Response (%) Biotin Concentration			
	0.5 µM	5 µM	50 µM	500 µM
180.3	53.93	66.33	70.55	82.46
210.3	49.33	63.60	68.16	86.59
240.3	45.26	67.25	64.81	86.78
270.4	42.00	54.60	54.67	80.08
300.4	38.39	47.53	46.28	69.59
330.4	33.38	43.53	41.92	60.11
360.4	30.17	44.85	43.20	56.01
390.5	29.75	46.43	45.33	58.27
420.5	29.33	47.08	47.06	58.95
450.5	29.93	47.20	47.70	59.47
480.6	30.48	46.85	48.34	60.19
510.6	32.97	48.05	50.37	63.74
540.6	33.73	48.15	51.49	64.22
570.6	34.68	50.33	52.80	67.20
600.7	35.12	50.94	53.73	68.80
630.7	36.65	52.62	53.98	68.12
660.7	37.05	51.16	53.64	64.42
690.8	36.24	50.02	52.83	62.33
720.8	33.43	47.19	50.99	62.11
750.8	32.39	48.28	54.41	64.66
780.8	32.18	48.17	60.96	67.01
810.9	31.56	48.15	65.90	67.05
840.9	30.73	49.36	66.72	67.34
870.9	32.13	53.70	69.90	69.06
901.0	33.56	49.03	66.89	66.28

Table B- 8. Student's T-Test of Biotin Sensor Response (2 tails, $\alpha = 0.05$)

Sample 1	Sample 2	P value	Significant Difference
Blank	0.5 µM	2.174E-06	Yes
Blank	5 µM	2.328E-14	Yes
Blank	50 µM	2.785E-12	Yes
Blank	500 µM	1.382E-14	Yes

B.2 CHAPTER 4 DATA

Table B- 9. Data for Table 4-2 and Table 4-3.

	Experimental Factors					Response	
	Pyrrole (%)	3TAA (g/mL)	FeCl3 (M)	5SSA (M)	Time (min)	R for regression	Resistance (Ω)
Run*	C1	C2	C3	C4	C5	y	
1	32.5	0.0125	0.075	0.15	97.5	0	53.8
2	32.5	0.0125	0.075	0.35	52.5	1	36.5
3	32.5	0.0125	0.125	0.15	52.5	1	23.3
4	32.5	0.0125	0.125	0.35	97.5	1	40.2
5	32.5	0.0375	0.075	0.15	52.5	0	82.6
6	32.5	0.0375	0.075	0.35	97.5	1	49.8
7	32.5	0.0375	0.125	0.15	97.5	0	53.2
8	32.5	0.0375	0.125	0.35	52.5	0	96.8
9	77.5	0.0125	0.075	0.15	52.5	0	267
10	77.5	0.0125	0.075	0.35	97.5	1	32.2
11	77.5	0.0125	0.125	0.15	97.5	0	65.6
12	77.5	0.0125	0.125	0.35	52.5	0	50.8
13	77.5	0.0375	0.075	0.15	97.5	0	55.8
14	77.5	0.0375	0.075	0.35	52.5	1	29.5
15	77.5	0.0375	0.125	0.15	52.5	1	34.1
16	77.5	0.0375	0.125	0.35	97.5	1	27.1
17	10	0.025	0.1	0.25	75	0	84.8
18	100	0.025	0.1	0.25	75	1	42.6
19	55	0	0.1	0.25	75	1	30
20	55	0.05	0.1	0.25	75	0	92.4
21	55	0.025	0.05	0.25	75	0	81.8
22	55	0.025	0.15	0.25	75	0	62.2
23	55	0.025	0.1	0.05	75	0	92.8
24	55	0.025	0.1	0.45	75	0	56.1
25	55	0.025	0.1	0.25	30	0	84.6
26	55	0.025	0.1	0.25	120	1	47
27	55	0.025	0.1	0.25	75	1	44.5
28	55	0.025	0.1	0.25	75	0	85.2
29	55	0.025	0.1	0.25	75	0	52.7
30	55	0.025	0.1	0.25	75	1	37
31	32.5	0.0125	0.075	0.15	97.5	0	75.2
32	32.5	0.0125	0.075	0.35	52.5	0	107
33	32.5	0.0125	0.125	0.15	52.5	1	25.9

Table B-9 (cont'd).

34	32.5	0.0125	0.125	0.35	97.5	1	43.6
35	32.5	0.0375	0.075	0.15	52.5	0	71.2
36	32.5	0.0375	0.075	0.35	97.5	0	117.6
37	32.5	0.0375	0.125	0.15	97.5	0	66.2
38	32.5	0.0375	0.125	0.35	52.5	1	49.3
39	77.5	0.0125	0.075	0.15	52.5	0	339
40	77.5	0.0125	0.075	0.35	97.5	0	82.3
41	77.5	0.0125	0.125	0.15	97.5	0	59.5
42	77.5	0.0125	0.125	0.35	52.5	1	31.6
43	77.5	0.0375	0.075	0.15	97.5	1	40.6
44	77.5	0.0375	0.075	0.35	52.5	0	51.6
45	77.5	0.0375	0.125	0.15	52.5	1	48
46	77.5	0.0375	0.125	0.35	97.5	1	26.4
47	10	0.025	0.1	0.25	75	1	48.7
48	100	0.025	0.1	0.25	75	1	30.4
49	55	0	0.1	0.25	75	0	86.2
50	55	0.05	0.1	0.25	75	0	71.1
51	55	0.025	0.05	0.25	75	0	134.9
52	55	0.025	0.15	0.25	75	1	45.4
53	55	0.025	0.1	0.05	75	0	115.9
54	55	0.025	0.1	0.45	75	0	73.4
55	55	0.025	0.1	0.25	30	1	42
56	55	0.025	0.1	0.25	120	1	31.5
57	55	0.025	0.1	0.25	75	1	38.6
58	55	0.025	0.1	0.25	75	0	61.4
59	55	0.025	0.1	0.25	75	1	49.1
60	55	0.025	0.1	0.25	75	1	44.4
61	32.5	0.0125	0.075	0.15	97.5	0	112.9
62	32.5	0.0125	0.075	0.35	52.5	0	75.4
63	32.5	0.0125	0.125	0.15	52.5	1	36.5
64	32.5	0.0125	0.125	0.35	97.5	1	20.1
65	32.5	0.0375	0.075	0.15	52.5	0	181
66	32.5	0.0375	0.075	0.35	97.5	0	101.7
67	32.5	0.0375	0.125	0.15	97.5	0	86.1
68	32.5	0.0375	0.125	0.35	52.5	0	59.2
69	77.5	0.0125	0.075	0.15	52.5	0	331
70	77.5	0.0125	0.075	0.35	97.5	1	49.6
71	77.5	0.0125	0.125	0.15	97.5	0	54.9
72	77.5	0.0125	0.125	0.35	52.5	1	39.9

Table B-9 (cont'd).

73	77.5	0.0375	0.075	0.15	97.5	0	68.6
74	77.5	0.0375	0.075	0.35	52.5	1	39.9
75	77.5	0.0375	0.125	0.15	52.5	1	49.6
76	77.5	0.0375	0.125	0.35	97.5	1	38.6
77	10	0.025	0.1	0.25	75	0	84.1
78	100	0.025	0.1	0.25	75	0	52.2
79	55	0	0.1	0.25	75	1	36.1
80	55	0.05	0.1	0.25	75	0	87.8
81	55	0.025	0.05	0.25	75	0	82.5
82	55	0.025	0.15	0.25	75	1	28.8
83	55	0.025	0.1	0.05	75	0	102.8
84	55	0.025	0.1	0.45	75	0	72.2
85	55	0.025	0.1	0.25	30	0	68.4
86	55	0.025	0.1	0.25	120	0	51.8
87	55	0.025	0.1	0.25	75	1	42.5
88	55	0.025	0.1	0.25	75	0	52.6
89	55	0.025	0.1	0.25	75	0	54.5
90	55	0.025	0.1	0.25	75	0	62.5
91	32.5	0.0125	0.075	0.15	97.5	1	46.6
92	32.5	0.0125	0.075	0.35	52.5	0	71.3
93	32.5	0.0125	0.125	0.15	52.5	0	67.8
94	32.5	0.0125	0.125	0.35	97.5	0	58.9
95	32.5	0.0375	0.075	0.15	52.5	1	32.4
96	32.5	0.0375	0.075	0.35	97.5	0	72.5
97	32.5	0.0375	0.125	0.15	97.5	0	99.8
98	32.5	0.0375	0.125	0.35	52.5	0	64.4
99	77.5	0.0125	0.075	0.15	52.5	0	226
100	77.5	0.0125	0.075	0.35	97.5	0	59.5
101	77.5	0.0125	0.125	0.15	97.5	0	62.2
102	77.5	0.0125	0.125	0.35	52.5	1	46.3
103	77.5	0.0375	0.075	0.15	97.5	1	41.4
104	77.5	0.0375	0.075	0.35	52.5	0	51.5
105	77.5	0.0375	0.125	0.15	52.5	1	45.7
106	77.5	0.0375	0.125	0.35	97.5	1	31.1
107	10	0.025	0.1	0.25	75	1	47.8
108	100	0.025	0.1	0.25	75	0	99.7
109	55	0	0.1	0.25	75	0	63.4
110	55	0.05	0.1	0.25	75	0	90.6
111	55	0.025	0.05	0.25	75	0	58.4

Table B-9 (cont'd).

112	55	0.025	0.15	0.25	75	1	27.6
113	55	0.025	0.1	0.05	75	1	47.2
114	55	0.025	0.1	0.45	75	1	29.5
115	55	0.025	0.1	0.25	30	1	26.8
116	55	0.025	0.1	0.25	120	1	40.9
117	55	0.025	0.1	0.25	75	0	80.6
118	55	0.025	0.1	0.25	75	1	39
119	55	0.025	0.1	0.25	75	1	37.1
120	55	0.025	0.1	0.25	75	1	42.9
121	32.5	0.0125	0.075	0.15	97.5	0	66.5
122	32.5	0.0125	0.075	0.35	52.5	0	62.7
123	32.5	0.0125	0.125	0.15	52.5	1	26.2
124	32.5	0.0125	0.125	0.35	97.5	1	46.7
125	32.5	0.0375	0.075	0.15	52.5	0	93.1
126	32.5	0.0375	0.075	0.35	97.5	0	116.9
127	32.5	0.0375	0.125	0.15	97.5	0	72.1
128	32.5	0.0375	0.125	0.35	52.5	0	52.9
129	77.5	0.0125	0.075	0.15	52.5	0	235
130	77.5	0.0125	0.075	0.35	97.5	0	78.4
131	77.5	0.0125	0.125	0.15	97.5	1	28.8
132	77.5	0.0125	0.125	0.35	52.5	0	70.4
133	77.5	0.0375	0.075	0.15	97.5	1	44.3
134	77.5	0.0375	0.075	0.35	52.5	0	52.1
135	77.5	0.0375	0.125	0.15	52.5	1	49.8
136	77.5	0.0375	0.125	0.35	97.5	1	29.3
137	10	0.025	0.1	0.25	75	0	60.6
138	100	0.025	0.1	0.25	75	1	37.4
139	55	0	0.1	0.25	75	0	62.6
140	55	0.05	0.1	0.25	75	0	51.2
141	55	0.025	0.05	0.25	75	0	102.6
142	55	0.025	0.15	0.25	75	0	55.5
143	55	0.025	0.1	0.05	75	0	93.8
144	55	0.025	0.1	0.45	75	0	59.5
145	55	0.025	0.1	0.25	30	0	58.6
146	55	0.025	0.1	0.25	120	0	51.2
147	55	0.025	0.1	0.25	75	0	76.1
148	55	0.025	0.1	0.25	75	1	28.7
149	55	0.025	0.1	0.25	75	1	31.5
150	55	0.025	0.1	0.25	75	0	54.7

Table B-9 (cont'd).

151	32.5	0.0125	0.075	0.15	97.5	1	39.9
152	32.5	0.0125	0.075	0.35	52.5	0	65.3
153	32.5	0.0125	0.125	0.15	52.5	1	27.2
154	32.5	0.0125	0.125	0.35	97.5	1	20.9
155	32.5	0.0375	0.075	0.15	52.5	0	120.6
156	32.5	0.0375	0.075	0.35	97.5	0	109.5
157	32.5	0.0375	0.125	0.15	97.5	0	65.2
158	32.5	0.0375	0.125	0.35	52.5	0	80.3
159	77.5	0.0125	0.075	0.15	52.5	0	136
160	77.5	0.0125	0.075	0.35	97.5	0	102.6
161	77.5	0.0125	0.125	0.15	97.5	0	83.6
162	77.5	0.0125	0.125	0.35	52.5	1	24.1
163	77.5	0.0375	0.075	0.15	97.5	0	53.5
164	77.5	0.0375	0.075	0.35	52.5	0	67.8
165	77.5	0.0375	0.125	0.15	52.5	1	38.5
166	77.5	0.0375	0.125	0.35	97.5	1	26.2
167	10	0.025	0.1	0.25	75	0	77.8
168	100	0.025	0.1	0.25	75	0	79.8
169	55	0	0.1	0.25	75	0	57.1
170	55	0.05	0.1	0.25	75	0	61.9
171	55	0.025	0.05	0.25	75	0	102.9
172	55	0.025	0.15	0.25	75	1	45.9
173	55	0.025	0.1	0.05	75	1	47.9
174	55	0.025	0.1	0.45	75	1	48.9
175	55	0.025	0.1	0.25	30	0	67.7
176	55	0.025	0.1	0.25	120	1	39.7
177	55	0.025	0.1	0.25	75	0	54.2
178	55	0.025	0.1	0.25	75	1	36.6
179	55	0.025	0.1	0.25	75	1	39.6
180	55	0.025	0.1	0.25	75	1	36.4
181	32.5	0.0125	0.075	0.15	97.5	0	123.2
182	32.5	0.0125	0.075	0.35	52.5	1	48.2
183	32.5	0.0125	0.125	0.15	52.5	0	68.3
184	32.5	0.0125	0.125	0.35	97.5	1	38.6
185	32.5	0.0375	0.075	0.15	52.5	0	73.4
186	32.5	0.0375	0.075	0.35	97.5	0	118.2
187	32.5	0.0375	0.125	0.15	97.5	0	53.5
188	32.5	0.0375	0.125	0.35	52.5	0	71.5
189	77.5	0.0125	0.075	0.15	52.5	0	181.8

Table B-9 (cont'd).

190	77.5	0.0125	0.075	0.35	97.5	0	58.6
191	77.5	0.0125	0.125	0.15	97.5	1	28.9
192	77.5	0.0125	0.125	0.35	52.5	0	60.2
193	77.5	0.0375	0.075	0.15	97.5	1	31.1
194	77.5	0.0375	0.075	0.35	52.5	1	37.8
195	77.5	0.0375	0.125	0.15	52.5	1	29.4
196	77.5	0.0375	0.125	0.35	97.5	1	33.9
197	10	0.025	0.1	0.25	75	0	87.7
198	100	0.025	0.1	0.25	75	1	32.2
199	55	0	0.1	0.25	75	0	78.1
200	55	0.05	0.1	0.25	75	1	48.9
201	55	0.025	0.05	0.25	75	0	94.7
202	55	0.025	0.15	0.25	75	1	28.9
203	55	0.025	0.1	0.05	75	1	41.2
204	55	0.025	0.1	0.45	75	1	32.1
205	55	0.025	0.1	0.25	30	0	92.5
206	55	0.025	0.1	0.25	120	0	63.2
207	55	0.025	0.1	0.25	75	1	38.1
208	55	0.025	0.1	0.25	75	1	46.6
209	55	0.025	0.1	0.25	75	1	35.2
210	55	0.025	0.1	0.25	75	1	36.4
211	32.5	0.0125	0.075	0.15	97.5	0	52.9
212	32.5	0.0125	0.075	0.35	52.5	0	86.6
213	32.5	0.0125	0.125	0.15	52.5	0	51.6
214	32.5	0.0125	0.125	0.35	97.5	1	42.9
215	32.5	0.0375	0.075	0.15	52.5	0	123.5
216	32.5	0.0375	0.075	0.35	97.5	0	132.7
217	32.5	0.0375	0.125	0.15	97.5	0	86.9
218	32.5	0.0375	0.125	0.35	52.5	0	54.6
219	77.5	0.0125	0.075	0.15	52.5	0	177.8
220	77.5	0.0125	0.075	0.35	97.5	0	107.2
221	77.5	0.0125	0.125	0.15	97.5	0	71.1
222	77.5	0.0125	0.125	0.35	52.5	1	40.4
223	77.5	0.0375	0.075	0.15	97.5	1	47.6
224	77.5	0.0375	0.075	0.35	52.5	0	79.6
225	77.5	0.0375	0.125	0.15	52.5	0	57.4
226	77.5	0.0375	0.125	0.35	97.5	1	48.4
227	10	0.025	0.1	0.25	75	0	80.6
228	100	0.025	0.1	0.25	75	0	52.9

Table B-9 (cont'd).

229	55	0	0.1	0.25	75	1	42.4
230	55	0.05	0.1	0.25	75	1	40.2
231	55	0.025	0.05	0.25	75	0	105.4
232	55	0.025	0.15	0.25	75	1	31.8
233	55	0.025	0.1	0.05	75	0	78.6
234	55	0.025	0.1	0.45	75	1	40.5
235	55	0.025	0.1	0.25	30	1	48.2
236	55	0.025	0.1	0.25	120	0	50.6
237	55	0.025	0.1	0.25	75	1	46.8
238	55	0.025	0.1	0.25	75	1	25.5
239	55	0.025	0.1	0.25	75	1	40.8
240	55	0.025	0.1	0.25	75	1	32
241	32.5	0.0125	0.075	0.15	97.5	0	93.2
242	32.5	0.0125	0.075	0.35	52.5	0	95.3
243	32.5	0.0125	0.125	0.15	52.5	0	82.8
244	32.5	0.0125	0.125	0.35	97.5	1	38.1
245	32.5	0.0375	0.075	0.15	52.5	0	141.7
246	32.5	0.0375	0.075	0.35	97.5	0	175.7
247	32.5	0.0375	0.125	0.15	97.5	0	60.4
248	32.5	0.0375	0.125	0.35	52.5	0	72.9
249	77.5	0.0125	0.075	0.15	52.5	0	148.8
250	77.5	0.0125	0.075	0.35	97.5	0	122.6
251	77.5	0.0125	0.125	0.15	97.5	1	42.2
252	77.5	0.0125	0.125	0.35	52.5	1	33.8
253	77.5	0.0375	0.075	0.15	97.5	1	25.5
254	77.5	0.0375	0.075	0.35	52.5	0	63.7
255	77.5	0.0375	0.125	0.15	52.5	1	27.9
256	77.5	0.0375	0.125	0.35	97.5	1	43.9
257	10	0.025	0.1	0.25	75	0	117.6
258	100	0.025	0.1	0.25	75	1	38.8
259	55	0	0.1	0.25	75	1	41.3
260	55	0.05	0.1	0.25	75	0	76.2
261	55	0.025	0.05	0.25	75	0	94.6
262	55	0.025	0.15	0.25	75	1	36.1
263	55	0.025	0.1	0.05	75	0	57.9
264	55	0.025	0.1	0.45	75	0	92.6
265	55	0.025	0.1	0.25	30	0	72.6
266	55	0.025	0.1	0.25	120	1	45.7
267	55	0.025	0.1	0.25	75	1	42.5

Table B-9 (cont'd).

268	55	0.025	0.1	0.25	75	1	34.9
269	55	0.025	0.1	0.25	75	1	36.5
270	55	0.025	0.1	0.25	75	1	49.8

Table B- 10. T-Test for model verification.

Hypothesis: 35.41 = 38.00	
df	9
n	10
□	38
μ	35.41
s	6.01
δ= s/sqrt(n)	1.90
t calc =(□-μ)/δ	1.36
t tab (α = 0.025, df =9)	2.26
t calc < t tab do not reject hypothesis	

B.3 CHAPTER 5 DATA

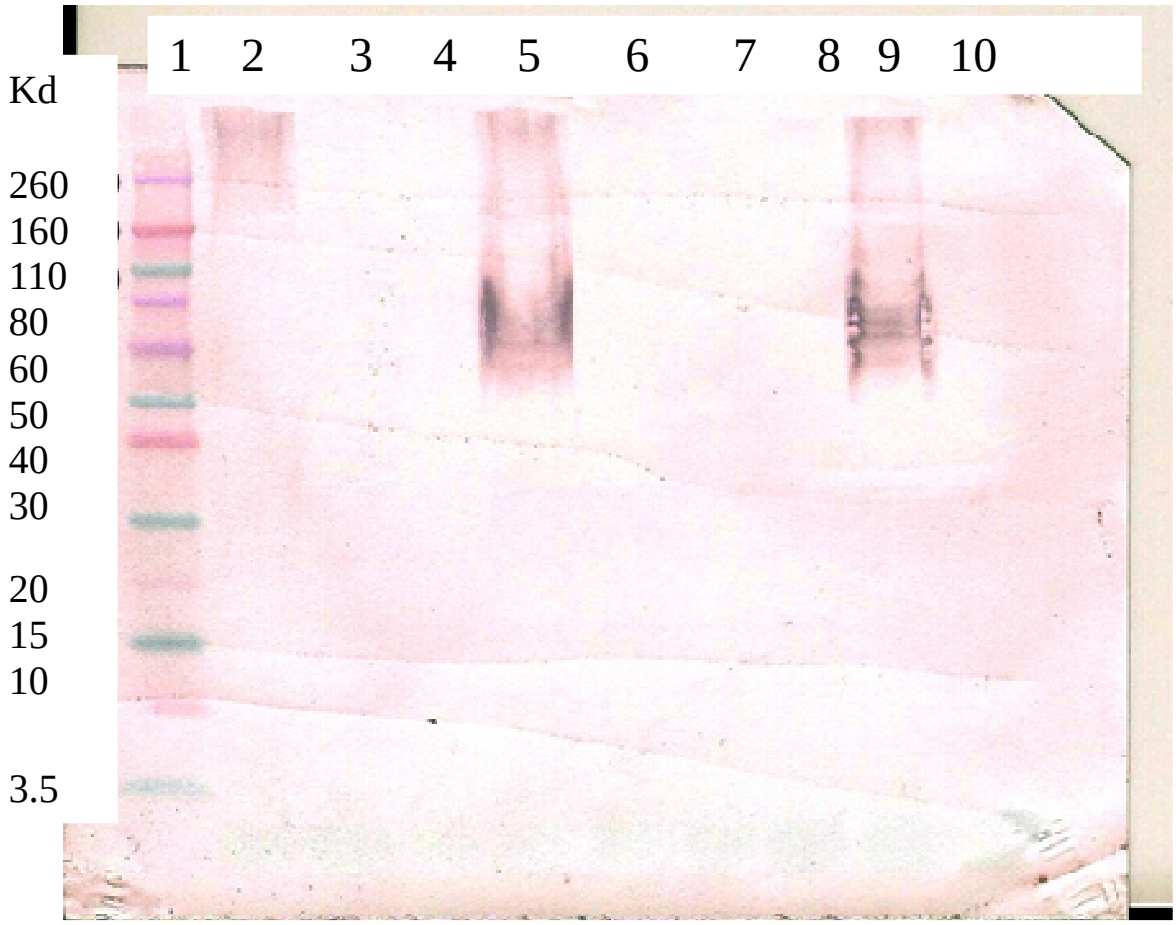

Figure B- 20. Western blot 1, where 1: ladder; 2: negative for *E.coli* O157:H19GT164; 3: negative for *E.coli* O157:H7GT126; 4: negative for *E.coli* O157:H7GT125; 5: positive for *E.coli* O157:H7 Sakai strain; 6: negative for *E.coli* O157:H7 AEEC strain; 7: negative for *E.coli* O26:H11; 8: negative for *E.coli* O55:H7; 9: positive for *E.coli* O157:H7 Spinach pGFPuv; and 10: negative for *Shigella boydii*.

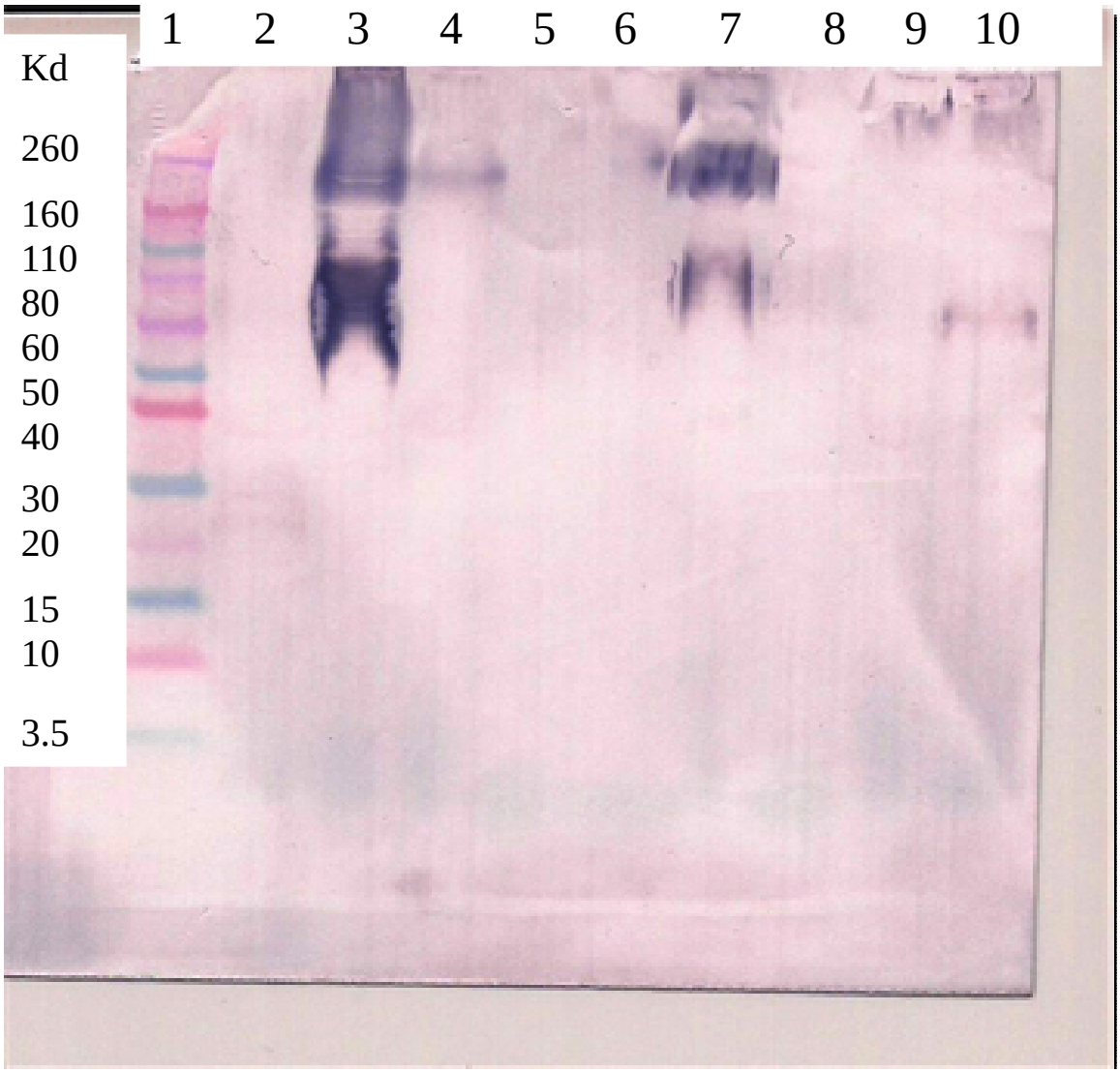

Figure B- 21. Western blot 2, where 1: ladder; 2: negative for *E.coli* O157:H38 Roe 1A164; 3: positive for *E.coli* O157:H45 166; 4: negative for *E.coli* Mastitis 1368; 5: negative for *Bacillus cereus*; 6: negative for *Bacillus anthracis* Sterne Strain; 7: positive for *Citrobacter freundii* GT4885; 8: negative *for Bacillus thuringiensis*; 9: negative for Bedmark generic *E.coli* K12; 10: negative for *Enterobacter agglomerans* GT1611.

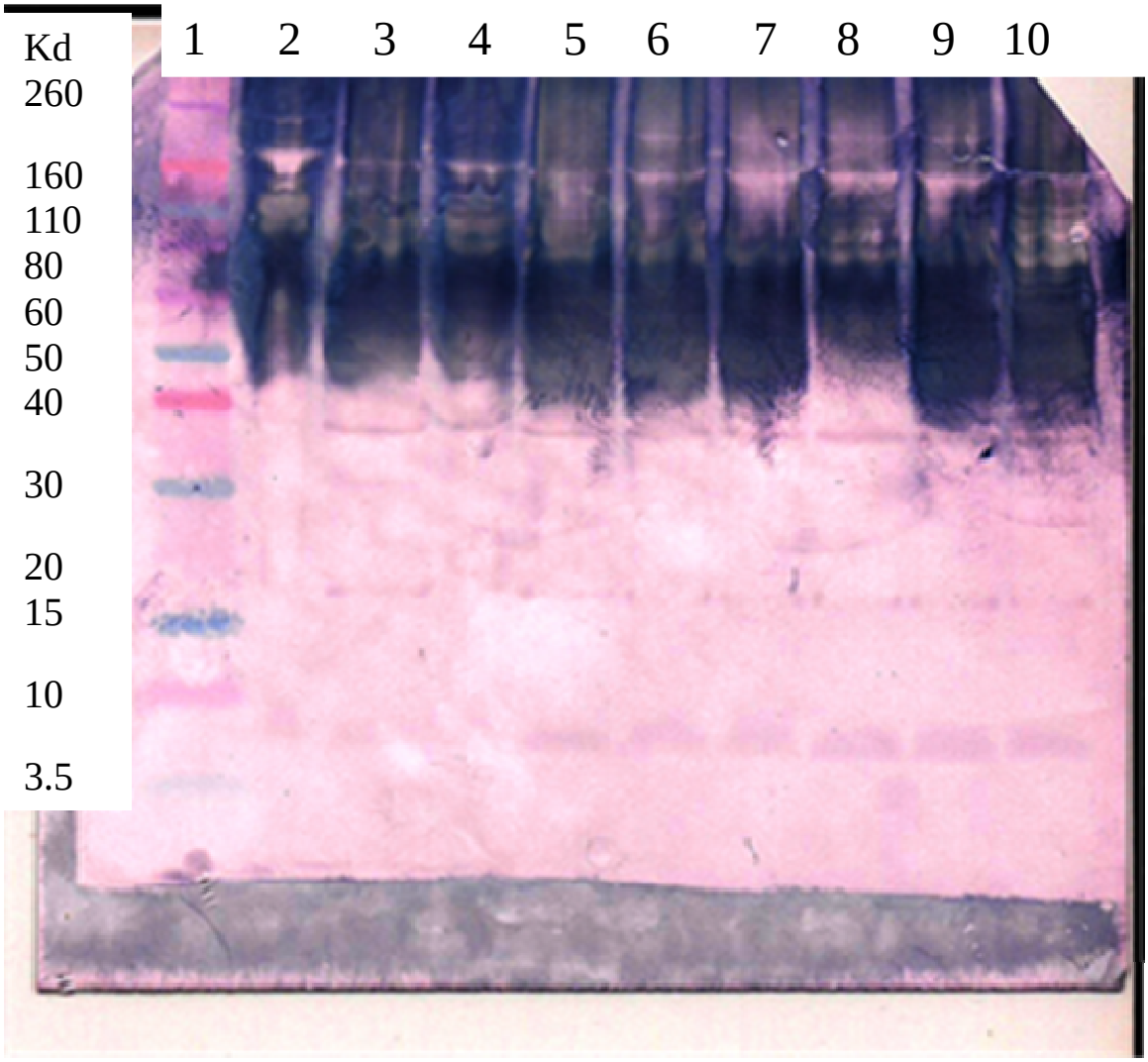

Figure B- 22. Western blot 3, where 1: ladder; 2: positive for SNP 17 *E.coli* O157:H7; 3: positive for SNP 18 *E.coli* O157:H7, 4: positive for SNP 19 *E.coli* O157:H7, 5: positive for SNP 20 *E.coli* O157:H7, 6: positive for EHEC1 #1 *E.coli* O157:H7, 7: positive for EHEC1 #2 *E.coli* O157:H7; 8: positive for EHEC1 #3 *E.coli* O157:H7; 9: positive for EHEC1 #4 *E.coli* O157:H7, and 10: positive for EHEC1 #5 *E.coli* O157:H7.

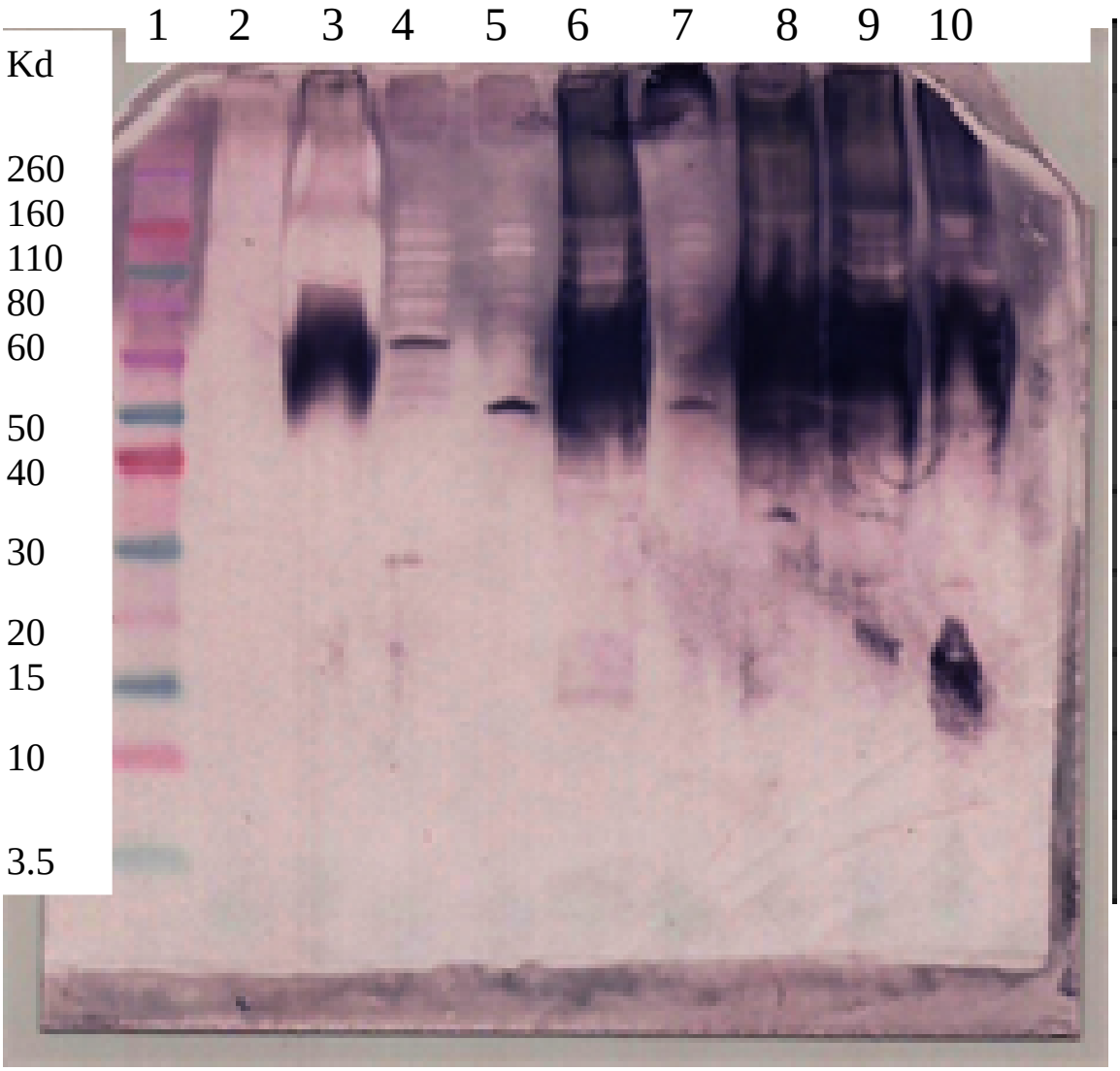

Figure B- 23. Western blot 4, where 1: ladder; 2: negative for *Pseudomonas aeruginosa*; 3: positive for *Escherichia hermannii*; 4: negative for *Staphylococcus aureus* 12600; 5: negative for *Staphylococcus aureus* Ent AT #4; 6: positive for *Enterococcus fecalis* ATCC 19433; 7: negative for *Staphylococcus aureus* ATCC 25923; 8: positive for *Citrobacter freundii* ATCC 8090; 9: positive for EHEC1 #8 *E.coli* O157:H7; 10: positive for *E.coli* O157:H7 Spinach TW 14359.

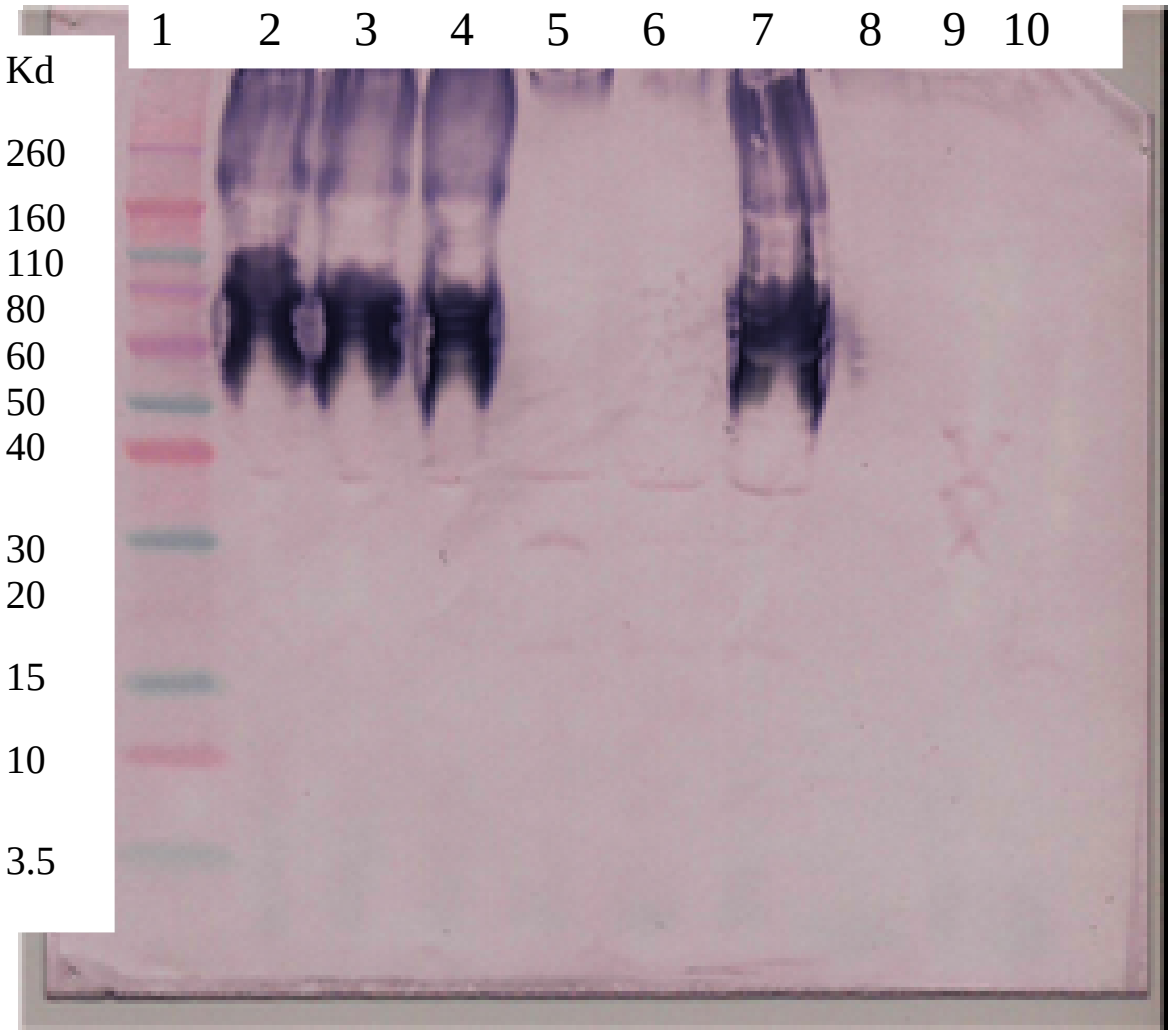

Figure B- 24. Western blot 5, where 1: ladder; 2: positive for EHEC1 #6 *E.coli* O157:NM; 3: positive for EHEC1 #7 *E.coli* O157:NM; 4: positive for *E.coli* O157:H7 Ao317; 5: negative for *Shigella flexneri*; 6: negative for *E.coli* O26:H11 BSL 326; 7: positive for *Citrobacter freundii* ATCC 8090; 8: negative for *Salmonella enteritis* Typhimurium 0648 10/12; 9: negative for *Klebsiella pneumoniae* 6-21; 10: negative for *Klebsiella pneumoniae* ATCC 13883.

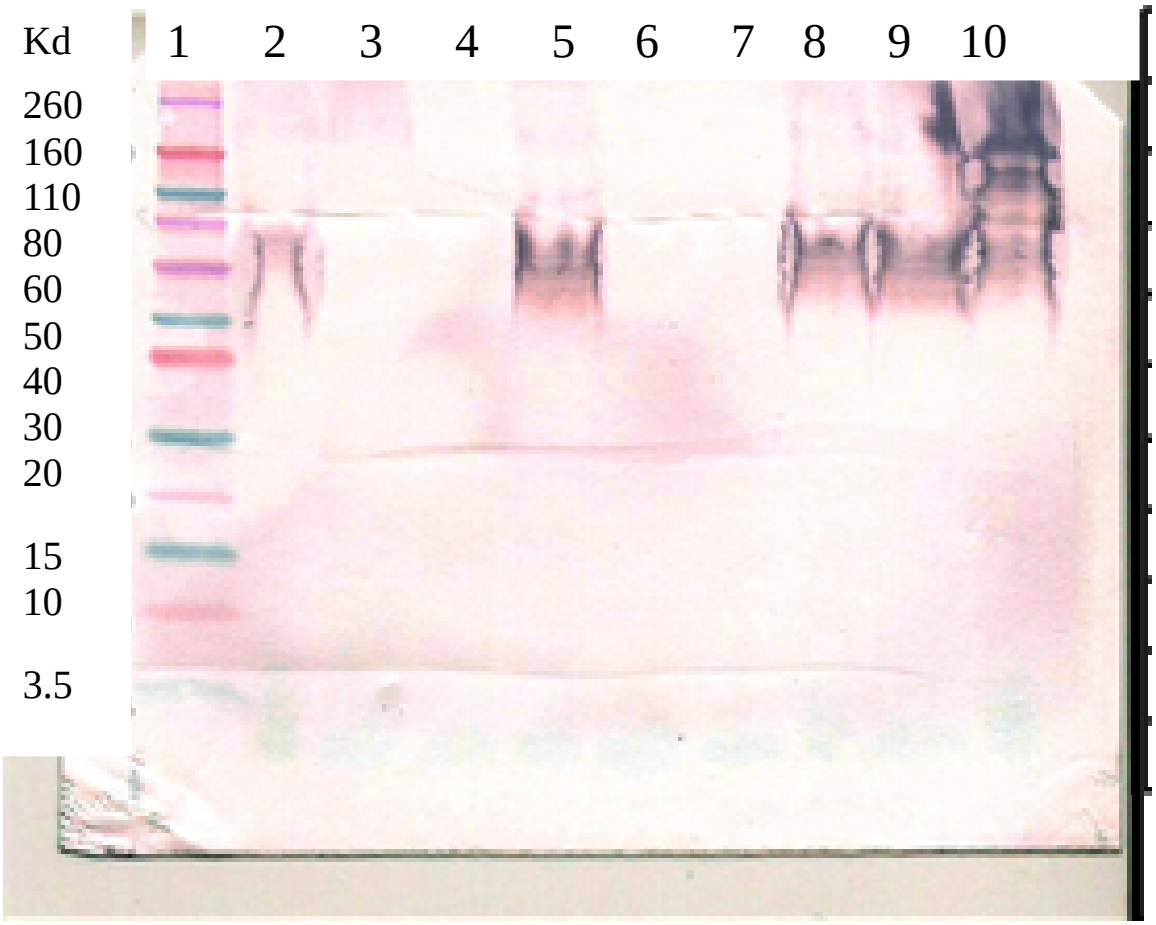

Figure B- 25. Western blot 6, where 1: ladder; 2: positive for *E.coli* O157:H43 GT 4316; 3: negative for *E.coli* O157:H19 GT164; 4: negative for *Enterobacter agglomerans* GT1611; 5: positive for *E.coli* O157:H7 GT632; 6: negative for *E.coli* O157:H7 GT126; 7: negative for *E.coli* O157:H7 GT125; 8: positive for *E.coli* O157:NM GT4141; 9: positive for *E.coli* O157:H7 A110; 10: positive for *Citrobacter freundii* (CF3) GT5142.

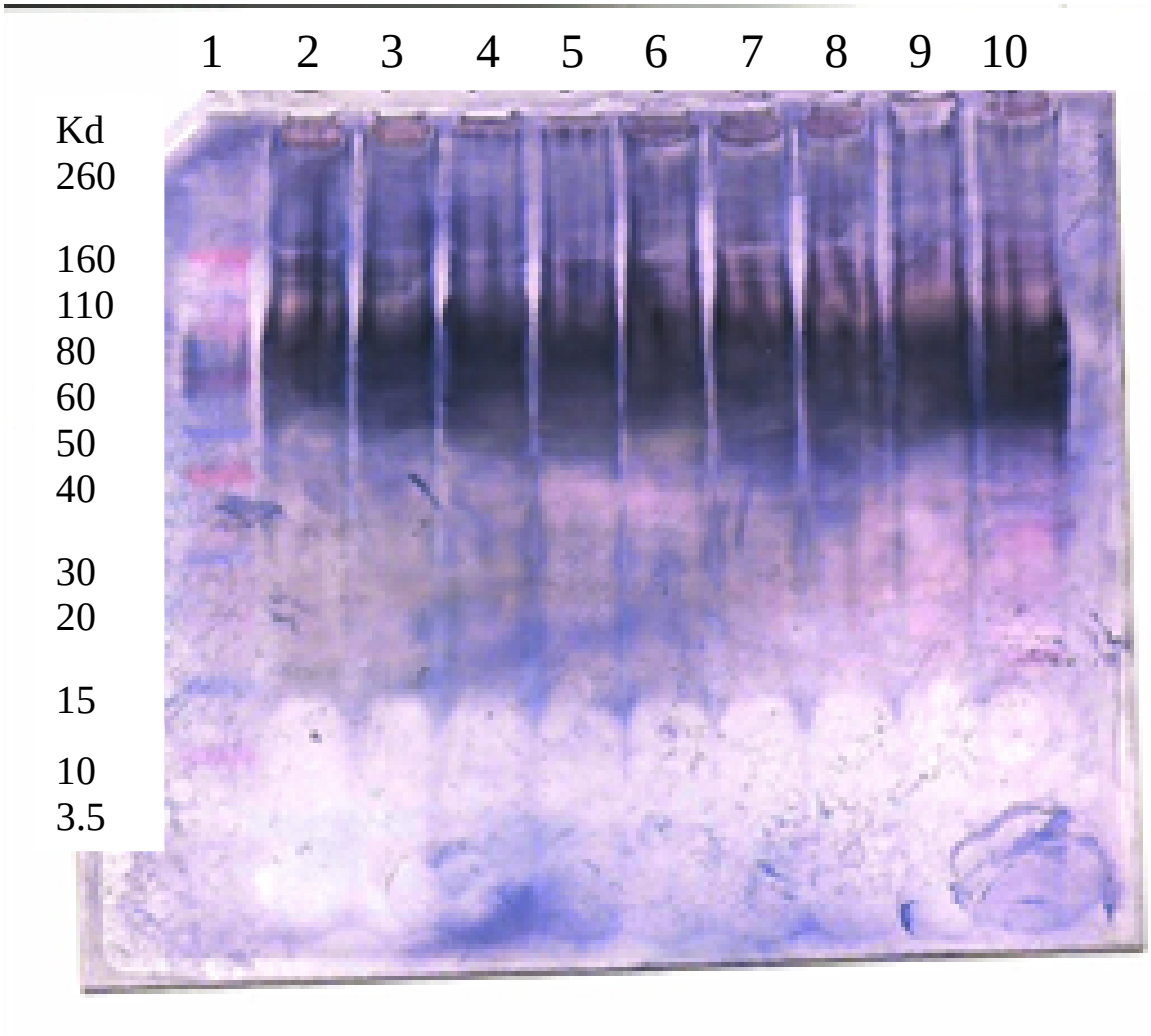

Figure B- 26. Western blot 7, where 1: ladder; 2: positive for SNP2 *E.coli* O157:H7; 3: positive for SNP3 *E.coli* O157:H7; 4: positive for SNP4 *E.coli* O157:H7; 5: positive for SNP5 *E.coli* O157:H7; 6: positive for SNP6 *E.coli* O157:H7; 7: positive for SNP7 *E.coli* O157:H7; 8: positive for SNP8 *E.coli* O157:H7; 9: positive for SNP9 *E.coli* O157:H7; 10: positive for SNP10 *E.coli* O157:H7.

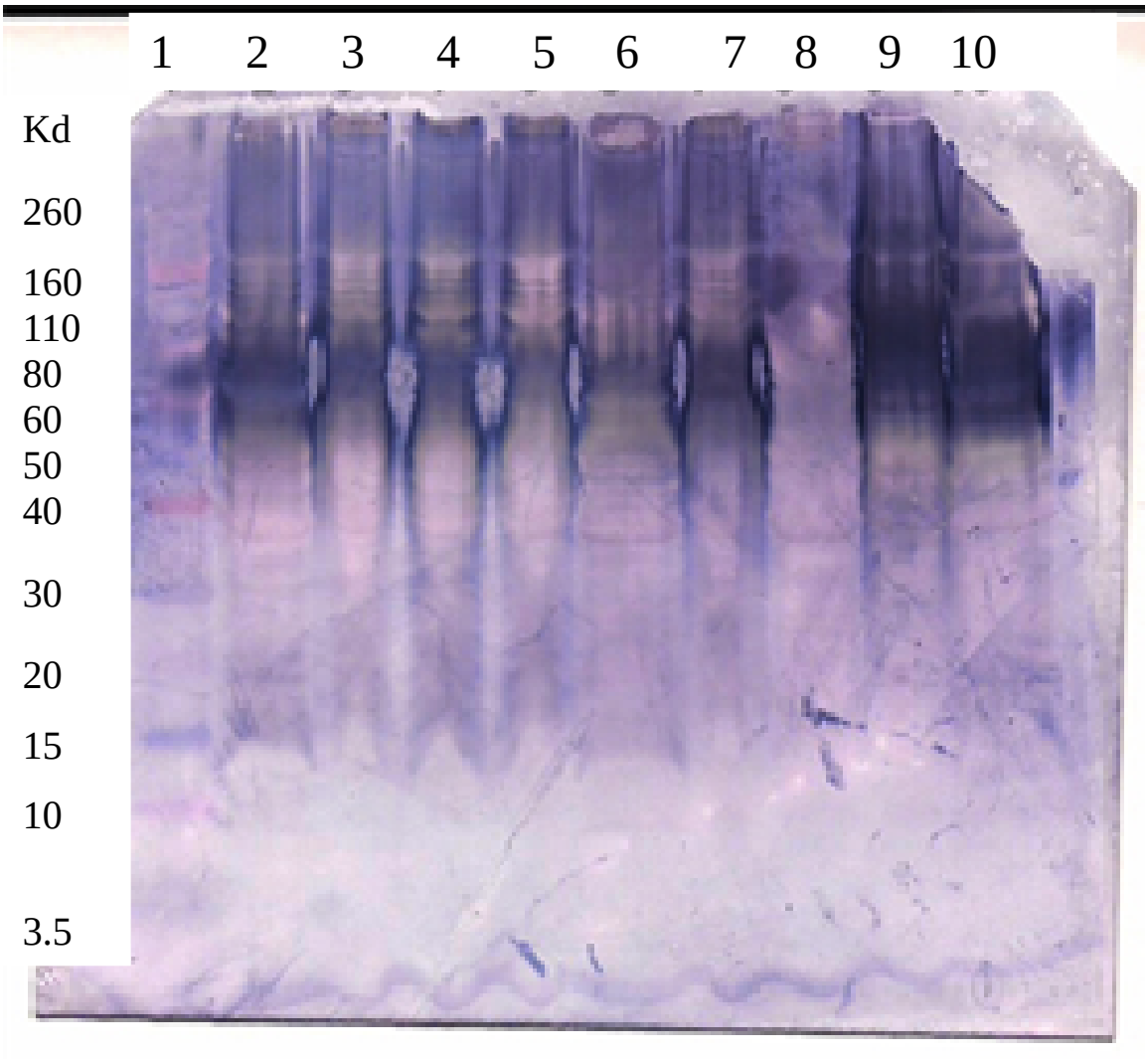

Figure B- 27. Western blot 8, where 1: ladder; 2: positive for SNP11 *E.coli* O157:H7; 3: positive for SNP12 *E.coli* O157:H7; 4: positive for SNP13 *E.coli* O157:H7; 5: positive for SNP14 *E.coli* O157:H7; 6: positive for SNP15 *E.coli* O157:H7; 7: positive for SNP16 *E.coli* O157:H7; 8: negative for 4-22-10 (BSL #1); 9: positive for BSL #2 Bio Systems; 10: positive for *E. coli* ATCC 43895(107).

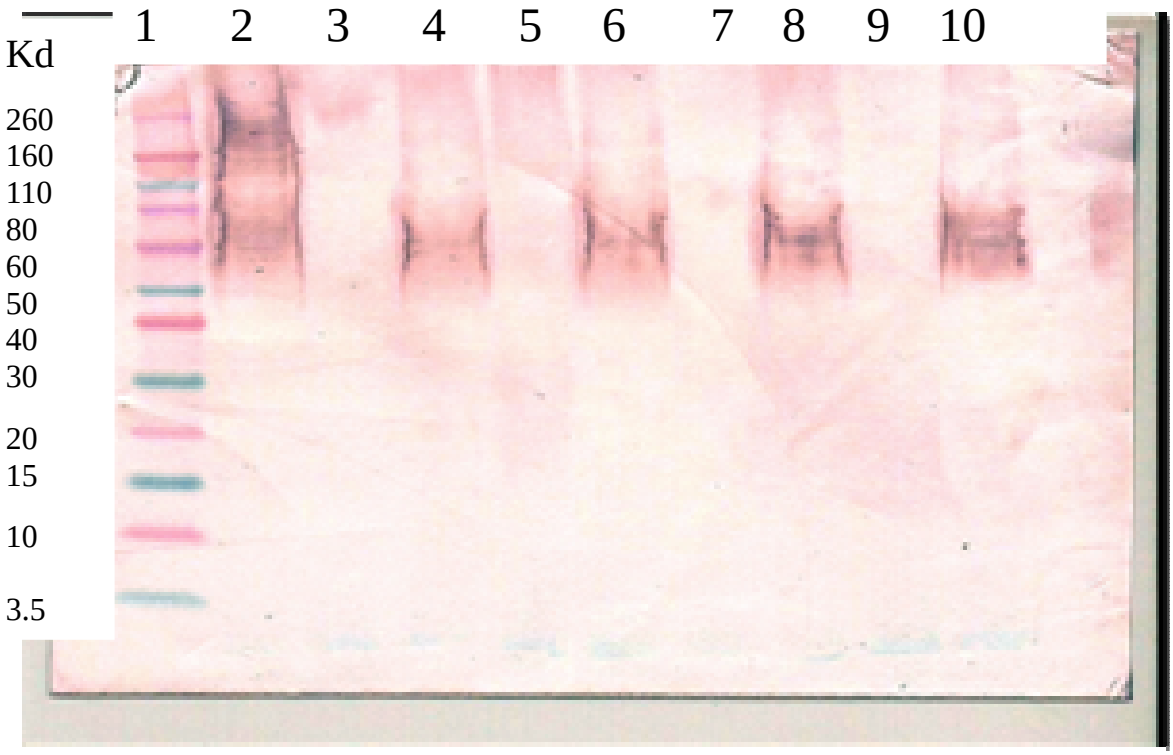

Figure B- 28. Western blot 9, where 1: ladder, 2: positive for *Citrobacter freundii* CF3GT5742; 3: negative for *Enterobacter agglomerans* GT1611; 4: positive for *E.coli* O157:H43 GT 4136; 5: negative for *E.coli* O157:H19 164; 6: positive for *E.coli* O157:H7 GT632; 7: negative for *E.coli* O157:H7 GT127; 8: positive for *E.coli* O157:H7 A110; 9: negative for *E.coli* O157:H7 125; 10: positive for *E.coli* O157:NM GT4141.

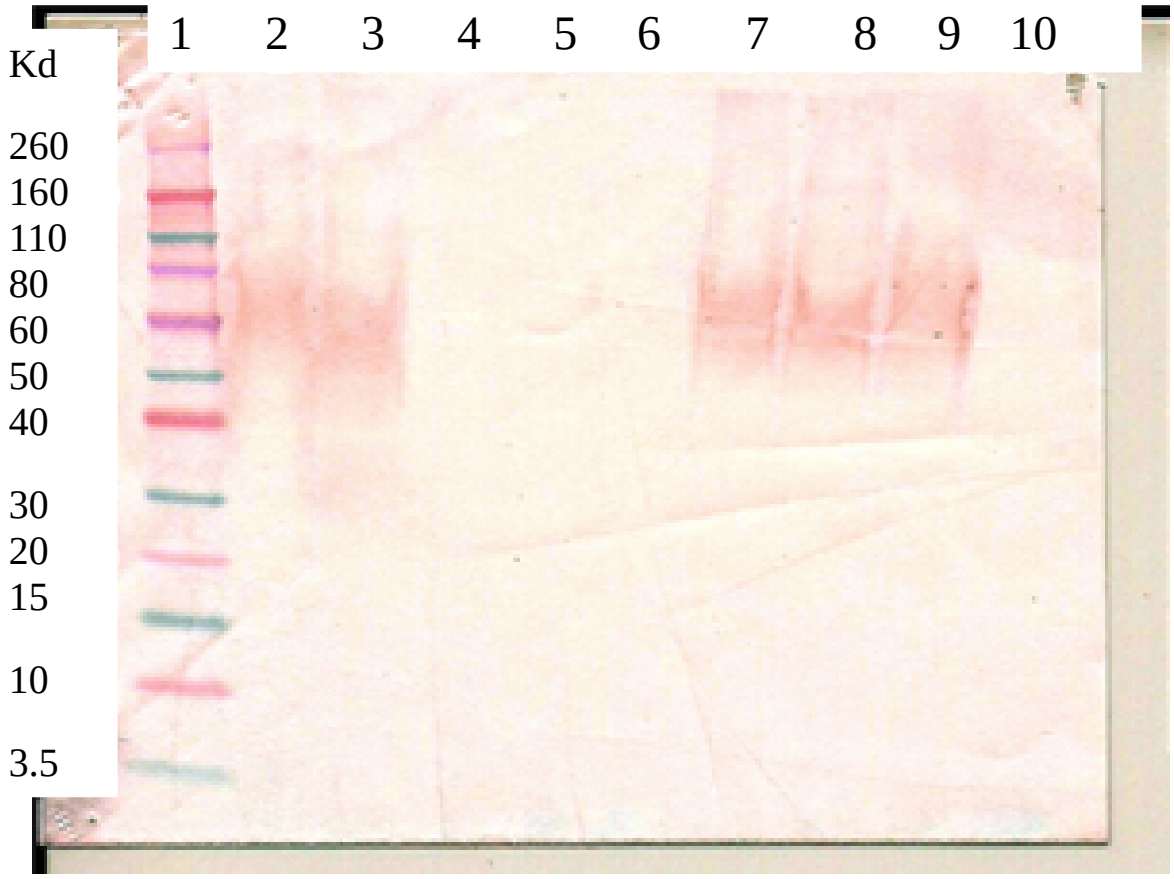

Figure B- 29. Western blot 10, where 1: ladder; 2: positive for *E.coli* O157:H16 GT4137; 3: positive for *E.coli* O157:H38 GT4138; 4: negative for *E. aerogenes* GT47; 5: negative for *E. cloacae* GT50; 6: negative for *C. freundii* GT9173; 7: positive for *E.coli* O157:H7 GT4135; 8: positive for *E.coli* O157:H7 GT4132; 9: positive for *E.coli* O157:H45; 10: negative for *C. freundii* GT 4885.

Table B- 11. Data for Figures 5-1 and 5-2, passive adsorption.

Controls	Fluorescent Output (RFU)			Average Fluorescent Output (RFU)	Standard Deviation
Neg (blank)	54.00	27.00	25.00	35.33	16.20
No antibody with PicoGreen cells	64.00	134.00	153.00	117.00	46.87
FITC					
1 ug/ml	45.00	60.00	58.00	54.33	8.14
10 ug/ml	93.00	147.00	188.00	142.67	47.65
100 ug/ml	185.00	239.00	403.00	275.67	113.53
PicoGreen Cells					
1 ug/ml	55.00	103.00	91.00	83.00	24.98
10 ug/ml	207.00	243.00	188.00	212.67	27.93
100 ug/ml	965.00	285.00	217.00	489.00	413.63

Table B- 12. Data for Figures 5-1 and 5-2, glutaraldehyde immobilization.

Controls	Fluorescent Output (RFU)			Average Fluorescent Output (RFU)	Standard Deviation
Neg (blank)	38.00	157.00	18.00	71.00	75.15
No antibody with PicoGreen cells	271.00	144.00	136.00	183.67	75.74
FITC					
1 ug/ml	31	61	36	42.67	16.07
10 ug/ml	129	81	60	90.00	35.37
100 ug/ml	100	146	134	126.67	23.86
PicoGreen Cells					
1 ug/ml	123	94	183	133.33	45.39
10 ug/ml	267	471	255	331.00	121.39
100 ug/ml	361	925	286	524.00	349.30

Table B- 13. Data for Figures 5-1 and 5-2, EDC / sulfo-NHS immobilization.

Controls	Fluorescent Output (RFU)			Average Fluorescent Output (RFU)	Standard Deviation
Neg (blank)	61.00	31.00	128.00	73.33	49.66
No antibody with PicoGreen cells	65.00	59.00	98.00	74.00	21.00
FITC					
1 ug/ml	78	52	91	73.67	19.86
10 ug/ml	272	186	248	235.33	44.38
100 ug/ml	458	168	170	265.33	166.86
PicoGreen Cells					
1 ug/ml	67	53	63	61.00	7.21
10 ug/ml	159	171	202	177.33	22.19
100 ug/ml	213	152	195	186.67	31.34

Table B- 14. Data for Figures 5-5, and 5-6 (0 washes).

0 Washes	Fluorescent Output (RFU)			Average Fluorescent Output (RFU)	Standard Deviation
No Cells					
No Block	21	10	15	15.33	5.507570547
BSA Block	20	15	17	17.33	2.516611478
Goat Block	17	8	19	14.67	5.859465277
E. coli O157:H7					
No Block	205	123	249	192.33	63.94789546
BSA Block	143	251	273	222.33	69.57969052
Goat Block	84	179	192	151.67	58.96043871
Salmonella Enteritidis					
No Block	286	355	737	459.33	242.9286589
BSA Block	1052	350	446	616.00	380.6258005
Goat Block	296	309	253	286.00	29.30870178

Table B- 15. Data for Figures 5-4, 5-5, and 5-6 (1 wash). Outlier removed from No Cells, Goat Block using Dixon's Q-test.

1 Wash	Fluorescent Output (RFU)			Average Fluorescent Output (RFU)	Standard Deviation
No Cells					
No Block	17	7	15	13.00	5.291502622
BSA Block	3	22	10	11.67	9.609023537
Goat Block		18	18	18.00	0
E. coli O157:H7					
No Block	385	541	312	412.67	116.9800553
BSA Block	134	196	220	183.33	44.37717131
Goat Block	338	280	482	366.67	104.0064101
Salmonella Enteritidis					
No Block	126	77	100	101.00	24.51530134
BSA Block	113	72	83	89.33	21.22105872
Goat Block	66	58	84	69.33	13.31665624

Table B- 16. Data for Figures 5-5 and 5-6 (3 washes). Outliers removed from *E. coli* O157:H7, BSA Block and *Salmonella* Enteritidis, Goat Block using Dixon's Q-test.

3 Washes	Fluorescent Output (RFU)			Average Fluorescent Output (RFU)	Standard Deviation
No Cells					
No Block	18	13	12	14.33	3.214550254
BSA Block	24	60	14	32.67	24.19366308
Goat Block	25	19	22	22.00	3
E. coli O157:H7					
No Block	58	112	350	173.33	155.361943
BSA Block		198	199	198.50	0.707106781
Goat Block	237	277	165	226.33	56.75679108
Salmonella Enteritidis					
No Block	48	52	56	52.00	4
BSA Block	77	121	104	100.67	22.18858565
Goat Block		34	34	34.00	0

B.4 CHAPTER 6 DATA

Table B- 17. Data for Figure 6-4.

Voltage (V)	Current (μA)			Average Current (μA)
-1.0	-2444.66	-3362.97	-3706.54	-3171.39
-0.9	-2093.41	-2952.59	-3299.89	-2781.96
-0.8	-1787.00	-2557.86	-2888.70	-2411.18
-0.7	-1496.54	-2178.66	-2495.20	-2056.80
-0.6	-1222.04	-1808.82	-2115.82	-1715.56
-0.5	-964.66	-1457.71	-1746.82	-1389.73
-0.4	-730.54	-1128.21	-1383.73	-1080.83
-0.3	-518.18	-817.14	-1028.77	-788.03
-0.2	-329.61	-523.07	-680.64	-511.11
-0.1	-159.68	-250.84	-337.93	-249.48
0.0	-0.36	0.75	0.86	0.41
0.1	160.33	239.27	339.79	246.46
0.2	330.09	472.28	679.25	493.87
0.3	514.78	698.13	1021.93	744.95
0.4	718.40	906.79	1366.07	997.09
0.5	945.44	1100.89	1715.50	1253.94
0.6	1188.38	1291.35	2066.07	1515.27
0.7	1440.76	1463.18	2421.98	1775.31
0.8	1684.90	1605.70	2780.21	2023.60
0.9	1921.66	1713.63	3137.72	2257.67
1.0	2160.11	1808.86	3486.52	2485.16

Table B- 18. Data for Figures 6-5 and 6-6.

Sample	Plate Counts		
Blank	0	0	0
D5	TNC	TNC	TNC
D6	97	74	80
D7	12	15	5
D8	0	0	0
SPC=(ΣD6)/(n*10^-7) SPC = 8.4 x 10^8 cfu/mL			

Sample	Concentration (CFU/mL)
Blank	0.00E+00
D0	8.37E+08
D3	8.37E+05
D5	8.37E+03
D8	8.37E+00

Table B- 19. Data for Figure 6-5, R_T.

	Resistance (kΩ)				
Time (min)	Blank	D8	D5	D3	D0
0.0	1.130	1.083	1.250	1.406	1.547
0.5	2.293	2.225	2.519	2.775	3.068
1.0	8.597	9.085	9.327	9.566	10.440
1.5	5.726	6.063	6.332	6.924	7.264
2.0	5.765	6.177	6.302	6.964	7.286
2.5	5.784	6.111	6.319	6.878	7.297
3.0	5.780	6.032	6.331	6.796	7.327
3.5	5.786	6.073	6.345	6.884	7.354
4.0	5.790	6.031	6.368	6.919	7.390
4.5	5.828	5.994	6.394	6.948	7.426
5.0	5.839	5.973	6.429	6.979	7.475
5.5	5.896	5.963	6.468	7.027	7.522
6.0	5.920	5.960	6.514	7.056	7.542
6.5	5.936	5.959	6.550	7.069	7.541
7.0	5.936	5.987	6.580	7.099	7.550
7.5	5.966	6.018	6.586	7.125	7.556
8.0	5.969	6.036	6.590	7.134	7.559
8.5	5.979	6.056	6.587	7.143	7.590
9.0	5.975	6.056	6.609	7.169	7.619
9.5	5.989	6.057	6.636	7.165	7.610
10.0	6.041	6.061	6.660	7.188	7.583
10.5	6.070	6.129	6.660	7.221	7.583
11.0	6.045	6.169	6.666	7.265	7.583
11.5	6.045	6.187	6.677	7.260	7.584
12.0	6.054	6.180	6.697	7.257	7.598
12.5	6.075	6.213	6.706	7.275	7.647
13.0	6.079	6.241	6.733	7.318	7.678
13.5	6.112	6.272	6.757	7.349	7.690
14.0	6.107	6.294	6.768	7.346	7.685
14.5	6.102	6.260	6.762	7.360	7.648

Table B- 20. Data for Figure 6-6, R_2.

	Resistance (kΩ)				
Time (min)	Blank	D8	D5	D3	D0
0.0	61.538	100.000	400.000	80.000	200.000
0.5	247.814	400.029	13970.664	297.906	1272.988
1.0	314.607	442.513	636.364	411.765	560.000
1.5	806.916	858.896	771.882	742.706	742.706
2.0	1040.892	1445.161	866.873	1040.892	1040.892
2.5	2413.793	3636.364	1341.317	2413.793	2413.793
3.0	35000.011	7417.219	3414.633	35000.011	35000.011
3.5	8000.000	5957.447	8549.619	8000.000	8000.000
4.0	7531.943	7671.233	8247.423	7593.220	7624.234
4.5	9180.329	13023.255	9003.215	9003.215	8917.197
5.0	26987.946	67469.882	22857.143	20180.177	17919.997
5.5	25454.542	13088.700	42424.258	57142.857	200000.000
6.0	15336.163	17041.349	22489.963	27654.317	37966.110
6.5	14997.324	16036.656	28806.589	32825.329	36842.101
7.0	13262.283	13757.100	22012.574	25431.419	24496.943
7.5	11049.724	11904.762	15730.334	17857.143	17623.916
8.0	10949.262	11879.193	13371.537	15611.062	15642.456
8.5	10538.201	11970.927	14470.285	15948.963	16149.965
9.0	11342.001	11377.949	15256.359	15938.068	15952.144
9.5	10930.668	206871.356	15397.516	15727.687	16009.606
10.0	10000.714	2337.678	15506.078	16711.431	17018.693
10.5	9818.015	1826.146	15512.467	15258.854	16986.171
11.0	11083.403	1948.755	14762.335	15295.530	18036.009
11.5	13634.860	8596.374	14352.091	15242.573	18919.557
12.0	8833.476	6395.541	14294.585	17498.493	20053.141
12.5	8188.271	20203.661	15247.431	16923.234	18673.857
13.0	8224.408	13930.347	15156.108	17398.463	18390.561
13.5	10439.093	13402.257	15437.245	16903.925	17990.666
14.0	10012.516	13559.322	16220.600	16981.533	17590.150
14.5	10767.160	12578.616	15255.530	19846.192	17901.096

Table B- 21. Calculated values of R_1.

	Resistance (kΩ)				
Time (min)	Blank	D8	D5	D3	D0
0.0	1.151	1.094	1.254	1.431	1.559
0.5	2.314	2.238	2.519	2.801	3.075
1.0	8.838	9.275	9.466	9.794	10.638
1.5	5.767	6.106	6.384	6.989	7.336
2.0	5.797	6.203	6.348	7.011	7.337
2.5	5.798	6.121	6.349	6.897	7.319
3.0	5.781	6.037	6.343	6.797	7.328
3.5	5.790	6.080	6.349	6.890	7.361
4.0	5.794	6.035	6.373	6.926	7.398
4.5	5.832	5.996	6.399	6.954	7.432
5.0	5.841	5.974	6.431	6.981	7.478
5.5	5.898	5.965	6.469	7.028	7.522
6.0	5.922	5.962	6.516	7.058	7.543
6.5	5.938	5.962	6.551	7.070	7.542
7.0	5.938	5.990	6.582	7.101	7.553
7.5	5.970	6.021	6.588	7.128	7.560
8.0	5.973	6.039	6.594	7.137	7.562
8.5	5.982	6.059	6.590	7.146	7.594
9.0	5.979	6.059	6.611	7.173	7.623
9.5	5.993	6.057	6.638	7.168	7.613
10.0	6.044	6.077	6.663	7.191	7.586
10.5	6.074	6.150	6.663	7.224	7.586
11.0	6.048	6.188	6.669	7.268	7.587
11.5	6.048	6.192	6.680	7.264	7.588
12.0	6.058	6.186	6.700	7.260	7.601
12.5	6.079	6.215	6.709	7.278	7.650
13.0	6.083	6.244	6.736	7.321	7.681
13.5	6.115	6.275	6.760	7.352	7.693
14.0	6.111	6.297	6.771	7.349	7.688
14.5	6.106	6.263	6.765	7.362	7.651

Table B- 22. Calculated values of ΔR.

	Change in R due to R2, ΔR (Ω)				
Time (min)	Blank	D8	D5	D3	D0
0.0	21.136	11.847	3.918	25.152	12.065
0.5	21.406	12.448	0.454	26.089	7.411
1.0	241.516	190.429	138.740	227.526	198.328
1.5	40.924	43.109	52.370	65.161	71.752
2.0	32.107	26.512	46.153	46.905	51.357
2.5	13.893	10.287	29.909	19.653	22.128
3.0	0.955	4.909	11.759	1.320	1.534
3.5	4.187	6.198	4.712	5.929	6.766
4.0	4.454	4.745	4.920	6.311	7.171
4.5	3.703	2.760	4.545	5.367	6.189
5.0	1.264	0.529	1.809	2.414	3.119
5.5	1.366	2.717	0.986	0.864	0.283
6.0	2.286	2.085	1.887	1.801	1.498
6.5	2.350	2.215	1.490	1.522	1.544
7.0	2.658	2.607	1.968	1.982	2.328
7.5	3.223	3.043	2.758	2.844	3.241
8.0	3.256	3.068	3.250	3.262	3.654
8.5	3.394	3.065	3.000	3.201	3.569
9.0	3.150	3.225	2.864	3.226	3.641
9.5	3.284	0.177	2.861	3.266	3.619
10.0	3.651	15.755	2.862	3.093	3.380
10.5	3.755	20.639	2.860	3.418	3.387
11.0	3.298	19.590	3.012	3.452	3.190
11.5	2.681	4.456	3.107	3.460	3.042
12.0	4.152	5.977	3.139	3.011	2.880
12.5	4.510	1.911	2.951	3.128	3.132
13.0	4.496	2.797	2.992	3.079	3.207
13.5	3.580	2.937	2.959	3.197	3.289
14.0	3.727	2.923	2.825	3.179	3.359
14.5	3.460	3.117	2.999	2.730	3.269

Table B- 23. Percent change due to R_2.

	Change Due to R2 (%)				
Time (min)	B	D8	D5	D3	D0
0.0	1.871	1.094	0.313	1.789	0.780
0.5	0.934	0.559	0.018	0.940	0.242
1.0	2.809	2.096	1.487	2.378	1.900
1.5	0.715	0.711	0.827	0.941	0.988
2.0	0.557	0.429	0.732	0.674	0.705
2.5	0.240	0.168	0.473	0.286	0.303
3.0	0.017	0.081	0.186	0.019	0.021
3.5	0.072	0.102	0.074	0.086	0.092
4.0	0.077	0.079	0.077	0.091	0.097
4.5	0.064	0.046	0.071	0.077	0.083
5.0	0.022	0.009	0.028	0.035	0.042
5.5	0.023	0.046	0.015	0.012	0.004
6.0	0.039	0.035	0.029	0.026	0.020
6.5	0.040	0.037	0.023	0.022	0.020
7.0	0.045	0.044	0.030	0.028	0.031
7.5	0.054	0.051	0.042	0.040	0.043
8.0	0.055	0.051	0.049	0.046	0.048
8.5	0.057	0.051	0.046	0.045	0.047
9.0	0.053	0.053	0.043	0.045	0.048
9.5	0.055	0.003	0.043	0.046	0.048
10.0	0.060	0.260	0.043	0.043	0.045
10.5	0.062	0.337	0.043	0.047	0.045
11.0	0.055	0.318	0.045	0.048	0.042
11.5	0.044	0.072	0.047	0.048	0.040
12.0	0.069	0.097	0.047	0.041	0.038
12.5	0.074	0.031	0.044	0.043	0.041
13.0	0.074	0.045	0.044	0.042	0.042
13.5	0.059	0.047	0.044	0.043	0.043
14.0	0.061	0.046	0.042	0.043	0.044
14.5	0.057	0.050	0.044	0.037	0.043

Table B- 24. Student's T-Test comparing R_T and R_1 (2 tails, $\alpha = 0.05$).

RT	R1	P Value	Significant Difference
Blank	Blank	0.962	No
D8	D8	0.967	No
D5	D5	0.973	No
D3	D3	0.964	No
D0	D0	0.969	No

Table B- 25. Resistances of blank sample.

Time (s)	Resistance (Ω)				
0	1129.94	1694.92	2056.56	5128.20	1951.22
30	2292.51	3604.15	4165.53	8004.71	4172.99
60	8596.87	17262.64	15258.85	14644.35	20756.11
90	5726.09	10164.63	10151.09	12864.69	11739.55
120	5764.99	10116.70	10081.73	12690.93	11091.30
150	5783.93	10069.23	9831.03	12575.22	10576.41
180	5780.35	10011.44	9620.34	12441.13	10395.40
210	5785.72	10046.46	9581.74	12544.80	10431.41
240	5790.03	10072.67	9648.52	12591.12	10403.43
270	5828.35	10134.68	9657.09	12654.79	10306.43
300	5839.29	10181.85	9663.90	12671.40	10204.68
330	5896.23	10265.75	9657.17	12740.07	10122.66
360	5919.79	10266.11	9652.34	12860.14	10050.25
390	5935.72	10278.15	9648.12	13016.17	9903.86
420	5935.60	10268.71	9644.34	13085.27	9752.12
450	5966.33	10276.64	9647.46	13134.99	9646.66
481	5969.26	10278.25	9623.17	13171.08	9602.46
511	5978.82	10286.89	9543.61	13329.46	9540.16
541	5975.50	10306.13	9462.33	13552.30	9533.73
571	5989.43	10338.28	9439.37	13669.34	9537.24
601	6040.60	10352.39	9453.39	13676.68	9505.22
631	6070.20	10359.24	9457.94	13708.76	9412.14
661	6044.51	10411.55	9454.35	13914.84	9367.68
691	6044.90	10466.20	9450.28	14046.64	9336.90
721	6053.92	10487.10	9443.19	14088.48	9318.43
751	6074.94	10468.46	9431.82	14173.77	9290.23
781	6078.63	10450.78	9430.47	14333.84	9246.32
811	6111.80	10438.48	9438.41	14495.23	9207.92
841	6106.87	10432.65	9447.01	14543.49	9187.57
871	6102.21	10426.17	9445.10	14582.57	9190.12
901		10427.53	9445.10	14643.97	9241.08
Average	5753.78	10020.80	9352.62	13018.66	9742.63
Total Average	9602.53				
Total StDev	3102.71				

Table B- 26. Data for Figures 6-7, 6-8, and 6-12 experiment A.

Sample	Plate Counts		
Blank	0	0	0
D5	TNC	TNC	TNC
D6	134	152	130
D7	12	15	10
D8	0	0	0
SPC=(ΣD6)/(n*10^-7) SPC = 1.39E+09 CFU/mL			

Sample	Concentration (CFU/mL)
Blank	0.00E+00
D0	1.39E+09
D3	1.39E+06
D5	1.39E+04
D8	1.39E+01

Table B- 27. Data for Figure 6-7, 6-8, and 6-12, experiment A resistance.

	Resistance (Ω)				
Time (s)	Blank	D8	D5	D3	D0
180	9620.34	10513.67	10729.61	11316.08	11860.38
210	9581.74	10546.14	10728.38	11425.10	11922.50
240	9648.52	10508.54	10803.93	11459.82	11927.38
270	9657.09	10469.44	10822.63	11505.97	11919.15
300	9663.90	10533.25	10916.22	11474.05	11850.70
330	9657.17	10547.81	10904.22	11495.46	11745.07
360	9652.34	10543.95	10917.87	11470.10	11718.86
390	9648.12	10559.62	10916.34	11553.30	11770.84
420	9644.34	10572.30	10942.58	11626.89	11848.83
450	9647.46	10591.18	10915.80	11725.83	11848.84
481	9623.17	10642.50	10908.68	11767.08	11870.28
511	9543.61	10697.35	10984.61	11784.71	11860.95
541	9462.33	10659.47	11096.67	11788.26	11885.48
571	9439.37	10619.66	11100.63	11769.40	11841.59
601	9453.39	10563.99	11020.59	11786.62	11786.59
631	9457.94	10518.05	10985.46	11782.87	11705.39
661	9454.35	10512.36	10979.47	11784.83	11686.92
691	9450.28	10549.20	10990.65	11779.80	11713.47
721	9443.19	10590.74	11002.01	11769.11	11764.36
751	9431.82	10644.04	11002.80	11755.57	11796.03
781	9430.47	10687.23	11028.86	11762.64	11820.13
811	9438.41	10669.27	10996.88	11776.58	11813.60
841	9447.01	10608.87	11006.67	11781.35	11834.82
871	9445.10	10559.66	11046.67	11778.56	11945.65
901	9445.10	10554.09	10966.42	11787.24	12208.15
180	12441.13	15973.53	25132.40	30663.94	32149.25
210	12544.80	15961.69	25152.15	31218.64	32825.33
240	12591.12	16340.73	25640.55	31361.21	33023.53
270	12654.79	16612.58	26042.15	31267.72	32777.66
300	12671.40	16986.58	26218.70	31186.30	32853.04
330	12740.07	17344.12	26192.22	31192.24	32776.14
360	12860.14	17612.06	26422.56	31188.38	33248.62
390	13016.17	17794.39	26479.29	31240.78	33706.51
420	13085.27	18002.73	26465.78	31286.66	33785.61
450	13134.99	18450.31	26549.09	31333.48	33797.65
481	13171.08	18911.76	26945.62	31281.42	33825.77
511	13329.46	19177.68	27414.70	31314.31	33836.25

Table B-27 (cont'd).

541	13552.30	19374.62	27723.59	31395.42	33992.70
571	13669.34	19728.38	27947.18	31647.81	33865.29
601	13676.68	20118.41	28048.81	31762.23	33998.90
631	13708.76	20542.55	28203.35	31914.74	34368.16
661	13914.84	20527.10	28401.89	32068.71	34781.30
691	14046.64	21068.40	28611.12	32251.88	34381.68
721	14088.48	21427.69	28662.38	32173.19	33970.69
751	14173.77	21901.34	28484.23	32004.34	34142.28
781	14333.84	21786.15	28411.96	31850.74	34714.46
811	14495.23	22083.41	28443.72	31802.06	35156.01
841	14543.49	22243.41	28965.71	31867.43	35199.77
871	14582.57	22421.52	29542.10	31923.38	35133.95
901	14643.97	22714.37	28766.63	31796.50	35026.27
180	10395.40	11234.15	12247.40	12731.70	13837.41
210	10431.41	11267.61	12330.80	12749.54	13926.07
240	10403.43	11261.53	12372.87	12748.95	13907.24
270	10306.43	11125.06	12431.01	12711.42	13887.00
300	10204.68	10904.37	12461.75	12677.50	13885.22
330	10122.66	10846.44	12475.21	12681.91	13916.70
360	10050.25	10863.87	12486.12	12705.98	13938.17
390	9903.86	10849.94	12521.69	12742.85	13978.28
420	9752.12	10788.61	12516.48	12809.15	14010.02
450	9646.66	10686.53	12502.01	12917.75	14073.25
481	9602.46	10467.09	12498.27	12931.83	14111.05
511	9540.16	10304.54	12513.91	12923.42	14162.66
541	9533.73	10129.44	12512.73	12967.52	14191.80
571	9537.24	10015.95	12520.07	13068.72	14243.85
601	9505.22	9895.60	12512.29	13108.37	14274.79
631	9412.14	9854.92	12521.41	13200.57	14315.59
661	9367.68	9805.78	12494.48	13253.68	14359.34
691	9336.90	9746.25	12488.35	13266.43	14386.90
721	9318.43	9680.31	12494.37	13270.52	14405.59
751	9290.23	9647.12	12528.52	13321.60	14442.48
781	9246.32	9648.49	12555.15	13331.94	14499.96
811	9207.92	9654.21	12605.57	13349.80	14539.68
841	9187.57	9661.71	12618.24	13424.56	14588.58
871	9190.12	9671.18	12588.51	13518.08	14598.54
901	9241.08	9716.99	12646.22	13603.13	14458.70

Table B- 28. Data for Figure 6-7, experiment A.

	Average Resistance (kΩ)				
Time (min)	Blank	D8	D5	D3	D0
3.0	10.82	12.57	16.04	18.24	19.28
3.5	10.85	12.59	16.07	18.46	19.56
4.0	10.88	12.70	16.27	18.52	19.62
4.5	10.87	12.74	16.43	18.50	19.53
5.0	10.85	12.81	16.53	18.45	19.53
5.5	10.84	12.91	16.52	18.46	19.48
6.0	10.85	13.01	16.61	18.45	19.64
6.5	10.86	13.07	16.64	18.51	19.82
7.0	10.83	13.12	16.64	18.57	19.88
7.5	10.81	13.24	16.66	18.66	19.91
8.0	10.80	13.34	16.78	18.66	19.94
8.5	10.80	13.39	16.97	18.67	19.95
9.0	10.85	13.39	17.11	18.72	20.02
9.5	10.88	13.45	17.19	18.83	19.98
10.0	10.88	13.53	17.19	18.89	20.02
10.5	10.86	13.64	17.24	18.97	20.13
11.0	10.91	13.62	17.29	19.04	20.28
11.5	10.94	13.79	17.36	19.10	20.16
12.0	10.95	13.90	17.39	19.07	20.05
12.5	10.97	14.06	17.34	19.03	20.13
13.0	11.00	14.04	17.33	18.98	20.34
13.5	11.05	14.14	17.35	18.98	20.50
14.0	11.06	14.17	17.53	19.02	20.54
14.5	11.07	14.22	17.73	19.07	20.56
15.0	11.11	14.33	17.46	19.06	20.56

Table B- 29. Data for Figure 6-8, experiment A.

	Blank	D8	D5	D3	D0
Average Resistance (kΩ)	10.90	13.43	16.95	18.76	19.98
Standard Deviation (kΩ)	1.92	4.45	7.50	9.14	9.97

Table B- 30. Student's T-Test of data, experiment A.

Sample 1	Sample 2	P Value	Significant Difference
Blank	D8	1.71E-05	Yes
Blank	D5	1.73E-09	Yes
Blank	D3	1.95E-10	Yes
Blank	D0	2.69E-11	Yes
D8	D5	0.001	Yes
D8	D3	1.49E-05	Yes
D8	D0	1.06E-06	Yes
D5	D3	0.187	No
D5	D0	0.037	Yes
D3	D0	0.436	No

Table B- 31. Data for Figures 6-9 and 6-12, experiment B.

Sample	Plate Counts		
Blank	0	0	0
D6	103	82	88
D7	14	5	8
D8	1	1	2
SPC=(ΣD6)/(n*10^-7) SPC = 9.10E+08 CFU/mL			

Sample	Concentration (CFU/mL)
Blank	0.00E+00
D0	9.10E+08
D3	9.10E+05
D5	9.10E+03
D8	9.10E+00

Table B- 32. Data for Figures 6-10 and 6-12, experiment C.

Sample	Plate Counts		
Blank	0	0	0
D5	TNC	TNC	354
D6	74	92	78
D7	4	2	9
D8	0	2	0
SPC=(ΣD6)/(n*10^-7) SPC = 7.30E+08 CFU/mL			

Sample	Concentration (CFU/mL)
Blank	0.00E+00
D0	7.30E+08
D3	7.30E+05
D5	7.30E+03
D8	7.30E+00

Table B- 33. Data for Figures 6-11 and 6-12, experiment D.

Sample	Plate Counts		
Blank	0	0	0
D5	TNC	TNC	TNC
D6	80	82	123
D7	4	6	4
D8	0	1	0
SPC=(ΣD6)/(n*10^-7) SPC = 9.50E+08 CFU/mL			

Sample	Concentration (CFU/mL)
Blank	0.00E+00
D0	9.50E+08
D3	9.50E+05
D5	9.50E+03
D8	9.50E+00

Table B- 34. Data for Figure 6-12, experiment E.

Sample	Plate Counts		
Blank	0	0	0
D5	TNC	TNC	TNC
D6	97	74	80
D7	12	15	5
D8	0	0	0
SPC=(ΣD6)/(n*10^-7) SPC = 8.37E+08 CFU/mL			

Sample	Concentration (CFU/mL)
Blank	0.00E+00
D0	8.37E+08
D3	8.37E+05
D5	8.37E+03
D8	8.37E+00

Table B- 35. Data for Figure 6-12, experiment F.

Sample	Plate Counts		
Blank	0	0	0
D5	TNC	TNC	294
D6	30	37	30
D7	3	1	5
D8	0	0	0
SPC=(ΣD6)/(n*10^-7) SPC = 3.23E+08 CFU/mL			

Sample	Concentration (CFU/mL)
Blank	0.00E+00
D0	3.23E+08
D3	3.23E+05
D5	3.23E+03
D8	3.23E+00

Table B- 36. Data for Figure 6-12, experiment G.

Sample	Plate Counts		
Blank	0	0	0
D5	TNC	TNC	TNC
D6	149	128	141
D7	10	13	19
D8	0	0	0
SPC=(ΣD6)/(n*10^-7) SPC = 1.39E+09 CFU/mL			

Sample	Concentration (CFU/mL)
Blank	0.00E+00
D0	1.39E+09
D3	1.39E+06
D5	1.39E+04
D8	1.39E+01

Table B- 37. Data for Figure 6-12, experiment H.

Sample	Plate Counts		
Blank	0	0	0
D5	TNC	TNC	TNC
D6	44	73	68
D7	1	19	17
D8	0	0	1
SPC=(ΣD6)/(n*10^-7) SPC = 6.17E+08 CFU/mL			

Sample	Concentration (CFU/mL)
Blank	0.00E+00
D0	6.17E+08
D3	6.17E+05
D5	6.17E+03
D8	6.17E+00

Table B- 38. Data for Figure 6-12, experiment A response.

	Response (%)			
Time (min)	D8	D5	D3	D0
3.0	9.29	11.53	17.63	23.28
3.5	10.06	11.97	19.24	24.43
4.0	8.91	11.97	18.77	23.62
4.5	8.41	12.07	19.15	23.42
5.0	9.00	12.96	18.73	22.63
5.5	9.22	12.91	19.04	21.62
6.0	9.24	13.11	18.83	21.41
6.5	9.45	13.14	19.75	22.00
7.0	9.62	13.46	20.56	22.86
7.5	9.78	13.15	21.54	22.82
8.0	10.59	13.36	22.28	23.35
8.5	12.09	15.10	23.48	24.28
9.0	12.65	17.27	24.58	25.61
9.5	12.50	17.60	24.68	25.45
10.0	11.75	16.58	24.68	24.68
10.5	11.21	16.15	24.58	23.76
11.0	11.19	16.13	24.65	23.61
11.5	11.63	16.30	24.65	23.95
12.0	12.15	16.51	24.63	24.58
12.5	12.85	16.66	24.64	25.07
13.0	13.33	16.95	24.73	25.34
13.5	13.04	16.51	24.77	25.17
14.0	12.30	16.51	24.71	25.28
14.5	11.80	16.96	24.71	26.47
15.0	11.74	16.11	24.80	29.25
3.0	28.39	102.01	146.47	158.41
3.5	27.24	100.50	148.86	161.66
4.0	29.78	103.64	149.07	162.28
4.5	31.27	105.79	147.08	159.01
5.0	34.05	106.91	146.12	159.27
5.5	36.14	105.59	144.84	157.27
6.0	36.95	105.46	142.52	158.54
6.5	36.71	103.43	140.02	158.96
7.0	37.58	102.26	139.10	158.20
7.5	40.47	102.12	138.55	157.31
8.0	43.59	104.58	137.50	156.82
8.5	43.87	105.67	134.93	153.85

Table B-38 (cont'd).

9.0	42.96	104.57	131.66	150.83
9.5	44.33	104.45	131.52	147.75
10.0	47.10	105.08	132.24	148.59
10.5	49.85	105.73	132.81	150.70
11.0	47.52	104.11	130.46	149.96
11.5	49.99	103.69	129.61	144.77
12.0	52.09	103.45	128.37	141.12
12.5	54.52	100.96	125.80	140.88
13.0	51.99	98.22	122.21	142.19
13.5	52.35	96.23	119.40	142.54
14.0	52.94	99.17	119.12	142.03
14.5	53.76	102.58	118.91	140.93
15.0	55.11	96.44	117.13	139.19
3.0	8.07	17.82	22.47	33.11
3.5	8.02	18.21	22.22	33.50
4.0	8.25	18.93	22.55	33.68
4.5	7.94	20.61	23.33	34.74
5.0	6.86	22.12	24.23	36.07
5.5	7.15	23.24	25.28	37.48
6.0	8.10	24.24	26.42	38.68
6.5	9.55	26.43	28.67	41.14
7.0	10.63	28.35	31.35	43.66
7.5	10.78	29.60	33.91	45.89
8.0	9.00	30.16	34.67	46.95
8.5	8.01	31.17	35.46	48.45
9.0	6.25	31.25	36.02	48.86
9.5	5.02	31.28	37.03	49.35
10.0	4.11	31.64	37.91	50.18
10.5	4.70	33.03	40.25	52.10
11.0	4.68	33.38	41.48	53.29
11.5	4.38	33.75	42.09	54.09
12.0	3.88	34.08	42.41	54.59
12.5	3.84	34.86	43.39	55.46
13.0	4.35	35.79	44.19	56.82
13.5	4.85	36.90	44.98	57.90
14.0	5.16	37.34	46.12	58.79
14.5	5.23	36.98	47.09	58.85
15.0	5.15	36.85	47.20	56.46

Table B- 39. Experiment A average response.

	Average Response (%)			
Time (min)	D8	D5	D3	D0
3.0	15.25	43.79	62.19	71.60
3.5	15.11	43.56	63.44	73.20
4.0	15.65	44.85	63.46	73.19
4.5	15.88	46.16	63.19	72.39
5.0	16.64	47.33	63.03	72.65
5.5	17.50	47.25	63.05	72.12
6.0	18.09	47.60	62.59	72.88
6.5	18.57	47.67	62.81	74.03
7.0	19.28	48.02	63.67	74.90
7.5	20.34	48.29	64.67	75.34
8.0	21.06	49.37	64.82	75.71
8.5	21.33	50.65	64.62	75.53
9.0	20.62	51.03	64.09	75.10
9.5	20.62	51.11	64.41	74.18
10.0	20.99	51.10	64.94	74.48
10.5	21.92	51.64	65.88	75.52
11.0	21.13	51.21	65.53	75.62
11.5	22.00	51.25	65.45	74.27
12.0	22.71	51.35	65.14	73.43
12.5	23.74	50.83	64.61	73.80
13.0	23.22	50.32	63.71	74.78
13.5	23.41	49.88	63.05	75.20
14.0	23.47	51.01	63.31	75.36
14.5	23.60	52.17	63.57	75.42
15.0	24.00	49.80	63.04	74.97

Table B- 40. Data for Figures 6-9 and 6-12, experiment B resistance.

	Resistance (Ω)				
Time (s)	B	D8	D5	D3	D0
180	56611.40	63240.92	72077.86	72407.54	70493.45
210	60375.08	63611.78	72141.70	73087.96	70818.84
240	62473.50	64043.00	71946.37	72101.77	71583.32
270	61201.27	64258.50	71461.38	71455.91	71753.47
300	60051.39	64220.37	71138.21	73763.80	71896.14
330	61097.35	64171.61	70701.71	74274.49	71922.58
360	62218.70	64369.02	68909.51	73857.19	72632.35
390	63783.48	64474.16	67464.99	73763.80	72475.49
421	65738.93	65236.22	67655.73	74740.91	73258.52
451	67097.18	65214.48	70311.13	74710.50	73239.00
481	67833.77	65267.01	71837.23	74204.12	74349.44
511	68427.86	64712.95	72235.69	75315.38	74074.07
541	67760.51	65617.94	70834.06	75180.40	73999.68
571	66166.08	64467.11	69684.67	75402.59	73094.64
601	64076.15	64152.13	69622.29	73898.12	73240.91
631	62058.45	64279.15	70387.57	74185.94	73197.83
661	59242.96	66539.92	71076.81	74768.35	73089.39
691	58778.46	67556.16	71358.03	75934.26	73437.80
721	59473.23	67673.71	71545.37	75817.06	74664.18
751	61859.65	67019.31	72338.80	75840.16	75522.59
781	62259.58	67020.91	73026.96	76032.33	75977.01
811	62584.16	67583.87	73465.75	75761.67	75874.58
841	62277.58	68736.96	72920.46	75153.29	76072.48
871	63593.00	69930.06	72926.16	74557.32	75400.57
901	65897.85	69204.15	71620.41	74005.55	72793.45
180	105144.58	89639.44	97357.45	115408.59	120911.15
210	110671.94	95076.39	101486.04	122132.06	125201.20
240	108573.44	112219.94	103907.68	120078.26	127278.51
270	106209.45	111124.32	108208.39	117484.16	130861.00
300	106072.66	111843.41	111964.18	118645.95	130584.82
330	105668.35	110488.52	114815.26	121754.22	127146.81
360	105940.22	112300.95	114034.37	123738.30	124747.95
390	108315.96	109982.91	113663.10	122654.57	124944.99
421	111390.68	112871.81	113614.70	123478.83	123874.35
451	111690.84	116784.17	115095.73	126164.82	120152.68
481	111007.21	113784.59	114820.71	129732.61	117571.65
511	109995.17	108198.97	114710.37	131311.83	117512.32

Table B-40 (cont'd).

541	110195.17	103484.08	114212.72	131053.63	119070.38
571	110068.64	104152.13	114426.50	129634.43	120897.44
601	107566.48	111013.32	115251.80	129134.30	121190.09
631	104327.74	115348.80	116191.93	128529.98	121960.65
661	103488.77	114768.08	115998.65	127052.47	120585.69
691	104113.11	109922.46	115074.93	127213.61	117920.55
721	105961.54	103181.58	114163.51	127729.65	119834.27
751	110043.83	98802.01	113838.53	130407.78	122970.98
781	111226.74	97721.85	113527.51	127849.80	127479.57
811	112196.55	98420.00	113282.79	129403.34	127477.85
841	113616.07	97623.47	113304.23	126081.24	128018.12
871	115025.16	97276.26	113010.31	121506.68	123342.58
901	111888.11	93984.96	111529.35	127327.71	120992.14
180	98039.22	123261.12	116424.11	173455.12	143076.13
210	116959.06	126949.56	125673.26	152061.28	158640.21
240	126748.46	128058.55	125532.38	157764.24	164790.69
270	123527.61	129425.91	126559.40	157691.80	165172.24
300	118363.20	130162.91	129557.64	156853.89	163300.98
330	114355.71	131381.36	135235.47	156772.15	163905.62
360	109430.55	131935.45	137083.54	156612.90	164858.61
390	103941.22	133590.33	136888.64	156179.48	167218.10
421	101190.42	137803.42	137085.04	154795.17	168522.15
451	101415.09	139981.80	140506.47	154094.93	167023.60
481	101935.59	143190.29	142830.37	154306.08	159556.66
511	101898.95	142966.53	142045.78	156138.90	155078.24
541	103156.87	142429.12	142142.77	155491.64	156109.11
571	102375.10	143763.72	148668.07	157669.62	159567.00
601	102584.68	151032.94	154773.94	159376.37	158587.58
631	105004.21	156137.14	155832.61	160020.12	157411.35
661	108624.39	154908.35	154694.64	156727.73	155681.37
691	109310.95	154301.84	154340.57	153555.06	153924.11
721	109347.65	153454.91	154342.95	152233.69	152576.72
751	114339.37	151789.89	153886.50	155829.99	153173.18
781	117676.21	148199.13	154703.88	157536.13	152382.48
811	115942.51	145013.83	152378.26	158485.79	152198.52
841	112562.80	143342.01	150248.92	158317.28	154281.04
871	109394.23	143292.14	148011.10	159140.64	159077.35
901	95192.77	145586.90	148478.10	157511.32	160610.32

Table B- 41. Data for Figures 6-9 and 6-12, experiment B response.

	Response (%)			
Time (min)	D8	D5	D3	D0
3.0	11.71	27.32	27.90	24.52
3.5	5.36	19.49	21.06	17.30
4.0	2.51	15.16	15.41	14.58
4.5	5.00	16.76	16.76	17.24
5.0	6.94	18.46	22.83	19.72
5.5	5.03	15.72	21.57	17.72
6.0	3.46	10.75	18.71	16.74
6.5	1.08	5.77	15.65	13.63
7.0	-0.76	2.92	13.69	11.44
7.5	-2.81	4.79	11.35	9.15
8.0	-3.78	5.90	9.39	9.61
8.5	-5.43	5.56	10.07	8.25
9.0	-3.16	4.54	10.95	9.21
9.5	-2.57	5.32	13.96	10.47
10.0	0.12	8.66	15.33	14.30
10.5	3.58	13.42	19.54	17.95
11.0	12.32	19.98	26.21	23.37
11.5	14.93	21.40	29.19	24.94
12.0	13.79	20.30	27.48	25.54
12.5	8.34	16.94	22.60	22.09
13.0	7.65	17.29	22.12	22.03
13.5	7.99	17.39	21.06	21.24
14.0	10.37	17.09	20.67	22.15
14.5	9.97	14.68	17.24	18.57
15.0	5.02	8.68	12.30	10.46
3.0	-14.75	-7.41	9.76	15.00
3.5	-14.09	-8.30	10.36	13.13
4.0	3.36	-4.30	10.60	17.23
4.5	4.63	1.88	10.62	23.21
5.0	5.44	5.55	11.85	23.11
5.5	4.56	8.66	15.22	20.33
6.0	6.00	7.64	16.80	17.75
6.5	1.54	4.94	13.24	15.35
7.0	1.33	2.00	10.85	11.21
7.5	4.56	3.05	12.96	7.58
8.0	2.50	3.44	16.87	5.91
8.5	-1.63	4.29	19.38	6.83

Table B-41 (cont'd).

9.0	-6.09	3.65	18.93	8.05
9.5	-5.38	3.96	17.78	9.84
10.0	3.20	7.14	20.05	12.67
10.5	10.56	11.37	23.20	16.90
11.0	10.90	12.09	22.77	16.52
11.5	5.58	10.53	22.19	13.26
12.0	-2.62	7.74	20.54	13.09
12.5	-10.22	3.45	18.51	11.75
13.0	-12.14	2.07	14.95	14.61
13.5	-12.28	0.97	15.34	13.62
14.0	-14.08	-0.27	10.97	12.68
14.5	-15.43	-1.75	5.63	7.23
15.0	-16.00	-0.32	13.80	8.14
3.0	25.73	18.75	76.92	45.94
3.5	8.54	7.45	30.01	35.64
4.0	1.03	-0.96	24.47	30.01
4.5	4.77	2.45	27.66	33.71
5.0	9.97	9.46	32.52	37.97
5.5	14.89	18.26	37.09	43.33
6.0	20.57	25.27	43.12	50.65
6.5	28.52	31.70	50.26	60.88
7.0	36.18	35.47	52.97	66.54
7.5	38.03	38.55	51.94	64.69
8.0	40.47	40.12	51.38	56.53
8.5	40.30	39.40	53.23	52.19
9.0	38.07	37.79	50.73	51.33
9.5	40.43	45.22	54.01	55.87
10.0	47.23	50.87	55.36	54.59
10.5	48.70	48.41	52.39	49.91
11.0	42.61	42.41	44.28	43.32
11.5	41.16	41.19	40.48	40.81
12.0	40.34	41.15	39.22	39.53
12.5	32.75	34.59	36.29	33.96
13.0	25.94	31.47	33.87	29.49
13.5	25.07	31.43	36.69	31.27
14.0	27.34	33.48	40.65	37.06
14.5	30.99	35.30	45.47	45.42
15.0	52.94	55.98	65.47	68.72

Table B- 42. Data for Figure 6-9, experiment B average response.

	Average Response (%)			
Time (min)	D8	D5	D3	D0
3.0	7.56	12.89	38.20	28.48
3.5	-0.06	6.21	20.47	22.02
4.0	2.30	3.30	16.83	20.61
4.5	4.80	7.03	18.34	24.72
5.0	7.45	11.16	22.40	26.93
5.5	8.16	14.21	24.63	27.12
6.0	10.01	14.55	26.21	28.38
6.5	10.38	14.14	26.38	29.95
7.0	12.25	13.46	25.84	29.73
7.5	13.26	15.46	25.42	27.14
8.0	13.06	16.49	25.88	24.02
8.5	11.08	16.42	27.56	22.42
9.0	9.61	15.32	26.87	22.86
9.5	10.83	18.17	28.58	25.39
10.0	16.85	22.22	30.25	27.19
10.5	20.95	24.40	31.71	28.25
11.0	21.94	24.83	31.09	27.74
11.5	20.56	24.37	30.62	26.34
12.0	17.17	23.06	29.08	26.06
12.5	10.29	18.33	25.80	22.60
13.0	7.15	16.94	23.65	22.05
13.5	6.93	16.59	24.36	22.04
14.0	7.88	16.77	24.10	23.96
14.5	8.51	16.08	22.78	23.74
15.0	13.99	21.45	30.52	29.11

Table B- 43. Data for Figures 6-10 and 6-12, experiment C resistance.

	Resistance (Ω)				
Time (s)	B	D8	D5	D3	D0
180	230234.80	288065.89	324825.93	514705.87	322878.32
210	249465.40	249276.60	348085.43	451248.88	314421.31
240	253450.99	258350.27	344870.16	482259.60	321950.04
270	251188.62	267660.79	329994.01	442897.65	319589.09
300	250682.61	280168.08	317784.56	379044.31	312849.22
330	254014.32	284466.05	312395.35	337874.59	312421.50
360	268430.58	287326.76	313725.49	338425.74	308437.87
390	273029.49	287654.56	307709.16	350811.22	308856.46
421	267958.01	289384.68	300903.73	360188.77	305187.14
451	259901.74	285297.91	299587.05	366727.27	310067.14
481	255925.18	284645.32	309741.37	368703.56	314148.69
511	255685.55	285051.18	319671.22	369599.41	319711.29
541	255964.62	288565.31	325570.01	365778.90	315871.13
571	258535.28	292562.59	324739.43	361746.08	314677.37
601	259723.39	296143.44	324224.15	359461.38	313598.97
631	259842.98	300360.73	313518.15	363273.88	315522.11
661	258892.04	303142.74	303152.48	363875.86	315802.50
691	258110.48	303606.79	299737.73	366319.96	312329.19
721	257991.81	304328.77	311964.59	362112.59	306760.70
751	256944.17	308038.26	326043.86	363579.78	305710.55
781	253808.91	309629.16	329075.97	356293.10	310113.10
811	247581.87	309812.19	327217.42	342026.51	315164.12
841	243769.97	312996.10	317485.51	334220.58	321137.80
871	239808.15	317965.02	311041.99	346921.08	324280.50
901	225035.16	303260.05	335289.19	342319.21	321285.14
180	156774.90	276679.82	291666.62	288065.89	511883.01
210	170212.77	245022.97	255009.14	249944.14	414354.22
240	170150.67	259499.50	268894.69	257122.55	404916.99
270	170212.77	256292.89	273838.61	258207.25	372389.83
300	171568.61	250738.80	277083.68	262448.73	357644.58
330	171442.54	247209.99	275863.74	262738.07	347826.09
360	172159.35	248517.72	270492.22	265787.09	361205.12
390	174064.40	248857.87	264515.42	271396.64	359642.89
421	181729.70	248459.30	262613.32	278139.20	350467.45
451	184746.51	248948.57	265397.57	276629.31	345543.46
481	183653.51	250677.08	266606.66	273826.16	353394.60
511	178732.16	251523.10	267415.57	272111.51	353072.93

Table B-43 (cont'd).

541	179340.03	252462.65	270452.57	270983.62	348158.87
571	185442.74	252642.00	273237.33	273170.31	348822.69
601	188959.33	252111.43	279611.09	271944.27	364251.22
631	191859.70	254546.07	280322.33	272734.31	369515.01
661	193713.98	252807.94	281874.51	273020.99	370149.93
691	201567.88	255731.06	281291.10	276960.13	367623.00
721	204400.41	262646.29	283062.72	273399.59	369754.11
751	208130.49	268407.52	276313.93	275812.00	365211.15
781	209111.23	265197.12	275528.24	282696.86	358047.18
811	212180.70	261873.75	280316.67	305767.01	350644.41
841	216585.79	256107.52	285839.73	315891.69	360133.25
871	222407.56	248601.62	283185.84	308522.95	372266.17
901	224466.89	259571.71	272944.39	314341.85	354139.00
180	230263.11	230078.64	282258.00	237690.94	242005.12
210	250000.00	251004.27	247459.09	257352.96	263653.42
240	250284.95	250514.43	258135.93	260368.25	267181.94
270	249203.17	251127.06	257566.00	263653.42	267713.53
300	247694.09	249669.81	259091.39	266641.21	267865.70
330	245334.23	250040.26	256433.80	268456.38	267291.06
360	242893.31	248629.92	255777.89	272638.69	266514.72
390	241227.99	248902.71	261211.05	273715.54	266736.52
421	238319.03	248569.11	267599.48	271091.90	267659.79
451	234447.46	248823.44	269837.95	268801.74	268775.88
481	230249.75	248095.13	272143.94	265919.54	271817.87
511	228435.36	246346.19	275511.85	264218.24	277118.54
541	225635.23	244733.46	274957.93	260479.62	278302.38
571	224180.77	244163.04	270560.14	257753.35	273123.45
601	222734.81	245055.15	266437.60	256201.49	267668.53
631	222603.42	248119.13	263115.80	260029.74	272668.57
661	221130.62	250936.49	263920.63	262074.15	271823.48
691	218185.31	251628.79	264647.72	261474.55	270560.72
721	215114.92	249473.74	267220.20	260138.37	271217.92
751	216994.96	249859.45	270375.35	261376.95	274919.53
781	220290.33	249440.38	271313.43	263765.25	270769.51
811	227462.87	254478.31	269970.53	271123.36	268752.76
841	237123.37	256163.29	268293.17	273552.31	270900.52
871	244349.42	255183.41	266577.81	268817.20	272294.08
901	236266.98	264375.41	265780.73	277777.78	271554.65

Table B- 44. Data for Figures 6-10 and 6-12, experiment C response.

	Response (%)			
Time (min)	D8	D5	D3	D0
3.0	25.12	41.08	123.56	40.24
3.5	-0.08	39.53	80.89	26.04
4.0	1.93	36.07	90.28	27.03
4.5	6.56	31.37	76.32	27.23
5.0	11.76	26.77	51.20	24.80
5.5	11.99	22.98	33.01	22.99
6.0	7.04	16.87	26.08	14.90
6.5	5.36	12.70	28.49	13.12
7.0	8.00	12.30	34.42	13.89
7.5	9.77	15.27	41.10	19.30
8.0	11.22	21.03	44.07	22.75
8.5	11.49	25.03	44.55	25.04
9.0	12.74	27.19	42.90	23.40
9.5	13.16	25.61	39.92	21.72
10.0	14.02	24.83	38.40	20.74
10.5	15.59	20.66	39.81	21.43
11.0	17.09	17.10	40.55	21.98
11.5	17.63	16.13	41.92	21.01
12.0	17.96	20.92	40.36	18.90
12.5	19.89	26.89	41.50	18.98
13.0	21.99	29.66	40.38	22.18
13.5	25.14	32.17	38.15	27.30
14.0	28.40	30.24	37.10	31.74
14.5	32.59	29.70	44.67	35.22
15.0	34.76	48.99	52.12	42.77
3.0	76.48	86.04	83.74	226.51
3.5	43.95	49.82	46.84	143.43
4.0	52.51	58.03	51.11	137.98
4.5	50.57	60.88	51.70	118.78
5.0	46.14	61.50	52.97	108.46
5.5	44.19	60.91	53.25	102.88
6.0	44.35	57.12	54.38	109.81
6.5	42.97	51.96	55.92	106.61
7.0	36.72	44.51	53.05	92.85
7.5	34.75	43.65	49.73	87.04
8.0	36.49	45.17	49.10	92.42
8.5	40.73	49.62	52.25	97.54

Table B-44 (cont'd).

9.0	40.77	50.80	51.10	94.13
9.5	36.24	47.34	47.31	88.10
10.0	33.42	47.97	43.92	92.77
10.5	32.67	46.11	42.15	92.60
11.0	30.51	45.51	40.94	91.08
11.5	26.87	39.55	37.40	82.38
12.0	28.50	38.48	33.76	80.90
12.5	28.96	32.76	32.52	75.47
13.0	26.82	31.76	35.19	71.22
13.5	23.42	32.11	44.11	65.26
14.0	18.25	31.98	45.85	66.28
14.5	11.78	27.33	38.72	67.38
15.0	15.64	21.60	40.04	57.77
3.0	-0.08	22.58	3.23	5.10
3.5	0.40	-1.02	2.94	5.46
4.0	0.09	3.14	4.03	6.75
4.5	0.77	3.36	5.80	7.43
5.0	0.80	4.60	7.65	8.14
5.5	1.92	4.52	9.42	8.95
6.0	2.36	5.30	12.25	9.73
6.5	3.18	8.28	13.47	10.57
7.0	4.30	12.29	13.75	12.31
7.5	6.13	15.10	14.65	14.64
8.0	7.75	18.20	15.49	18.05
8.5	7.84	20.61	15.66	21.31
9.0	8.46	21.86	15.44	23.34
9.5	8.91	20.69	14.98	21.83
10.0	10.02	19.62	15.03	20.17
10.5	11.46	18.20	16.81	22.49
11.0	13.48	19.35	18.52	22.92
11.5	15.33	21.29	19.84	24.01
12.0	15.97	24.22	20.93	26.08
12.5	15.15	24.60	20.45	26.69
13.0	13.23	23.16	19.74	22.91
13.5	11.88	18.69	19.19	18.15
14.0	8.03	13.14	15.36	14.24
14.5	4.43	9.10	10.01	11.44
15.0	11.90	12.49	17.57	14.94

Table B- 45. Data for Figure 6-10, experiment C average response.

	Average Response (%)			
Time (min)	D8	D5	D3	D0
3.0	33.84	49.90	70.18	90.62
3.5	14.76	29.44	43.56	58.31
4.0	18.18	32.41	48.47	57.25
4.5	19.30	31.87	44.61	51.15
5.0	19.57	30.96	37.27	47.13
5.5	19.37	29.47	31.90	44.94
6.0	17.92	26.43	30.90	44.81
6.5	17.17	24.32	32.62	43.44
7.0	16.34	23.03	33.74	39.69
7.5	16.88	24.67	35.16	40.33
8.0	18.49	28.13	36.22	44.41
8.5	20.02	31.75	37.49	47.97
9.0	20.66	33.29	36.48	46.96
9.5	19.44	31.21	34.07	43.88
10.0	19.15	30.81	32.45	44.56
10.5	19.91	28.32	32.92	45.51
11.0	20.36	27.32	33.34	45.33
11.5	19.94	25.66	33.06	42.46
12.0	20.81	27.88	31.68	41.96
12.5	21.33	28.08	31.49	40.38
13.0	20.68	28.19	31.77	38.77
13.5	20.14	27.66	33.82	36.90
14.0	18.23	25.12	32.77	37.42
14.5	16.27	22.04	31.13	38.01
15.0	20.77	27.69	36.58	38.49

Table B- 46. Data for Figures 6-11 and 6-12, experiment D resistance.

	Resistance (Ω)				
Time (s)	B	D8	D5	D3	D0
180	230263.11	237690.94	301724.11	307017.44	507246.37
210	250000.00	258189.38	264525.21	334108.91	417443.11
240	250738.80	257494.90	275130.11	331674.96	413528.33
270	249066.00	257177.17	277502.43	325108.94	372241.50
300	239952.01	258702.36	283659.13	317460.32	359827.69
330	231684.96	265096.59	292703.37	317154.64	344466.96
360	229819.02	269224.23	297086.94	315777.57	351169.71
390	233248.23	269146.98	296648.23	313188.62	349493.20
421	234867.82	266666.67	295184.30	309837.34	347820.04
451	240141.82	267309.49	294884.00	313641.07	348178.50
481	249472.12	267724.86	295233.63	321086.25	350047.64
511	251274.34	267324.78	300596.93	327479.53	351550.44
541	251114.32	268964.41	300261.17	327034.00	347887.56
571	248204.98	273496.19	300948.29	324253.79	341983.46
601	250324.04	277485.96	297501.99	322567.53	337304.30
631	247732.75	277227.02	297833.56	323098.02	335051.25
661	250929.82	275685.33	295358.67	321784.07	329764.62
691	250367.16	274540.49	297864.96	324289.34	325297.61
721	251671.86	275167.96	299911.95	320456.33	328027.60
751	256342.82	276228.75	303616.56	316243.33	339225.45
781	258119.27	276553.72	306246.07	318087.81	347583.08
811	260664.57	273517.14	304463.50	320336.84	350433.56
841	260525.63	270849.60	304291.55	324923.87	356818.66
871	261780.10	271831.46	312012.48	335008.38	365965.23
901	269632.63	277874.26	319233.84	332640.33	347222.22
180	68176.28	81693.67	82171.67	95398.31	97582.22
210	67323.87	82403.22	84058.83	98606.30	100000.00
240	66916.80	81554.19	84500.24	97703.96	100034.83
270	66111.02	79997.13	86148.54	95665.16	99978.58
300	67123.74	78431.37	87502.72	94051.26	99356.84
330	68119.88	77615.54	87456.27	93502.41	99083.48
360	68884.07	78330.45	87089.03	93448.58	99582.99
390	68946.83	79986.28	86775.95	93679.94	100150.23
421	68487.29	81063.08	86483.81	93802.33	100086.68
451	68261.05	81081.87	86943.02	94349.15	100239.85
481	68744.34	80309.76	87958.34	94527.54	101069.35
511	69097.78	80054.89	88397.79	94984.48	101852.43

Table B-46 (cont'd).

541	69055.70	80286.73	88548.05	95015.09	102090.11
571	69002.06	80894.46	88835.30	95457.25	101952.58
601	69108.27	81046.66	88978.58	95027.98	101705.75
631	69250.57	82544.73	89090.40	95460.51	101303.37
661	69401.44	85003.03	89109.53	96715.13	101243.47
691	69329.23	86719.51	89110.42	97073.92	100822.77
721	69181.92	86518.54	89105.99	96359.00	100119.42
751	69456.50	86024.14	89935.45	96765.27	100112.27
781	70598.32	85973.95	89410.44	97796.09	101055.30
811	72181.68	86951.12	89965.79	97683.49	102251.73
841	73101.32	87170.38	90573.84	98022.05	103152.78
871	73193.05	86299.89	91324.20	98887.52	104275.29
901	73800.74	87145.97	91220.07	97323.60	105111.02
180	115798.18	149492.79	164997.06	150375.94	166865.29
210	126182.97	131009.47	148128.53	163265.31	177103.05
240	126446.52	136181.78	160339.00	164299.93	176812.34
270	126915.05	135830.00	152905.20	160375.72	178788.08
300	124951.18	137837.65	146344.02	154278.47	179360.68
330	123587.58	140042.02	140951.40	150634.81	176202.57
360	123874.48	140585.17	141614.38	151884.97	175804.27
390	125513.98	140009.63	141960.48	151516.80	175912.51
421	126271.97	139969.18	142899.40	149459.27	176585.97
451	126735.26	142521.73	143185.16	148619.94	177745.04
481	127310.01	143712.07	143413.96	150037.51	180039.72
511	127878.25	143718.51	143878.60	151366.90	180124.55
541	128486.58	143455.10	144177.52	152246.72	180111.12
571	128252.09	143570.61	144232.75	152592.69	179617.57
601	128089.16	142381.67	144519.49	153196.32	179593.31
631	127788.70	141477.01	145440.84	153359.09	179135.19
661	127950.28	141209.11	147157.38	153782.13	179539.79
691	127351.77	140885.47	148133.14	153656.05	180210.70
721	126794.78	141299.62	149439.30	153565.20	180232.33
751	126946.31	143605.95	148990.84	153465.89	179699.30
781	129219.07	146148.45	149187.73	154025.58	179407.53
811	129847.23	147314.93	149892.14	154100.87	179335.78
841	130678.54	146854.44	150925.49	154218.98	180079.34
871	132868.29	146439.69	150375.94	154231.73	180750.11
901	133489.07	144822.59	151601.29	154469.97	179211.47

Table B- 47. Data for Figures 6-11 and 6-12, experiment D response.

	Response (%)			
Time (min)	D8	D5	D3	D0
3.0	3.23	31.03	33.33	120.29
3.5	3.28	5.81	33.64	66.98
4.0	2.69	9.73	32.28	64.92
4.5	3.26	11.42	30.53	49.45
5.0	7.81	18.21	32.30	49.96
5.5	14.42	26.34	36.89	48.68
6.0	17.15	29.27	37.40	52.80
6.5	15.39	27.18	34.27	49.84
7.0	13.54	25.68	31.92	48.09
7.5	11.31	22.80	30.61	44.99
8.0	7.32	18.34	28.71	40.32
8.5	6.39	19.63	30.33	39.91
9.0	7.11	19.57	30.23	38.54
9.5	10.19	21.25	30.64	37.78
10.0	10.85	18.85	28.86	34.75
10.5	11.91	20.22	30.42	35.25
11.0	9.87	17.71	28.24	31.42
11.5	9.66	18.97	29.53	29.93
12.0	9.34	19.17	27.33	30.34
12.5	7.76	18.44	23.37	32.33
13.0	7.14	18.65	23.23	34.66
13.5	4.93	16.80	22.89	34.44
14.0	3.96	16.80	24.72	36.96
14.5	3.84	19.19	27.97	39.80
15.0	3.06	18.40	23.37	28.78
3.0	19.83	20.53	39.93	43.13
3.5	22.40	24.86	46.47	48.54
4.0	21.87	26.28	46.01	49.49
4.5	21.00	30.31	44.70	51.23
5.0	16.85	30.36	40.12	48.02
5.5	13.94	28.39	37.26	45.45
6.0	13.71	26.43	35.66	44.57
6.5	16.01	25.86	35.87	45.26
7.0	18.36	26.28	36.96	46.14
7.5	18.78	27.37	38.22	46.85
8.0	16.82	27.95	37.51	47.02
8.5	15.86	27.93	37.46	47.40

Table B-47 (cont'd).

9.0	16.26	28.23	37.59	47.84
9.5	17.23	28.74	38.34	47.75
10.0	17.27	28.75	37.51	47.17
10.5	19.20	28.65	37.85	46.29
11.0	22.48	28.40	39.36	45.88
11.5	25.08	28.53	40.02	45.43
12.0	25.06	28.80	39.28	44.72
12.5	23.85	29.48	39.32	44.14
13.0	21.78	26.65	38.52	43.14
13.5	20.46	24.64	35.33	41.66
14.0	19.25	23.90	34.09	41.11
14.5	17.91	24.77	35.11	42.47
15.0	18.08	23.60	31.87	42.43
3.0	29.10	42.49	29.86	44.10
3.5	3.83	17.39	29.39	40.35
4.0	7.70	26.80	29.94	39.83
4.5	7.02	20.48	26.36	40.87
5.0	10.31	17.12	23.47	43.54
5.5	13.31	14.05	21.89	42.57
6.0	13.49	14.32	22.61	41.92
6.5	11.55	13.10	20.72	40.15
7.0	10.85	13.17	18.36	39.85
7.5	12.46	12.98	17.27	40.25
8.0	12.88	12.65	17.85	41.42
8.5	12.39	12.51	18.37	40.86
9.0	11.65	12.21	18.49	40.18
9.5	11.94	12.46	18.98	40.05
10.0	11.16	12.83	19.60	40.21
10.5	10.71	13.81	20.01	40.18
11.0	10.36	15.01	20.19	40.32
11.5	10.63	16.32	20.65	41.51
12.0	11.44	17.86	21.11	42.14
12.5	13.12	17.37	20.89	41.56
13.0	13.10	15.45	19.20	38.84
13.5	13.45	15.44	18.68	38.11
14.0	12.38	15.49	18.01	37.80
14.5	10.21	13.18	16.08	36.04
15.0	8.49	13.57	15.72	34.25

Table B- 48. Data for Figure 6-11, experiment D average response.

	Average Response (%)			
Time (min)	D8	D5	D3	D0
3.0	17.38	31.35	34.37	69.17
3.5	9.83	16.02	36.50	51.96
4.0	10.76	20.94	36.07	51.42
4.5	10.43	20.73	33.87	47.19
5.0	11.66	21.90	31.96	47.17
5.5	13.89	22.92	32.01	45.57
6.0	14.78	23.34	31.89	46.43
6.5	14.32	22.05	30.29	45.08
7.0	14.25	21.71	29.08	44.69
7.5	14.18	21.05	28.70	44.03
8.0	12.34	19.65	28.02	42.92
8.5	11.54	20.02	28.72	42.72
9.0	11.67	20.00	28.77	42.18
9.5	13.12	20.82	29.32	41.86
10.0	13.09	20.14	28.66	40.71
10.5	13.94	20.90	29.43	40.57
11.0	14.24	20.37	29.26	39.21
11.5	15.12	21.27	30.07	38.95
12.0	15.28	21.94	29.24	39.07
12.5	14.91	21.76	27.86	39.34
13.0	14.01	20.25	26.98	38.88
13.5	12.95	18.96	25.63	38.07
14.0	11.86	18.73	25.61	38.62
14.5	10.65	19.05	26.39	39.43
15.0	9.88	18.52	23.65	35.15

Table B- 49. Student's T-Tests of responses (2 tails, $\alpha = 0.05$).

Experiment A			
Sample 1	Sample 2	P Value	Significant Difference
Blank	D8	1.184E-15	Yes
Blank	D5	4.789E-17	Yes
Blank	D3	5.119E-17	Yes
Blank	D0	4.609E-18	Yes
D8	D5	5.841E-08	Yes
D8	D3	3.520E-10	Yes
D8	D0	5.520E-12	Yes
D5	D3	0.047	Yes
D5	D0	0.002	Yes
D3	D0	0.241	No

Experiment B			
Sample 1	Sample 2	P Value	Significant Difference
Blank	D8	6.987E-07	Yes
Blank	D5	1.118E-13	Yes
Blank	D3	2.023E-23	Yes
Blank	D0	4.766E-21	Yes
D8	D5	0.053	No
D8	D3	6.691E-08	Yes
D8	D0	5.612E-07	Yes
D5	D3	9.785E-05	Yes
D5	D0	4.830E-04	Yes
D3	D0	0.778	No

Experiment C			
Sample 1	Sample 2	P Value	Significant Difference
Blank	D8	5.356E-17	Yes
Blank	D5	5.274E-24	Yes
Blank	D3	1.184E-23	Yes
Blank	D0	2.594E-14	Yes
D8	D5	4.952E-04	Yes
D8	D3	1.624E-07	Yes
D8	D0	1.895E-06	Yes
D5	D3	0.019	Yes
D5	D0	0.002	Yes
D3	D0	0.086	No

Experiment D			
Sample 1	Sample 2	P Value	Significant Difference
Blank	D8	6.389E-30	Yes
Blank	D5	4.912E-40	Yes
Blank	D3	8.101E-45	Yes
Blank	D0	5.567E-47	Yes
D8	D5	3.020E-12	Yes
D8	D3	6.822E-29	Yes
D8	D0	5.474E-41	Yes
D5	D3	3.800E-11	Yes
D5	D0	9.559E-30	Yes
D3	D0	6.303E-15	Yes

Experiment E			
Sample 1	Sample 2	P Value	Significant Difference
Blank	D8	5.694E-08	Yes
Blank	D5	7.213E-34	Yes
Blank	D3	7.093E-36	Yes
Blank	D0	1.306E-35	Yes
D8	D5	5.093E-23	Yes
D8	D3	1.842E-36	Yes
D8	D0	1.231E-46	Yes
D5	D3	4.055E-40	Yes
D5	D0	5.939E-39	Yes
D3	D0	1.606E-30	Yes

Experiment F			
Sample 1	Sample 2	P Value	Significant Difference
Blank	D8	3.276E-04	Yes
Blank	D5	1.023E-04	Yes
Blank	D3	1.054E-07	Yes
Blank	D0	5.397E-07	Yes
D8	D5	0.071	No
D8	D3	7.520E-05	Yes
D8	D0	4.623E-05	Yes
D5	D3	0.020	Yes
D5	D0	0.003	Yes
D3	D0	0.274	No

Experiment G			
Sample 1	Sample 2	P Value	Significant Difference
Blank	D8	2.02E-21	Yes
Blank	D5	5.50E-18	Yes
Blank	D3	4.24E-32	Yes
Blank	D0	4.00E-36	Yes
D8	D5	3.29E-09	Yes
D8	D3	8.38E-29	Yes
D8	D0	6.01E-36	Yes
D5	D3	1.80E-09	Yes
D5	D0	3.42E-22	Yes
D3	D0	1.29E-10	Yes

Experiment H			
Sample 1	Sample 2	P Value	Significant Difference
Blank	D8	5.237E-19	Yes
Blank	D5	2.111E-18	Yes
Blank	D3	1.642E-19	Yes
Blank	D0	1.085E-20	Yes
D8	D5	4.976E-13	Yes
D8	D3	2.299E-16	Yes
D8	D0	2.371E-18	Yes
D5	D3	4.851E-05	Yes
D5	D0	9.095E-07	Yes
D3	D0	0.363	No

Table B- 50. Data for Figure 6-12, experiment E resistance.

	Resistance (Ω)				
Time (s)	B	D8	D5	D3	D0
180	5780.35	6032.01	6330.76	6795.79	7326.77
210	5785.72	6073.49	6344.57	6884.00	7353.91
240	5790.03	6030.58	6367.62	6919.39	7390.40
270	5828.35	5993.53	6394.30	6948.41	7425.68
300	5839.29	5973.33	6429.32	6978.89	7475.04
330	5896.23	5962.52	6468.16	7026.70	7521.62
360	5919.79	5960.24	6514.05	7056.27	7541.53
390	5935.72	5959.35	6549.71	7068.56	7540.87
421	5935.60	5987.13	6580.18	7099.21	7550.48
451	5966.33	6017.66	6585.64	7125.41	7556.34
481	5969.26	6035.52	6590.41	7133.94	7558.63
511	5978.82	6056.18	6586.88	7143.22	7590.34
541	5975.50	6055.63	6608.61	7169.38	7619.05
571	5989.43	6056.71	6635.58	7164.97	7609.73
601	6040.60	6060.87	6660.32	7187.78	7582.63
631	6070.20	6128.93	6659.85	7220.59	7582.94
661	6044.51	6168.89	6666.15	7264.61	7583.45
691	6044.90	6187.16	6676.52	7260.09	7584.48
721	6053.92	6179.92	6696.76	7256.71	7598.27
751	6074.94	6213.38	6706.27	7274.62	7646.62
781	6078.63	6241.08	6732.51	7317.58	7678.18
811	6111.80	6272.12	6756.59	7349.27	7690.09
841	6106.87	6294.26	6768.19	7346.19	7684.92
871	6102.21	6259.78	6762.47	7359.71	7648.18

Table B- 51. Data for Figure 6-12, experiment F resistance.

	Resistance (Ω)				
Time (s)	B	D8	D5	D3	D0
180	10011.44	10574.42	12062.73	13818.97	15603.23
210	10046.46	10641.53	12232.95	13904.75	15516.76
240	10072.67	10748.77	12226.97	13908.12	15599.23
270	10134.68	10813.44	12326.44	13947.77	15705.01
300	10181.85	10882.49	12441.35	14039.52	15608.88
330	10265.75	10892.99	12490.13	14141.92	15577.54
360	10266.11	10944.51	12535.26	14164.84	15568.87
390	10278.15	10941.90	12614.20	14200.42	15633.72
421	10268.71	10966.72	12718.25	14182.46	15715.33
451	10276.64	11046.28	12745.00	14180.07	15834.32
481	10278.25	11082.22	12796.49	14167.53	15884.59
511	10286.89	11133.33	12789.59	14250.81	15887.70
541	10306.13	11156.27	12805.09	14352.35	15928.33
571	10338.28	11223.30	12874.51	14427.04	15891.03
601	10352.39	11212.87	12974.13	14461.17	15900.28
631	10359.24	11272.50	13050.33	14506.27	15995.24
661	10411.55	11296.38	13142.70	14558.31	16165.35
691	10466.20	11388.55	13229.14	14594.96	16211.59
721	10487.10	11443.89	13277.69	14679.28	16233.67
751	10468.46	11539.59	13279.58	14727.00	16227.93
781	10450.78	11612.18	13338.67	14800.64	16256.48
811	10438.48	11733.99	13396.36	14828.23	16306.09
841	10432.65	11765.64	13471.25	14932.46	16399.59
871	10426.17	11737.09	13531.80	15034.77	16423.73
180	15924.47	16257.23	15311.95	15110.22	15476.46
210	15733.21	16117.10	15091.90	15392.23	15371.10
240	15848.94	16110.19	15021.96	15531.05	15205.86
270	15871.30	16071.36	14862.55	15536.35	15123.45
300	15938.16	16082.25	14886.91	15730.51	15043.14
330	15886.89	16022.15	14965.74	15882.69	14941.54
360	15952.24	15962.76	15102.40	15925.01	14963.74
390	16014.96	15933.26	15236.85	15948.46	15000.00
421	16055.60	16042.97	15293.36	15944.33	15007.73
451	16019.45	16098.15	15317.29	16052.37	14966.36
481	15976.76	16128.36	15291.94	16012.90	14958.01
511	15979.78	16111.30	15256.94	15937.98	15058.45
541	15982.42	16105.70	15115.28	15769.40	15047.28

Table B-51 (cont'd).

571	16011.71	16061.57	15047.29	15597.45	15073.56
601	16050.58	16023.72	14992.08	15547.78	15074.67
631	16108.71	15952.54	14950.48	15647.47	14983.04
661	16175.62	15889.70	14926.87	15665.69	14799.00
691	16219.85	15876.97	14908.84	15712.85	14748.56
721	16243.56	15878.32	14848.34	15544.89	14927.20
751	16329.96	15880.25	14756.88	15419.25	15177.71
781	16441.38	15838.98	14752.68	15320.81	15458.77
811	16422.38	15813.41	14856.55	15463.89	15640.97
841	9893.75	15762.39	14946.32	15481.59	15695.86
871	16447.37	15717.09	14953.27	15533.98	15710.92

Table B- 52. Data for Figure 6-12, experiment G resistance.

	Resistance (Ω)				
Time (s)	B	D8	D5	D3	D0
180	26987.96	28498.73	29595.96	31624.11	35193.57
210	27068.83	28928.61	29535.87	31474.81	35445.28
240	27351.76	29179.73	29544.59	31722.65	36021.19
270	27897.89	29136.02	29545.52	32173.54	35764.46
300	28000.98	29016.14	29832.62	32611.32	35572.15
330	28049.36	29375.05	30058.72	32674.78	35459.51
360	28210.88	29466.24	30013.28	32594.93	35506.85
390	28171.00	29707.90	29874.31	32590.64	35496.26
421	28195.81	29731.25	29875.02	32825.44	35465.92
451	28322.02	29918.05	29982.76	33035.42	35451.41
481	28446.90	29811.02	30064.88	33068.98	35448.87
511	28188.87	30091.35	30161.51	33005.24	35605.28
541	27892.34	30472.87	30147.89	32955.75	35592.61
571	27918.19	31046.51	30240.77	33073.20	35656.06
601	28030.13	30990.59	30141.89	33233.65	35504.61
631	28045.99	30652.15	30080.91	33512.58	35669.24
661	27898.86	30264.46	30220.94	34061.66	35691.98
691	27709.60	30019.46	30533.61	34511.65	35863.40
721	27854.18	29600.27	30614.82	34609.24	35723.85
751	28387.78	29383.88	30639.17	34572.36	35617.51
781	28953.43	29735.36	30625.86	34694.25	35769.04
811	29037.81	30156.82	30554.26	35005.33	36116.44
841	29108.15	30490.80	30640.62	34837.14	36406.19
871	29143.90	30698.39	30983.73	34379.03	36613.27
901	28149.19	30429.82	31043.85	35211.27	37383.18
180	36377.82	38633.99	41925.10	45441.45	50197.20
210	35804.13	39695.20	42195.98	45964.42	49991.05
240	36189.87	40394.70	42081.17	45974.73	50350.43
270	36191.60	40525.96	42251.57	46057.61	50398.18
300	35952.81	40160.06	42852.58	46126.78	50379.64
330	35708.22	40057.23	43707.13	46107.43	50375.28
360	36036.35	40122.94	44287.80	45929.25	50101.99
390	35783.53	40065.84	44392.32	45958.12	49647.55
421	35946.55	39859.06	44329.03	46030.56	49555.78
451	36432.00	39308.18	44764.20	46395.45	50011.61
481	37193.97	39292.45	45129.98	46789.62	50542.66
511	36724.98	38881.88	45305.98	47010.64	50811.16

Table B-52 (cont'd).

541	36325.20	38021.25	45264.97	46748.46	51330.23
571	36593.23	37457.20	45276.69	46623.92	51894.14
601	36246.65	37942.43	45099.45	46955.46	52034.21
631	36220.23	38354.06	45207.75	47365.89	52086.24
661	36203.55	37972.02	45362.09	47639.65	52193.04
691	36819.39	37810.24	45307.42	47647.41	52334.50
721	36530.64	38073.22	45393.51	47795.57	51991.22
751	36417.85	38231.53	45111.09	47521.24	51706.24
781	36366.89	38321.90	45020.02	47599.96	50951.71
811	36645.98	38313.65	45181.69	48191.10	50210.42
841	36987.56	38706.79	45154.72	49267.15	48585.81
871	37243.95	39005.36	44469.15	49597.02	47365.30
901	36934.44	38186.16	45325.78	49291.44	49720.32

Table B- 53. Data for Figure 6-12, experiment H resistance.

	Resistance (Ω)				
Time (s)	B	D8	D5	D3	D0
180	55456.53	72774.53	103780.58	116569.52	120249.08
210	55688.14	73413.73	110182.01	125000.00	125000.00
240	55843.64	72768.85	107226.28	125184.43	125058.62
270	56556.52	72799.12	106082.70	124533.00	124816.11
300	57340.03	73356.03	106601.69	123147.28	124521.22
330	57760.54	75708.41	109443.39	122205.08	124365.09
360	58118.41	76523.64	111084.67	121883.26	124285.79
390	57764.12	76946.33	110348.31	121460.81	124021.66
421	58158.25	78600.90	109383.53	121016.18	124243.82
451	58045.52	80114.44	110431.86	121501.40	124713.28
481	59863.59	80728.86	110970.62	121548.86	124548.20
511	60235.78	79776.63	108798.28	121888.05	123860.67
541	61091.36	79974.86	107566.53	121488.23	123594.24
571	60971.62	81350.42	109466.94	121873.73	124175.63
601	62592.21	82046.46	112511.25	122948.30	125263.55
631	63091.47	83729.56	112218.16	123097.50	126286.54
661	63919.64	87697.31	109661.58	122188.18	127593.33
691	65095.08	94931.35	108017.19	121271.42	127026.16
721	66835.34	100639.77	108632.81	122391.65	126380.58
751	68209.49	100160.96	109572.30	121872.66	125420.50
781	68945.14	100589.15	109145.62	121472.03	125825.73
811	70170.16	102594.18	108814.76	121076.90	125529.58
841	71580.13	106890.62	107878.59	122292.09	125791.23
871	73193.05	106100.80	106951.87	123039.06	125845.52
901	74074.07	105263.16	109036.39	121784.14	126043.80

Table B- 54. Data for Figure 6-12, cumulative response experiments A-H.

		Response (%)			
	Time (min)	D8	D5	D3	D0
Exp E	3.0	4.35	9.52	17.57	26.75
	3.5	4.97	9.66	18.98	27.10
	4.0	4.15	9.98	19.51	27.64
	4.5	2.83	9.71	19.22	27.41
	5.0	2.30	10.10	19.52	28.01
	5.5	1.12	9.70	19.17	27.57
	6.0	0.68	10.04	19.20	27.40
	6.5	0.40	10.34	19.09	27.04
	7.0	0.87	10.86	19.60	27.21
	7.5	0.86	10.38	19.43	26.65
	8.0	1.11	10.41	19.51	26.63
	8.5	1.29	10.17	19.48	26.95
	9.0	1.34	10.60	19.98	27.50
	9.5	1.12	10.79	19.63	27.05
	10.0	0.34	10.26	18.99	25.53
	10.5	0.97	9.71	18.95	24.92
	11.0	2.06	10.28	20.19	25.46
	11.5	2.35	10.45	20.10	25.47
	12.0	2.08	10.62	19.87	25.51
	12.5	2.28	10.39	19.75	25.87
	13.0	2.67	10.76	20.38	26.31
	13.5	2.62	10.55	20.25	25.82
	14.0	3.07	10.83	20.29	25.84
	14.5	2.58	10.82	20.61	25.33
Exp F	3.0	5.62	20.49	38.03	55.85
	3.5	5.92	21.76	38.40	54.45
	4.0	6.71	21.39	38.08	54.87
	4.5	6.70	21.63	37.62	54.96
	5.0	6.88	22.19	37.89	53.30
	5.5	6.11	21.67	37.76	51.74
	6.0	6.61	22.10	37.98	51.65
	6.5	6.46	22.73	38.16	52.11
	7.0	6.80	23.85	38.11	53.04
	7.5	7.49	24.02	37.98	54.08
	8.0	7.82	24.50	37.84	54.55
	8.5	8.23	24.33	38.53	54.45
	9.0	8.25	24.25	39.26	54.55

Table B-54 (cont'd).

	9.5	8.56	24.53	39.55	53.71
	10.0	8.31	25.33	39.69	53.59
	10.5	8.82	25.98	40.03	54.41
	11.0	8.50	26.23	39.83	55.26
	11.5	8.81	26.40	39.45	54.89
	12.0	9.12	26.61	39.97	54.80
	12.5	10.23	26.85	40.68	55.02
	13.0	11.11	27.63	41.62	55.55
	13.5	12.41	28.34	42.05	56.21
	14.0	12.78	29.13	43.13	57.19
	14.5	12.57	29.79	44.20	57.52
	3.0	2.09	-3.85	-5.11	-2.81
	3.5	2.44	-4.08	-2.17	-2.30
	4.0	1.65	-5.22	-2.01	-4.06
	4.5	1.26	-6.36	-2.11	-4.71
	5.0	0.90	-6.60	-1.30	-5.62
	5.5	0.85	-5.80	-0.03	-5.95
	6.0	0.07	-5.33	-0.17	-6.20
	6.5	-0.51	-4.86	-0.42	-6.34
	7.0	-0.08	-4.75	-0.69	-6.53
	7.5	0.49	-4.38	0.21	-6.57
	8.0	0.95	-4.29	0.23	-6.38
	8.5	0.82	-4.52	-0.26	-5.77
	9.0	0.77	-5.43	-1.33	-5.85
	9.5	0.31	-6.02	-2.59	-5.86
	10.0	-0.17	-6.59	-3.13	-6.08
	10.5	-0.97	-7.19	-2.86	-6.99
	11.0	-1.77	-7.72	-3.15	-8.51
	11.5	-2.11	-8.08	-3.13	-9.07
	12.0	-2.25	-8.59	-4.30	-8.10
	12.5	-2.75	-9.63	-5.58	-7.06
	13.0	-3.66	-10.27	-6.82	-5.98
	13.5	-3.71	-9.53	-5.84	-4.76
	14.0	59.32	51.07	56.48	58.64
	14.5	-4.44	-9.08	-5.55	-4.48
Exp G	3.0	5.60	9.66	17.18	30.40
	3.5	6.87	9.11	16.28	30.95
	4.0	6.68	8.02	15.98	31.70
	4.5	4.44	5.91	15.33	28.20

Table B-54 (cont'd).

	5.0	3.63	6.54	16.46	27.04
	5.5	4.73	7.16	16.49	26.42
	6.0	4.45	6.39	15.54	25.86
	6.5	5.46	6.05	15.69	26.00
	7.0	5.45	5.96	16.42	25.78
	7.5	5.64	5.86	16.64	25.17
	8.0	4.80	5.69	16.25	24.61
	8.5	6.75	7.00	17.09	26.31
	9.0	9.25	8.09	18.15	27.61
	9.5	11.21	8.32	18.46	27.72
	10.0	10.56	7.53	18.56	26.67
	10.5	9.29	7.26	19.49	27.18
	11.0	8.48	8.32	22.09	27.93
	11.5	8.34	10.19	24.55	29.43
	12.0	6.27	9.91	24.25	28.25
	12.5	3.51	7.93	21.79	25.47
	13.0	2.70	5.78	19.83	23.54
	13.5	3.85	5.22	20.55	24.38
	14.0	4.75	5.26	19.68	25.07
	14.5	5.33	6.31	17.96	25.63
	15.0	8.10	10.28	25.09	32.80
	3.0	6.20	15.25	24.92	37.99
	3.5	10.87	17.85	28.38	39.62
	4.0	11.62	16.28	27.04	39.13
	4.5	11.98	16.74	27.26	39.25
	5.0	11.70	19.19	28.30	40.13
	5.5	12.18	22.40	29.12	41.07
	6.0	11.34	22.90	27.45	39.03
	6.5	11.97	24.06	28.43	38.74
	7.0	10.88	23.32	28.05	37.86
	7.5	7.89	22.87	27.35	37.27
	8.0	5.64	21.34	25.80	35.89
	8.5	5.87	23.37	28.01	38.36
	9.0	4.67	24.61	28.69	41.31
	9.5	2.36	23.73	27.41	41.81
	10.0	4.68	24.42	29.54	43.56
	10.5	5.89	24.81	30.77	43.80
	11.0	4.88	25.30	31.59	44.17
	11.5	2.69	23.05	29.41	42.14

Table B-54 (cont'd).

	12.0	4.22	24.26	30.84	42.32
	12.5	4.98	23.87	30.49	41.98
	13.0	5.38	23.79	30.89	40.10
	13.5	4.55	23.29	31.50	37.01
	14.0	4.65	22.08	33.20	31.36
	14.5	4.73	19.40	33.17	27.18
	15.0	3.39	22.72	33.46	34.62
Exp A	3.0	9.29	11.53	17.63	23.28
	3.5	10.06	11.97	19.24	24.43
	4.0	8.91	11.97	18.77	23.62
	4.5	8.41	12.07	19.15	23.42
	5.0	9.00	12.96	18.73	22.63
	5.5	9.22	12.91	19.04	21.62
	6.0	9.24	13.11	18.83	21.41
	6.5	9.45	13.14	19.75	22.00
	7.0	9.62	13.46	20.56	22.86
	7.5	9.78	13.15	21.54	22.82
	8.0	10.59	13.36	22.28	23.35
	8.5	12.09	15.10	23.48	24.28
	9.0	12.65	17.27	24.58	25.61
	9.5	12.50	17.60	24.68	25.45
	10.0	11.75	16.58	24.68	24.68
	10.5	11.21	16.15	24.58	23.76
	11.0	11.19	16.13	24.65	23.61
	11.5	11.63	16.30	24.65	23.95
	12.0	12.15	16.51	24.63	24.58
	12.5	12.85	16.66	24.64	25.07
	13.0	13.33	16.95	24.73	25.34
	13.5	13.04	16.51	24.77	25.17
	14.0	12.30	16.51	24.71	25.28
	14.5	11.80	16.96	24.71	26.47
	15.0	11.74	16.11	24.80	29.25
	3.0	28.39	102.01	146.47	158.41
	3.5	27.24	100.50	148.86	161.66
	4.0	29.78	103.64	149.07	162.28
	4.5	31.27	105.79	147.08	159.01
	5.0	34.05	106.91	146.12	159.27
	5.5	36.14	105.59	144.84	157.27
	6.0	36.95	105.46	142.52	158.54

Table B-54 (cont'd).

	6.5	36.71	103.43	140.02	158.96
	7.0	37.58	102.26	139.10	158.20
	7.5	40.47	102.12	138.55	157.31
	8.0	43.59	104.58	137.50	156.82
	8.5	43.87	105.67	134.93	153.85
	9.0	42.96	104.57	131.66	150.83
	9.5	44.33	104.45	131.52	147.75
	10.0	47.10	105.08	132.24	148.59
	10.5	49.85	105.73	132.81	150.70
	11.0	47.52	104.11	130.46	149.96
	11.5	49.99	103.69	129.61	144.77
	12.0	52.09	103.45	128.37	141.12
	12.5	54.52	100.96	125.80	140.88
	13.0	51.99	98.22	122.21	142.19
	13.5	52.35	96.23	119.40	142.54
	14.0	52.94	99.17	119.12	142.03
	14.5	53.76	102.58	118.91	140.93
	15.0	55.11	96.44	117.13	139.19
	3.0	8.07	17.82	22.47	33.11
	3.5	8.02	18.21	22.22	33.50
	4.0	8.25	18.93	22.55	33.68
	4.5	7.94	20.61	23.33	34.74
	5.0	6.86	22.12	24.23	36.07
	5.5	7.15	23.24	25.28	37.48
	6.0	8.10	24.24	26.42	38.68
	6.5	9.55	26.43	28.67	41.14
	7.0	10.63	28.35	31.35	43.66
	7.5	10.78	29.60	33.91	45.89
	8.0	9.00	30.16	34.67	46.95
	8.5	8.01	31.17	35.46	48.45
	9.0	6.25	31.25	36.02	48.86
	9.5	5.02	31.28	37.03	49.35
	10.0	4.11	31.64	37.91	50.18
	10.5	4.70	33.03	40.25	52.10
	11.0	4.68	33.38	41.48	53.29
	11.5	4.38	33.75	42.09	54.09
	12.0	3.88	34.08	42.41	54.59
	12.5	3.84	34.86	43.39	55.46
	13.0	4.35	35.79	44.19	56.82

Table B-54 (cont'd).

	13.5	4.85	36.90	44.98	57.90
	14.0	5.16	37.34	46.12	58.79
	14.5	5.23	36.98	47.09	58.85
	15.0	5.15	36.85	47.20	56.46
Exp H	3.0	31.23	87.14	110.20	116.83
	3.5	31.83	97.86	124.46	124.46
	4.0	30.31	92.01	124.17	123.94
	4.5	28.72	87.57	120.19	120.69
	5.0	27.93	85.91	114.77	117.16
	5.5	31.07	89.48	111.57	115.31
	6.0	31.67	91.14	109.72	113.85
	6.5	33.21	91.03	110.27	114.70
	7.0	35.15	88.08	108.08	113.63
	7.5	38.02	90.25	109.32	114.85
	8.0	34.85	85.37	103.04	108.05
	8.5	32.44	80.62	102.35	105.63
	9.0	30.91	76.07	98.86	102.31
	9.5	33.42	79.54	99.89	103.66
	10.0	31.08	79.75	96.43	100.13
	10.5	32.71	77.87	95.11	100.16
	11.0	37.20	71.56	91.16	99.62
	11.5	45.83	65.94	86.30	95.14
	12.0	50.58	62.54	83.12	89.09
	12.5	46.84	60.64	78.67	83.88
	13.0	45.90	58.31	76.19	82.50
	13.5	46.21	55.07	72.55	78.89
	14.0	49.33	50.71	70.85	75.73
	14.5	44.96	46.12	68.10	71.94
	15.0	42.11	47.20	64.41	70.16
Exp B	3.0	11.71	27.32	27.90	24.52
	3.5	5.36	19.49	21.06	17.30
	4.0	2.51	15.16	15.41	14.58
	4.5	5.00	16.76	16.76	17.24
	5.0	6.94	18.46	22.83	19.72
	5.5	5.03	15.72	21.57	17.72
	6.0	3.46	10.75	18.71	16.74
	6.5	1.08	5.77	15.65	13.63
	7.0	-0.76	2.92	13.69	11.44
	7.5	-2.81	4.79	11.35	9.15

Table B-54 (cont'd).

	8.0	-3.78	5.90	9.39	9.61
	8.5	-5.43	5.56	10.07	8.25
	9.0	-3.16	4.54	10.95	9.21
	9.5	-2.57	5.32	13.96	10.47
	10.0	0.12	8.66	15.33	14.30
	10.5	3.58	13.42	19.54	17.95
	11.0	12.32	19.98	26.21	23.37
	11.5	14.93	21.40	29.19	24.94
	12.0	13.79	20.30	27.48	25.54
	12.5	8.34	16.94	22.60	22.09
	13.0	7.65	17.29	22.12	22.03
	13.5	7.99	17.39	21.06	21.24
	14.0	10.37	17.09	20.67	22.15
	14.5	9.97	14.68	17.24	18.57
	15.0	5.02	8.68	12.30	10.46
	3.0	-14.75	-7.41	9.76	15.00
	3.5	-14.09	-8.30	10.36	13.13
	4.0	3.36	-4.30	10.60	17.23
	4.5	4.63	1.88	10.62	23.21
	5.0	5.44	5.55	11.85	23.11
	5.5	4.56	8.66	15.22	20.33
	6.0	6.00	7.64	16.80	17.75
	6.5	1.54	4.94	13.24	15.35
	7.0	1.33	2.00	10.85	11.21
	7.5	4.56	3.05	12.96	7.58
	8.0	2.50	3.44	16.87	5.91
	8.5	-1.63	4.29	19.38	6.83
	9.0	-6.09	3.65	18.93	8.05
	9.5	-5.38	3.96	17.78	9.84
	10.0	3.20	7.14	20.05	12.67
	10.5	10.56	11.37	23.20	16.90
	11.0	10.90	12.09	22.77	16.52
	11.5	5.58	10.53	22.19	13.26
	12.0	-2.62	7.74	20.54	13.09
	12.5	-10.22	3.45	18.51	11.75
	13.0	-12.14	2.07	14.95	14.61
	13.5	-12.28	0.97	15.34	13.62
	14.0	-14.08	-0.27	10.97	12.68
	14.5	-15.43	-1.75	5.63	7.23

Table B-54 (cont'd).

	15.0	-16.00	-0.32	13.80	8.14
	3.0	25.73	18.75	76.92	45.94
	3.5	8.54	7.45	30.01	35.64
	4.0	1.03	-0.96	24.47	30.01
	4.5	4.77	2.45	27.66	33.71
	5.0	9.97	9.46	32.52	37.97
	5.5	14.89	18.26	37.09	43.33
	6.0	20.57	25.27	43.12	50.65
	6.5	28.52	31.70	50.26	60.88
	7.0	36.18	35.47	52.97	66.54
	7.5	38.03	38.55	51.94	64.69
	8.0	40.47	40.12	51.38	56.53
	8.5	40.30	39.40	53.23	52.19
	9.0	38.07	37.79	50.73	51.33
	9.5	40.43	45.22	54.01	55.87
	10.0	47.23	50.87	55.36	54.59
	10.5	48.70	48.41	52.39	49.91
	11.0	42.61	42.41	44.28	43.32
	11.5	41.16	41.19	40.48	40.81
	12.0	40.34	41.15	39.22	39.53
	12.5	32.75	34.59	36.29	33.96
	13.0	25.94	31.47	33.87	29.49
	13.5	25.07	31.43	36.69	31.27
	14.0	27.34	33.48	40.65	37.06
	14.5	30.99	35.30	45.47	45.42
	15.0	52.94	55.98	65.47	68.72
Exp C	3.0	25.12	41.08	123.56	40.24
	3.5	-0.08	39.53	80.89	26.04
	4.0	1.93	36.07	90.28	27.03
	4.5	6.56	31.37	76.32	27.23
	5.0	11.76	26.77	51.20	24.80
	5.5	11.99	22.98	33.01	22.99
	6.0	7.04	16.87	26.08	14.90
	6.5	5.36	12.70	28.49	13.12
	7.0	8.00	12.30	34.42	13.89
	7.5	9.77	15.27	41.10	19.30
	8.0	11.22	21.03	44.07	22.75
	8.5	11.49	25.03	44.55	25.04
	9.0	12.74	27.19	42.90	23.40

Table B-54 (cont'd).

	9.5	13.16	25.61	39.92	21.72
	10.0	14.02	24.83	38.40	20.74
	10.5	15.59	20.66	39.81	21.43
	11.0	17.09	17.10	40.55	21.98
	11.5	17.63	16.13	41.92	21.01
	12.0	17.96	20.92	40.36	18.90
	12.5	19.89	26.89	41.50	18.98
	13.0	21.99	29.66	40.38	22.18
	13.5	25.14	32.17	38.15	27.30
	14.0	28.40	30.24	37.10	31.74
	14.5	32.59	29.70	44.67	35.22
	15.0	34.76	48.99	52.12	42.77
	3.0	76.48	86.04	83.74	226.51
	3.5	43.95	49.82	46.84	143.43
	4.0	52.51	58.03	51.11	137.98
	4.5	50.57	60.88	51.70	118.78
	5.0	46.14	61.50	52.97	108.46
	5.5	44.19	60.91	53.25	102.88
	6.0	44.35	57.12	54.38	109.81
	6.5	42.97	51.96	55.92	106.61
	7.0	36.72	44.51	53.05	92.85
	7.5	34.75	43.65	49.73	87.04
	8.0	36.49	45.17	49.10	92.42
	8.5	40.73	49.62	52.25	97.54
	9.0	40.77	50.80	51.10	94.13
	9.5	36.24	47.34	47.31	88.10
	10.0	33.42	47.97	43.92	92.77
	10.5	32.67	46.11	42.15	92.60
	11.0	30.51	45.51	40.94	91.08
	11.5	26.87	39.55	37.40	82.38
	12.0	28.50	38.48	33.76	80.90
	12.5	28.96	32.76	32.52	75.47
	13.0	26.82	31.76	35.19	71.22
	13.5	23.42	32.11	44.11	65.26
	14.0	18.25	31.98	45.85	66.28
	14.5	11.78	27.33	38.72	67.38
	15.0	15.64	21.60	40.04	57.77
	3.0	-0.08	22.58	3.23	5.10
	3.5	0.40	-1.02	2.94	5.46

Table B-54 (cont'd).

	4.0	0.09	3.14	4.03	6.75
	4.5	0.77	3.36	5.80	7.43
	5.0	0.80	4.60	7.65	8.14
	5.5	1.92	4.52	9.42	8.95
	6.0	2.36	5.30	12.25	9.73
	6.5	3.18	8.28	13.47	10.57
	7.0	4.30	12.29	13.75	12.31
	7.5	6.13	15.10	14.65	14.64
	8.0	7.75	18.20	15.49	18.05
	8.5	7.84	20.61	15.66	21.31
	9.0	8.46	21.86	15.44	23.34
	9.5	8.91	20.69	14.98	21.83
	10.0	10.02	19.62	15.03	20.17
	10.5	11.46	18.20	16.81	22.49
	11.0	13.48	19.35	18.52	22.92
	11.5	15.33	21.29	19.84	24.01
	12.0	15.97	24.22	20.93	26.08
	12.5	15.15	24.60	20.45	26.69
	13.0	13.23	23.16	19.74	22.91
	13.5	11.88	18.69	19.19	18.15
	14.0	8.03	13.14	15.36	14.24
	14.5	4.43	9.10	10.01	11.44
	15.0	11.90	12.49	17.57	14.94
Exp D	3.0	3.23	31.03	33.33	120.29
	3.5	3.28	5.81	33.64	66.98
	4.0	2.69	9.73	32.28	64.92
	4.5	3.26	11.42	30.53	49.45
	5.0	7.81	18.21	32.30	49.96
	5.5	14.42	26.34	36.89	48.68
	6.0	17.15	29.27	37.40	52.80
	6.5	15.39	27.18	34.27	49.84
	7.0	13.54	25.68	31.92	48.09
	7.5	11.31	22.80	30.61	44.99
	8.0	7.32	18.34	28.71	40.32
	8.5	6.39	19.63	30.33	39.91
	9.0	7.11	19.57	30.23	38.54
	9.5	10.19	21.25	30.64	37.78
	10.0	10.85	18.85	28.86	34.75
	10.5	11.91	20.22	30.42	35.25

Table B-54 (cont'd).

	11.0	9.87	17.71	28.24	31.42
	11.5	9.66	18.97	29.53	29.93
	12.0	9.34	19.17	27.33	30.34
	12.5	7.76	18.44	23.37	32.33
	13.0	7.14	18.65	23.23	34.66
	13.5	4.93	16.80	22.89	34.44
	14.0	3.96	16.80	24.72	36.96
	14.5	3.84	19.19	27.97	39.80
	15.0	3.06	18.40	23.37	28.78
	3.0	19.83	20.53	39.93	43.13
	3.5	22.40	24.86	46.47	48.54
	4.0	21.87	26.28	46.01	49.49
	4.5	21.00	30.31	44.70	51.23
	5.0	16.85	30.36	40.12	48.02
	5.5	13.94	28.39	37.26	45.45
	6.0	13.71	26.43	35.66	44.57
	6.5	16.01	25.86	35.87	45.26
	7.0	18.36	26.28	36.96	46.14
	7.5	18.78	27.37	38.22	46.85
	8.0	16.82	27.95	37.51	47.02
	8.5	15.86	27.93	37.46	47.40
	9.0	16.26	28.23	37.59	47.84
	9.5	17.23	28.74	38.34	47.75
	10.0	17.27	28.75	37.51	47.17
	10.5	19.20	28.65	37.85	46.29
	11.0	22.48	28.40	39.36	45.88
	11.5	25.08	28.53	40.02	45.43
	12.0	25.06	28.80	39.28	44.72
	12.5	23.85	29.48	39.32	44.14
	13.0	21.78	26.65	38.52	43.14
	13.5	20.46	24.64	35.33	41.66
	14.0	19.25	23.90	34.09	41.11
	14.5	17.91	24.77	35.11	42.47
	15.0	18.08	23.60	31.87	42.43
	3.0	29.10	42.49	29.86	44.10
	3.5	3.83	17.39	29.39	40.35
	4.0	7.70	26.80	29.94	39.83
	4.5	7.02	20.48	26.36	40.87
	5.0	10.31	17.12	23.47	43.54

Table B-54 (cont'd).

	5.5	13.31	14.05	21.89	42.57
	6.0	13.49	14.32	22.61	41.92
	6.5	11.55	13.10	20.72	40.15
	7.0	10.85	13.17	18.36	39.85
	7.5	12.46	12.98	17.27	40.25
	8.0	12.88	12.65	17.85	41.42
	8.5	12.39	12.51	18.37	40.86
	9.0	11.65	12.21	18.49	40.18
	9.5	11.94	12.46	18.98	40.05
	10.0	11.16	12.83	19.60	40.21
	10.5	10.71	13.81	20.01	40.18
	11.0	10.36	15.01	20.19	40.32
	11.5	10.63	16.32	20.65	41.51
	12.0	11.44	17.86	21.11	42.14
	12.5	13.12	17.37	20.89	41.56
	13.0	13.10	15.45	19.20	38.84
	13.5	13.45	15.44	18.68	38.11
	14.0	12.38	15.49	18.01	37.80
	14.5	10.21	13.18	16.08	36.04
	15.0	8.49	13.57	15.72	34.25

Table B- 55. Data for Figure 6-12, cumulative average response.

	Average Response (%)			
Time (min)	D8	D5	D3	D0
3.0	15.40	30.67	45.42	58.04
3.5	10.10	24.33	39.79	49.49
4.0	11.21	24.83	39.85	48.92
4.5	11.51	25.14	38.75	47.34
5.0	12.18	26.19	37.76	46.76
5.5	12.94	27.01	37.16	45.86
6.0	13.18	26.83	36.92	46.06
6.5	13.24	26.33	37.08	46.10
7.0	13.63	25.89	37.03	45.45
7.5	14.13	26.52	37.38	45.11
8.0	13.89	26.88	37.08	44.69
8.5	13.74	27.64	37.80	45.10
9.0	13.49	27.62	37.35	44.93
9.5	13.83	28.04	37.31	44.67
10.0	14.73	28.53	37.16	44.68
10.5	15.94	28.57	37.85	45.17
11.0	16.24	28.06	37.74	44.87
11.5	16.60	27.53	37.46	43.56
12.0	16.55	27.67	36.62	42.97
12.5	15.33	26.50	35.28	41.86
13.0	14.40	25.73	34.47	41.42
13.5	14.24	25.12	34.54	40.79
14.0	17.68	28.00	37.83	44.44
14.5	13.49	23.97	33.89	40.72
15.0	17.30	28.84	38.96	44.72

Table B- 56. Student's T-Test cumulative responses of experiments A – H (2 tails, $\alpha = 0.05$)

Sample 1	Sample 2	P Value	Significant Difference
Blank	10^0 CFU/mL	1.544E-45	Yes
Blank	10^1 CFU/mL	4.759E-20	Yes
Blank	10^3 CFU/mL	5.118E-57	Yes
Blank	10^4 CFU/mL	7.782E-21	Yes
Blank	10^5 CFU/mL	4.086E-72	Yes
Blank	10^6 CFU/mL	7.392E-23	Yes
Blank	10^8 CFU/mL	3.775E-67	Yes
Blank	10^9 CFU/mL	5.329E-26	Yes
10^0 CFU/mL	10^1 CFU/mL	0.588	No
10^0 CFU/mL	10^3 CFU/mL	8.696E-11	Yes
10^0 CFU/mL	10^4 CFU/mL	6.794E-10	Yes
10^0 CFU/mL	10^5 CFU/mL	5.894E-29	Yes
10^0 CFU/mL	10^6 CFU/mL	4.534E-14	Yes
10^0 CFU/mL	10^8 CFU/mL	3.060E-34	Yes
10^0 CFU/mL	10^9 CFU/mL	5.694E-18	Yes
10^1 CFU/mL	10^3 CFU/mL	1.645E-06	Yes
10^1 CFU/mL	10^4 CFU/mL	9.530E-09	Yes
10^1 CFU/mL	10^5 CFU/mL	1.629E-19	Yes
10^1 CFU/mL	10^6 CFU/mL	3.875E-13	Yes
10^1 CFU/mL	10^8 CFU/mL	2.097E-26	Yes
10^1 CFU/mL	10^9 CFU/mL	3.841E-17	Yes

Table B-56 (cont'd).

10^3 CFU/mL	10^4 CFU/mL	0.001	Yes
10^3 CFU/mL	10^5 CFU/mL	1.470E-07	Yes
10^3 CFU/mL	10^6 CFU/mL	2.395E-08	Yes
10^3 CFU/mL	10^8 CFU/mL	3.954E-14	Yes
10^3 CFU/mL	10^9 CFU/mL	2.443E-12	Yes
10^4 CFU/mL	10^5 CFU/mL	0.592	No
10^4 CFU/mL	10^6 CFU/mL	0.013	Yes
10^4 CFU/mL	10^8 CFU/mL	0.152	No
10^4 CFU/mL	10^9 CFU/mL	3.404E-05	Yes
10^5 CFU/mL	10^6 CFU/mL	0.001	Yes
10^5 CFU/mL	10^8 CFU/mL	0.002	Yes
10^5 CFU/mL	10^9 CFU/mL	2.882E-07	Yes
10^6 CFU/mL	10^8 CFU/mL	0.090	No
10^6 CFU/mL	10^9 CFU/mL	0.092	No
10^8 CFU/mL	10^9 CFU/mL	2.904E-04	Yes

REFERENCES

REFERENCES

1. Sanders, J.W., et al., *Military importance of diarrhea: lessons from the Middle East.* Current Opinion in Gastroenterology, 2005. **21**(1): p. 9-14.

2. Hyams, K.C., et al., *The Impact of Infectious Diseases on the Health of U.S. Troops Deployed to the Persian Gulf During Operations Desert Shield and Desert Storm.* Clinical Infectious Diseases, 1995. **20**(6): p. 1497-1504.

3. Sharpe, A.N., *Food Sample Preparation and Enrichment for Rapid Detection*, in *Rapid Detection Assays: For Food and Water*, S.T. Clarke, et al., Editors. 2001, Royal Society of Chemistry: Cornwall. p. 129-137.

4. Oyofo, B.A., et al., *A survey of enteropathogens among United States military personnel during Operation Bright Star '94, in Cairo, Egypt.* Mil Med, 1995. **160**(7): p. 331-334.

5. Feng, P., et al., *Enumeration of Escherichia coli and the Coliform Bacteria*, in *Bacteriological Analytical Manual (BAM)*, T. Hammack, et al., Editors. 1998, U.S. Food and Drug Administration.

6. Feng, P., S.D. Weagant, and K. Jinneman, *Diarrheagenic Escherichia coli*, in *Bacteriological Analytical Manual (BAM)*, T. Hammack, et al., Editors. 1998, U.S. Food and Drug Administration.

7. Swaminathan, B. and P. Feng, *Rapid Detection of Food-Borne Pathogenic Bacteria.* Annual Review of Microbiology, 1994. **48**(1): p. 401-426.

8. Radke, S.M. and E.C. Alocilja, *A high density microelectrode array biosensor for detection of E. coli O157:H7.* Biosensors and Bioelectronics, 2005. **20**(8): p. 1662-1667.

9. Rodriguez, M.I. and E.C. Alocilja, *Embedded DNA-polypyrrole biosensor for rapid detection of Escherichia Coli.* Sensors Journal, IEEE, 2005. **5**(4): p. 733-736.

10. Muhammad-Tahir, Z. and E.C. Alocilja, *Fabrication of a disposable biosensor for Escherichia Coli O157:H7 detection.* Sensors Journal, IEEE, 2003. **3**(4): p. 345-351.

11. Setterington, E.B. and E.C. Alocilja, *Electrochemical Biosensor for Rapid and Sensitive Detection of Magnetically Extracted Bacterial Pathogens.* Biosensors, 2012. **2**(1): p. 15-31.

12. Granato, F., et al., *Disposable Electrospun Electrodes Based on Conducting Nanofibers.* Electroanalysis, 2008. **20**(12): p. 1374-1377.

13. Bhattacharyya, D., et al., *High Surface Area Flexible Chemiresistive Biosensor by Oxidative Chemical Vapor Deposition.* Advanced Functional Materials, 2011. **21**(22): p. 4328-4337.

14. Gregory, R.V., W.C. Kimbrell, and H.H. Kuhn, *Electrically Conductive Non-Metallic Textile Coatings.* Journal of Industrial Textiles, 1991. **20**(3): p. 167-175.

15. Ryder, K.S., D.G. Morris, and J.M. Cooper, *Role of conducting polymeric interfaces in promoting biological electron transfer.* Biosensors and Bioelectronics, 1997. **12**(8): p. 721-727.

16. Kuhn, H.H. and W.C. Kimbrell, *Electrically Conductive Textile Materials and Method for Making Same*, in *USPTO*, USPTO, Editor 1989, Milliken Research Corporation: United States.

17. Vaddiraju, S., K. Seneca, and K.K. Gleason, *Novel Strategies for the Deposition of □COOH Functionalized Conducting Copolymer Films and the Assembly of Inorganic Nanoparticles on Conducting Polymer Platforms.* Advanced Functional Materials, 2008. **18**(13): p. 1929-1938.

18. McGraw, S., et al., *Synthesis of a Functionalized Polypyrrole Coated Electrotextile for Use in Biosensors.* Biosensors, 2012. **2**(4): p. 465-478.

19. McGraw, S.K., et al., *Antibody Immobilization on Conductive Polymer Coated Nonwoven Fibers for Biosensors.* Sensors & Transducers Journal, 2011. **13**(Special Issue): p. 142-149.

20. McGraw, S.K., et al., *A Resistance Based Biosensor That Utilizes Conductive Microfibers for Microbial Pathogen Detection.* Open Journal of Applied Biosensor, 2012. **1**(3): p. 36-43.

21. Prevention, C.f.D.C.a., *CDC 2011 Estimates: Findings*, in *CDC Estimates of Foodborne Illness in the United States*2010, Centers for Disease Control and Prevention: Atlanta.

22. Baylis, C.L., et al., *Escherichia coli and Shigella spp.*, in *Principles and Practice of Clinical Bacteriology*, S.H. Gillespie and P.M. Hawkey, Editors. 2006, John Wiley and Sons: West Sussex, UK. p. 347-365.

23. Feng, P., *Escherichia coli (ETEC, EPEC, EHEC, and EIEC)*, in *FDA Bad Bug Book -- Foodborne Pathogenic Microorganisms and Natural Toxins Handbook*, K.A. Lampel, S. Al-Khaldi, and S.M. Cahill, Editors. 2012, U.S. Food and Drug Administration: Silver Spring, MD. p. 69-81.

24. Prevention, C.f.D.C.a., *Vital Signs: Incidence and Trends of Infection with Pathogens Transmitted Commonly Through Food -- Foodborne Diseases Active Surveillance Network, 10 U.S. Sites, 1996 -- 2010.* MMWR, 2011. **60**(22): p. 749-755.

25. Prevention, C.f.D.C.a. *Trends in Foodborne Illness in the United States*. CDC Estimates of Foodborne Illness in the United States 2013 02/04/2013 [cited 2013 02/15/2013].

26. James, J., A. Frelin, and R. Jeffery, *Disease and nonbattle injury rates and military medicine.* Med Bull, 1982. **39**: p. 17-27.

27. Harman, D., T. Hooper, and G. Gackstetter, *Aeromedical evacuations from Operation Iraqi Freedom: a descriptive study.* Mil Med, 2005. **170**: p. 521-527.

28. Aronson, N.E., J.W. Sanders, and K.A. Moran, *In Harm's Way: Infections in Deployed American Military Forces.* Clinical Infectious Diseases, 2006. **43**(8): p. 1045-1051.

29. Sanders, J.W., et al. *A cross-sectional, case-finding study of travelers' diarrhea among U.S. military personnel deployed to Iraq*. in *Annual Meeting of the American Society of Tropical Medicine and Hygiene*. 2005. Washington, DC: American Society of Tropical Medicine and Hygiene.

30. Sanders, J.W., et al., *Impact of illness and non-combat injury during operations Iraqi Freedom and Enduring Freedom (Afghanistan).* Am J Trop Med Hyg, 2005. **73**: p. 713-719.

31. Putnam, S.D., et al., *Self-Reported Description of Diarrhea Among Military Populations in Operations Iraqi Freedom and Enduring Freedom.* Journal of Travel Medicine, 2006. **13**(2): p. 92-99.

32. Lazcka, O., F.J.D. Campo, and F.X. Muñoz, *Pathogen detection: A perspective of traditional methods and biosensors.* Biosensors and Bioelectronics, 2007. **22**(7): p. 1205-1217.

33. Fratamico, P.M., *Comparison of culture, polymerase chain reaction (PCR), TaqMan Salmonella, and Transia Card Salmonella assays for detection of Salmonella spp. in naturally-contaminated ground chicken, ground turkey, and ground beef.* Molecular and Cellular Probes, 2003. **17**(5): p. 215-221.

34. Janeway, C., *Immunobiology : the immune system in health and disease*. 6th ed. 2005, New York: Garland Science. xxiii, 823 p.

35. Echko, M.M. and S.K. Dozier. *Recombinant Antibody Technology for the Production of Antibodies Without the Use of Animals*. 2010 [cited 2013 02/15/2013].

36. Gu, H., et al., *Biofunctional magnetic nanoparticles for protein separation and pathogen detection.* Chemical Communications, 2006. **0**(9): p. 941-949.

37. Mine, Y., *Separation of Salmonella enteritidis from Experimentally Contaminated Liquid Eggs Using a Hen IgY Immobilized Immunomagnetic Separation System.* Journal of Agricultural and Food Chemistry, 1997. **45**(10): p. 3723-3727.

38. Pérez, F.G., et al., *Immunomagnetic Separation with Mediated Flow Injection Analysis Amperometric Detection of Viable Escherichia coli O157.* Analytical Chemistry, 1998. **70**(11): p. 2380-2386.

39. Navarro, A., et al., *Antibody responses to Escherichia coli O157 and other lipopolysaccharides in healthy children and adults.* Clin Diagn Lab Immunol, 2003. **10**(5): p. 797-801.

40. Mullis, K., et al., *Specific Enzymatic Amplification of DNA In Vitro: The Polymerase Chain Reaction.* Cold Spring Harbor Symposia on Quantitative Biology, 1986. **51**: p. 263-273.

41. Cady, N.C., et al., *Real-time PCR detection of Listeria monocytogenes using an integrated microfluidics platform.* Sensors and Actuators B: Chemical, 2005. **107**(1): p. 332-341.

42. Rodriguez-Lazaro, D., et al., *Real-time PCR-based methods for detection of Mycobacterium avium subsp. paratuberculosis in water and milk.* Int J Food Microbiol, 2005. **101**(1): p. 93-104.

43. Jofré, A., et al., *Simultaneous detection of Listeria monocytogenes and Salmonella by multiplex PCR in cooked ham.* Food Microbiology, 2005. **22**(1): p. 109-115.

44. Touron, A., et al., *Detection of Salmonella in environmental water and sediment by a nested-multiplex polymerase chain reaction assay.* Research in Microbiology, 2005. **156**(4): p. 541-553.

45. Fratamico, P. and C. DebRoy, *Detection of Escherichia coli O157:H7 in Food Using Real-Time Multiplex PCR Assays Targeting the stx 1, stx 2, wzy O157, and the fliC h7 or eae Genes.* Food Analytical Methods, 2010. **3**(4): p. 330-337.

46. Weagant, S.D. and A.J. Bound, *Comparison of Methods for Enrichment and Isolation of Escherichia coli O157:H7 from Artificially Contaminated Salad Mixes*, in *Laboratory Information Bulleting*2001.

47. Jinneman, K.C., K.J. Yoshitomi, and S.D. Weagant, *Multiplex real-time PCR method to identify Shiga toxin genes stx1 and stx2 and Escherichia coli O157:H7/H- serotype.* Appl Environ Microbiol, 2003. **69**(10): p. 6327-33.

48. Jinneman, K.C., K.J. Yoshitomi, and S.D. Weagant, *Multiplex real-time PCR protocol for the identification of shiga toxins, stx1 and stx2, and E. coli O157:H7/H- serogroup*, in *Laboratory Information Bulletin*2003.

49. Yoshitomi, K.J., K.C. Jinneman, and S.D. Weagant, *Optimization of a 3′-minor groove binder-DNA probe targeting the uidA gene for rapid identification of Escherichia coli O157:H7 using real-time PCR.* Molecular and Cellular Probes, 2003. **17**(6): p. 275-280.

50. Feng, P. and K.A. Lampel, *Genetic analysis of uidA expression in enterohaemorrhagic Escherichia coli serotype 0157:H7.* Microbiology, 1994. **140**(8): p. 2101-2107.

51. Feng, P. and S.R. Monday, *Multiplex PCR for detection of trait and virulence factors in enterohemorrhagic Escherichia coli serotypes.* Molecular and Cellular Probes, 2000. **14**(6): p. 333-337.

52. Nayak, M., et al., *Detection of microorganisms using biosensors—A smarter way towards detection techniques.* Biosensors and Bioelectronics, 2009. **25**(4): p. 661-667.

53. Thevenot, D.R., et al., *Electrochemical Biosensors: Recommended Definitions and Classification*, in *Pure Applied Chemistry*1999, International Union of Pure and Applied Chemistry: Great Britain. p. 2333-2348.

54. Cahn, T.M., *Biosensors*. Sensor Physics and Technology Series, ed. K.T.V. Grattan and A. Augousti. 1993, London: Chapman and Hall.

55. DeMarco, D.R., et al., *Rapid detection of Escherichia coli O157:H7 in ground beef using a fiber-optic biosensor.* J Food Prot, 1999. **62**(7): p. 711-6.

56. Hoyle, B., *High-Tech Biosensor Speeds Bacteria Detection*, in *ASM News*2001, American Society for Microbiology. p. 434-435.

57. Seo, K.H., et al., *Development of a rapid response biosensor for detection of Salmonella typhimurium.* J Food Prot, 1999. **62**(5): p. 431-7.

58. Cunningham, B.T., *Label-free optical biosensors: An introduction*, in *LABEL-FREE BIOSENSORS : TECHNIQUES AND APPLICATIONS [electronic resource]* M.A. Cooper, Editor 2009, CAMBRIDGE UNIV PRESS: New York. p. 1-27.

59. Griffiths, D. and G. Hall, *Biosensors what real progress is being made?* Trends in biotechnology, 1993. **11**(4): p. 122-130.

60. Luong, J.H.T., P. Bouvrette, and K.B. Male, *Developments and applications of biosensors in food analysis.* Trends in biotechnology, 1997. **15**(9): p. 369-377.

61. Bae, Y.M., et al., *Detection of insulin-antibody binding on a solid surface using imaging ellipsometry.* Biosens Bioelectron, 2004. **20**(4): p. 895-902.

62. Baeumner, A.J., et al., *RNA biosensor for the rapid detection of viable Escherichia coli in drinking water.* Biosens Bioelectron, 2003. **18**(4): p. 405-13.

63. Tschmelak, J., G. Proll, and G. Gauglitz, *Sub-nanogram per litre detection of the emerging contaminant progesterone with a fully automated immunosensor based on evanescent field techniques.* Analytica Chimica Acta, 2004. **519**(2): p. 143-146.

64. Willardson, B.M., et al., *Development and Testing of a Bacterial Biosensor for Toluene-Based Environmental Contaminants.* Appl Environ Microbiol, 1998. **64**(3): p. 1006-1012.

65. Ramakrishna, S., et al., *Polymer nanofibers for biosensor applications*, in *Molecular Building Blocks for Nanotechnology: From Diamondoids to Nanoscale Materials and Applications*, G.A. Mansoori, et al., Editors. 2007, Springer: New York. p. 377-392.

66. Higgins, J.A., et al., *A handheld real time thermal cycler for bacterial pathogen detection.* Biosensors and Bioelectronics, 2003. **18**(9): p. 1115-1123.

67. Ko, S. and S.A. Grant, *Development of a novel FRET method for detection of Listeria or Salmonella.* Sensors and Actuators B: Chemical, 2003. **96**(1–2): p. 372-378.

68. Cooper, M.A., *Label-free screening of bio-molecular interactions.* Analytical and Bioanalytical Chemistry, 2003. **377**(5): p. 834-42.

69. Oh, B.-K., et al., *The fabrication of protein chip based on surface plasmon resonance for detection of pathogens.* Biosensors and Bioelectronics, 2005. **20**(9): p. 1847-1850.

70. Taylor, A.D., et al., *Comparison of E. coli O157:H7 preparation methods used for detection with surface plasmon resonance sensor.* Sensors and Actuators B: Chemical, 2005. **107**(1): p. 202-208.

71. O'Sullivan, C.K. and G.G. Guilbault, *Commercial quartz crystal microbalances – theory and applications.* Biosensors and Bioelectronics, 1999. **14**(8–9): p. 663-670.

72. Plomer, M., G.G. Guilbault, and B. Hock, *Development of a piezoelectric immunosensor for the detection of enterobacteria.* Enzyme and Microbial Technology, 1992. **14**(3): p. 230-235.

73. Vaughan, R.D., C.K. O'Sullivan, and G.G. Guilbault, *Development of a quartz crystal microbalance (QCM) immunosensor for the detection of Listeria monocytogenes.* Enzyme and Microbial Technology, 2001. **29**(10): p. 635-638.

74. Wong, Y.Y., et al., *Immunosensor for the differentiation and detection of Salmonella species based on a quartz crystal microbalance.* Biosensors and Bioelectronics, 2002. **17**(8): p. 676-684.

75. Wang, J., *Analytical electrochemistry*. 2nd ed. Vol. XVI. 2000, New York: John Wiley & Sons. xvi, 209 p.

76. Bergveld, P., *Thirty years of ISFETOLOGY: What happened in the past 30 years and what may happen in the next 30 years.* Sensors and Actuators B: Chemical, 2003. **88**(1): p. 1-20.

77. Schoning, M.J. and A. Poghossian, *Recent advances in biologically sensitive field-effect transistors (BioFETs).* Analyst, 2002. **127**(9): p. 1137-1151.

78. Barsoukov, E. and J.R. Macdonald, *Impedance spectroscopy theory, experiment, and applications*, 2005, Wiley-Interscience,: Hoboken, N.J. p. xvii, 595 p. ill.

79. Katz, E. and I. Willner, *Probing Biomolecular Interactions at Conductive and Semiconductive Surfaces by Impedance Spectroscopy: Routes to Impedimetric Immunosensors, DNA-Sensors, and Enzyme Biosensors.* Electroanalysis, 2003. **15**(11): p. 913-947.

80. Muhammad-Tahir, Z. and E.C. Alocilja, *A conductometric biosensor for biosecurity.* Biosensors and Bioelectronics, 2003. **18**(5–6): p. 813-819.

81. Deitzel, J.M., et al., *The effect of processing variables on the morphology of electrospun nanofibers and textiles.* Polymer, 2001. **42**(1): p. 261-272.

82. Dhawan, A., *Development of robust fiber optic sensors suitable for incorporation into textiles and a mechanic analysis of electronic textile circuits*, in *Fiber and Polymer Science / Electrical Engineering*2008, North Carolina State University: Raleigh, NC.

83. Bhat, G.S., *Nonwovens as Three-Dimensional Textiles for Composites.* Materials and Manufacturing Processes, 1995. **10**(4): p. 667-688.

84. Broughton, R.M. and P.H. Brady, *Nonwoven fabrics*, in *Wellington Sears handbook of industrial textiles*, S. Adanur, Editor. 1995, Technomic Pub.: Lancaster, PA. p. 141-154.

85. Burger, C., B.S. Hsiao, and B. Chu, *Nanofibrous Materials and Their Applications.* Annual Review of Materials Research, 2006. **36**(1): p. 333-368.

86. Lu, P. and B. Ding, *Applications of Electrospun Fibers.* Recent Patents on Nanotechnology, 2008. **2**(3): p. 169-182.

87. Zhang, C.-H., et al., *Preparation and characterization of hydrophilic modification of polypropylene non-woven fabric by dip-coating PVA (polyvinyl alcohol).* Separation and Purification Technology, 2008. **61**(3): p. 276-286.

88. Bhardwaj, N. and S.C. Kundu, *Electrospinning: a fascinating fiber fabrication technique.* Biotechnol Adv, 2010. **28**(3): p. 325-47.

89. Grafe, T. and K. Graham *Polymeric Nanofibers and Nanofiber Webs: A New Class of Nonwovens*. International Nonwovens Journal, 2003. **12**.

90. Doshi, J. and D.H. Reneker, *Electrospinning process and applications of electrospun fibers.* Journal of Electrostatics, 1995. **35**(2–3): p. 151-160.

91. Kubo, E. and M. Watanabe, *Spinning for nonwovens*, in *Advance Fiber Spinning Technology*, T. Nakajima, Editor. 1994, Woodhead Publishing, Ltd.: Cambridge, UK. p. 105-114.

92. Matabola, K.P., et al., *Single polymer composites: a review*. Journal of Materials Science, 2009. **44**(23): p. 6213-6222.

93. Agarwal, S., A. Greiner, and J.H. Wendorff, *Electrospinning of Manmade and Biopolymer Nanofibers—Progress in Techniques, Materials, and Applications.* Advanced Functional Materials, 2009. **19**(18): p. 2863-2879.

94. Greiner, A. and J.H. Wendorff, *Electrospinning: A Fascinating Method for the Preparation of Ultrathin Fibers (Angew. Chem. Int. Ed. 30/2007).* Angewandte Chemie International Edition, 2007. **46**(30): p. 5633-5633.

95. Huang, J., et al., *Polyaniline Nanofibers: Facile Synthesis and Chemical Sensors.* Journal of the American Chemical Society, 2002. **125**(2): p. 314-315.

96. Liang, D., B.S. Hsiao, and B. Chu, *Functional electrospun nanofibrous scaffolds for biomedical applications.* Advanced Drug Delivery Reviews, 2007. **59**(14): p. 1392-1412.

97. Schiffman, J.D. and C.L. Schauer, *A Review: Electrospinning of Biopolymer Nanofibers and their Applications.* Polymer Reviews, 2008. **48**(2): p. 317-352.

98. Subbiah, T., et al., *Electrospinning of nanofibers.* Journal of Applied Polymer Science, 2005. **96**(2): p. 557-569.

99. Formhals, A., *Process and apparatus for preparing artificial threads*, in *USPTO*, U.S.P. Office, Editor 1934, Schreiber-Gastell, R.
Formhals, A.: USA.

100. Moon, J., et al., *Semiconducting ZnO nanofiber as gas sensors and gas response improvement by SnO2 coating.* ETRI Journal, 2009. **31**(6): p. 636-641.

101. Sawicka, K., P. Gouma, and S. Simon, *Electrospun biocomposite nanofibers for urea biosensing.* Sensors and Actuators B: Chemical, 2005. **108**(1–2): p. 585-588.

102. Ding, B., et al., *Electrospun nanomaterials for ultrasensitive sensors.* Materials Today, 2010. **13**(11): p. 16-27.

103. Li, H., Y. Ke, and Y. Hu, *Polymer nanofibers prepared by template melt extrusion.* Journal of Applied Polymer Science, 2006. **99**(3): p. 1018-1023.

104. So, J.-H., et al. *Highly stretchable conductive fibers*. in *2010 Innovative Nonwovens Conference*. 2010. Raleigh, NC: TAPPI.

105. Karaguzel, B., H.V. Tafreshi, and B. Pourdeyhimi, *Potentials and challenges in jetting microdroplets onto nonwoven fabrics.* Journal of The Textile Institute, 2008. **99**(6): p. 581-589.

106. Held, R.P., *Ink jet printing of textiles*, in *USPTO*, U.S.P. Office, Editor 1998, E. I. du Pont de Nemours and Company: USA.

107. de Gans, B.J., P.C. Duineveld, and U.S. Schubert, *Inkjet Printing of Polymers: State of the Art and Future Developments.* Advanced Materials, 2004. **16**(3): p. 203-213.

108. Kang, T.H., et al. *Sensors on Textile Substrates for Home-Based Healthcare Monitoring*. in *Distributed Diagnosis and Home Healthcare, 2006. D2H2. 1st Transdisciplinary Conference on*. 2006.

109. Puurunen, R.L., *Surface chemistry of atomic layer deposition: A case study for the trimethylaluminum / water process.* J. Appl. Phys., 2005. **97**(12).

110. George, S.M., *Atomic layer deposition: An overview.* Chemical Reviews, 2009. **110**(1): p. 111-131.

111. Langereis, E., et al., *Plasma-assisted atomic layer deposition of Al2O3 moisture permeation barriers on polymers.* Appl. Phys. Lett., 2006. **89**(8).

112. Jur, J.S., et al., *Atomic Layer Deposition of Conductive Coatings on Cotton, Paper, and Synthetic Fibers: Conductivity Analysis and Functional Chemical Sensing Using "All-Fiber" Capacitors.* Advanced Functional Materials, 2011. **21**(11): p. 1993-2002.

113. Rahman, M., et al., *Electrochemical Sensors Based on Organic Conjugated Polymers.* Sensors, 2008. **8**(1): p. 118-141.

114. Walton, D.J., F.J. Davis, and P.J. Langley, *The synthesis of conducting polymers based on heterocyclic compounds*, in *Polymer Chemistry: A Practical Approach*, F.J. Davis, Editor. 2004, Oxford University Press: Oxford, UK. p. 158-187.

115. Ramanavičius, A., A. Ramanavičienė, and A. Malinauskas, *Electrochemical sensors based on conducting polymer—polypyrrole.* Electrochimica Acta, 2006. **51**(27): p. 6025-6037.

116. Tenhaeff, W.E. and K.K. Gleason, *Initiated and Oxidative Chemical Vapor Deposition of Polymeric Thin Films: iCVD and oCVD.* Advanced Functional Materials, 2008. **18**(7): p. 979-992.

117. Nair, S., S. Natarajan, and S.H. Kim, *Fabrication of Electrically Conducting Polypyrrole-Poly(ethylene oxide) Composite Nanofibers.* Macromolecular Rapid Communications, 2005. **26**(20): p. 1599-1603.

118. Malinauskas, A., *Chemical deposition of conducting polymers.* Polymer, 2001. **42**(9): p. 3957-3972.

119. Child, A.D. and H.H. Kuhn, *Enhancement of the thermal stability of chemically synthesized polypyrrole.* Synthetic Metals, 1997. **84**(1–3): p. 141-142.

120. Jolly, R., J.P. Boutrois, and C. Petrescu, *Process of polypyrrole deposit on textile. Product characteristics and applications.* Synthetic Metals, 1997. **85**(1): p. 1405-1406.

121. Kuhn, H.H. and W.C. Kimbrell, *Method for making electrically conductive textile materials*, U.S.P. Office, Editor 1989, Milliken Research Corporation: United States.

122. Kuhn, H.H., et al., *Properties and applications of conductive textiles.* Synthetic Metals, 1993. **57**(1): p. 3707-3712.

123. Li, H., et al., *Polypyrrole-carbon fiber composite film prepared by chemical oxidative polymerization of pyrrole.* Journal of Applied Polymer Science, 1997. **64**(11): p. 2149-2154.

124. Yin, X.H., et al., *Percolation conduction in polymer composites containing polypyrrole coated insulating polymer fiber and conducting polymer.* Synthetic Metals, 1995. **69**(1–3): p. 367-368.

125. Anbarasan, R., et al., *Chemical grafting of aniline and o-toluidine onto poly(ethylene terephthalate) fiber.* Journal of Applied Polymer Science, 1999. **73**(1): p. 121-128.

126. Bartlett, P.N., *Modified electrode surface in amperometric biosensors.* Medical and Biological Engineering and Computing, 1990. **28**(3): p. B10-B17.

127. Munoz-Berbel, X., et al., *Impedance-Based Biosensors for Pathogen Detection*, in *Principles of Bacterial Detection: Biosensors, Recognition Receptors and Microsystems*, M. Zourob, S. Elwary, and A. Turner, Editors. 2008, Springer Science + Business Media LLC: New York. p. 341-371.

128. Bakshi, U.A. and V.U. Bakshi, *Electrical Engineering*. 1st ed. 2009, Pune, India: Technical Publications Pune.

129. Layton, K.N. and M.R. Abidian. *Conducting polymer nanofiber-based biosensor for detection of neurochemicals*. in *Neural Engineering (NER), 2011 5th International IEEE/EMBS Conference on*. 2011.

130. Marx, S., et al., *Electrospun gold nanofiber electrodes for biosensors.* Biosensors and Bioelectronics, 2011. **26**(6): p. 2981-2986.

131. Luo, Y., et al., *Surface functionalization of electrospun nanofibers for detecting E. coli O157:H7 and BVDV cells in a direct-charge transfer biosensor.* Biosensors and Bioelectronics, 2010. **26**(4): p. 1612-1617.

132. Pal, S., E.C. Alocilja, and F.P. Downes, *Nanowire labeled direct-charge transfer biosensor for detecting Bacillus species.* Biosensors and Bioelectronics, 2007. **22**(9–10): p. 2329-2336.

133. Arecchi, A., et al., *Biocatalytic nylon nanofibrous membranes.* Analytical and Bioanalytical Chemistry, 2010. **398**(7-8): p. 3097-3103.

134. Manesh, K.M., et al., *A novel glucose biosensor based on immobilization of glucose oxidase into multiwall carbon nanotubes–polyelectrolyte-loaded electrospun nanofibrous membrane.* Biosensors and Bioelectronics, 2008. **23**(6): p. 771-779.

135. Arecchi, A., et al., *Nanofibrous membrane based tyrosinase-biosensor for the detection of phenolic compounds.* Analytica Chimica Acta, 2010. **659**(1–2): p. 133-136.

136. Muhammad-Tahir, Z., E.C. Alocilja, and D.L. Grooms, *Rapid detection of bovine viral diarrhea virus as surrogate of bioterrorism agents.* Sensors Journal, IEEE, 2005. **5**(4): p. 757-762.

137. Okafor, C., et al., *Fabrication of a Novel Conductometric Biosensor for Detecting Mycobacterium avium subsp. paratuberculosis Antibodies.* Sensors, 2008. **8**(9): p. 6015-6025.

138. Chambers, J.P., et al., *Biosensor recognition elements.* Curr. Issues Mol. Biol., 2008. **10**: p. 1-12.

139. Setterington, E.B., et al., *Rapid, sensitive, and specific immunomagnetic separation of foodborne pathogens.* International Journal of Food Safety, Nutrition and Public Health, 2011. **4**(1): p. 83-100.

140. Torres-Chavolla, E. and E.C. Alocilja, *Aptasensors for detection of microbial and viral pathogens.* Biosensors and Bioelectronics, 2009. **24**(11): p. 3175-3182.

141. Zhang, D., M.C. Huarng, and E.C. Alocilja, *A multiplex nanoparticle-based bio-barcoded DNA sensor for the simultaneous detection of multiple pathogens.* Biosensors and Bioelectronics, 2010. **26**(4): p. 1736-1742.

142. Ivnitski, D., et al., *Biosensors for detection of pathogenic bacteria.* Biosensors and Bioelectronics, 1999. **14**(7): p. 599-624.

143. Scott, A.O., *Biosensors for food analysis*. Special publication, ed. R.S.o.C.G.B.b.F.C. Group. 1998, Cambridge: Royal Society of Chemistry, Woodhead Publishing. viii, 200 p.

144. Heisey, C.L., et al., *Surface and Adhesion Properties of Polypyrrole-Coated Textiles.* Textile Research Journal, 1993. **63**(5): p. 247-256.

145. Senecal, A., et al., *Development of functional nanofibrous membrane assemblies towards biological sensing.* Reactive and Functional Polymers, 2008. **68**(10): p. 1429-1434.

146. Marks, R., et al., *An innovative strategy for immobilization of receptor proteins on to an optical fiber by use of poly(pyrrole–biotin).* Analytical and Bioanalytical Chemistry, 2002. **374**(6): p. 1056-1063.

147. Konry, T., et al., *Optical Fiber Immunosensor Based on a Poly(pyrrole−benzophenone) Film for the Detection of Antibodies to Viral Antigen.* Analytical Chemistry, 2005. **77**(6): p. 1771-1779.

148. Kwon, O.S., S.J. Park, and J. Jang, *A high-performance VEGF aptamer functionalized polypyrrole nanotube biosensor.* Biomaterials, 2010. **31**(17): p. 4740-4747.

149. Alocilja, E.C. and S.M. Radke, *Market analysis of biosensors for food safety.* Biosensors and Bioelectronics, 2003. **18**(5–6): p. 841-846.

150. Swain, A., *Biosensors: a new realism.* Annales de biologie clinique, 1992. **50**(3): p. 175-179.

151. Warsinke, A., *Biosensors for food analysis*, in *Frontiers in Biosensorics II: Practical Applications*, F.W. Scheller, F. Schubert, and J. Fedrowitz, Editors. 2000, Birkhauser Basel: Basel, Switzerland. p. 121-140.

152. Armes, S.P., *Optimum reaction conditions for the polymerization of pyrrole by iron(III) chloride in aqueous solution.* Synthetic Metals, 1987. **20**(3): p. 365-371.

153. Eisazadeh, H., *Studying the characteristics of polypyrrole and its composites.* World Journal of Chemistry, 2007. **2**(2): p. 67-74.

154. Myers, R., *Chemical oxidative polymerization as a synthetic route to electrically conducting polypyrroles.* Journal of Electronic Materials, 1986. **15**(2): p. 61-69.

155. Novák, P., *Limitations of polypyrrole synthesis in water and their causes.* Electrochimica Acta, 1992. **37**(7): p. 1227-1230.

156. Stanke, D., M.L. Hallensleben, and L. Toppare, *Oxidative polymerization of some N-alkylpyrroles with ferric chloride.* Synthetic Metals, 1995. **73**(3): p. 267-272.

157. Hermanson, G.T., *Bioconjugate techniques*, 2008, Elsevier Academic Press,: Amsterdam ; Boston. p. 1202.

158. Avlyanov, J.K., et al., *In-situ deposited thin films of polypyrrole: conformational changes induced by variation of dopant and substrate surface.* Synthetic Metals, 1997. **84**(1–3): p. 153-154.

159. Turner, A.P.F. and J.D. Newman, *An introduction to biosensors*, in *Biosensors for food analysis*, A.O. Scott, Editor. 1998, Woodhead Publishing Limited: Cambridge. p. 13-27.

160. Suh, M. *E-Textiles for Wearability: Review of Integration Technologies*. Textile World, 2010.

161. Liao, W., et al., *Studying the effects of reaction conditions on components of dairy manure and cellulose accumulation using dilute acid treatment.* Bioresource Technology, 2007. **98**(10): p. 1992-1999.

162. Liu, Y., W. Liao, and S. Chen, *Study of pellet formation of filamentous fungi Rhizopus oryzae using a multiple logistic regression model.* Biotechnology and Bioengineering, 2008. **99**(1): p. 117-128.

163. Montgomery, D.C., E.A. Peck, and G.G. Vining, *Introduction to Linear Regression Analysis*. Wiley Series in Probability and Statistics. 2012, Hoboken, NJ: John Wiley and Sons, Inc.

164. Neter, J., W. Wasserman, and M.H. Kutner, *Applied linear statistical models : regression, analysis of variance, and experimental designs*. 3rd ed. 1990, Homewood, IL: Irwin. xvi, 1181 p.

165. Haaland, P.D., *Experimental design in biotechnology*. Statistics, textbooks, and monographs. 1989, New York: Marcel Dekker. xv, 259 p.

166. Gregory, R.V., W.C. Kimbrell, and H.H. Kuhn, *Conductive textiles.* Synthetic Metals, 1989. **28**(1–2): p. 823-835.

167. Ahuja, T., et al., *Biomolecular immobilization on conducting polymers for biosensing applications.* Biomaterials, 2007. **28**(5): p. 791-805.

168. Sargent, A. and O.A. Sadik, *Monitoring antibody–antigen reactions at conducting polymer-based immunosensors using impedance spectroscopy.* Electrochimica Acta, 1999. **44**(26): p. 4667-4675.

169. Yokoyama, K., et al., *Complete nucleotide sequence of the prophage VT1-Sakai carrying the Shiga toxin 1 genes of the enterohemorrhagic Escherichia coli O157:H7 strain derived from the Sakai outbreak.* Gene, 2000. **258**(1-2): p. 127-39.

170. Cloutier, B.C., *Development of mitigation strategies toward preventative postures in food defense*, 2012, Michigan State University: United States -- Michigan. p. 385.

171. Gagna, C.E., et al., *Novel DNA Staining Method and Processing Technique for the Quantification of Undamaged Double-stranded DNA in Epidermal Tissue Sections by PicoGreen Probe Staining and Microspectrophotometry.* Journal of Histochemistry & Cytochemistry, 2007. **55**(10): p. 999-1014.

172. Muhammad-Tahir, Z. and E.C. Alocilja, *A Disposable Biosensor for Pathogen Detection in Fresh Produce Samples.* Biosystems Engineering, 2004. **88**(2): p. 145-151.

173. Senecal, A. and P. Marek, *Military Food Safety Technologies*, in *Military Food Engineering and Ration Technology*, A.H. Barrett and A.V. Cardello, Editors. 2012, DEStech Publications: Lancaster, PA. p. 157-194.

174. Federation, I.D., *Milk and Milk Products*, in *Enumeration of Microorganisms: Colony Count at 3 Degrees C*1987, International Dairy Federation: Brussels.

175. Niemela, S., *Statistical Evaluation of Results from Quantitative Microbiological Examinations*, 1983, Nordic Committee in Food Analysis: Uppsala.

176. Cattaneo, M.V., J.H.T. Luong, and S. Mercille, *Monitoring glutamine in mammalian cell cultures using an amperometric biosensor.* Biosensors and Bioelectronics, 1992. **7**(5): p. 329-334.

177. Darain, F., S.-U. Park, and Y.-B. Shim, *Disposable amperometric immunosensor system for rabbit IgG using a conducting polymer modified screen-printed electrode.* Biosensors and Bioelectronics, 2003. **18**(5–6): p. 773-780.

178. Tahir, Z., E. Alocilja, and D. Grooms, *Indium Tin Oxide-Polyaniline Biosensor: Fabrication and Characterization.* Sensors, 2007. **7**(7): p. 1123-1140.

179. Tsiafoulis, C.G., M.I. Prodromidis, and M.I. Karayannis, *Development of an amperometric biosensing method for the determination of l-fucose in pretreated urine.* Biosensors and Bioelectronics, 2004. **20**(3): p. 620-627.

180. Radke, S.M. and E.C. Alocilja, *Design and fabrication of a microimpedance biosensor for bacterial detection.* Sensors Journal, IEEE, 2004. **4**(4): p. 434-440.

181. Tien, H.T. and A. Ottova-Leitmannova, *Membrane biophysics : as viewed from experimental bilayer lipid membranes (planar lipid bilayers and spherical liposomes).* 1st ed. Membrane science and technology series. Vol. 5. 2000, Amsterdam ; New York: Elsevier. ix, 640 p.

182. Diaz deLeon, S. and N. Carter, *Method of Making Electro-Conductive Substrates*, in *USPTO*, USPTO, Editor 2005, Polymer Group, Inc.: United States.

183. Bartlett, P.N. and D.H. Dawson, *Electrochemistry of poly(3-thiopheneacetic acid) in aqueous solution: evidence for an intramolecular chemical reaction.* Journal of Materials Chemistry, 1994. **4**(12): p. 1805-1810.

184. Kiralp, S., et al., *Synthesis and Characterization of Conducting Copolymers of Menthyl Ester of 3-Thiophene Acetic Acid with Pyrrole.* Journal of Macromolecular Science, Part A, 2003. **40**(3): p. 251-264.

185. Sahmetlioglu, E., et al., *Synthesis and characterization of conducting copolymers of poly(vinyl alcohol) with thiophene side-groups and pyrrole.* Polymer International, 2004. **53**(12): p. 2138-2144.

186. Haiyun, W., et al. *A biosensor model based on multivariate regression of corrected Cole-Cole parameters*. in *Image and Signal Processing (CISP), 2011 4th International Congress on*. 2011.

187. Ju, J., Y.-a. Han, and S.-m. Kim, *Design Optimization of Structural Parameters for Highly Sensitive Photonic Crystal Label-Free Biosensors.* Sensors, 2013. **13**(3): p. 3232-3241.

188. Mattias Sandstrom, K.J., et al., *Multivariate evaluation of factors influencing the performance of a formic acid biosensor for use in air monitoring.* Analyst, 2001. **126**(11): p. 2008-2014.

189. Roy, N.K., W.D. Potter, and D.P. Landau, *Polymer property prediction and optimization using neural networks.* Neural Networks, IEEE Transactions on, 2006. **17**(4): p. 1001-1014.

190. Saravis, C.A., *Improved blocking of nonspecific antibody binding sites on nitrocellulose membranes.* ELECTROPHORESIS, 1984. **5**(1): p. 54-55.

191. Sattar, S.A., et al., *Transfer of bacteria from fabrics to hands and other fabrics: development and application of a quantitative method using Staphylococcus aureus as a model.* Journal of Applied Microbiology, 2001. **90**(6): p. 962-970.